Adaptation of plants to low-oxygen stress

Dissertation

zur Erlangung des Doktorgrades der Fakultät für Biologie

der Ludwig-Maximilians-Universität München

vorgelegt von

Benjamin Faix

München September 2016

Erstgutachter: Prof. Peter Geigenberger

Zweitgutachter: Prof. Wolfgang Frank

Datum der Abgabe: 11.10.2016

Datum der mündlichen Prüfung: 08.03.2017

Summary

Plants are obligate aerobic organisms and, therefore, need oxygen for survival. However, unlike animals, plants do not possess an active oxygen transport system to supply their organs with oxygen. Hence, oxygen can fall to low levels inside plant tissues if the diffusion of oxygen cannot keep pace with the rate of oxygen consumption. As a consequence, plants have developed special mechanisms to save oxygen. Studies show that plants actively regulate their respiration and metabolism in relation to the internal oxygen concentration. Nevertheless, the sequences of metabolic events leading to this adaptation are not yet known.

Therefore, an experiment was developed to treat potato tuber slices with 4% oxygen (v/v) and analyze the metabolic response in a time dependent manner. The low-oxygen treatment led to a rapid inhibition of respiration and a general metabolic depression at different sites, while fermentation was activated at a later point in time. Regulatory sites have been identified in glycolysis and in the tricarboxylic acid (TCA) cycle. The experiments also revealed cytosolic pyruvate kinase (PKc) as important control site in glycolysis.

PKc is crucial under low-oxygen conditions as it provides pyruvate for respiration and for fermentation. To further investigate the role of PKc under low-oxygen conditions transgenic potato tubers with decreased expression of PKc mediated by RNA interference were treated with 4% oxygen, and a comprehensive metabolic profile was performed. Indeed, the results indicate that PKc regulates the availability of pyruvate for fermentation, thereby influencing the metabolic performance under low-oxygen.

Whereas potato tuber discs are an easy system to manipulate the surrounding oxygen concentration, there are only limited tools available for genetic manipulation. Therefore, *Arabidopsis thaliana* was used as model system for reverse genetic studies.

Transgenic Arabidopsis plants carrying a T-DNA insertion in the catalytic subunit of mitochondrial NAD-dependent isocitrate dehydrogenase (IDH) were used to investigate the importance of the mitochondrial alpha-ketoglutarate provision for the reorganization of the TCA cycle under low-oxygen. The *idhv* mutant showed an improved low-oxygen tolerance accompanied by specific alterations of hypoxic metabolism compared to wild type, thus, suggesting that mitochondrial alpha-ketoglutarate production through IDH is dispensable under low-oxygen conditions in Arabidopsis. Moreover, the experiments showed that an increased activity of extramitochondrial pathways for 2-oxoglutarate production is beneficial for plant survival under low-oxygen.

In addition to the modifications in primary metabolism for an improved survival under low-oxygen, changes in the redox state are also common characteristics of hypoxia. NADPH-

Summary

dependent thioredoxin reductases (NTRs) modulate the activity of redox-regulated enzymes depending on the cellular redox-state. To explore the role of the NTR system under low-oxygen, a knockout of the plastidial NADPH-dependent thioredoxin reductase (NTRC) and a double knockout of the extraplastidial NADPH-dependent thioredoxin reductase A (NTRA) and NADPH-dependent thioredoxin reductase B (NTRB) in *Arabidopsis thaliana* were treated with hypoxia, and the relevant redox related parameters were measured. The results show opposed effects of the low-oxygen treatment for the *ntrc* and the *ntrantrb* mutant. Whereas the *ntrantrb* mutant revealed an increased resistance to hypoxia, the *ntrc* mutant displayed the opposite behavior. Apparently, the plastidial and extraplastidial NTR systems play different roles in the adaptation to low-oxygen, although the underlying reasons for this phenomenon are not yet fully understood.

A further area of plant metabolism being affected by low-oxygen is the cellular energy status. With falling oxygen concentrations inside the cell the production of ATP through respiration decreases and the energy status declines. This in turn affects the biosynthesis pathways and, ultimately, the plant growth which needs to be adjusted to the energy deficit. A possible regulator that connects energy homeostasis with plant growth is the sucrose non-fermenting-1-related protein kinase (SnRK1). Transgenic Arabidopsis plants with beta-estradiol inducible transcriptional silencing of the regulatory SNF4 subunit of SnRK1 were used to study the function of SnRK1 under low-oxygen. The transgenic plants displayed a lower anoxic survival rate, a decrease in hypoxia marker genes expression and alterations in primary metabolism compared to wild type. Altogether, these results suggest an important role of SnRK1 in the low-oxygen response in *Arabidopsis thaliana*.

Zusammenfassung

Pflanzen sind obligat aerobe Organismen und benötigen daher Sauerstoff zum Überleben. Allerdings besitzen Pflanzen im Gegensatz zu Tieren kein aktives Sauerstofftransportsystem, um ihre Organe mit Sauerstoff zu versorgen. Daher kann es im pflanzlichen Gewebe zu Sauerstoffarmut kommen, wenn die Diffusion von Sauerstoff zu langsam ist, um mit dem Sauerstoffverbrauch mitzuhalten. Als Konsequenz haben Pflanzen spezielle Mechanismen entwickelt um Sauerstoff zu sparen. Studien zeigen, dass Pflanzen in der Lage sind ihre Atmung und ihren Stoffwechsel in Abhängigkeit von der Sauerstoffkonzentration aktiv zu regulieren. Jedoch ist die Abfolge der metabolen Ereignisse, die zur Anpassung an niedrige Sauerstoffkonzentrationen führen nicht bekannt.

Infolgedessen wurde ein Experiment entwickelt, bei dem Kartoffelknollenscheibchen mit 4% Sauerstoff (v/v) begast wurden und die Antwort des Stoffwechsels in Abhängigkeit von der Zeit analysiert wurde. Die Niedrig-Sauerstoff Behandlung führte zu einer raschen Inhibierung der Atmung und einer generellen Stoffwechseldepression an verschiedenen Stellen, während die Gärungsprozesse erst zu einem späteren Zeitpunkt aktiviert wurden. Es konnten verschiedene Regulationsstellen in der Glykolyse und im Tricarbonsäurezyklus (TCA-Zyklus) identifiziert werden. Die Experimente haben ebenso gezeigt, dass die cytosolische Pyruvatkinase (PKc) eine wichtige Kontrollstelle in der Glykolyse darstellt.

Bei limitierenden Sauerstoffbedingungen ist PKc entscheidend, da sie Pyruvat bereitstellt, welches nicht nur ein Substrat für die Atmung, sondern auch ein Substrat für die Gärung ist. Um die Rolle von PKc unter Niedrig-Sauerstoff zu untersuchen, wurden transgene Kartoffelknollen, welche mittels RNA-Interferenz eine verminderte Expression von PKc aufweisen, mit 4% Sauerstoff begast und ein umfassendes Stoffwechselprofil aufgenommen. Tatsächlich zeigen die Ergebnisse, dass PKc die Verfügbarkeit von Pyruvat für die Gärung reguliert und somit die Stoffwechselleistung unter Niedrig-Sauerstoff beeinflusst.

Während Kartoffelknollenscheibchen ein einfaches System für die Beeinflussung der Sauerstoffkonzentration in unmittelbarer Umgebung darstellen, so gibt es leider nur eine begrenzte Anzahl an Methoden zur genetischen Manipulation. Aus diesem Grund wurde *Arabidopsis thaliana* verwendet, welche ein Modell-System für reverse Genetik ist.

Mit transgenen Arabidopsis Pflanzen, die eine T-DNA Insertion in der katalytischen Untereinheit der mitochondrialen NAD-abhängigen Isocitrat-Dehydrogenase (IDH) tragen, wurde die Bedeutung der mitochondrialen 2-oxoglutarate Produktion für die Reorganisation des TCA Zyklus unter Niedrig-Sauerstoff untersucht. Die *idhv*-Mutante zeigte eine verbesserte Toleranz gegenüber Niedrig-Sauerstoff begleitet von spezifischen Änderungen im hypoxischen Stoffwechsel im Vergleich zum Wildtyp. Diese Ergebnisse deuten darauf hin, dass die mitochondriale Produktion von 2-Oxoglutarat durch IDH unter Niedrig-Sauerstoff für

Zusammenfassung

Arabidopsis entbehrlich ist. Weiterhin zeigen die Ergebnisse der *idhv*-Mutante, dass eine erhöhte Aktivität der extramitochondrialen 2-Oxoglutarat Produktion vorteilhaft für das Überleben der Pflanze bei Niedrig-Sauerstoff ist.

Abgesehen von den Modifikationen im Primärstoffwechsel, zur Verbesserung des Überlebens bei Sauerstoffmangel, ist die Änderung im Redoxstatus ein allgemeines Merkmal unter Hypoxie. NADPH-abhängige Thioredoxin-Reduktasen (NTRs) beeinflussen die Aktivität von Redox-regulierten Enzymen in Abhängigkeit vom zellulären Redoxstatus. Um die Rolle des NTR-Systems unter Niedrig-Sauerstoff zu untersuchen, wurde ein Knockout der plastidären NADPH-abhängigen Thioredoxin-Reduktase C (NTRC) und ein Doppelknockout der extraplastidären NADPH-abhängigen Thioredoxin-Reduktase A (NTRA) und NADPH-abhängigen Thioredoxin-Reduktase B (NTRB) in *Arabidopsis thaliana* mit Hypoxie behandelt und Redox-abhängige Parameter untersucht. Die Ergebnisse zeigen gegensätzliche Effekte der Niedrig-Sauerstoffbehandlung für die *ntrc*-Mutante im Vergleich zur *ntrantrb*-Mutante. Während die *ntrantrb*-Mutante eine erhöhte Resistenz gegenüber Anoxie aufwies, zeigte die *ntrc*-Mutante das entgegengesetzte Verhalten. Offenbar erfüllen das plastidäre und das extra-plastidäre NTR-System unterschiedliche Aufgaben bei der Anpassung an Sauerstoffarmut, wobei die zugrunde liegende Ursache für dieses Phänomen noch nicht vollständig verstanden ist.

Ein weiterer durch Niedrig-Sauerstoff beeinflusster Bereich im pflanzlichen Stoffwechsel ist der Energiestatus der Zelle. Mit fallender Sauerstoffkonzentration in der Zelle sinkt der Energiestatus ab, da sich die atmungsabhängige Produktion von ATP verringert. Dies führt wiederum zu einem Energiedefizit, welches sich auf die Biosynthesewege und das Pflanzenwachstum auswirkt. Ein möglicher Regulator, der die Energiehomöostase mit dem Pflanzenwachstum verbindet, ist die SNF1-related kinase (SnRK1). Die Funktion von SnRK1 unter Niedrig-Sauerstoff wurde mit Hilfe transgener Arabidopsis-Pflanzen untersucht, welche eine beta-estradiol induzierbare Verringerung der Transkription der regulatorischen SNF4 Untereinheit aufweisen. Die transgenen Pflanzen zeigten eine verringerte Überlebensrate bei Anoxie, eine erniedrigte Expression der Hypoxie-Markergene und einen veränderten Primärstoffwechsel im Vergleich zum Wildtyp. Zusammengenommen sprechen diese Ergebnisse für eine entscheidende Rolle von SnRK1 bei der Anpassung an Niedrig-Sauerstoff in *Arabidopsis thaliana*.

Index

Index

Abbreviations

ACBP	acyl-CoA-binding protein
ADH	alcohol dehydrogenase
AMPK	AMP-activated protein kinase
AlaAT	alanine aminotransferase
AOX	alternative oxidase
ASN	glutamine dependent asparagine synthetase
COX	cytochrome c oxidase
D2HGDH	D-2-hydroxyglutarate dehydrogenase
ERF	ethylene response factor
F6P	fructose-6-phosphate
FBP	fructose-1,6-bisphosphate
FK	fructokinase
G6P	glucose-6-phosphate
G6PDH	glucose-6-phosphate dehydrogenase
GABA	gamma-aminobutyric acid
GDC	glutamate decarboxylase
GR	glutathione reductase
GS/GOGAT	glutamine synthetase/glutamate synthase
GSH	reduced glutathione
GSSG	oxidized glutathione
Hb	hemoglobin
HK	hexokinase
HRE	hypoxia responsive ERF
IDH	NAD-dependent isocitrate dehydrogenase
LDH	lactate dehydrogenase
mETC	mitochondrial electron transport chain

Abbreviations

NERP	N-end rule pathway
NR	nitrate reductase
NTR	NADPH-dependent thioredoxin reductase
NTRA	NADPH-dependent thioredoxin reductase A
NTRB	NADPH-dependent thioredoxin reductase B
NTRC	NADPH-dependent thioredoxin reductase C
PEP	phosphoenolpyruvate
PEPC	phosphoenolpyruvate carboxylase
PFK	ATP-dependent phosphofructokinase
PKc	cytosolic pyruvate kinase
PKp	plastidial pyruvate kinase
PP_i	pyrophosphate
RAP2	related to APETALA2
RNS	reactive nitrogen species
ROS	reactive oxygen species
SDH	succinate dehydrogenase
SNF1	sucrose non-fermenting-1
SnRK1	sucrose-non-fermenting-1-related protein kinase-1
SuSy	sucrose synthase
TCA	tricarboxylic acid
Trx	thioredoxin

1 Introduction

1.1 Oxygen is essential for plant survival

Plants, like animals and most fungi are obligate aerobic organisms. Hence, they need oxygen as terminal electron acceptor for the cytochrome c oxidase (COX) which reduces oxygen to water. During the process of respiration 38 mol ATP per one mol glucose are generated. However, when oxygen becomes limiting plants have to switch to glycolytic substrate level phosphorylation yielding only two mol ATP per one mol glucose. Therefore, plants are not able to survive longer periods without oxygen. In addition, oxygen is involved in the secondary plant metabolism in the biosynthesis of phenylpropanoids, flavanoids, anthocyanins and lignin. Also, oxygen takes part in the biosynthesis of haem, sterols, fatty acids and hormones (jasmonic acid, gibberellins and brassinosteroids). Taken together, oxygen is of extreme importance for plant metabolism and growth.

1.2 Internal or external factors can cause oxygen deficiency

Unlike animals, plants possess no active oxygen transport system to supply the organs with oxygen. The uptake of oxygen in the tissue and further transport occurs only by diffusion. Usually, plants do not have difficulties with the delivery of oxygen into their cells for aerobic respiration. However, even at normal ambient oxygen concentrations (21% O_2 (v/v)) oxygen can become a limiting factor for plant growth. Such can happen in plant organs with a small surface to volume ratio as well as in plant cells which are highly metabolically active or poorly vacuolated (Geigenberger et al. 2000). This applies to seeds of peas, beans, barley (Borisjuk & Rolletschek 2009) and rapeseed (Vigeolas et al. 2003). Likewise, roots (Armstrong et al. 2009), phloem tissue (van Dongen et al. 2003), storage organs (potato tuber) (Geigenberger et al. 2000) and fruits (melon, apple) (Biais et al. 2010; Ho et al. 2010) can suffer from oxygen limitation inside the cell. If oxygen decreases to low levels inside the plant cell and limits the production of ATP by mitochondrial respiration, it is termed hypoxia. Anoxia is the complete absence of oxygen inside the plant cell (Albrecht et al. 2004). External factors that induce low-oxygen stress are waterlogging and submergence caused by flooding (Bailey-Serres & Voesenek 2008; Voesenek & Bailey-Serres 2013). Indeed, the occurrence of floods worldwide increased over the past six decades (Bailey-Serres et al. 2012). If plants are submerged, the availability of oxygen for respiration is strongly decreased, since oxygen diffuses 10,000 times slower in water than in air (Bailey-Serres & Voesenek 2008).

Therefore, floods are a major factor contributing to the loss of crop productivity worldwide, as most crops are not flood tolerant (Setter & Waters 2003).

1.3 Molecular responses to hypoxia

Cellular oxygen depletion results in various molecular responses. There is an activation of low-oxygen responsive transcription factors leading to a change in gene expression. Additionally, hypoxic plants show a selective repression of translation to promote the conservation of energy.

1.3.1 Regulation and sensing by ethylene response factors

Low-oxygen leads to a reprogramming of gene expression (Klok et al. 2002; Dongen et al. 2009; Hsu et al. 2011) which is partly mediated by the transcription factors (TFs) of the plant specific group VII Ethylene Response Factor (ERF) family (Bailey-Serres et al. 2012; Gibbs et al. 2015). The group VII ERF TFs are members of the APETALA2/Ethylene Responsive Factor family being involved in the control of primary and secondary metabolism, growth and developmental programs as well as responses to plant abiotic stress (Mizoi et al. 2012; Licausi, Ohme-Takagi, et al. 2013). The group VII ERF TFs share a conserved 60-70 amino acids long DNA binding domain and are regulated by the N-end rule pathway (NERP) for protein degradation (Licausi et al. 2010; Gibbs et al. 2011). The N-end rule pathway of targeted proteolysis has not only been identified in animals and plants, but also in yeast and bacteria (Tasaki et al. 2012). The substrates of NERP have an N-terminal motif (MCGGAI/L) recognized by specific aminopeptidases that cleave the N-terminal methionine (Liao et al. 2004). This leaves an N-terminal cysteine residue exposed for oxidation by plant cysteine oxidases (Weits et al. 2014). The oxidized cysteine is arginylated by arginine-tRNA protein transferases signaling the ubiquitin ligases to polyubiquitinate the nearby lysine residues. The 26S proteasome recognizes the polyubiquitin tail and subsequently degrades the target protein (Bailey-Serres et al. 2012). The oxygen dependent proteolytic degradation makes group VII ERF TFs ideal candidates for oxygen sensors. Indeed, RAP2.12 belonging to the group VII ERF family was shown to be constitutively expressed in many cell types and degraded in the presence of oxygen. Under normoxia some of the RAP2.12 proteins bind to the plasma membrane with the help of acyl-CoA-binding protein 1 and 2 (ACBP1 and ACBP2) (Licausi et al. 2011). Under hypoxia RAP2.12 is released from the plasma membrane in a time and oxygen dependent manner and moves to the nucleus where it

triggers the expression of its target genes (Licausi et al. 2011; Kosmacz et al. 2015) (Fig. 1.2). In addition, recent studies have shown that the RAP2.12 related TFs RAP2.2 and RAP2.3 can also activate the expression of core hypoxia responsive genes (Papdi et al. 2015; Gasch et al. 2015; Bui et al. 2015). Among those genes are *HYPOXIA RESPONSIVE ERF1 (HRE1)* and *HRE2*, both belonging to the group VII ERF family (Mustroph et al. 2009; Sasidharan & Mustroph 2011). HRE1 and HRE2 are targets of NERP and recognized as regulators of the low oxygen response (Licausi et al. 2010; Hess et al. 2011; Gibbs et al. 2011). Overexpression of HRE1 in Arabidopsis enhances ethanol fermentation, whereas *hre1 hre2* knockouts show a delay in induction and decreased expression of hypoxia core responsive genes (Licausi et al. 2010). Therefore, HRE1 and HRE2 have been suggested to be involved in the later steps of the low-oxygen response, whereas the RAP TFs are principal activators of the core hypoxia responsive genes (Bui et al. 2015; Gasch et al. 2015).
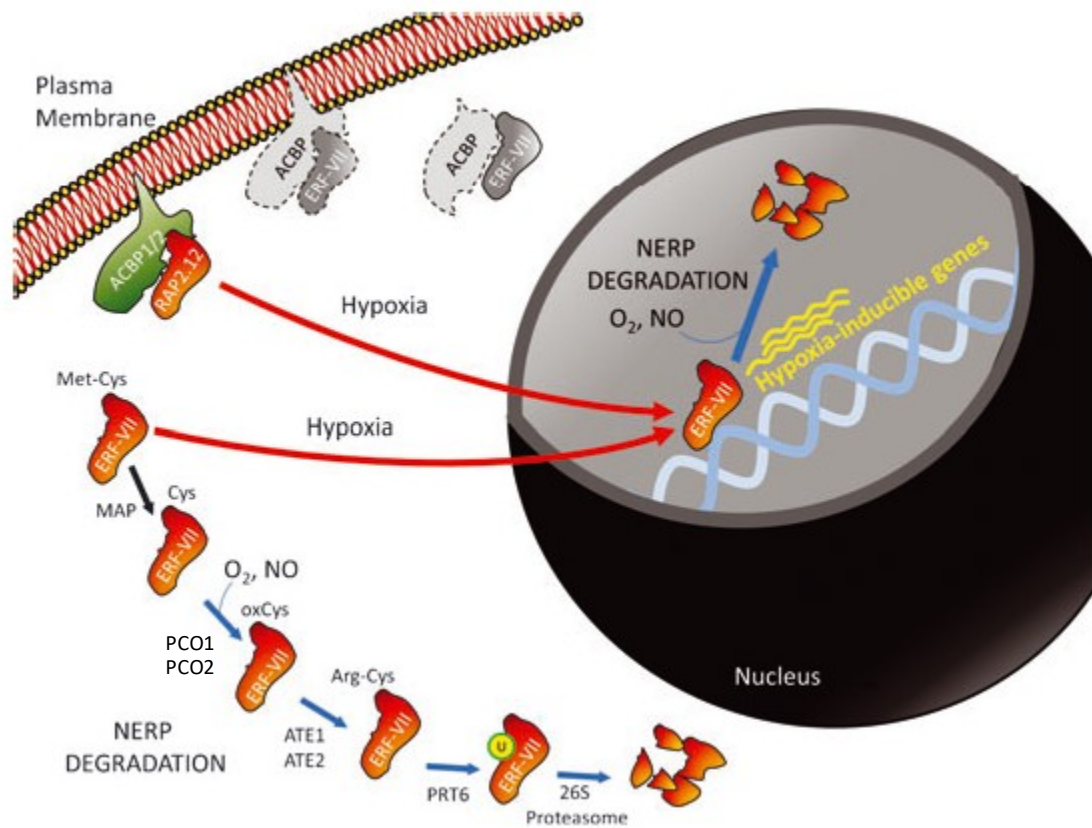
Fig. 1.1: Schematic representation of oxygen signaling in plants. Under aerobic conditions most of the RAP2.12 TFs are bound to the membrane localized protein ACBP1/2, whereas the remaining proteins are either in the cytosol or in the nucleus. In case oxygen is present, RAP2.12 and other group VII ERF TFs are degraded via NERP. Under hypoxia the lack of oxygen prevents the degradation of the group VII ERF TFs and RAP2.12. The stabilized TFs move into the nucleus and activate the expression of hypoxia responsive genes. Figure was taken from Licausi (2013).

1.3.2 Selective transcription and translation of mRNA

In addition to the induction of the core hypoxic response genes by the RAP TF family, there are several hundred other genes whose expression changes depending on the cellular oxygen concentration (Klok et al. 2002; Liu et al. 2005; Branco-Price et al. 2005; Dongen et al. 2009; Narsai et al. 2011; Christianson et al. 2010). The differentially expressed genes can be grouped into functional categories. A microarray analysis of the anaerobic response in Arabidopsis and rice revealed an upregulation of genes involved in photosynthesis, major carbohydrate metabolism and protein degradation function. In contrast, the expression of cell wall and secondary metabolism function genes were downregulated (Narsai et al. 2011). Furthermore, Christianson et al. (2010) compared the transcriptome response of three dicotyledonous species under hypoxia and showed that more than 120 genes were commonly regulated under low-oxygen in all three species. Those genes belong to the functional categories of fermentation, ethylene hormone metabolism, abiotic stress, regulation of transcription, cell wall degradation, secondary metabolism and receptor kinase signaling. A comparison of the mRNA expression under low-oxygen in 21 different cell types of Arabidopsis thaliana revealed a core set of 49 genes whose expression was changed across all cell types upon treatment with hypoxia (Mustroph et al. 2009; Sasidharan & Mustroph 2011). Among those genes were *ADH1*, *HB1*, *SUS1* and *SUS4* which are all vital for tolerance to low-oxygen in Arabidopsis (Hunt et al. 2002; Hinz et al. 2010) and are, therefore, commonly used as hypoxia marker genes (Licausi et al. 2010; Licausi et al. 2011; Weits et al. 2014; Kosmacz et al. 2015). SUS1 and SUS4 are isoforms of sucrose synthase (SuSy) which is involved in the breakdown of sucrose under oxygen deprivation (Santaniello et al. 2014). ADH1 is the most important isoform of alcohol dehydrogenase being responsible for the production of ethanol from acetaldehyde in the ethanol fermentation pathway (Ismond et al. 2003). The ethanol fermentation is important under low-oxygen, as it produces NAD required to keep glycolysis running (Plaxton 1996). Similarly, *HB1* functions also in the oxidation of NADH. It is part of the hemoglobin/nitric oxide (Hb/NO) cycle that uses NO and NADH to produce NO_3^- and NAD (Igamberdiev et al. 2005).

In addition to changes in transcription, translation is likewise altered under low-oxygen. With limited ATP availability under low-oxygen, the energy-costly mRNA translation needs to be adjusted. Branco-Price et al. (2008) demonstrated that *Arabidopsis thaliana* decreases the level of polysomal associated mRNA in alignment with the energy state of the cell. While the majority of mRNA is restricted from polysome complexes, the hypoxia induced genes are preferably translated under hypoxia (Mustroph et al. 2009). Reoxygenation completely reverses the hypoxic selective inhibition of translation (Branco-Price et al. 2008).

1.4 Metabolic responses to hypoxia

The aforementioned response to low-oxygen on the molecular level is associated with alterations in primary metabolism. Hypoxia leads to changes in the flux through glycolysis being accompanied by the induction of fermentation to maintain the cellular redox balance. Furthermore, the TCA cycle is reorganized to support ATP production, whereas the respiratory electron chain is inhibited under low-oxygen stress.

1.4.1 Induction of fermentation

A conserved mechanism of all plants examined under low-oxygen conditions is the induction of fermentation having the oxidation of NADH as function which otherwise would inhibit glycolysis. The substrate for fermentation is pyruvate used in the TCA cycle for respiration and being likewise the end product of glycolysis. When oxygen becomes limiting, the respiratory activity decreases, whereas glycolytic flux increases, ultimately leading to the accumulation of pyruvate (Branco-Price et al. 2008; Kreuzwieser et al. 2009; Zabalza et al. 2008; António et al. 2015). This is detrimental for plant survival under low-oxygen, since pyruvate stimulates mitochondrial oxygen consumption (Zabalza et al. 2008). To circumvent this negative effect, plants are able to control the level of pyruvate with the induction of fermentation.

There are three main fermentation pathways in plants: 1.) ethanol fermentation, 2.) lactate fermentation and 3.) alanine fermentation (Fig. 1.2) with ethanol fermentation as the most important pathway (Gibbs & Greenway 2003). Ethanol fermentation involves two reactions, catalyzed by pyruvate decarboxylase (PDC) and ADH. PDC uses pyruvate to produce acetaldehyde being toxic to plant cells (Tadege et al. 1999; Ismond et al. 2003). Therefore, acetaldehyde has to be efficiently converted to ethanol by ADH additionally producing NAD. The expression of both genes is induced by mannitol and abscisic acid and cold stress (Dolferus et al. 1994; de Bruxelles et al. 1996; Kursteiner et al. 2003). However, the strongest induction occurs under conditions of oxygen deficiency mediated by the oxygen sensor RAP2.12 (Licausi et al. 2011; Mithran et al. 2014). The importance of both enzymes for the tolerance to low-oxygen stress was demonstrated by several studies. Overexpression of PDC and ADH together and alone enhances anoxia survival, whereas knockdown of both or single enzymes decreases anoxia survival (Ellis et al. 1999; Kursteiner et al. 2003; Mithran et al. 2014; Ismond et al. 2003).

Another main fermentation pathway is the production of lactate by lactate dehydrogenase (LDH) from pyruvate which is linked to the oxidation of NADH to NAD. Both, ethanol and lactate fermentation, enable the plant to sustain glycolytic ATP production under low-oxygen which would normally be inhibited by high NAD levels (Kennedy et al. 1992; Ismond et al. 2003; Rocha et al. 2010). Similar to ADH and PDC, LDH expression is not only induced by hypoxia, but also by other abiotic stresses (Dolferus et al. 2008) However, hypoxic LDH expression is not regulated by the oxygen sensor RAP2.12 (Hinz et al. 2010; Licausi et al. 2011). The role of LDH in the tolerance to low-oxygen was demonstrated by Dolferus et al. (2008). Overexpression of LDH in Arabidopsis improves this tolerance, whereas knockout of LDH decreases the tolerance. Although lactate and ethanol fermentation individually are each necessary for low-oxygen tolerance, the activity of both pathways has to be tightly controlled by the cell, as they both compete for the same substrate. In fact, it was proved that lactate accumulation preceded ethanol fermentation under low-oxygen in several plant species correlating with a change in cytosolic pH. This observation led to the pH-stat hypothesis from Davies & Roberts according to which the cytosolic pH determines the switch from lactate to ethanol fermentation under low-oxygen (Davies et al. 1974; J. Roberts et al. 1984; Roberts et al. 1985; Dolferus et al. 2008). At the beginning of hypoxia lactate is produced by LDH which acidifies the cytosol. The resulting lower cytosolic pH favors the activity of PDC, whereas LDH is inhibited by low pH.

A third major product of pyruvate metabolism under low-oxygen is alanine. Alanine aminotransferase (AlaAT) catalyzes the reversible transfer of an amino group from glutamate to pyruvate to form 2-oxoglutarate and alanine. AlaAT expression is distinctly induced by hypoxia in several plant species, but is also regulated by light and nitrogen availability (Miyashita et al. 2007). In contrast to the cytosolic localization of the other fermentation enzymes, the main AlaAT isoforms are located in the mitochondria (Heazlewood et al. 2004; Taylor et al. 2011; Salvato et al. 2013). Hypoxic alanine accumulation was found in many plant species. Likewise, it was observed that alanine can become the most abundant amino acid under low-oxygen in plant roots (REGGIANI 1985; Good & Muench 1993; Sousa & Sodek 2002; Miyashita et al. 2007; Narsai et al. 2011). However, the function of alanine fermentation remained unclear for over two decades. In contrast to ethanol and lactate fermentation, the production of alanine is not coupled to the oxidation of NADH. Instead, alanine fermentation yields an additional ATP and is linked to the reorganization of the TCA cycle under low-oxygen (Rocha et al. 2010; António et al. 2015). For details, see chapter 1.4.3.

PYRUVATE   GLUTAMATE

NADH

LDH   PDC   AlaAT

NAD⁺ CO_2

LACTATE   ACETALDEHYDE   ALANINE
                                +
            NADH   2-OXOGLUTARATE

                        ADH

            NAD⁺
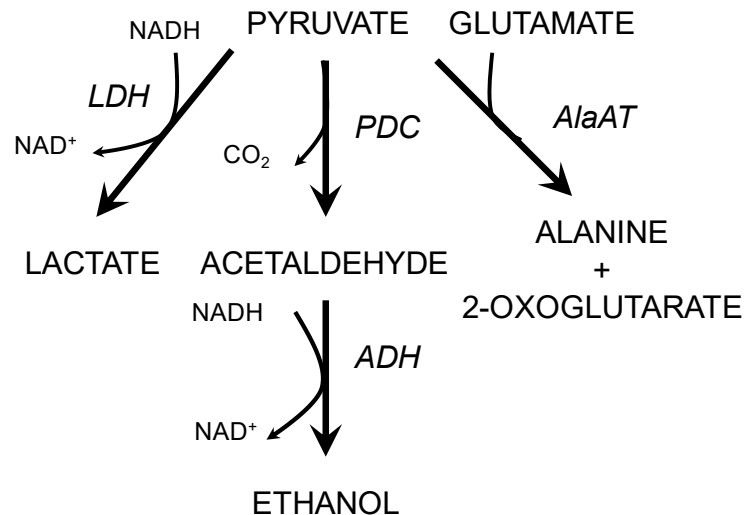
                ETHANOL

Fig. 1.2: Fermentation pathways in plants under low-oxygen. All three main fermentation pathways use pyruvate as a substrate. Lactate and ethanol fermentation produce NAD, whereas alanine fermentation produces 2-oxoglutarate.

1.4.2 Regulation of glycolysis

When plants face low-oxygen conditions, respiration gets inhibited and energy has to be generated via glycolytic substrate-level phosphorylation. Under strict anoxic conditions glycolysis is the exclusive producer of cellular ATP. In contrast, under hypoxia respiration and glycolysis contribute to the cellular energy generation (Ricard et al. 1994; Geigenberger 2003). The glycolytic flux in plant cells decreases under hypoxia, whereas under anoxia the flux through glycolysis increases again for maximization of the substrate level ATP production (Bouny & Saglio 1996; Geigenberger et al. 2000; Vigeolas et al. 2003; Alonso et al. 2007).

Important regulatory sites of glycolysis are the ATP-dependent phosphofructokinase (PFK) and the PKc (Plaxton 1996). PFK is sensitive to inhibition by phosphoenolpyruvate (PEP) being the substrate for PKc. If PKc is inhibited under hypoxia, PEP accumulates and inhibits PFK leading to the restriction of glycolytic flux. PKc catalyzes the final step of glycolysis, thereby converting PEP to pyruvate and producing ATP. The main isoform of PKc is a heterotetramer and subject to tight allosteric regulation (Smith 2000; Turner & Plaxton 2000; Turner et al. 2005). Potential allosteric inhibitors of PKc are alpha-ketoglutarate and citrate indicating a regulation of PKc by respiratory metabolism (Auslender et al. 2015). This regulatory circuit allows the plant to control glycolytic activity dependent on the activity of the TCA cycle and the mitochondrial electron transport chain (Fig. 1.2). It is speculated that this mechanism contributes to the adaptation of respiratory metabolism to a decrease in cellular oxygen concentration (Zabalza et al. 2008)
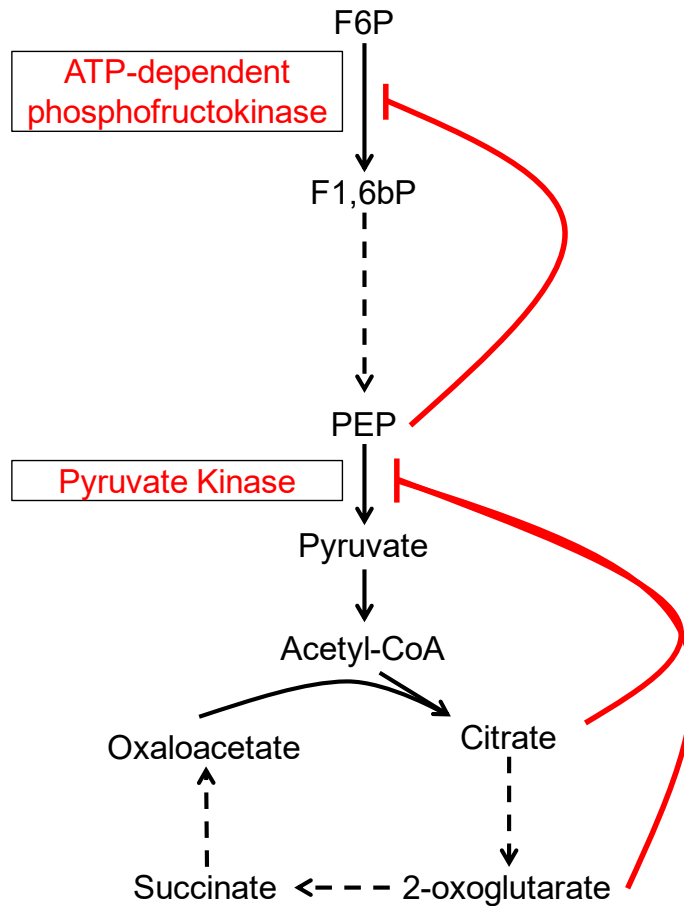
Fig. 1.3: Regulation of plant glycolysis. Plant glycolysis is regulated from the "bottom up" via PKc and PFK. When respiration is inhibited, citrate and 2-oxoglutarate accumulate affecting in turn PKc. This leads to an increase in PEP which is a potent inhibitor of PFK. Subsequently, overall flux of glycolysis is decreased (Plaxton 1996; Auslender et al. 2015).

1.4.3 Reorganization of the TCA cycle

The TCA cycle is an important part of respiratory metabolism, as it connects the mitochondrial electron transport chain (mETC) with glycolysis. It provides energy and reducing equivalents for metabolism to support plant growth. Moreover, the TCA cycle plays a multifaceted role in plant metabolism, as it influences photosynthesis, photorespiration, nitrate assimilation and stomata function (Sweetlove et al. 2010; Araújo et al. 2011; Araújo et al. 2014). Furthermore, the TCA cycle intermediates oxaloacetate and 2-oxoglutarate are precursors for several amino acids.

In addition to its essential function in the glutamine synthetase/glutamate synthase (GS/GOGAT) cycle (Hodges et al. 2003; Lemaitre & Hodges 2006), 2-oxoglutarate is also important during the reorganization of the TCA cycle under low-oxygen. Rocha et al. (2010) demonstrated that the production of alanine is coupled to the production of succinate yielding

an additional ATP in *Lotus japonicus* roots under hypoxia. Alanine is produced in a transamination reaction by AlaAT from pyruvate and glutamate with 2-oxoglutarate as a side product. This metabolite can enter the TCA cycle and is further metabolized to succinate in a 2-step reaction sequence. Thereby, ATP and NADH are produced. The observed accumulation of succinate in different plant species under hypoxia can be explained by the inhibition of succinate dehydrogenase which uses succinate to generate fumarate in the TCA cycle (Narsai et al. 2011; António et al. 2015). The NADH is reoxidized to NAD by the reduction of oxaloacetate to malate catalyzed by malate dehydrogenase. The oxaloacetate used in this reaction is a result of the deamination of aspartate which is coupled to the amination of 2-oxoglutarate to form glutamate (Fig. 1.2). Interestingly, the normal route of 2-oxoglutatrate production via the mitochondrial NAD-dependent isocitrate dehydrogenase (IDH) was inhibited under low oxygen in *Lotus japonicus* roots (Rocha et al. 2010). Under normoxic conditions IDH is the main producer for mitochondrial 2-oxoglutarate (Hodges et al. 2003; Lemaitre & Hodges 2006) required for the assimilation of ammonia in the GS/GOGAT cycle. Despite this essential function in primary metabolism, knockdown of IDH in tomato and Arabidopsis showed no visible phenotype. However, decrease in IDH activity was accompanied by changes in primary metabolism suggesting a compensatory mechanism (Lemaitre et al. 2007; Sienkiewicz-Porzucek et al. 2010). The question whether the reorganized TCA cycle is also functional in other dicotyledonous plant species like *Arabidopsis thaliana* remains open. Moreover, the contribution of the different pathways to the 2-oxoglutarate production under low-oxygen is not yet clear.

In summary, the reorganized TCA cycle helps the plant to survive low-oxygen conditions by improving the energy yield per mol carbon that is consumed by the plant under hypoxia.

Fig. 1.4: Metabolic model of hypoxia induced reorganization of primary metabolism in *Lotus japonicus*. Grey arrows indicate reactions which are suppressed under hypoxia, whereas black arrows indicate reactions which are enhanced under low-oxygen. At 21% oxygen the TCA cycle runs in a cyclic flux mode and 2-oxoglutarate is produced by mitochondrial IDH from isocitrate. However, under low-oxygen 2-oxoglutarate is produced from glutamate via transamination of pyruvate to alanine. This mechanisms attenuates the accumulation of pyruvate which should be avoided to prevent the activation of respiratory oxygen consumption (Zabalza et al. 2008). Simultaneously, the TCA cycle splits in two branches to support ATP coupled production of succinate and reoxidation of NADH. Abbreviations are as follows: AlaAT, alanine aminotransferase; AspAT, aspartate aminotransferase; GABA-T, GABA transaminase; GAD, glutamate decarboxylase; GOGAT, glutamine oxoglutarate aminotransferase; IDH, NAD-dependent isocitrate dehydrogenase; MDH, malate dehydrogenase; ME, malic enzyme; OGDH, 2-oxoglutarate dehydrogenase; PEP, phosphoenolpyruvate; PEPC, phosphoenolpyruvate carboxylase; SDH, succinate dehydrogenase; Figure was taken and modified from Rocha et al. (2010).

1.4.4 Inhibition of respiration

When oxygen availability decreases, the rate of respiratory oxygen consumption is diminished (Zabalza et al. 2008; Nikoloski & van Dongen 2011). This phenomenon is described for different tissues like leaves, roots, seeds and fruits (van Dongen et al. 2004; Laisk et al. 2007; Maricle & Lee 2007; Ho et al. 2010). The level of oxygen at which the respiration starts to decline in roots of pea and Arabidopsis is around 20% of air saturation (Zabalza et al. 2008). This value is 400 times higher than the K_m of the cytochrome c oxidase (COX) which catalyzes the reduction of oxygen into water in the respiratory electron chain. Yet, a direct inhibition of COX cannot explain the kinetics of the respiratory oxygen consumption depending on the external oxygen concentration. Rather, it was concluded that plants are able to proactively adapt their respiratory metabolism to a change in cellular oxygen concentration to avoid internal anoxia (Geigenberger 2003; Gupta et al. 2009; Zabalza et al. 2008; Nikoloski & van Dongen 2011). For example, glycolysis is able to regulate the amount of pyruvate that becomes available for respiration in the TCA cycle (Zabalza et al. 2008). Furthermore, under hypoxia the TCA cycle itself operates in a non-cyclic flux mode at the inhibitory site of succinate dehydrogenase (SDH) (Rocha et al. 2010; António et al. 2015). This enzyme connects the TCA cycle with the mETC. Thus, an inhibition of SDH also affects the activity of the mETC and leads to a decrease in respiration which was shown for tomato (*Solanum lycopersicum*) SDH (Araújo, et al. 2011).

Additionally, the formation of supercomplexes in the mETC is changed under low-oxygen. The respiratory complexes I (NADH dehydrogenase), III (cytochrome c reductase) and IV (cytochrome c oxidase) are organized in supercomplexes with different compositions (Eubel et al. 2004). Hypoxia changes the organization of the respiratory complexes within the supercomplexes. For instance, the activity of the single complex I monomer increases during prolonged hypoxia, whereas its activity within the supercomplex decreases (Ramirez-Aguilar et al. 2011). The transcriptional regulation of mETC components under low-oxygen is not conserved among different plant species. The mRNA levels of complex I, III and V are upregulated in poplar, whereas they are downregulated in Arabidopsis (Narsai et al. 2011).

Apart from COX, the alternative oxidase (AOX) also transfers electrons from the ubiquinol pool to oxygen, thereby reducing oxygen to water. However, this process does not translocate protons across the mitochondrial membrane. Therefore, less ATP is produced via the AOX pathway compared with the production via the COX pathway. So, an active AOX would be counterproductive for the generation of ATP under low-oxygen. Studies of leaves and roots in different species showed a change in AOX capacity depending on the cellular oxygen concentration. Certainly, the response was not conserved among the examined species (Vanlerberghe 2013). Overall, the affinity for oxygen as well as the capacity of AOX

under low-oxygen is much less compared to COX (Ribas-Carbo et al. 1994; Gupta et al. 2009; Zabalza et al. 2008). A possible role of AOX is to prevent the over-reduction of the mitochondrial ubiquinol pool under low-oxygen subsequently leading to the formation of harmful reactive oxygen species (ROS). Moreover, AOX diminishes the mitochondrial oxygen concentration and may, therefore, function as regulator of the oxygen homeostasis in mitochondria (Gupta et al. 2009). The precise functions of the other respiratory complexes under low-oxygen remain elusive, as the available plants lines that are genetically modified in one of the mETC components have not yet been investigated under low-oxygen.

1.5 Consequences of hypoxia

Although plants are able to adapt to a decrease in the external oxygen concentration, they have to deal with the negative consequences of the oxygen deficit to survive prolonged periods of low-oxygen stress. The main consequence of low-oxygen stress is the decrease in the efficiency of oxidative phosphorylation which ultimately leads to a lower energy status of the cell. Likewise, the diminished availability of oxygen to function as electron acceptor leads to a backlog of electrons further causing redox imbalances in the plant cellular system. Additionally, low-oxygen enhances the production of ROS and reactive nitrogen species (RNS) which can damage the cell structure.

1.5.1 Energy deficit

With the decrease in oxygen concentration in the surrounding atmosphere plant respiration is inhibited. Eventually, this leads to a decline in oxidative phosphorylation and ATP production. The deficit in energy production restricts plant growth and can ultimately cause cell death (Hochachka et al. 1996; Vartapetian & Jackson 1997). However, plants have evolved numerous strategies to counteract the energy crisis. First of all, plants progressively decrease their biosynthetic activities. This includes the biosynthesis of lipids, starch, protein and cell wall (Geigenberger et al. 2000; Gibon et al. 2002; Vigeolas et al. 2003).

The transport of sugars and amino acids within the phloem sap from source to sink tissues is also affected by low-oxygen stress (van Dongen et al. 2003; van Dongen et al. 2004). The decrease in biosynthetic activity is associated with the inhibition of plant growth under low-oxygen (Hunt et al. 2002; Kreuzwieser et al. 2009). When the oxygen levels inside the plant become anoxic, only few plant species are able to continue growing (Gibbs & Greenway 2003; Bailey-Serres & Voesenek 2008). For instance, embryos and coleoptiles of rice can

germinate and grow under anoxia, but their further development depends on the availability of oxygen (Drew 1997). The advantage of rice compared to anoxia intolerant plant species is the ability to increase the flux of ATP substrate level phosphorylation under anoxic conditions to mitigate the decline in aerobic ATP generation (Pasteur effect) (Narsai et al. 2009). Still, the efficiency of aerobic respiration is up to ten times higher than of anaerobic substrate level phosphorylation (Gibbs & Greenway 2003). To improve the ATP yield under low-oxygen, plants have developed a split TCA cycle by which the amount of ATP can be doubled compared with the operation of glycolysis alone (Rocha et al. 2010).

Apart from the amelioration of ATP generation under low-oxygen, plants use pyrophosphate (PP_i) as alternative energy donor (Plaxton & Podestá 2006). PP_i is produced as a byproduct in the synthesis of polymers and reaches concentrations of up to 0.5 mM in the cytosol of plants (Plaxton & Tran 2011). In contrast to ATP, which sharply declines under low-oxygen, the cytosolic PP_i pool remains stable under environmental perturbations (Plaxton & Podestá 2006). This is important for the function of the PP_i dependent enzymes being crucial for anoxia survival of plants (Gibbs & Greenway 2003; Atwell et al. 2015). One known example of a PP_i dependent enzyme is the H^+-transporting pyrophosphatase at the tonoplast. This enzyme is required for the transport of H^+ from the cytosol to the vacuole by hydrolysis of PP_i, which is necessary to maintain the energy dependent solute compartmentation between cytosol and vacuole (Felle 2005). Another energy consuming process is the phosphorylation of hexoses as the substrate for glycolytic energy generation. An alternative PPi dependent pathway uses SuSy and uridine diphosphate-glucose pyrophosphorylase to cleave sucrose into two hexose phosphates at the expense of 1 PP_i. This process improves the energy yield by 50% compared with the work of invertase and hexokinase (Atwell et al. 2015).

The ability of plants to switch to an energy efficient metabolism under low-oxygen requires a metabolic sensor that is able to sense changes in the cellular energy state. A putative plant energy sensor is Sucrose-non-fermenting-1-related protein kinase-1 (SnRK1). It is a serine-threonine protein kinase with a high homology to the yeast sucrose non-fermenting-1 (SNF1) and the animal AMP-activated protein kinase (AMPK). SnRK1/Snf1/AMPK kinases are metabolic energy sensors which are activated under conditions of energy depletion (extended darkness, hypoxia) to promote cell survival (Baena-González et al. 2007; Ghillebert et al. 2011; Robaglia et al. 2012; Tome et al. 2014).

SnRK1 is located in the cytosol and in the nucleus where it can influence gene expression (Bitrián et al. 2011; Cho et al. 2012). SnRK1 is a heterotrimer consisting of a catalytic α-subunit (Kin10 and KIN11) and regulatory β (AKINβ1, AKINβ2 and AKINβ3) and γ subunits (AKINγ1, AKINγ2 and AKINβγ) (Tome et al. 2014). For kinase activity, a conserved threonine residue in the activation loop has to be phosphorylated by upstream kinases (Chris Sugden et al. 1999; Ghillebert et al. 2011). So far, SnRK1-activating kinase 1 and 2 (AtSnAK1 and

1. Introduction

AtSnAK2) have been identified as possible upstream kinases in Arabidopsis (Shen & Hanley-Bowdoin 2006; Crozet et al. 2010). In animal cells AMP directly enhances phosphorylation efficiency, thereby activating AMPK. In plant cells AMP cannot directly activate SnRK1. Instead, SnRK1 interacts with an Adenosine kinase (ADK). ADK produces 5'-AMP which in turn inhibits t-loop dephosphorylation and, subsequently, the inactivation of SnRK1 (Chris Sugden et al. 1999; Mohannath et al. 2014). The regulatory β-subunit regulates substrate specificity, subcellular localization and complex activity of SnRK1 (Tome et al. 2014; Emanuelle et al. 2015). While a functional SnRK1 heterotrimer can contain either Kin10 or KIN11 as catalytic α-subunit as well as AKINβ1, AKINβ2 or AKINβ3 as regulatory β-subunit, only AKINβγ is a functional γ-subunit (Emanuelle et al. 2015). The AKINβγ subunit is plant specific and the only γ-subunit that complements a yeast γ-subunit mutant (snf4) (Kleinow et al. 2000; Lumbreras et al. 2001).

The importance of SnRK1 for the regulation of cellular metabolism has been shown by Baena-González et al. (2007) who transiently expressed AKIN10 in protoplasts and found more than 1000 genes to be regulated by SnRK1. SnRK1 can influence gene expression through the activation of transcription factors (basic leucine zipper family TF), micro RNA (miRNA) mediated RNA modification or through direct binding of DNA (Baena-González et al. 2007; Dietrich et al. 2011; Cho et al. 2012; Confraria et al. 2013; Tome et al. 2014). In addition to the change in gene expression, SnRk1 also inactivates proteins by phosphorylation. Enzymes of central metabolism like sucrose phosphate synthase, trehalose phosphate synthase and nitrate reductase (NR) were identified as target proteins (Baena-González & Sheen 2008; Tome et al. 2014).

As SnRK1 is part of the low energy signaling network (Tome et al. 2014), a function of SnRK1 in the low-oxygen response in plants was already assumed in the year 2003 (Geigenberger 2003). This is hardly surprising, bearing in mind that the SnRK1 homolog AMPK is involved in the low-oxygen response in animals (Marsin et al. 2002; Lee et al. 2003). The role of SnRK1 in plants under hypoxia has been demonstrated by Baena-González et al. in 2007. Experiments with Arabidopsis protoplasts revealed an activation of SnRK1 catalytic subunits KIN10 and KIN11 under hypoxic conditions. Likewise, KIN10/KIN11 deficiency abrogates the switch in metabolic reprogramming under low-oxygen conditions (Baena-González et al. 2007). Inactivation of SnRK1 through mutation of the ATP binding site and catalytic site in Arabidopsis leads to decreased fitness under submergence conditions. More importantly, SnRK1 is able to regulate the expression of ethanol fermentation pathway enzymes PDC and ADH through direct association with target gene chromatins (Cho et al. 2012). Furthermore, SnRK1A as the rice homolog of Arabidopsis SnRK1 controls the breakdown of starch, thereby producing sugars which become available for fermentation (Lee et al. 2009; Lee et al. 2014). A similar function of SnRK1 in Arabidopsis

has been suggested by Baena-González et al. (2007) and Fragoso et al. (2009). In conclusion, the aforementioned results highlight the importance of SnRK1 for the adaptation of plants to low-oxygen.

1.5.2 Redox imbalances

When plants face low-oxygen conditions, not only is the energy generation affected, but also the redox state of the cell. The redox state is determined by the ratio of oxidant versus antioxidant pool sizes and is under tight control. It regulates gene expression and protein function, thereby controlling developmental and metabolic processes (Shigeoka & Maruta 2014; Mock & Dietz 2016). With the inhibition of respiration NADH cannot be oxidized and accumulates in the cytosol of the plant cell. High NADH/NAD ratios in the cytosol limit the activity of the glycolytic enzyme NAD-glyceraldehyde-3-phosphate dehydrogenase (GAPDH) leading to a restriction of the flux through glycolysis (Geigenberger & Fernie 2014). Therefore, plants activate fermentation pathways to reoxidize NADH to NAD to keep glycolysis running.

Another mechanism contributing to the decrease in the cytosolic NADH/NAD ratio under low oxygen is the hemoglobin/nitric oxide cycle. The oxidation of NADH to NAD is coupled to the oxidation of NO to NO_3^- under consumption of molecular oxygen and with the support of reduced non-symbiotic hemoglobin (Igamberdiev et al. 2005). Non-symbiotic hemoglobins are cytoplasmic oxygen binding proteins which are induced under low-oxygen conditions and can be found in numerous species. Their primary function is the scavenging of the signaling molecule NO (Dordas, Rivoal, et al. 2003; Hill 2012). NO belongs to the RNS and can influence the protein function through S-nitrosylation of protein thiols (Lindermayr et al. 2005). NO is produced from the reduction of nitrite occurring in the cytosol via nitrate reductase or in the mitochondria at complex III and IV (Yamasaki & Sakihama 2000; Gupta & Kaiser 2010; Igamberdiev et al. 2010; Gupta et al. 2011). Among others, NO is involved in the control of seed germination and stomatal closure as well as in the regulation of the oxygen sensor RAP2.12 (Beligni et al. 2002; Desikan et al. 2002; Siddiqui et al. 2011; Gibbs et al. 2014). Under hypoxia NO regulates plant respiration at complex IV and participates in the inhibition of the TCA cycle enzyme aconitase (Gupta et al. 2012).

In addition to RNS, ROS also play a major role in the acclimation of plants to low-oxygen. Though it is a paradox that a low-oxygen environment leads to an increase in ROS, ROS accumulation had been measured under hypoxia and even under anoxia in plants (Baxter-Burrell et al. 2002; Banti et al. 2010; Pucciariello et al. 2012; Gonzali et al. 2015). Most likely, NADPH oxidase is responsible for the accumulation of ROS under low-oxygen. This enzyme

1. Introduction

generates superoxide (O_2^-) and hydrogen peroxide (H_2O_2) by transferring electrons from NADPH to O_2 (Baxter-Burrell et al. 2002; Torres et al. 2002). Evidence for a potential crosstalk between low-oxygen and ROS signaling was recently found by Gonzali et al. (2015). They proved that HYPOXIA RESPONSIVE UNIVERSAL STRESS PROTEIN 1, whose expression is induced by the oxygen sensor RAP2.12, is able to interact with the NADPH OXIDASE RESPIRATORY BURST OXIDASE HOMOLOG D (RBOHD). The respiratory burst of ROS under low-oxygen helps the plant to acclimatize to the hypoxic stress (Pucciariello & Perata 2016). For instance, ROS together with the hormone ethylene induce the formation of aerenchyma to improve the transport of oxygen inside the plant under conditions of submergence or waterlogging (Steffens et al. 2011; Steffens et al. 2013).

The response of plants to a change in the cellular redox state is partly mediated by NTRs and thioredoxins (Trxs), also known as the NTR-Trx system. Trxs are small thiol-disulfide oxidoreductases which reduce disulfide bridges of their target proteins. There are more than 20 Arabidopsis isoforms of Trx located in all subcellular compartments including chloroplast, cytosol, mitochondria, nucleus, peroxisome membranes and, thus, having around 400 potential targets in plants (Montrichard et al. 2009; Belin et al. 2014; Du et al. 2015). Oxidized Trxs are reduced by NTRs and ferredoxin dependent thioredoxin reductases. NTRs occur in the cytosol, mitochondria and chloroplast (Reichheld et al. 2005; Serrato et al. 2004; Pérez-Ruiz et al. 2006). Cytosolic and mitochondrial targeted NTRs of Arabidopsis are encoded by two genes (*AtNTRA* and *AtNTRB*). Both NTRs are dually targeted to the cytosol and mitochondria (Reichheld et al. 2005). Reichheld et al. (2005) have shown that NTRA is the main cytosolic isoform and NTRB the main mitochondrial isoform. The chloroplast NTRC protein is an unusual NTR with a Trx domain as part of the functional enzyme (Serrato et al. 2004). Due to this specialty NTRC can directly reduce target proteins like ADP-glucose pyrophosphorylase, Mg-chelatase or 2-Cys Peroxiredoxin independently from the chloroplastic Trx system (Cejudo et al. 2012).

The knockout of NTRA or NTRB separately revealed no phenotype, though Arabidopsis mutants lacking both proteins showed wrinkled seeds, slower shoot and root growth as well as diminished pollen fitness (Reichheld et al. 2007; Cha et al. 2014). The loss of plastidial NTRC leads to a more severe phenotype than the knockout of NTRA and NTRB (Cejudo et al. 2012). NTRC knockout plants show inhibited growth, pale-green leaves, abnormal chloroplast structure and hypersensitivity to abiotic induced ROS stress (Serrato et al. 2004; Pérez-Ruiz et al. 2006). The hypersensitivity of the *ntrc* mutant towards ROS stress is attributed to the decreased reduction state of the chloroplastic antioxidant 2-Cys peroxiredoxin which is a direct target of NTRC (Cejudo et al. 2012). NTRA and NTRB appear to have a function in ROS scavenging, as they participate in the reduction of the cytosolic and mitochondrial peroxiredoxin system (Cha et al. 2014; Cha et al. 2015). Thus, it is

plausible to assume that the NTR system could even contribute to ROS homeostasis under low-oxygen conditions. The low-oxygen signaling molecule NO in conjunction with auxin is able to regulate the activity of the NTR system providing a rationale for a potential crosstalk between ROS, NO and hormone signaling through the NTR system (Correa-Aragunde et al. 2015).

Additionally, NTRs are supposed to be involved in the regulation of primary metabolism under low-oxygen with different functions. For instance, NTRC regulates starch and chlorophyll biosynthesis in the chloroplast (Michalska et al. 2009; Richter et al. 2013; Perez-Ruiz et al. 2014) and NTRA and NTRB regulate enzymes of the TCA cycle and the fatty acid biosynthesis (Daloso et al. 2015).

1.6 Aims and objectives of the thesis

The aim of this thesis was to investigate the adaptation of primary plant metabolism to low-oxygen concentrations.

1.) In order to better understand the mechanisms leading to low-oxygen adaptation, a simplified experimental system using potato tuber slices was developed which allowed the taking of biological samples within minutes after the stress application. With this system, the sequence of metabolic events occurring during the hypoxic acclimation phase could be determined.

2.) The experiments with potato tuber slices under hypoxia identified PKc as one of the possible regulatory sites. Therefore, transgenic potato tubers with decreased PKc activity generated by Oliver et al. (2008) were used to resolve the function of PKc in the adaptive response to low-oxygen.

3.) In addition to changes in glycolytic activity, hypoxia also leads to alterations in the TCA cycle. Studies with *Lotus japonicus* revealed a reorientation of the TCA cycle under hypoxia related to the production of 2-oxoglutarate which is crucial for plant survival (Rocha et al. 2010). In Arabidopsis 2-oxoglutarate is mainly produced by IDH in the mitochondria. To test the role of the mitochondrial IDH in the reorganization of the TCA cycle in Arabidopsis, the t-DNA insertion lines, which lack the major catalytic subunit of mitochondrial IDH, were treated with low-oxygen up to 24 h. Afterwards a comprehensive metabolite profile using GCMS and enzyme assays was performed.

4.) Changes in redox metabolism are commonly induced by low-oxygen, as the availability of oxygen as electron acceptor decreases with falling cellular oxygen levels. Plant NTRs are master regulators of redox metabolism in plants, but their function under low-oxygen is yet unknown. To compare the role of the different NTRs under low-oxygen, an *ntrantrb* double

mutant and an *ntrc* single mutant were treated with hypoxia. After the hypoxia treatment, the redox state of cellular redox marker like pyridine nucleotides as well as glutathione and ascorbate was measured.

5.) With the decline in oxygen availability respiration gets inhibited and the energy production slows down. To adapt to the changes in the cellular energy status plants must be able to actually sense the energy status. A putative energy sensor in plants is SNRK1. Transgenic Arabidopsis plants with a beta-estradiol inducible downregulation of the SnRK1 subunit SNF4 were used to identify the role of SnRK1 in the regulation of the energy metabolism under hypoxia.

2 Materials and methods

All chemicals and enzymes were obtained from Sigma Aldrich (St. Louis MO USA), unless stated otherwise. Enzymes were at least 95% pure.

2.1 Plant material and growth conditions

2.1.1 Solanum tuberosum

Potato tubers from *Solanum tuberosum cv* Desiree (Saatzucht Lange AG) were used as plant material. Oliver et al. (2009) generated 5 independent RNAi lines with decreased expression of the *PKCYT1* gene. Line 6 (PKC-6) and 15 (PKC-15) had only 2% and 1% of wild type transcript left, respectively. These lines were used for all experiments in this thesis. Wild type as well as transgenic plants were grown in tissue culture and then transferred to greenhouse conditions as described by Oliver et al. (2008).

2.1.2 Arabidopsis thaliana

Arabidopsis homozygous t-DNA insertion lines *idhv* (SAIL_806_A06) (Lemaitre et al. 2007), *ntrc* (SALK_012208) (Pérez-Ruiz et al. 2006), *ntrantrb* (Reichheld et al. 2007) and beta-estradiol inducible amiRSNF4 seeds (kindly provided by Csaba Koncz MPIZ Köln) and the respective Col-0 wild type were used for the experiments. For metabolite and qPCR measurements, plants were grown for 14 days on a vertical plate with 2% agar dissolved in half strength MS (Murashige and Skoog) medium supplemented with 1% sucrose, except for experiments with the *ntrantrb* mutant, the *ntrc* mutant and the respective Col-0 background, where no sucrose was put in the growth media. Plant growth conditions were as follows: 16 h light with 8 h darkness, 100 µmol s^{-1} m^{-2} light intensity and 22°C day, 18°C night temperature.

2.1.2.1 Seed sterilization

Arabidopsis thaliana seeds were surface sterilized with 1 ml of 0.5 % SDS in 70 % ethanol under shaking for 7 min. After short centrifugation, the supernatant was discarded and 1 ml

of 100 % ethanol was added. The seeds were shaken for another 10 min and subsequently washed several times with 1 ml of sterile water.

2.1.2.2 Beta-estradiol induction

For the anoxia survival and SNF4 expression analysis amiRSNF4 and Col-0 seeds were grown on 0.8% agar dissolved in half strength MS medium supplemented with 1% sucrose and 10 µM beta-estradiol. In all other experiments 9-day-old amiRSNF4 and Col-0 seedlings were transferred from vertical plates with 2% agar dissolved in half strength MS medium supplemented with 1% sucrose to vertical plates with 2% agar dissolved in half strength MS medium supplemented with 1% sucrose and 10 µM beta-estradiol.

2.2 Low-oxygen treatment and plant harvesting

2.2.1 Low-oxygen treatment and harvesting of potato tuber discs

Tubers from 12-week old transgenic (PKC-6, PKC-15) and wild type potato plants were harvested and cut into discs (see respiration measurement with Clark electrodes). Tuber discs were placed into a 2l beaker filled with 25 mM imidazole buffer pH 6.5 and gassed with normal air (21% oxygen) under continuous stirring. After 1 h half of the slices were transferred into a second beaker being equilibrated to 4% oxygen. Samples were collected at 21% oxygen 1 min before the transfer and 15, 30 and 60 min after the transfer to low-oxygen. At 4% oxygen tuber slices were harvested 1, 2, 3, 4, 5, 6, 7, 15, 30 and 60 min after the transfer. Samples were collected and flash frozen in liquid nitrogen within 10 sec. The oxygen concentration inside the beaker was regularly checked with the FIBOX 3 (Presens, Regensburg) oxygen sensor.

2.2.2 Low-oxygen treatment and harvesting of Arabidopsis seedlings

For metabolite and qPCR analysis 14-day-old Arabidopsis seedlings grown on vertical plates were treated for 16 h or 24 h with 21%, 1% and 0% oxygen in an acrylic glass box in the dark. Col-0 and *idhv* seedlings were either treated for 16 h (from 6 p.m. to 10 a.m.) or 24 h (at the end of the night; from 8 a.m. to 8 a.m.) with 21%, 1% and 0% oxygen. Col-0, the *ntrantrb* mutant and the *ntrc* mutant were treated for 16 h (from 6 p.m. to 10 a.m.) with 21%

and 1% oxygen. Col-0 and amiRSNF4 seedlings were treated for 24 h (at the end of the night; from 8 a.m. to 8 a.m.) with 21%, 1% and 0% oxygen. The oxygen concentration inside the acrylic glass box was regularly checked with a noninvasive oxygen sensor FIBOX 3 (Presens, Regensburg). After the low-oxygen treatment 10-14 vertical plates with 14-day-old Arabidopsis seedlings were taken out of the acrylic glass box and put upside down (the seedlings on the bottom) into a box filled with liquid nitrogen. The Arabidopsis shoot was then scratched with a spatula into a 15 ml falcon tube and stored at -80°C until further processing. This procedure allowed rapid harvesting (< 15 sec.) of several genotypes in parallel.

2.3 Respiration measurement with Clark electrodes

The Clark electrodes (Hansatech, Norfolk) were calibrated with a 2-point calibration method before the start of the measurements. At first, pure nitrogen was blown into the chamber filled with 25 mM imidazole buffer pH 6.5 for the calibration of 0% oxygen and then normal air was blown inside for the calibration of 21% oxygen. 11 to 12-week-old potato tubers (wild type and transgenic lines) were cut into slices (diameter 9 mm, height 1.5 - 2 mm) using a single tuber slice (50 - 70 mg) for the oxygen consumption measurement at 25°C.

2.4 Anoxia survival assay

Sterilized seeds were put on 0.8% agar dissolved in half strength MS medium supplemented with 1% sucrose and grown for 7 days in the sterile growth chamber. Then, 7-day-old seedlings were treated for 8 h (from to 10 a.m. to 6 p.m.) with 0% oxygen in the dark. Afterwards the seedlings were placed back in the sterile growth chamber for another 7 days, and the surviving seedlings were scored. For the induction of the SNF4 amiRNA construct, amiRSNF4 seeds were put on 0.8% agar dissolved in half strength MS medium with 10 µM beta-estradiol and supplemented with 1% sucrose.

2.5 Root growth assay

Sterilized seeds were put on vertical plates filled with 2% agar dissolved in half strength MS medium supplemented with 1% sucrose. The roots of the seedlings grew only on top of the agar, thereby allowing the free diffusion of oxygen into the roots. After 14 days, the vertical

plates were taken out of the growth chamber and the length of the root was marked at the bottom of the vertical plate. Subsequently, the seedlings were treated with 21%, 8%, 4%, 1% (v/v) oxygen in the dark for 48 h. Thereafter, the tip of the root was marked again and the root growth evaluated with the software program ImageJ (ImageJ 1.44n, National Institutes of Health, Bethesda).

2.6 RNA isolation and quantitative real-time PCR

Approximately 50 mg of plant material was weighted and the total RNA extracted with the RNeasy kit (Qiagen) according to the manufacturer's instructions. DNase treatment was done using RNasefree DNase I (New England Biolabs). The concentration of total RNA was measured with a Nanodrop ND-2000 (Peqlab) and 500 ng of extracted RNA was reverse transcribed using the iScript reverse transcriptase (Biorad). Then, the cDNA was diluted as in Kleine et al. (2007) and used for Real time PCR amplification with the iQ Sybr-green Supermix (Biorad) on a iQ5 multicolor real-time PCR detection system (Biorad). The following Primer were used in the analysis: *ADH1* (AT1G77120) forward primer 5'-TATTCGATGCAAAGCTGCTGTG-3', reverse primer 5'- CGAACTTCGTGTTTCTGCGGT-3'; *HB1* (AT2G16060) forward primer 5'-TTTGAGGTGGCCAAGTATGCA-3', reverse primer 5'-TGATCATAAGCCTGACCCCAA-3'; *SUS1* (AT5G20830) forward primer 5'-ACGCTGAACGTATGATAACGCG-3', reverse primer 5'-AACCCTGGAAAGCAAGGCAAG-3'; *SUS4* AT3G43190 forward primer 5'- CGCAGAACGTGTAATAACGCG-3', reverse primer 5'-CAACCCTTGAGAGCAAAGCAAA-3'; *SNF4* (AT1G09020) forward primer 5'-GCCACTTGTTCAGGTTGGAC-3', reverse primer 5'-CTGCGGATATGAACCATCCT-3'; *AOX1A* (At3g22370) forward primer 5'- GACGGTCCGTACGGTTTCG-3'; reverse primer 5'-CTTCTGATTCGCGTCCTCTC-3'; *RCE1* (AT4G36800) forward primer 5'-CTGTTCACGGAACCCAATTC-3', reverse primer 5'-GGAAAAAGGTCTGACCGACA-3'. As a housekeeping gene *RCE1* (AT4G36800) was used according to Kleine et al. (2007). Calculations were done as described in Kleine et al. (2007).

2.7 TCA extraction from potato tuber and Arabidopsis

The extraction was performed as described by Jelitto et al. (1992) with following modifications. 600 µl ice-cooled 16% (w/v) TCA (trichloroacetic acid) in water containing 5 mM EGTA (ethylene glycol tetraacetic acid) was added to 50 mg of frozen Arabidopsis powder. After vigorous mixing for 45 sec, the mixture was incubated under shaking at 4° C for 1 h. The homogenate was centrifuged for 10 min at 14000 rpm and the supernatant was washed with 5 ml water saturated diethylether and then with 3 ml water saturated diethylether. The pH of the sample was adjusted between 6 and 7 with 1-2 µl 5 M KOH, 1 M Triethanolamine. The remaining diethylether was led to evaporate under the fume hood for 1 h and the extract was subsequently used for metabolite analysis or stored at -80°C for further analysis. The pellet remaining after centrifugation was washed 3 times with 80% ethanol and dried in a SpeedVac (Eppendorf AG, Hamburg).

For the extraction of metabolites from potato tuber material, 1 ml 16% (w/v) TCA in diethylether (-20°C) was added to 200 mg of frozen potato tuber powder, vortexed for 1 min and then incubated at 4°C for 20 min. After the addition of 600 µl ice cooled 16% TCA (w/v) in water containing 5 mM EGTA, the suspension was incubated under shaking at 4°C for 2 h. For the separation of the different phases the suspension was centrifuged for 10 min at 14000 rpm at 4°C. The lower water phase (around 600 µl) was transferred into a 5 ml falcon and the subsequent steps were done as described above.

2.8 Determination of metabolites

2.8.1 Extraction and measurement of polar metabolites with GCMS

Metabolites for GC–TOF–MS were extracted and derivatized using a modified method described in Roessner et al. (2001), Lisec et al. (2006) and Erban et al. (2007). For the extraction 50 mg plant material (fresh weight) was grounded in 180 µl cold (-20°C) methanol containing 10 µl ribitol (0.2 mg ml-1 in water) and 10 µl 13C-sorbitol (0.2 mg ml-1 in water), which were added as internal standards for the quantification of metabolite abundances. After the incubation at 70°C for 15 min, the extract was carefully mixed with 100 µl of chloroform and 200 µl of water. To separate the polar and non-polar phase a 15 min centrifugation step of 25000 g was performed. For the further analysis, 50 µl of the upper (polar) phase was dried in vacuo. The pellet was resuspended in 10 µl of methoxyaminhydrochloride (20 mg ml-1 in pyridine) and derivatized for 90 min at 37°C. After

the addition of 20 µl of BSTFA (N,O-Bis[trimethylsilyl]trifluoroacetamide) containing 5 µl retention time standard mixture of linear alkanes (n-decane, n-dodecane, n-pentadecane, n-nonadecane, n-docosane, n-octacosane, n-dotriacontane), the mix was incubated at 37°C for further 45 min. A volume of 1 µl of each sample was injected into a GC–TOF–MS system (Pegasus HT, Leco, St Joseph, USA). Samples were derivatized and injected by an autosampler system (Combi PAL, CTC Analytics AG, Zwingen, Switzerland). Helium acted as carrier gas at a constant flow rate of 1 ml/min. Gas chromatography was performed on an Agilent GC (7890A, Agilent, Santa Clara, USA) using a 30 m VF-5ms column with 10 m EZ-Guard column. The injection temperature of the CIS injector (CIS4, Gerstel, Mühlheim, Germany) increased with a rate of 12°C s-1 from initially 70°C to finally 275°C. Transfer line and ion source were set to 250°C. The initial oven temperature (70°C) was permanently increased to a final temperature of 320°C by 9°C per minute. To avoid solvent contaminations the solvent delay was set to 340 sec. Because of the chemical and physical properties of the different metabolites the mixture was separated on the column over time. Metabolites that passed the column were released into the TOF-MS. The transferline connecting the GC and the TOF-MS was set to 250°C as well as the ion source where the in streaming metabolites got ionized and fractionated by an ion pulse of 70 eV. Charged mass fragments flew through the vacuum flight tube until they reached the mass detector. Each fragment had a specific time of flight, depending of its mass charge ratio (m/z) until its impact with the detector. Mass spectra were recorded at 20 scans per sec with an m/z 35 – 800 scanning range. Chromatograms and mass spectra were evaluated using ChromaTOF 4.5 and TagFinder 4.1 software (Luedemann et al. 2008).

2.8.2 Determination of sugars (glucose, fructose and sucrose) and starch

20-40 µl of TCA extract was used for the measurement of glucose, fructose and glucose, being carried out in accordance with Thormählen et al. (2013). For the determination of starch, the pellet remaining after TCA extraction was washed three times with 80% ethanol and dried in a SpeedVac (Eppendorf AG, Hamburg). Starch extraction and measurement was done as described by Thormählen et al. (2013).

2.8.3 Determination of phosphoenolpyruvate and pyruvate

The measurement of phosphoenolpyruvate and pyruvate was performed according to Geigenberger et al. (1998). 50 - 100 µl of TCA extract was mixed with a master mix containing 50 mM HEPES (4-(2-hydroxyethyl)-1-piperazineethanesulfonic acid)/KOH pH 7.5, 10 µM NADH, 1 mM ADP and 1 mM $MgCl_2$ in a 200 µl volume in a well of a 96-well microplate. For the determination of pyruvate 2 µl of lactate dehydrogenase (2U µl^{-1}) (Roche) and for the determination of phosphoenolpyruvate 2 µl of pyruvate kinase (5,5U µl^{-1}) (Roche) was added and the fluorescence intensity of NADH was measured at 360 nm with a FilterMax F5 Multi-Mode Microplate reader (Molecular Devices, Sunnyvale, USA). Metabolites were quantified by measuring the fluorescence intensity of known amounts of NADH at the same wavelength.

2.8.4 Determination of isocitrate

50 - 100 µl of TCA extract was mixed with a master mix containing 50 mM HEPES/KOH pH 7.8, 187.5 µM NADP, 50 µM EDTA (Ethylenediaminetetraacetic acid) and 2.5 mM $MnSO_4$ in a 200 µl volume in a well of a 96-well plate. The reaction was started with 2 µl isocitrate dehydrogenase (0.5 mU µl-$^{1)}$ (Fluka), and the fluorescence intensity of NADPH was measured at 360 nm with a FilterMax F5 Multi-Mode Microplate reader (Molecular Devices, Sunnyvale, USA). Isocitrate was quantified by measuring the fluorescence intensity of known amounts of NADPH at the same wavelength.

2.8.5 Determination of ATP and ADP

The determination of ATP and ADP was based on Stitt et al. (1989) with some modifications. For the determination of ADP, 50 - 100 µl of TCA extract was mixed with a master mix containing 50 mM HEPES/KOH pH 7, 20 µM NADH, 0.86 mM PEP, 15.4 mM $MgCl_2$ and 2,75 U lactate dehydrogenase (Roche) in a 200 µl volume in a well of a 96-well microplate. The reaction was started with 2 µl pyruvate kinase (1U µl-^{1}) (Roche), and fluorescence intensity of NADH was measured at 360 nm with a FilterMax F5 Multi-Mode Microplate reader (Molecular Devices, Sunnyvale, USA). ADP was quantified by measuring the fluorescence intensity of known amounts of NADH at the same wavelength.

For the determination of ATP, 50 - 100 µl of TCA extract was mixed with a master mix containing 50 mM HEPES/KOH pH 7, 0.38 mM NADP, 12.62 mM glucose, 5 mM $MgCl_2$, 1.4

U phosphoglucoisomerase (Roche) and 0.14 U glucose-6-phosphate dehydrogenase (Roche) in a 200 µl volume in a well of a 96-well microplate. The reaction was started with 2 µl hexokinase (0.15 U µl^{-1}) (Roche), and fluorescence intensity of NADPH was measured at 360 nm with a FilterMax F5 Multi-Mode Microplate reader (Molecular Devices, Sunnyvale, USA). ATP was quantified by measuring the fluorescence intensity of known amounts of NADPH at the same wavelength.

2.8.6 Determination of nucleotides and nucleotide sugars in potato tubers with HPLC

Nucleotides and nucleotide sugars were analyzed as described by Geigenberger et al. (1996). A DEAE (diethyl-aminoethyl)-Anion exchange column with a phosphate gradient was used to separate nucleotides and nucleotide sugars in 20 µl of TCA extract. Nucleotides and nucleotide sugars absorb UV-light and can, therefore, be detected with a UV-photometer at 254 nm. Identification and quantification of metabolite amounts were achieved by comparing the retention time of sample peaks with an authentic standard containing 20 µM AMP, GMP, UMP, 50 µM ADPG, UDPG, ADP, UDP, GDP and 100 µM ATP, UTP, GTP using Chromeleon 6.6 software from Dionex.

Column:	Partisil 10 SAX (Knauer)
Precolumn:	Partisil 10 SAX self filled
Flow rate:	1ml/ min
Pressure:	250 bar
Injection volume:	20 µl (Autosampler)
Buffer A:	40 mM NH$_4$PO$_4$ pH 2.8 adjust with H$_3$PO$_4$
Buffer B:	750 mM NH$_4$PO$_4$ pH 3.7 adjust with H$_3$PO$_4$
Gradient program:	

Time in min	0	3	12	20	25	32	37	38	44
% buffer A	100	100	85	50	14	0	0	100	100

2.8.7 Extraction and determination of pyridine nucleotides

The extraction and analysis of pyridine nucleotides were performed as described by Lintala et al. (2014) with the following modifications for the analysis of potato tuber material. Pyridine nucleotides were extracted from 40 mg of frozen potato tuber powder and the pH was adjusted to 8.0 - 8.5 with 400 µl of 0.2 M Tris (2-Amino-2-hydroxymethyl-propane-1,3-diol) (pH 8.4), 0.1 M KOH or with 400µl 0.2 M Tris (pH 8.4), 0.1 M HClO4.

For the quantification of NAD(H), 20 - 40 µl of a sample was mixed with a detection mix containing 100 mM Tricine/KOH (pH 9), 4 mM EDTA, 500 mM EtOH, 0.1mM phenazine ethosulfate (PES), 0.6 mM methylthiazolyldiphenyl-tetrazoliumbromide (MTT) and 6 U ml-1 alcohol dehydrogenase in a 150 µl volume in a 96-well microplate. Afterwards the change in absorbance at 570 nm was recorded.

For the quantification of NADP(H), 20 - 40 µl of a sample was mixed with a detection mix containing 100 mM Tricine/KOH (pH 9), 4 mM EDTA, 3 mM glucose 6-phosphate, 0.1 mM PES, 0.6 mM MTT and 6 U ml-1 G6PDH in a 150 µl volume in a 96-well microplate, and the change in absorbance at 570 nm was recorded.

2.8.8 Extraction of glutathione and ascorbate

The Extraction of glutathione and ascorbate was done according to Queval & Noctor (2007). 250 µl 0.2 M HCl was added to 25 mg of frozen Arabidopsis powder and the solution was vortexed for 2 min. After centrifugation with 16000g for 10 min at 4°C, 200 µl of the supernatant was transferred into a new Eppendorf tube and 20 µl 0.2 M NaH_2PO_4 (pH 5.6) was added. The extract was neutralized with 170 µl 0.2 M NaOH to adjust the pH between 5 and 6.

2.8.8.1 Determination of glutathione

The method for the quantification of glutathione was based on Griffith (1980) and Queval & Noctor (2007). For the measurement of GSH (reduced glutathione) 20 µl of extract was mixed with a reaction mix containing 0.1 M NaH_2PO_4 (pH 7.5), 10 mM ETDA, 0.5 mM NADP and 0.5 mM DTNB (5,5'-dithiobis-(2-nitrobenzoic acid)) in a 200 µl volume in a well of a 96-well microplate. The reaction was started by adding 10 µl glutathione reductase (GR) (0.02 U µl-[1]) (Sigma Aldrich) and the reaction slope was measured at 412 nm for 5 min with a FilterMax F5 Multi-Mode Microplate reader (Molecular Devices, Sunnyvale, USA).

For the measurement of GSSG (oxidized glutathione) one drop of 2-vinylpyridin (VPD) was added to 100 µl extract and the extract was incubated for 30 min at room temperature. After the extract was centrifuged twice for 1 min at 14000 rpm, 20 µl of supernatant was used for the measurement as described above.

GSH was quantified by measuring the slope at 412 nm of an authentic GSH standard with the following concentrations 0, 0.125, 0.25, 0.5, 1, 2.5, 5 µM. GSSG was quantified using 1 ml of 10 mM GSSG standard, which was treated with one drop of 2-vinylpyridin (VPD) and incubated for 30 min at room temperature. The suspension was centrifuged twice for 1 min at 14000 rpm and the supernatant was used for the measurement as described above.

The following concentrations of GSSG were used for the calibration curve: 0, 0.125, 0.25, 0.5, 1, 2.5, 5 µM GSSG.

2.8.8.2 Determination of ascorbate

The amount of ascorbate in the sample was determined as described by Griffith (1980) and Queval & Noctor (2007). For the measurement of reduced ascorbate, 20 µl extract was mixed with a master mix containing 0.1 M NaH_2PO_4 (pH 5.6) in a 200 µl volume in a well of a 96-well UV-microplate. The reaction was started with 5 µl ascorbate oxidase (0.04 U µl^{-1}) (Sigma Aldrich) and the difference in absorbance at 265 nm before and after the addition of the enzyme was measured. For the determination of the total ascorbate pool 100 µl of extract was incubated with 140 µl 0.12 M NaH_2PO_4 pH (7.5) and 10 µl 25 mM DTT (Dithiothreitol) for 30 min at room temperature. 20 µl of this solution was used for the measurement as described above. The following concentrations of reduced ascorbate were used for the calibration curve: 0, 0.125, 0.25, 0.5, 1, 2.5, 5 µM.

2.9 Determination of total amino acids

5 - 10 µl of TCA extract was mixed with 200 µl of reaction mix containing 50 µl 50% EtOH, 50 µl citric acid ph 5.2 in 0.2% (w/v) ascorbic acid and 100 µl 1% (w/v) ninhydrin in 70% EtOH in a well of a 96-well plate. After 15 min incubation at 95° C, the absorbance was measured at 570 nm with a FilterMax F5 Multi-Mode Microplate reader (Molecular Devices, Sunnyvale, USA). The total amount of amino acids in the sample was quantified using a standard curve with 5 and 10 µl of 0, 0.1, 0.2, 0.5, 1, 2, 4, 6 mM leucine in Aqua bidest mixed with 200 µl reaction mix.

2.10 Determination of protein content

The dried pellet of the TCA extraction was dissolved in 400 µl water with addition of 600 µl of 0.1 M NaOH. After incubation at 95°C for 30 min the solution was centrifuged for 10 min at 14000 rpm. 5 µl of supernatant was mixed with 225 µl of Bio-Rad Bradford mix (DC Protein Assay, Bio-Rad, Hercules, California) according to manufacturer's instructions in a well of a 96-well microplate and the absorbance was measured at 750 nm. The sample protein amount was quantified with a standard curve containing 0.0, 0.2, 0.4, 0.8, 1.6, 2 mg/ml BSA (bovine serum albumin) in NaOH.

2.11 Extraction and measurement of pyruvate kinase activity

100 mg frozen potato tuber powder was mixed with 500 µl of extraction buffer containing 50 mM HEPES, 5 mM $MgCl_2$, 1 mM EDTA pH 8, 5 mM DTT, 2 mM benzamidine, 2 mM ε-aminocaproic acid, 0.5 mM PMSF (phenylmethylsulfonyl fluoride), 0.1% TritonX-100 and 10% glycerol. The vortexed solution was centrifuged at 4°C for 10 min at 14000 rpm. In order to remove the salts in the protein extracts, the supernatant was pipetted on a preequilibrated NAP5 column (GE Healthcare, England). In the next step, the bound proteins were eluted with 1 ml of extraction buffer. The eluate was captured in Eppendorf tubes, divided into 100 µl aliquots and stored at -80°C for further analysis.

10 µl of the protein extract was mixed with 285 µl master mix containing 50 mM MOPS (3-(N-morpholino)propanesulfonic acid) buffer, 100 mM KCl, 15 mM $MgCl_2$, 0,2 mM NADH, 1 mM ADP and 1.5 U lactate dehydrogenase (Roche) in a well of a 96-well microplate. The reaction was started by adding 4 µl of 4 mM phosphoenolpyruvate. The decrease in absorption at 340 nm was measured for 10 min with the Anthos reader HT-3 (Anthos Mikrosysteme GmbH, Krefeld, Germany) and the slope determined.

2.12 Extraction and measurement of NAD and NADP dependent isocitrate dehydrogenase activity

Approximately 100 mg of fresh Arabidopsis seedlings was extracted with 1 ml extraction buffer containing 50 mM TRIS-Acetate pH 7.2 and 10 mM DTT in a precooled (-20°C) mortar with a pestle at 4°C. After 1 min of grinding time, the solution was transferred into an Eppendorf tube and centrifuged for 5 min at 1400 g, 12 min at 8000 g and 5 min at 1400 g. After each centrifugation step, the supernatant was transferred into a new Eppendorf tube.

For the measurement of the NAD dependent isocitrate dehydrogenase a master mix containing 50 mM TRIS-Acetate pH 7.2, 20 mM isocitrate, 2 mM NAD and 20 mM $MnCl_2$ was pipetted in a 200 µl volume in a well of a 96-well microplate, and the reaction was started by adding 100 µl of enzyme extract to a final volume of 200 µl. The increase in absorption was measured at 340 nm for 20 min with the Anthos reader HT-3 (Anthos Mikrosysteme GmbH, Krefeld, Germany) and the slope was calculated.

For the measurement of the NADP dependent isocitrate dehydrogenase a master mix containing 50 mM TRIS-Acetate pH 7.2, 20 mM isocitrate, 2 mM NADP and 20 mM $MnCl_2$ was pipetted in a 200 µl volume in a well of a 96-well microplate and the reaction was started by adding 20 µl of enzyme extract to a final volume of 200 µl. The increase in absorption was measured at 340 nm for 20 min with the Anthos reader HT-3 (Anthos Mikrosysteme GmbH, Krefeld, Germany) and the slope calculated.

3 Results

3.1 Time-resolved analysis of the metabolic response of potato tuber tissue to a sudden transfer from 21% to 4% oxygen

In previous studies, potato tubers were used as a model system to investigate low-oxygen responses at the metabolic level (Geigenberger et al. 2000; Bologa et al. 2003). The use of tuber slices allowed oxygen concentrations to be manipulated in a simple manner. By using this simplified model system Geigenberger et al. (2000) provided evidence that hypoxia results in a partial inhibition of respiration, which in turn leads to a decrease in the cellular energy status accompanied by a decrease in biosynthetic activity. By analyzing the levels of selected metabolites the authors could identify several potential control sites in primary metabolism, but were not able to resolve the metabolic changes on a shorter time scale.

To determine which metabolic site responds first to the decrease in oxygen, a detailed time course of the changes in metabolite levels was recorded. Potato tuber discs were sampled in the time range between 1 and 60 min after the low-oxygen treatment, due to the fact that changes in metabolism upon environmental perturbations can occur within minutes (Hatzfeld & Stitt 1991; Arrivault et al. 2009; Szecowka et al. 2013).

3.1.1 Time-resolved effect of low-oxygen on the respiration rate of potato tuber tissue

To investigate how fast respiration is inhibited under hypoxic conditions, oxygen consumption rates were measured in a detailed time course.
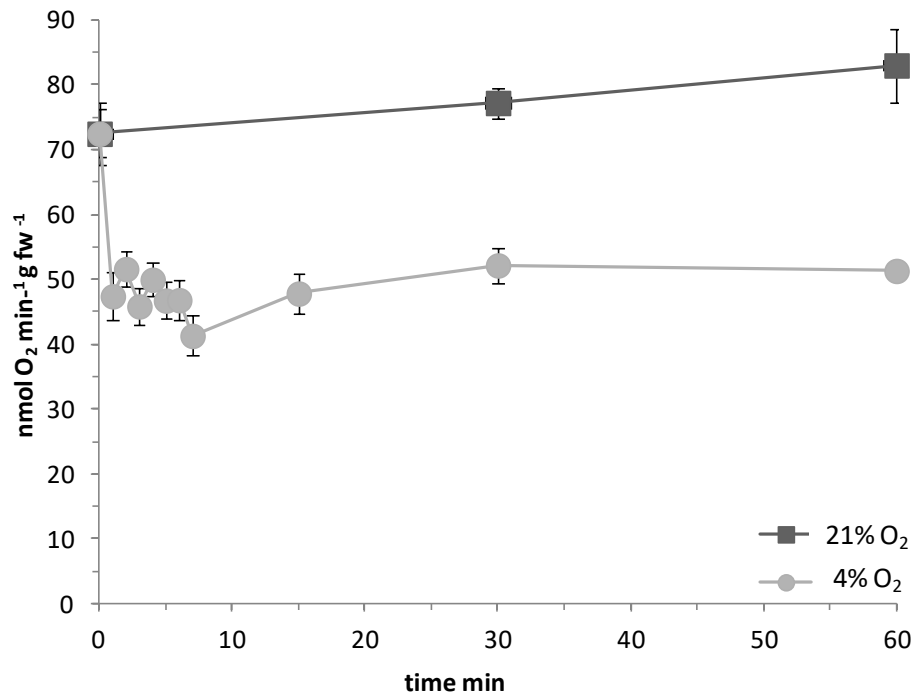
Fig. 3.1: Time-resolved oxygen consumption rate of potato tuber discs incubated with 21% and 4% oxygen in the measuring chamber of an oxygen electrode. Potato plants were grown in the greenhouse under long day conditions (16 h light/8 h dark). Tubers were harvested from 12-week-old plants. Potato tuber discs were incubated in 25 mM imidazole buffer pH 6.5 for 1 h with 21% oxygen (not shown in the graph). Then half of the discs were transferred into 25 mM imidazole buffer pH 6.5 solution equilibrated with 4% oxygen. The time of the transfer is indicated as min 0. In the case of the 21% O_2 control, respiration was measured 30 and 60 min after transfer. Tuber discs transferred to 4% O_2 were sampled 1, 2, 3, 4, 5, 6, 7, 15, 30 and 60 min after transfer. Results are the mean ± SE of 6 biological replicates.

Oxygen consumption rates of tuber discs incubated with 21% oxygen increased slightly within the 60 minutes time interval, while the respiration rate of tuber slices transferred to 4% oxygen decreased by 35% already within the first minute compared to 21% oxygen and remained at this level for the next 59 minutes (Fig. 3.1).

3.1.2 Time-resolved effect of low-oxygen on metabolite levels of potato tuber tissue

The results from the oxygen consumption measurements (3.1.1) indicated an immediate response of mitochondrial respiration to decreased oxygen availability. To investigate possible regulatory sites in respiratory metabolism, metabolite levels were analyzed in a parallel set of potato tuber discs using the same experimental setup (Fig. 3.1).
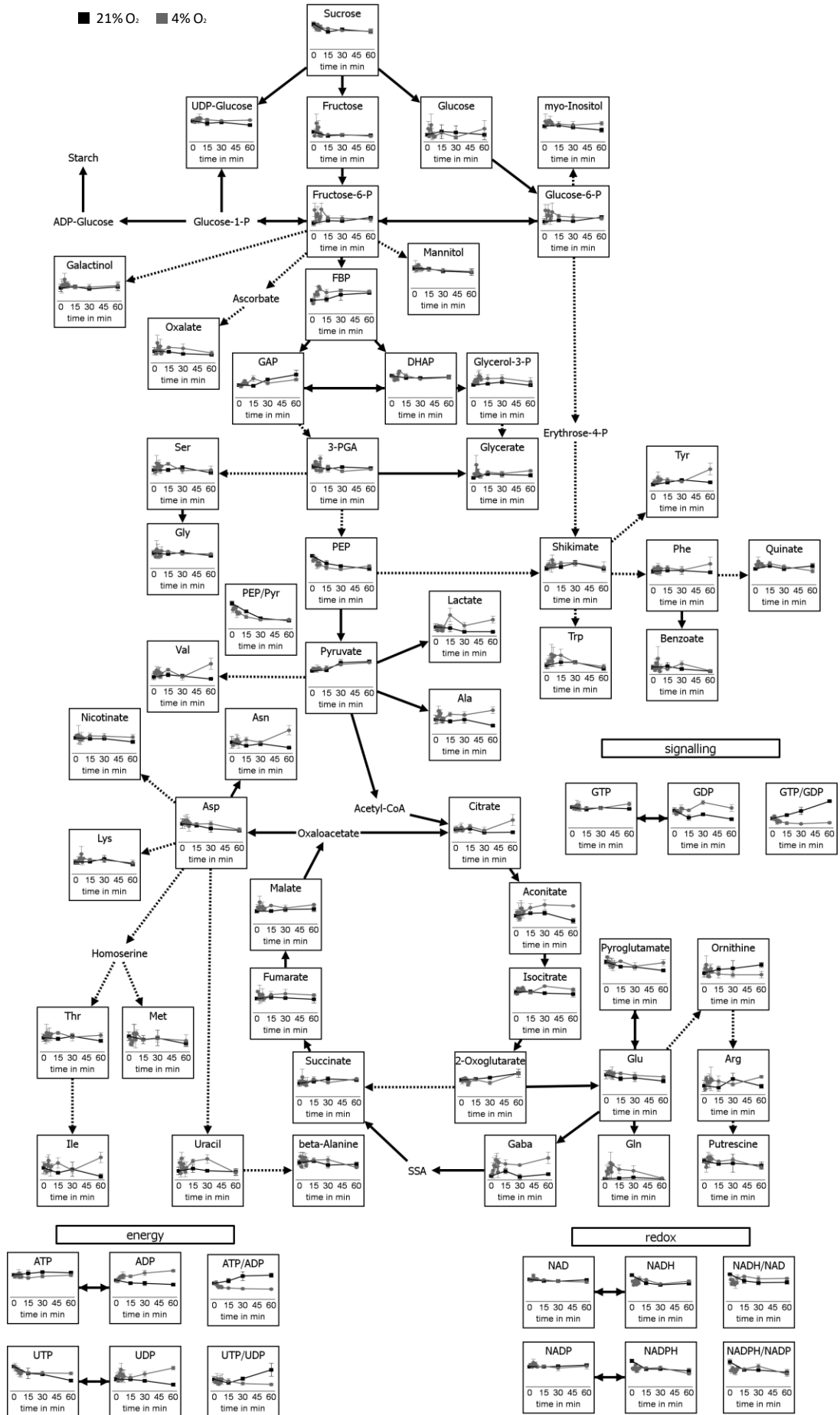
Fig. 3.2: Time-resolved changes in the levels of metabolites in wild type potato tubers incubated with 21% and 4% oxygen. Potato plants were grown in the greenhouse under long day conditions (16 h light/8 h dark). Tubers were harvested from 12-week-old plants. After 60 min of pre-incubation in buffer equilibrated with 21% oxygen, potato tuber slices were transferred to 4% oxygen and sampled at different time points as indicated in Fig. 3.1. After 0, 15, 30, 60 min (21% oxygen) and 1, 2, 3, 4, 5, 6, 7, 15, 30, 60 min (4% oxygen) tuber discs were sampled by direct shock-freezing in liquid nitrogen to immediately quench the metabolism in the tissue. The y-axis displays metabolite abundance, which was measured by profiling via GC-MS or by enzymatic assays. For details, see supplemental table 1 and 2. Results are the mean ± SE, *n* = 3 biological replicates.

The potato tuber discs incubated at 4% oxygen showed a different response in the metabolite levels compared to the 21% oxygen control. The fastest change was visible in the adenylate pool. ADP rose after 2 minutes of the 4% treatment and increased up to 2-fold until 60 minutes, while ATP decreased slightly by 10% at this time point. The ratio of ATP to ADP at 4% oxygen decreased in parallel with the increase of ADP being obviously a direct consequence of the inhibition in respiration (Fig. 3.1). Other important nucleotides like the guanylates and uridinylates displayed a similar pattern like ATP and ADP in potato tubers treated with 4% oxygen, but the respective changes occurred at later time points.

To investigate whether the inhibition of respiration under hypoxia is influencing the redox state of the tissue, the NADH/NAD ratio was measured. It is an indicator for the redox state and is controlled through the activity of glycolysis, the TCA cycle and the respiratory electron transport. When oxygen was decreased to 4% the NADH/NAD ratio decreased transiently by 30% in the first 5 minutes and increased later to values 20% higher than the 21% oxygen control. The phosphorylated pyridine nucleotide NADPH and the ratio of NADPH/NADP showed a decrease at 4% oxygen in the first 10 minutes, followed by an increase to levels similar to the normoxic control. Other metabolites showing a fast response to the decrease in oxygen from 21% to 4% are involved in glycolysis and in the amino acid metabolism. The hexose phosphates and fructose-1,6-bisphosphate (FBP) increased at 4% oxygen in the first 10 minutes, followed by a decrease back to 21% oxygen control levels after 60 minutes of treatment. In contrast, PEP displayed the opposite response. The amino acids glutamine and glutamate both being part of the GS-GOGAT ammonium assimilation pathway responded differently. While glutamine increased 12-fold in the first 10 minutes under low-oxygen and later decreased back to the level at 21% oxygen, glutamate increased by 30% at 4% oxygen within the first 15 minutes and remained at this level compared to the normoxic control. Gamma-aminobutyric acid (GABA) typically increasing under abiotic stress (Allan et al. 2008; Fait et al. 2008) showed similar kinetics to glutamine at 4% oxygen in the first 10 minutes. At later time points, GABA remained increased at 4-fold level in comparison to the 21% oxygen control. Alanine and lactate which are known low-oxygen fermentation products increased 15 minutes after the transfer to 4% oxygen and accumulated up to 3-fold and 4-fold after 1 h of low-oxygen treatment. The branched-chain amino acids valine and isoleucine being both

derived from pyruvate accumulated 3-fold and 6-fold, respectively after 60 minutes of hypoxia treatment. Also asparagine, arginine, tyrosine, phenylalanine, threonine, pyroglutamate, glycerate and myo-inositol were clearly increased after 1 h of low-oxygen treatment compared to the normoxic control. Moreover, the levels of organic acids involved in the TCA cycle showed changes in response to low-oxygen. The TCA cycle enzyme aconitase catalyses the conversion of citrate into isocitrate via the intermediate product aconitate. This enzyme appears to be blocked under low-oxygen, as citrate and aconitate increased 2.5-fold and 3-fold after 60 minutes of low-oxygen treatment. Furthermore, the nonproteinogenic amino acid ornithine was one of the few measured metabolites that decreased under hypoxic conditions in potato tuber slices. This could reflect possible alterations in polyamine and alkaloid synthesis (Kalamaki et al. 2009) (Fig. 3.2).

3.2 Investigation of the low-oxygen response of transgenic potato tubers with decreased expression of cytosolic pyruvate kinase compared to wild type

One aspect of the adaptation of plants to low-oxygen is the induction of fermentation. Pyruvate being the end product of glycolysis is the substrate for various fermentative pathways. Under aerobic conditions, pyruvate is imported into the mitochondria and fed into the TCA cycle, thereby linking cytosolic glycolysis and mitochondrial respiration. Thus, the distribution of pyruvate between the different pathways has to be under tight control. The activity of glycolysis and respiration declines with decreasing oxygen concentrations, while fermentation is induced. Therefore, it is even more important for the plant to regulate the cellular levels of pyruvate (Gupta et al. 2009; Zabalza et al. 2008). It is produced in plants by pyruvate kinase existing as both, plastidial and cytosolic, isoforms denoted PKp and PKc, respectively (Plaxton 1996; Givan 1999). While PKp was shown to be responsible for fatty acid biosynthesis in Arabidopsis seeds (Andre et al. 2007; Andre & Benning 2007), the role of PKc is more related to sink-source metabolism (Gottlob-McHugh et al. 1992; Knowles et al. 1998; Oliver et al. 2008; Zhang et al. 2012). In order to understand the impact of altered pyruvate provision on respiratory metabolism under oxygen limiting conditions, potato tuber with decreased expression of PKc (Oliver et al. 2008) were treated for 1 h with 4% oxygen.

3.2.1 Enzyme activity measurement of transgenic tubers with decreased PKc activity and wild type

Oliver et al. (2008) generated transgenic potato tubers by RNA interference induced gene silencing showing a substantial decrease in PKc levels. The two independent lines (PKC-6 and PKC-15) with the lowest PKc expression were chosen for all subsequent experiments. To confirm the decreased expression of pyruvate kinase in the transgenic lines, the pyruvate kinase activity in potato-tuber extracts was determined.
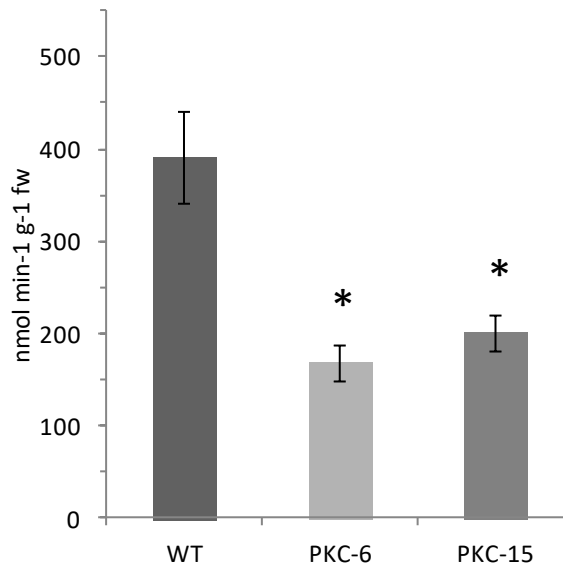
Fig. 3.3: Pyruvate kinase activity measurements of transgenic tubers with decreased PKc activity (PKC-6, PKC-15) relative to wild type potato tubers (WT). Potato plants were grown in the greenhouse under long day conditions (16 h light/8 h dark). Tubers were harvested from 12-week-old plants to analyze enzyme activity using an assay that does not distinguish between cytosolic and plastidial PK isoforms. Results are the mean ± SE, n = 3 biological replicates. Significant changes between the transgenic lines PKC-6, PKC-15 and wild type were evaluated by using Student's t-test (p < 0.05) and are shown by asterisk.

The transgenic lines PKC-6 and PKC-15 showed a significant decrease in pyruvate kinase enzyme activity compared to wild type. The pyruvate kinase activity in line 6 was decreased by 60%, while it was decreased by 50% in line 15. These results are in compliance with Oliver et al. (2008) (Fig. 3.3).

3.2.2 Changes in respiration rates in transgenic tubers with decreased PKc activity and wild type across different oxygen concentrations

The decrease in PKc activity might affect plant respiration, as pyruvate is an important substrate for the TCA cycle. Therefore, it is interesting to investigate the effect of decreased pyruvate supply on respiration under low-oxygen.
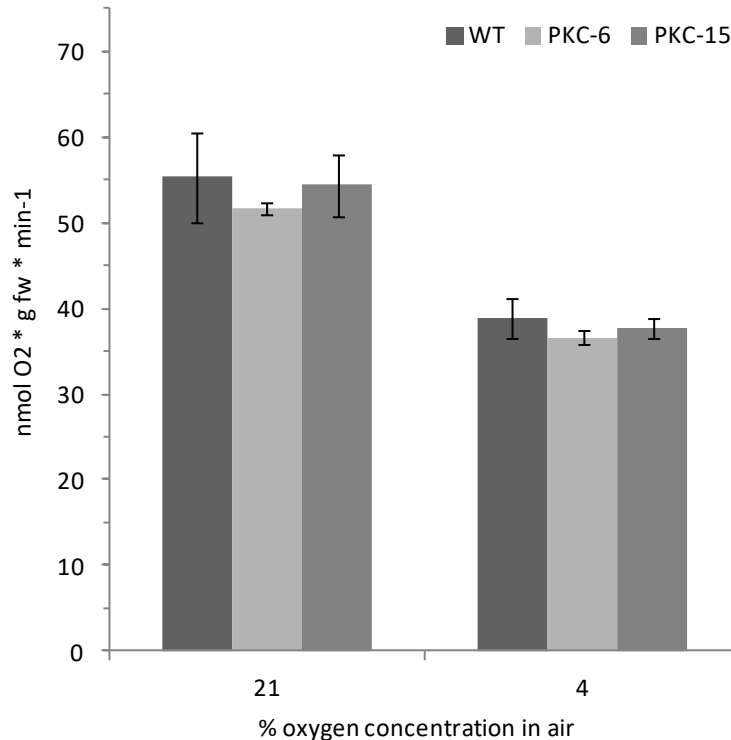
Fig. 3.4: Oxygen consumption rate of transgenic tubers with decreased PKc activity (PKC-6, PKC-15) relative to wild type at 21% and 4% oxygen. Potato plants were grown in the greenhouse under long day conditions (16 h light/8 h dark). Tubers were harvested from 12-week-old plants. Potato tuber slices were incubated for 5 min in the chamber of Clark electrodes equilibrated with 21% oxygen, and oxygen consumption was measured. Afterwards the oxygen concentration was changed to 4%, and oxygen consumption was measured for another 5 min. Results are the mean ± SE, n = 3-4 biological replicates. Significant changes between the transgenic lines PKC-6, PKC-15 and wild type were evaluated by using Student's t-test ($p < 0.05$) and are shown by asterisk.

Under normal oxygen conditions, the respiration rate in the transgenic lines was similar to the wild type. Likewise, Oliver et al. (2008) could not find significant differences in the oxygen consumption rate between the transgenic lines and the wild type. At 4% oxygen the respiration was clearly decreased by 30% in all genotypes compared to 21% oxygen. However, there was no difference between the wild type and the transgenic lines (Fig. 3.4).

3.2.3 Changes in metabolite levels in transgenic tubers with decreased PKc activity and wild type across different oxygen concentrations

To investigate the influence of decreased pyruvate availability on primary metabolism in potato tubers under low-oxygen, wild type and transgenic potato tubers with decreased cytosolic pyruvate kinase activity were treated for 1 h with 4% oxygen. Subsequently, a comprehensive metabolic profile of primary metabolism including energy and redox parameters was carried out in all genotypes.
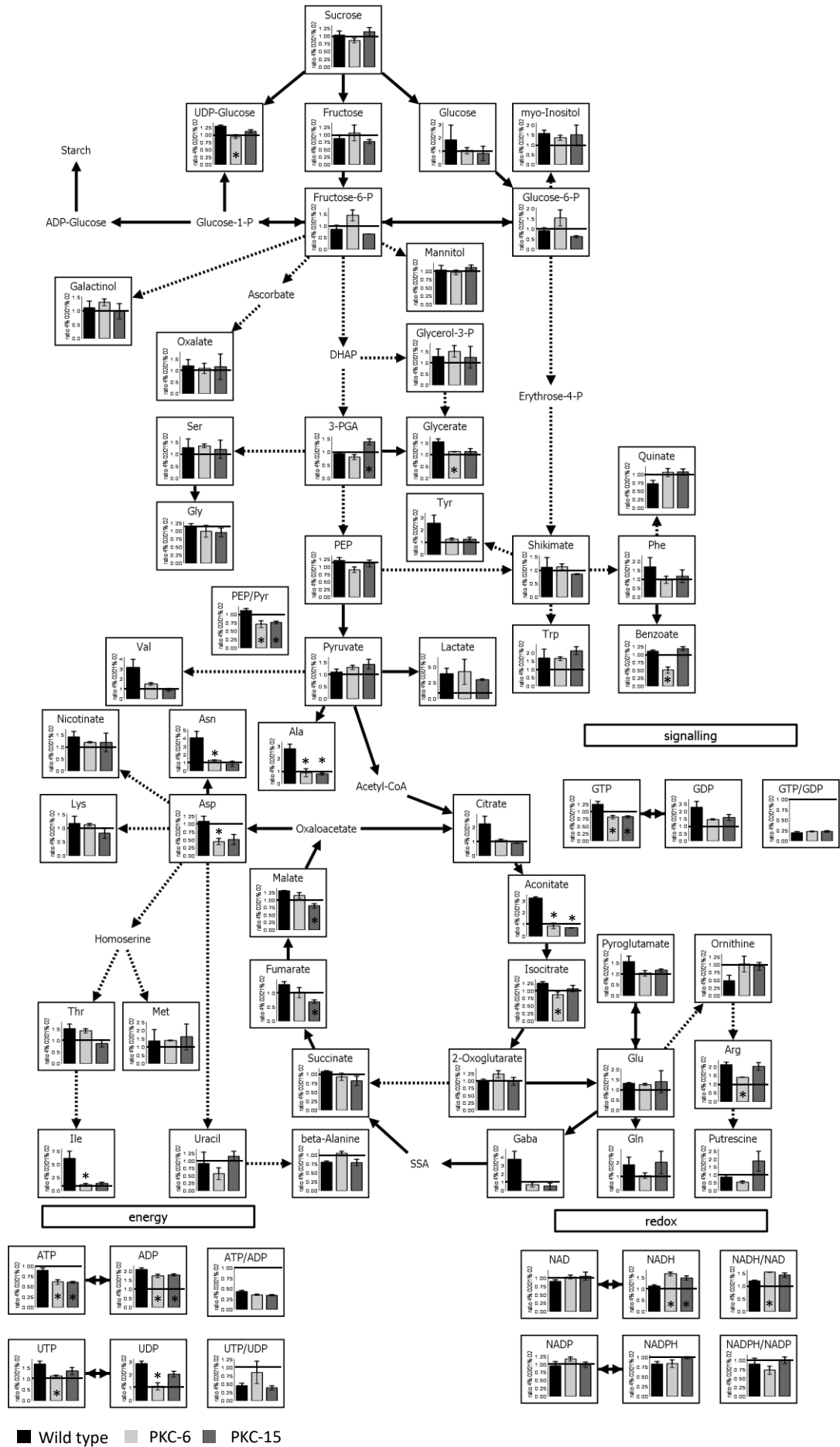
Wild type   PKC-6   PKC-15

Fig. 3.5: Low-oxygen induced changes in the levels of metabolites in transgenic tubers with decreased PKc activity (PKC-6, PKC-15) relative to wild type. Potato plants were grown in the greenhouse under long day conditions (16 h light/8 h dark). Tubers were harvested from 12-week-old plants. After 60 min of pre-incubation in buffer equilibrated with 21% oxygen potato tuber slices were transferred into 4% oxygen and harvested after another hour. Sampling of the discs was performed in order to immediately quench the metabolism of the discs by direct shock-freezing directly in liquid nitrogen. Metabolite levels were measured by GC-MS profiling or enzymatic assays. For details, see supplemental table 3. Results are expressed as fold change of metabolite level in 4% oxygen relative to 21% oxygen in all genotypes. A horizontal black line marks the point, where the 4% oxygen value equals the 21% oxygen value. Results are the mean ± SE, n = 3 biological replicates. Significant changes between the transgenic lines PKC-6, PKC-15 and wild type were evaluated by using Student's t-test ($p < 0.05$) and are shown by asterisk.

Figure 3.5 shows the fold change of the relative metabolite abundance in 4% oxygen relative to 21% oxygen for the wild type and the transgenic lines PKC-6 and PKC-15 after 1 h of low-oxygen treatment.

When oxygen was decreased to 4%, the wild type responded with a strong increase in metabolites derived from pyruvate. Alanine, valine and lactate rose 3-fold to 4-fold compared to the 21% oxygen control. The amino acid metabolism in the wild type was also affected by the low-oxygen treatment, as asparagine, isoleucine, tyrosine, GABA and arginine were at least 2-fold increased at 4% oxygen compared to 21% oxygen. Moreover, the TCA cycle intermediates citrate and aconitate increased 2-fold to 3-fold compared to the normoxic control. The nucleoside diphosphates ADP, UDP and GDP were at least 2-fold higher at low-oxygen compared to normoxia, leading to the decrease in the ATP/ADP, UTP/UDP and GTP/GDP ratio under hypoxia by 55%, 60% and 80%, respectively.

The decreased activity of PKc in the transgenic potato tubers affected the response of the metabolite levels to low-oxygen compared to wild type. First of all, PEP and pyruvate being substrate and product of PKc, respectively, showed only slight changes in the transgenic lines compared to wild type. PEP was slightly decreased and pyruvate was slightly increased. Nevertheless, the ratio of PEP/pyruvate was significantly decreased in both transgenic lines relative to wild type affecting also downstream reactions. For example, alanine being derived from pyruvate significantly decreased by 70% compared to wild type. Also, the pyruvate dependent amino acids valine and isoleucine were considerably lower in both transgenic lines, albeit significant only for PKC-6. However, the accumulation of lactate was not altered in the transgenic lines compared to wild type. In addition to the role of pyruvate in fermentation pathways, pyruvate is imported into the mitochondrion to feed into the TCA cycle. In general, the measured TCA cycle intermediates tended to decrease in the transgenic lines relative to wild type. Citrate and aconitate belonging to the initial reactions of the cycle decreased at least 2-fold in comparison with the wild type. Isocitrate was significantly decreased in line 6, while malate and fumarate were significantly lower in PKC-15 relative to wild type. The TCA cycle associated amino acids like GABA, glutamate,

glutamine, aspartate and asparagine were differentially regulated in the transgenic lines compared to wild type. GABA was decreased in both transgenic lines to 20% of the wild type levels. Glutamate and glutamine remained unchanged, while aspartate and asparagine were significantly decreased in both transgenic lines compared to wild type. The changes in the TCA cycle intermediates were accompanied by alterations in the energy state in the transgenic lines. For example, ATP and ADP were significantly decreased in the transgenic lines by 30% and 20%, respectively, while the ATP/ADP ratio was about 20% lower in the transgenic lines relative to the wild type. The nucleotides UTP and UDP participating in sugar and cell wall metabolism were decreased in both transgenic lines, albeit significantly only in PKC-6 compared to wild type. Furthermore, GDP and GTP showed a decrease in both transgenic lines relative to wild type, yet significantly only for GTP. The redox related parameters were changed as well in the transgenic lines compared to wild type. NADH was significantly increased in both transgenic lines, while the NADH/NAD ratio was significantly higher in PKC-6.

The metabolites upstream of the PKc reaction displayed only a few changes compared to metabolites downstream of PKc. The metabolites upstream of PKc UDP-glucose, 3-phosphoglyceric acid and glycerate were significantly changed in the transgenic lines in comparison with the wild type. UDP-glucose was significantly decreased by 30% in PKC-6, while 3-phosphoglyceric acid was significantly increased by 50% in PKC-15 relative to wild type. Furthermore, glycerate was decreased in both lines by 30%, although only significantly in PKC-6. Taken together, these results show that a deficiency in PKc activity leads to a strong attenuation in the low-oxygen induced increase in the levels of specific amino acids and organic acids which are indicators of a rearrangement of the TCA cycle under these conditions. This was accompanied by an increase in the NADH/NAD ratio and a decrease in the ATP/ADP ratio, suggesting that PKc is important for the adaptation of the energy and redox status to low-oxygen conditions assumably by promoting a reorganization of the TCA cycle (Fig. 3.5).

3.3 Investigation of the low-oxygen response of an Arabidopsis mutant lacking the major catalytic subunit of NAD-isocitrate dehydrogenase in comparison to wild type

The afore-described experiments were carried out with potato tubers as a simplified experimental model system to analyze time-resolved responses of metabolism to low-oxygen. However, the possibilities for genetic manipulations are somewhat restricted in potato tubers compared to Arabidopsis. Therefore, for the further experiments the model system was switched from *Solanum tuberosum* to *Arabidopsis thaliana*, which provides a huge collection of different mutants and transgenic lines. Moreover, the use of Arabidopsis allows an easier analysis of the plant hypoxic resistance and low-oxygen effects on growth.

In the preceding chapter it could be demonstrated that a decrease in PKc activity in potato tuber led to an impaired metabolic response to low-oxygen indicating that the reorganization of the TCA cycle under these conditions has been severely compromised. The importance of this non-cyclic TCA cycle for anoxia survival was demonstrated by Rocha et al. (2010) in *Lotus japonicus*. However, the significance of the mitochondrial 2-oxoglutarate production for the operation of this reorganized TCA cycle under low-oxygen had not yet been investigated. Therefore, *Arabidopsis thaliana* plants with a defect in the catalytic subunit of IDH were used to identify the role of the mitochondrial 2-oxoglutarate production in the reorganization of the TCA cycle under low-oxygen.

3.3.1 Enzyme activity measurement of NAD-and NADP-isocitrate dehydrogenase in the idhv mutant and wild type

The activity of NAD-dependent isocitrate dehydrogenase in mitochondrial enriched fractions of Arabidopsis was measured to study the effect of the deficiency of the catalytical subunit of IDH in the *idhv* mutant compared to wild type. Moreover, the activity of the NADP-dependent isocitrate dehydrogenase (ICDH) in both genotypes was determined to investigate whether ICDH shows a compensatory increase in activity in the *idhv* mutant.
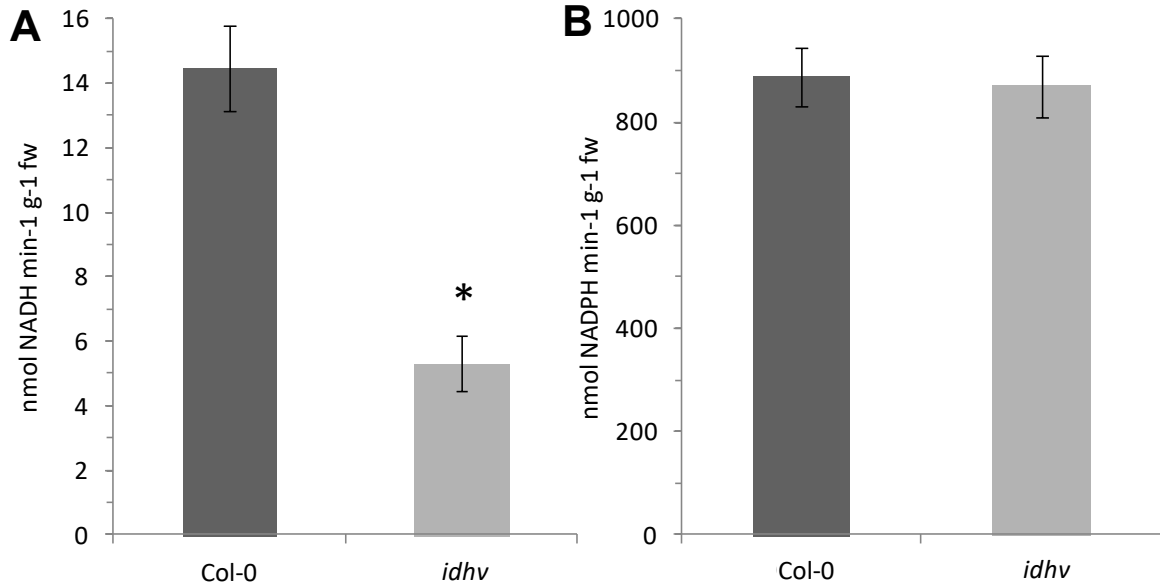
Fig. 3.6: Enzyme activity measurements of *idhv* seedlings relative to wild type Col-0. A, maximal catalytic activity of NAD-dependent isocitrate dehydrogenase in *idhv* and wild type seedlings. B, maximal catalytic activity of NADP-dependent isocitrate dehydrogenase in *idhv* and wild type seedlings. Seedlings were grown for two weeks under long day conditions (16 h light /8 h dark with 100 μmol photons m² s⁻1) on vertical plates with 2% agar and 1% sucrose. Then, seedlings were harvested and used for protein extraction. Results are the mean ± SE, *n* = 7-8 biological replicates. Significant changes between *idhv* and wild type were evaluated by using Student's t-test (p < 0.05) and are shown by asterisk.

The deficiency of the catalytic subunit of IDH in *idhv* plants led to a significant 75% decrease in IDH activity relative to wild type (Fig. 3.6A). This decrease was not as strong as observed by Lemaitre et al. (2007) being attributable to differences in plant age and growth conditions in the different studies. The activity of ICDH showed no difference between the *idhv* mutant and the wild type. Apparently, there is no compensatory increase in ICDH activity which concurs with the findings of Lemaitre et al. (2007) (Fig. 3.6B).

3.3.2 Anoxia tolerance assay in the idhv mutant and wild type

Arabidopsis plants are not able to survive longer periods without oxygen (Vartapetian & Jackson 1997). However, shorter periods of anoxia can be partially tolerated leading to the survival of a certain percentage of plants depending on the conditions (Ellis et al. 1999; Licausi et al. 2010). To verify the ability of Arabidopsis plants to survive a specific period of anoxic treatment, an anoxia tolerance assay was used in which 7-day-old seedlings were treated for 8 h under anoxia in the dark. 7 days after the treatment, the percentage number of surviving plants was counted.
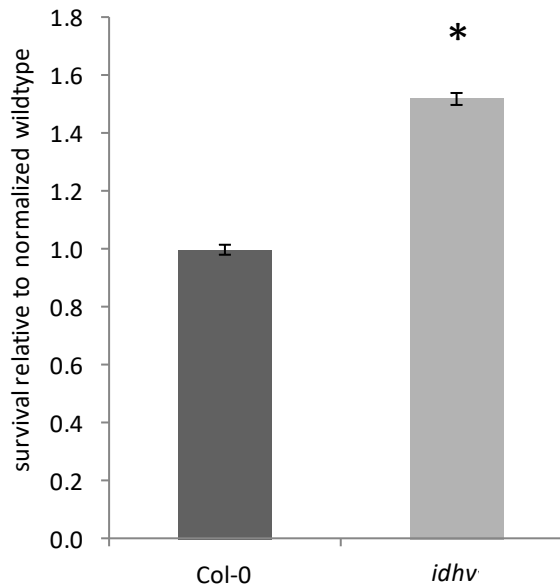
Fig. 3.7: Anoxic survival rate of *idhv* seedlings relative to wild type Col-0. Seedlings were grown for 1 week under long day conditions (16 h light /8 h dark with 100 µmol photons m² s⁻1) on 0.8% agar and 1% sucrose in 21% oxygen. On day 7, seedlings were exposed for 8 h to anoxic conditions in the dark. Then, they were transferred back to the normoxic growth chamber with 21% oxygen for another 7 days, and the surviving plants were counted. Results are the mean ± SE n= 15-19 plates, with each plate containing 30 seedlings. Significant changes between *idhv* and wild type were evaluated by using Student's t-test (p < 0.05) and are shown by asterisk.

The *idhv* mutant showed a significant 50% increase in anoxic survival rate in comparison with the wild type (Fig. 3.7).

3.3.3 Analysis of root growth in the idhv mutant and wild type across different oxygen conditions

The results of the anoxia survival experiment indicate an improved tolerance to low-oxygen of the *idhv* mutant compared to wild type. However, the anoxic survival experiment only provides information about the tolerance of the different genotypes to strict anoxic conditions. Therefore, the measurement of the root growth decrease caused by hypoxia (Dongen et al. 2009) was used as tool to compare the tolerance of the *idhv* mutant and the wild type to different low-oxygen conditions, giving information on the biosynthetic capacity of roots under hypoxia.
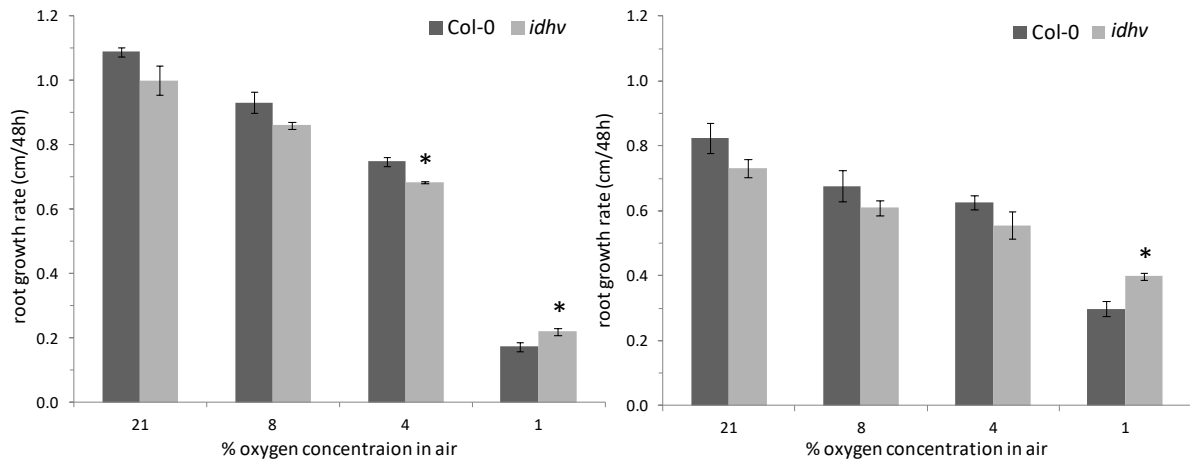
Fig. 3.8: Root growth rate of *idhv* seedlings relative to wild type Col-0 at different oxygen concentrations in 2 separate experiments: A, experiment of April 2012 B, experiment of August 2012. Seedlings were grown for two weeks under long day conditions (16 h light /8 h dark with 100 µmol photons m² s⁻1) on vertical plates with 2% agar and 1% sucrose. Then, they were exposed for 48 h to 21%, 8%, 4% and 1% (v/v) oxygen in the dark, and root extension growth was measured. Results are the mean ± SE, *n*= 5-6 plates, with each plate containing 8-10 seedlings. Significant changes between *idhv* and wild type were evaluated by using Student's t-test ($p < 0.05$) and are shown by asterisk.

The two independent experiments conducted in 2012 showed similar results. The root growth rate decreased in alignment with the decrease in oxygen in all genotypes (Fig. 3.8A and B). The *idhv* mutant revealed a slight (10%) decrease in root growth relative to the wild type at 21%, 8%, and 4% oxygen (Fig. 3.8A and B). Interestingly, at 1% oxygen the *idhv* mutant showed a significant increase in root growth by about 30% compared to wild type in both experiments (Fig. 3.8A and B). This is consistent with the findings of the anoxia survival experiment which revealed an improved performance of the *idhv* mutant compared to wild type under anoxia (Fig. 3.7).

3.3.4 Transcript expression analysis of hypoxic marker genes in the idhv mutant and wild type exposed for 16 h and 24 h to different oxygen concentrations

Low-oxygen leads to a reprogramming of metabolism, accompanied by changes in gene expression. It has been shown in several experiments that specific genes are upregulated by hypoxic stress (Branco-Price et al. 2005; Gonzali et al. 2005; Dongen et al. 2009). Based on these findings, Licausi et al. (2010) selected 4 genes as distinct markers of the low-oxygen response. These hypoxia marker genes are *ADH1, HB1, SUS1* and *SUS4*. The up-regulation of these genes under hypoxia enables the plant to cope with the low-oxygen stress leading to increased fermentation (*ADH1*), improved scavenging of NO to promote conversion of NADH

to NAD (*HB1*) and stimulation of an energy-saving route of sucrose breakdown (*SUS1* and *SUS4*). To investigate the increase in mRNA levels of these genes in the *idhv* mutant and wild type, seedlings were exposed to different oxygen concentrations for 16 h and 24 h.

Fig. 3.9: Expression of hypoxia marker genes *ADH1* (A), *HB1* (B), *SUS1* (C) and *SUS4* (D) in *idhv* seedlings compared to wild type Col-0 at different oxygen concentrations. Marker gene expression was normalized to the housekeeping gene *RCE1* and is displayed as fold change. Seedlings were grown for two weeks under long day conditions (16 h light /8 h dark with 100 µmol photons m² s⁻1) on vertical plates with 2% agar and 1% sucrose. Then, seedlings were exposed for 16 h to 21%, 1% and 0% (v/v) oxygen in the dark and shoots were harvested to analyze mRNA levels. Results are the mean ± SE, n = 3-4 biological replicates. Significant changes between *idhv* and wild type were evaluated by using Student's t-test (p < 0.05) and are shown by asterisk.

Both genotypes showed the typical pattern of increased induction with the decrease in oxygen levels in the 16 h low-oxygen treatment (Fig. 3.9). However, the induction of *ADH1*, *SUS1* and *SUS4* transcript levels was significantly attenuated in the *idhv* plants compared to wild type at 0% oxygen (Fig. 3.9A, B, C). The expression of *ADH1* and *SUS4* was diminished

by 30% in the *idhv* mutant relative to the wild type, whereas the transcript levels of *SUS1* decreased by 45% in the *idhv* mutant compared to wild type (Fig. 3.9A, C, D).
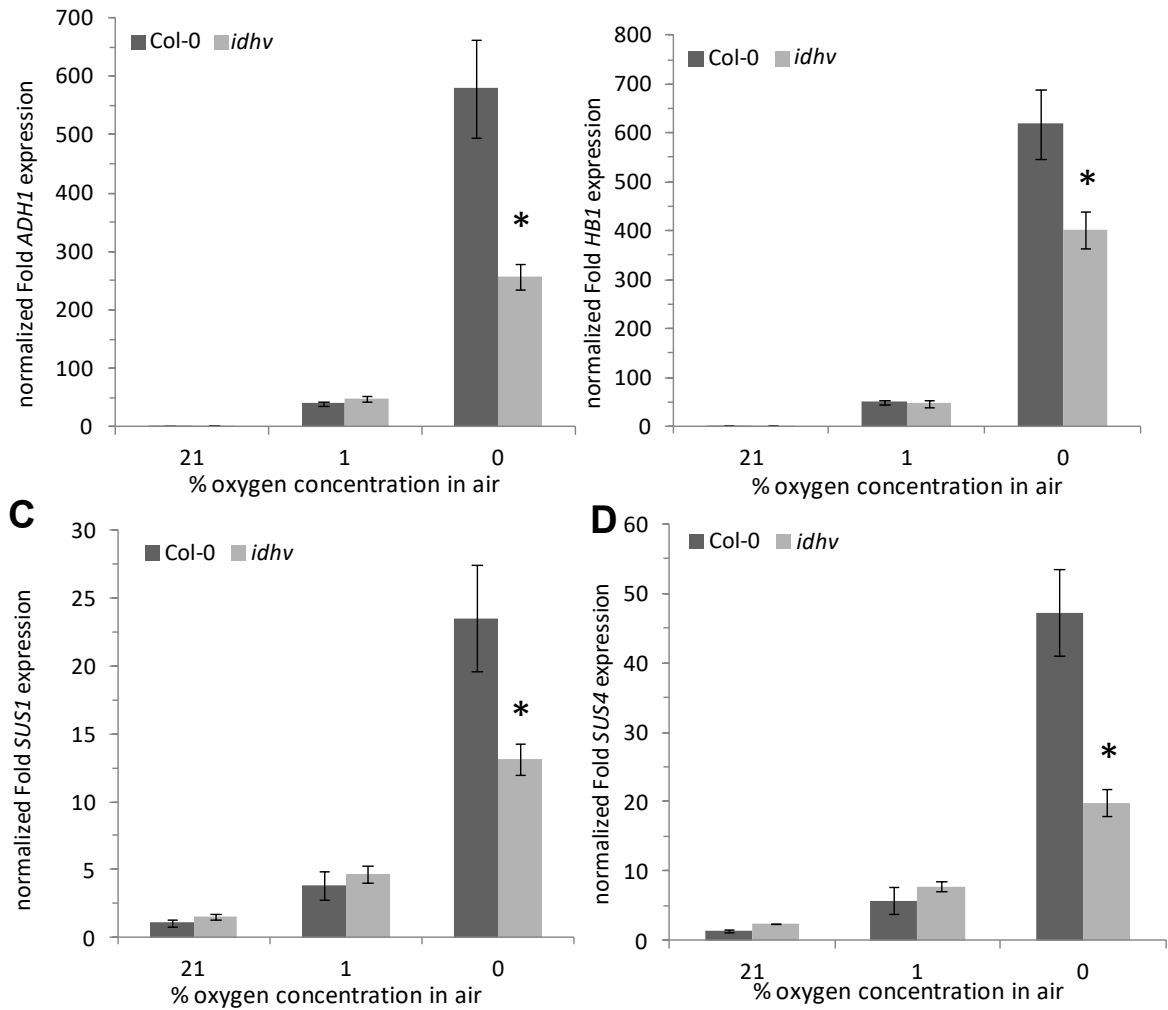
Fig. 3.10: Expression of the hypoxia marker genes *ADH1* (A), *HB1* (B), *SUS1* (C) and *SUS4* (D) in *idhv* seedlings compared to wild type Col-0 at different oxygen concentrations. Marker gene expression was normalized to the housekeeping gene *RCE1* and is displayed as fold change. Seedlings were grown for two weeks under long day conditions (16 h light /8 h dark with 100 µmol photons m² s⁻1) on vertical plates with 2% agar and 1% sucrose. Then, seedlings were exposed for 24 h to 21%, 1% and 0% (v/v) oxygen in the dark and shoots were harvested to analyze mRNA levels. Results are the mean ± SE, *n* = 3-4 biological replicates. Significant changes between *idhv* and wild type were evaluated by using Student's t-test ($p < 0.05$) and are shown by asterisk.

The 24 h low-oxygen treatment revealed a similar expression of hypoxia marker genes of the *idhv* mutant compared to wild type at 21% and 1% oxygen concentration. Under anoxic conditions there was a significant decrease of expression in the *idhv* mutant by 55%, 35%, 45% and 60% for *ADH1*, *HB1*, *SUS1* and *SUS4* transcript levels, respectively, compared to wild type (Fig. 3.10A to D).

3.3.5 Metabolic analysis of the *idhv* mutant and wild type exposed for 16 h to different oxygen concentrations

The experimental results described in the chapters 3.3.2 and 3.3.3 demonstrated an improved tolerance to low-oxygen conditions of the *idhv* mutant, whereas the transcript expression analysis revealed a decreased induction of hypoxia marker genes in *idhv* plants compared to wild type (see 3.3.4). Apparently, the increased tolerance to low-oxygen of the *idhv* plants cannot be explained by an increased expression of hypoxia marker genes. Possible reasons for the improved low-oxygen tolerance of the *idhv* mutant are changes at the metabolic level to circumvent the decrease in mitochondrial IDH activity. To test this hypothesis, a metabolite profile of primary metabolism was conducted using GCMS and enzyme based assays.

Fig. 3.11: Changes in the levels of metabolites in *idhv* seedlings relative to wild type Col-0 at different oxygen concentrations. Seedlings were grown for two weeks under long day conditions (16 h light /8 h dark with 100 µmol photons m² s⁻1) on vertical plates with 2% agar and 1% sucrose. Then, seedlings were exposed for 16 h to 21%, 1% and 0% (v/v) oxygen in the dark (bars 1-2, 3-4 and 5-6 from left to right, respectively), and shoots were directly harvested in liquid nitrogen. The y-axis displays metabolite abundance, which was measured by profiling via GC-MS or by enzymatic assays. For details, see supplemental table 4. Results are the mean ± SE, *n* = 4-6 biological replicates. Significant changes between *idhv* and wild type were evaluated by using Student's t-test (p < 0.05) and are shown by asterisk.

Fig. 3.11 shows metabolite abundances of the different genotypes at 21%, 1% and 0% oxygen. The changes between the wild type and the *idhv* mutant at 21% oxygen are discussed at first in the following.

The *idhv* gene codes for the catalytic subunit of IDH (Lemaitre et al. 2007). This mitochondrial enzyme catalyzes the conversion of isocitrate to 2-oxoglutarate being part of the TCA cycle. Hence, a decrease in IDH activity should lead to alterations in the ratio of isocitrate to 2-oxoglutarate. However, there was no visible change in isocitrate or 2-oxoglutarate levels relative to wild type under normoxic conditions. Yet, altered IDH activity in the *idhv* mutant might influence the metabolism of amino acids, as 2-oxoglutarate is the precursor for amino acid synthesis. The levels of most of the detected amino acids and some of the nonproteinogenic amino acids like ornithine and beta-alanine were significantly decreased in *idhv* plants compared to wild type. Only glutamine, asparagine and glycine were unaltered. Overall, there was a 15% decrease in the total amino acid pool in *idhv* plants relative to the wild type. In addition to the changes of the pool of amino acids, TCA cycle intermediates such as citrate, fumarate and malate were also found to be significantly decreased in *idhv* plants in comparison with the wild type. This could be due to a blockage in glycolysis, as glucose and sucrose were significantly higher in the transgenic plants compared to wild type. Furthermore, the *idhv* mutant exhibited a significant decrease in 2-hydroxyglutarate. This compound is thought to be involved in linking lysine catabolism with an alternative pathway for respiration through the action of D-2-hydroxyglutarate dehydrogenase (D2HGDH) (Araújo et al. 2010). D2HGDH uses D-2-hydroxyglutarate to generate 2-oxoglutaratarate and can, therefore, help to balance the mitochondrial 2-oxoglutarate pool, if IDH activity is decreased. Moreover, reduced ascorbate as well as the ratio of reduced to oxidized ascorbate was significantly decreased by 80% in the *idhv* mutant relative to wild type.

At 1% oxygen isocitrate decreased significantly, while 2-oxoglutarate remained unchanged in the *idhv* mutant compared to wild type. The other TCA cycle intermediates like citrate, succinate, fumarate and malate were significantly higher in *idhv* plants than in the wild type. However, the increase in the TCA cycle acids did not affect the total amino acids pool in the *idhv* mutant. Yet, glutamine and arginine were significantly decreased, while the amino acids

aspartate, alanine, lysine, proline and o-acetylserine were significantly increased in the *idhv* mutant compared to wild type. GABA and 4-hydroxybutyrate, being part of the GABA shunt, were also increased in *idhv* plants relative to wild type. Furthermore, the idhv mutant showed alterations in the levels of certain sugar and sugar phosphates. Glucose-6-phosphate (G6P) and fructose-6-phosphate (F6P) were higher in the transgenic plants compared to wild type, while starch accumulated to almost 150% of wild type levels in the *idhv* mutant. An indicator for the energy status of plants is the ATP/ADP ratio. Interestingly, at 1% oxygen ADP was significantly lower, and, subsequently the ATP/ADP ratio was significantly increased in the *idhv* plants relative to wild type. The redox status was also affected in the transgenic plants, as the levels of NAD and oxidized ascorbate were both significantly increased in the *idhv* mutant compared to wild type.

A further oxygen decrease to anoxic levels revealed some additional changes in the *idhv* plants compared to the wild type at 21% and 1% oxygen. Starch, succinate, lysine, 4-hydroxybutyrate and guanine were significantly increased under anoxia in the transgenic plants compared to wild type. Also, trehalose, arabinose, pyruvate, malonate and glycerate were significantly higher in the *idhv* plants than in wild type. Similar to then result at 1% oxygen, the ATP/ADP ratio was significantly higher under anoxia in the *idhv* mutant compared to wild type, because ADP was significantly decreased, while the ATP level remained unchanged relative to wild type (Fig. 3.11).

3.3.6 Metabolic analysis of the idhv mutant and wild type exposed for 24 h to different oxygen concentrations

The metabolic profile of the 16 h low-oxygen treatment already revealed some interesting differences. To get a further insight into the low-oxygen response, both genotypes were treated for 24 h with 21%, 1% and 0% oxygen. This should lead to even more dramatic changes in the metabolite profile between the wild type and *idhv* plants.

Fig. 3.12: Changes in the levels of metabolites in *idhv* seedlings relative to wild type Col-0 at different oxygen concentrations. Seedlings were grown for two weeks under long day conditions (16 h light /8 h dark with 100 µmol photons m² s⁻1) on vertical plates with 2% agar and 1% sucrose. Afterwards, seedlings were exposed for 24 h to 21%, 1% and 0% (v/v) oxygen in the dark (bars 1-2, 3-4 and 5-6 from left to right, respectively) and shoots were directly harvested in liquid nitrogen. The y-axis displays metabolite abundance which was measured by profiling via GC-MS or by enzymatic assays. For details, see supplemental table 5. Results are the mean ± SE, *n* = 4-6 biological replicates. Significant changes between *idhv* and wild type were evaluated by using Student's t-test (p < 0.05) and are shown by asterisk.

Fig. 3.11 shows the metabolite levels of the *idhv* mutant and the wild type at 21%, 1% and 0% oxygen.

Treatment of the *idhv* mutant and wild type plants with 21% oxygen for 24 h revealed specific alterations between the two genotypes. The levels of glucose, sucrose and starch were significantly increased, while glycerate, 2-hydroxyglutarate, alanine, serine, ethanolamine, ascorbate and the ratio of ascorbate to dehydroascorbate were significantly decreased in the *idhv* mutant relative to wild type. Additional changes were observed for galactinol and myo-inositol being significantly increased, whereas uracil was significantly decreased in *idhv* plants relative to wild type.

A decrease in oxygen to 1% resulted in a significant increase in alanine, glutamine, proline, guanine, GABA and 4-hydroxybutyrate in the *idhv* mutant compared to wild type. Furthermore, metabolites associated with starch and sugar metabolism were also affected in the mutant plants. Starch, sucrose, G6P, F6P, myo-inositol and mannose were significantly higher in the *idhv* plants than in the wild type. In glycolysis, there was a significant 30% decrease in pyruvate, and subsequently, a 50% increase in the PEP/pyruvate ratio in the *idhv* plants relative to wild type.

Applying anoxic conditions to the plants for 24 h led to alterations in 33 different metabolites in the transgenic plants compared to wild type. This includes different compound classes like sugars, sugar alcohols, organic and amino acids, sugar phosphates, polyamines and pyridine nucleotides. The *idhv* plants revealed a significant increase in starch, myo-inositol, xylitol, trehalose, galactinol, ribose, galactonate, fucose, myo-inositol 1-phosphate, pyruvate, citrate, succinate, fumarate, malate, malonate, 2-hydroxyglutarate, 4-hydroxybutyrate, glycine, phenylalanine, aspartate, lysine, homoserine, glutamate, beta-alanine, guanine, putrescine and a significant decrease in glutamine in comparison with the wild type. The pyridine nucleotides NADH and NADPH were significantly higher in the *idhv* plants relative to wild type, although the ratio of NADH/NAD and NADPH/NADP was not altered between the genotypes (Fig. 3.12).

3.4 Characterization of the low-oxygen response of Arabidopsis mutants with deletions in genes encoding for different isoforms of NADPH-dependent thioredoxin reductases compared to wild type

The decrease in the activity of enzymes which are part of glycolysis and the TCA cycle showed opposing responses to low-oxygen (see chapter 3.2 and 3.3).

On the one hand, silencing cytosolic pyruvate kinase in potato tubers led to a decreased performance under low-oxygen conditions. On the other hand, knocking out IDH in Arabidopsis promoted survival under anoxia. Although alterations in the respiratory pathways as well as low-oxygen stress are often accompanied by changes in the cellular redox state, only little is known about the role of redox regulating enzymes in the low-oxygen response in plants.

Therefore, Arabidopsis mutants were analyzed lacking either the cytosolic and the mitochondrial NTRA and NTRB (Reichheld et al. 2005) or the plastidial NTRC (Serrato et al. 2004; Pérez-Ruiz et al. 2006; Lepistö et al. 2009) to determine the influence of changes in the subcellular redox state on the low-oxygen response.

3.4.1 Anoxia tolerance assay in the ntrc mutant, the ntrantrb double mutant and wild type

To compare the low-oxygen tolerance of the different genotypes, an anoxia tolerance assay was carried out as described in chapter 3.3.2.
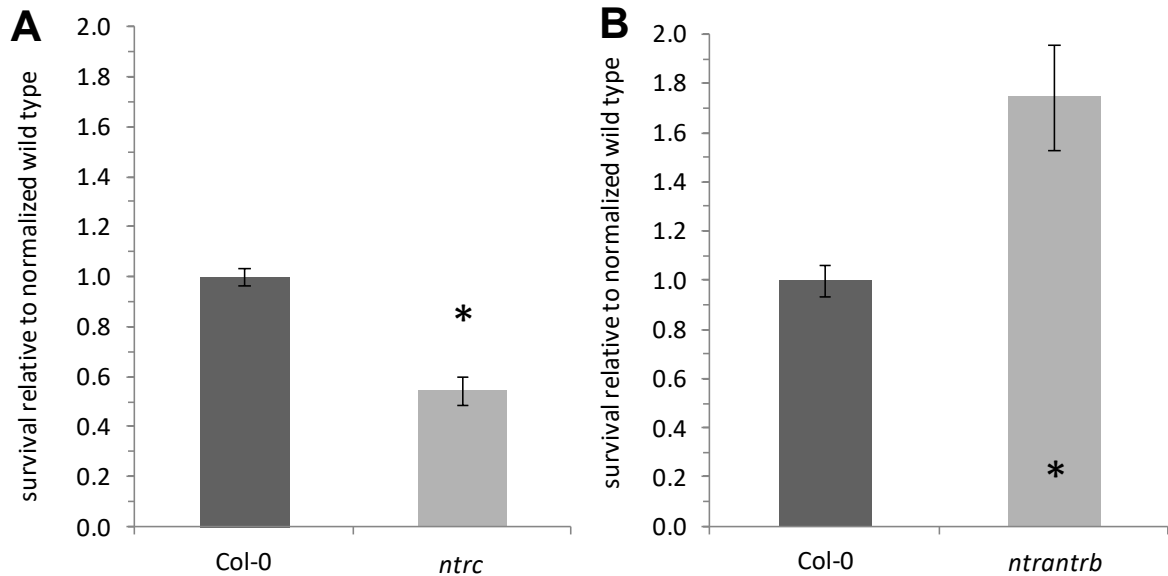
Fig. 3.13: Anoxic survival rate of *ntrc* seedlings relative to wild type Col-0 (A) and of *ntrantrb* seedlings relative to wild type Col-0 (B). Seedlings were grown for 1 week under long day conditions (16 h light /8 h dark with 100 µmol photons m² s⁻1) on 0.8% agar, 1% sucrose. On day 7, seedlings were exposed for 8 h to anoxic conditions in the dark. Then, they were transferred back to the normoxic growth chamber with 21% oxygen for another 7 days and the surviving plants were counted. Results are the mean ± SE, *n* = 12-15 plates, with each plate containing 30 seedlings. Significant changes between *ntrc* and wild type, and *ntrantrb* and wild type were evaluated by using Student's t-test ($p < 0.05$) and are shown by asterisk.

The survival of *ntrc* knockout plants was decreased by 55% relative to the wild type (Fig. 3.13A), whereas the *ntrantrb* double knockout plants had a significant 75% higher survival rate than the wild type (Fig. 3.13B).

3.4.2 Analysis of root growth in the ntrc mutant, the ntrantrb double mutant and wild type across different oxygen concentrations

The anoxia survival assay only gives information about the tolerance to complete anoxic conditions. To elucidate the response of all genotypes to a moderate decrease in oxygen levels the root growth was measured at 21%, 8%, 4% and 1% oxygen as described in chapter 3.3.3
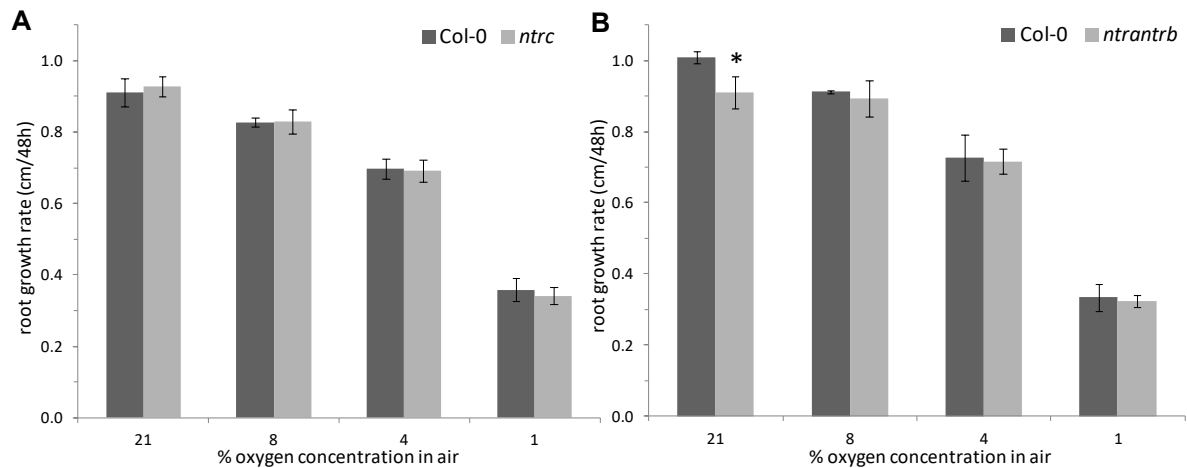
Fig. 3.14: Root growth rate of *ntrc* seedlings relative to Col-0 (A) and of *ntrantrb* seedlings relative to wild type Col-0 (B) at different oxygen concentrations. Seedlings were grown for two weeks under long day conditions (16 h light /8 h dark with 100 µmol photons m² s⁻1) on vertical plates with 2% agar and 1% sucrose. Then, they were exposed for 48 h to 21%, 8%, 4% and 1% (v/v) oxygen in the dark, and root growth was measured. Results are the mean ± SE *n*= 5-6 plates with each plate containing 8-10 seedlings. Significant changes between *ntrc* and wild type, and *ntrantrb* and wild type were evaluated by using Student's t-test ($p < 0.05$) and are shown by asterisk.

All genotypes showed the oxygen dependent decrease in root growth (Fig. 3.14A and B). While the *ntrc* mutant was not different from the wild type, the *ntrantrb* mutant showed a significant 10% decrease in root growth at 21% oxygen (Fig. 3.14A and B). The inhibition in root growth for the *ntrantrb* mutant at normoxia was already published by Reichheld et al. (2007).

The root growth at 8%, 4% and 1% oxygen of both mutants did not change compared to the wild type (Fig. 3.14A and B).

3.4.3 Transcript expression analysis of specific genes in the ntrc mutant, the ntrantrb double mutant and wild type exposed to different oxygen concentrations

The adaptation to low oxygen is accompanied by an induction of specific low-oxygen marker genes like *ADH1* and *HB1*. To examine, whether the difference in survival rate and root growth correlates with an altered expression of *ADH1* and *HB1*, both mRNA levels were measured via qRT-PCR. Moreover, the expression of AOX which is known to be regulated by ROS and redox dependent signals was tested in all genotypes (Clifton et al. 2006). Yoshida et al. (2013) hypothesized that NTRs might control AOX expression through Trx o1. To test whether the difference in anoxia survival of *ntrc* and *ntrantrb* plants may be attributed

to a different induction of AOX, the expression of the most induced AOX isoform AOX1A was studied (Clifton et al. 2006).

3.4.3.1 ADH1 expression
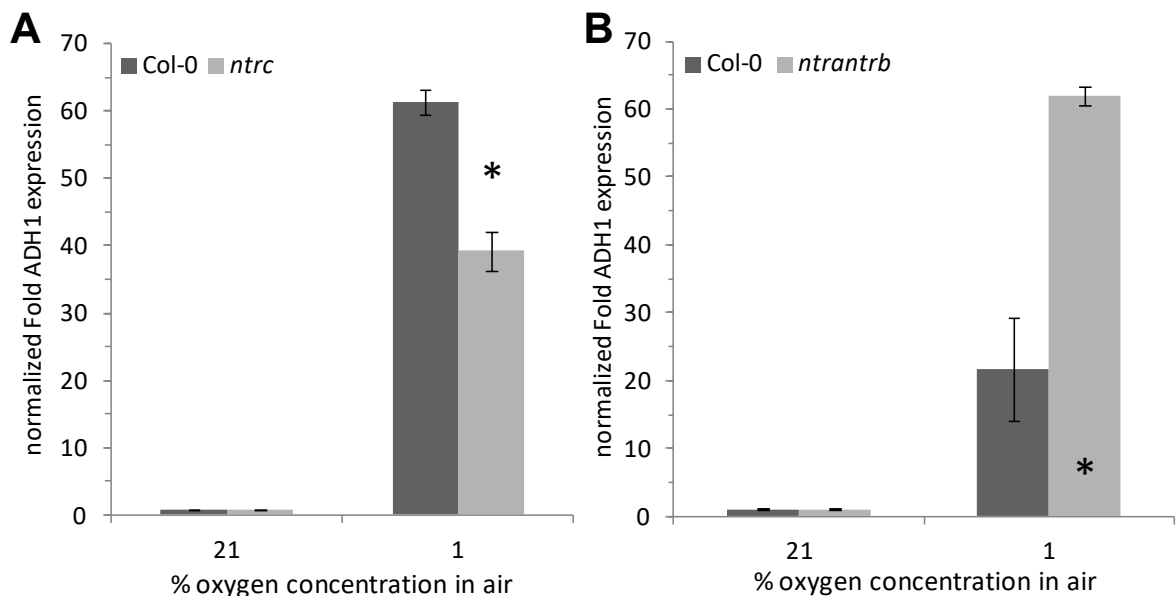
Fig. 3.15: Expression of *ADH1* in *ntrc* seedlings relative to wild type Col-0 (A) and *ntrantrb* seedlings compared to wild type Col-0 (B) at different oxygen concentrations. *ADH1* expression was normalized to the housekeeping gene *RCE1* and is displayed as fold change. A, *ntrc* and wild type seedlings were grown for 21 days under long day conditions (16 h light /8 h dark with 100 μmol photons m² s⁻1) on vertical plates with 2% agar and 1% sucrose. Then, seedlings were exposed for 6 h to 21% and 1% (v/v) oxygen in the dark and whole seedlings were harvested to analyze mRNA levels. B, *ntrantrb* and wild type seedlings were grown for 10 days under long day conditions (16 h light /8 h dark with 100 μmol photons m² s⁻1) on vertical plates with 2% agar and 1% sucrose. Then, seedlings were exposed for 6 h to 21% and 1% (v/v) oxygen in the dark, and whole seedlings were harvested to analyze mRNA levels. Results are the mean ± SE, *n* = 3-4 biological replicates. Significant changes between *ntrc* and wild type and *ntrantrb* and wild type were evaluated by using Student's t-test (p < 0.05) and are shown by asterisk.

All genotypes displayed the typical pattern of hypoxia induction of *ADH1* (Fig. 3.15A and B). The *ntrc* mutant showed a significant 35% decrease in expression of *ADH1* at 1% oxygen relative to wild type (Figure 3.15A). In contrast, the expression of *ADH1* was significantly increased by 2.8-fold in the *ntrantrb* plants in comparison with the wild type (Fig. 3.15B). These findings confirm the results from the anoxic survival experiment (3.4.1).

3.4.3.2 HB1 expression
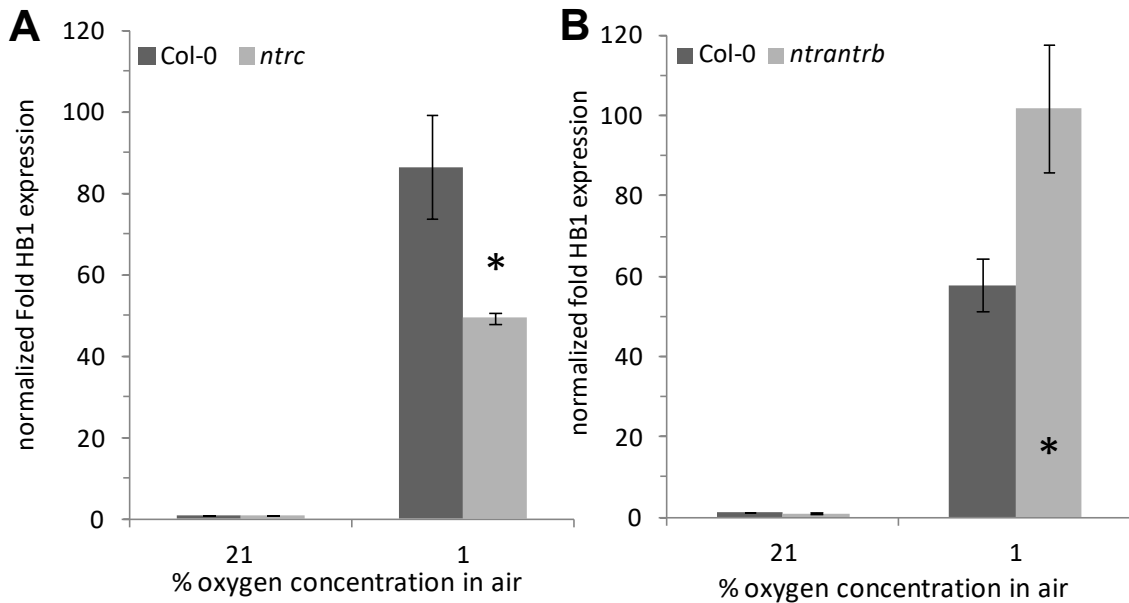
Fig. 3.16: Expression of *HB1* in *ntrc* seedlings relative to wild type Col-0 (A) and in *ntrantrb* seedlings relative to wild type Col-0 (B) at different oxygen concentrations. *HB1* expression was normalized to the housekeeping gene *RCE1* and is displayed as fold change. A, *ntrc* and wild type seedlings were grown for 21 days under long day conditions (16 h light /8 h dark with 100 µmol photons m² s⁻1) on vertical plates with 2% agar and 1% sucrose. Then, seedlings were exposed for 6 h to 21% and 1% (v/v) oxygen in the dark and whole seedlings were harvested to analyze mRNA levels. B, *ntrantrb* and wild type seedlings were grown for 10 days under long day conditions (16 h light /8 h dark with 100 µmol photons m² s⁻1) on vertical plates with 2% agar and 1% sucrose. Then, seedlings were exposed for 6 h to 21% and 1% (v/v) oxygen in the dark, and whole seedlings were harvested to analyze mRNA levels. Results are the mean ± SE, *n* = 3-4 biological replicates. Significant changes between *ntrc* and wild type and *ntrantrb* and wild type were evaluated by using Student's t-test ($p < 0.05$) and are shown by asterisk.

HB1 expression was also induced in all tested genotypes at 1% oxygen compared to 21% oxygen (Fig. 3.16A and B). The *ntrc* mutant displayed a significant decrease in *HB1* expression, whereas hemoglobin expression was significantly increased in the *ntrantrb* mutant relative to wild type (Fig. 3.16A and B). This pattern is similar to the expression of *ADH1* in the *ntrc* and *ntrantrb* mutants compared to wild type at 21% oxygen and 1% oxygen (Fig. 3.15A and B).

3.4.3.3 AOX1a expression
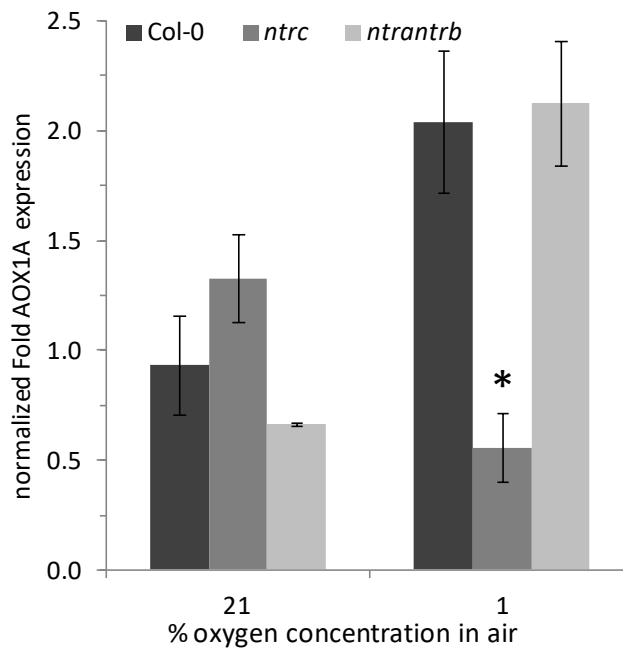
Fig. 3.17: Expression of AOX1a in *ntrc* and *ntrantrb* seedlings relative to wild type Col-0 at different oxygen concentrations. AOX1a expression was normalized to the housekeeping gene *RCE1* and is displayed as fold change. Seedlings were grown for 10 days under long day conditions (16 h light /8 h dark with 100 µmol photons m² s⁻1) on vertical plates with 2% agar and 1% sucrose. Then, seedlings were exposed for 6 h to 21% and 1% (v/v) oxygen in the dark, and whole seedlings were harvested to analyze mRNA levels. Results are the mean ± SE, *n* = 3-5 biological replicates. Significant changes between *ntrc, ntrantrb* and wild type were evaluated by using one-way ANOVA ($p < 0.05$) and are shown by asterisk

The expression of *AOX1a* at 1% oxygen was clearly induced in the wild type and in the *ntrantrb* plants compared to 21% oxygen. However, the *ntrc* mutant showed a significant 70% decrease in *AOX1a* expression relative to *ntrantrb* and wild type at 1% oxygen (Fig. 3.17).

3.4.4 Metabolic analysis in the ntrc mutant, the ntrantrb double mutant and wild type exposed for 16 h to different oxygen concentrations

The transcript expression analysis data showed a differential expression for *ADH1* in *ntrc* and *ntrantrb* plants compared to wild type. The gene product of *ADH1* alcohol dehydrogenase is an important enzyme involved in ethanol fermentation. This pathway uses pyruvate as substrate and is therefore dependent on glycolytic activity. Hence, starch, soluble sugars as well as the glycolytic end products PEP and pyruvate were measured.

Furthermore, a possible link between the survival rate and the redox and energy status of *ntrc* and *ntrantrb* plants in comparison with the wild type was investigated under low-oxygen conditions.
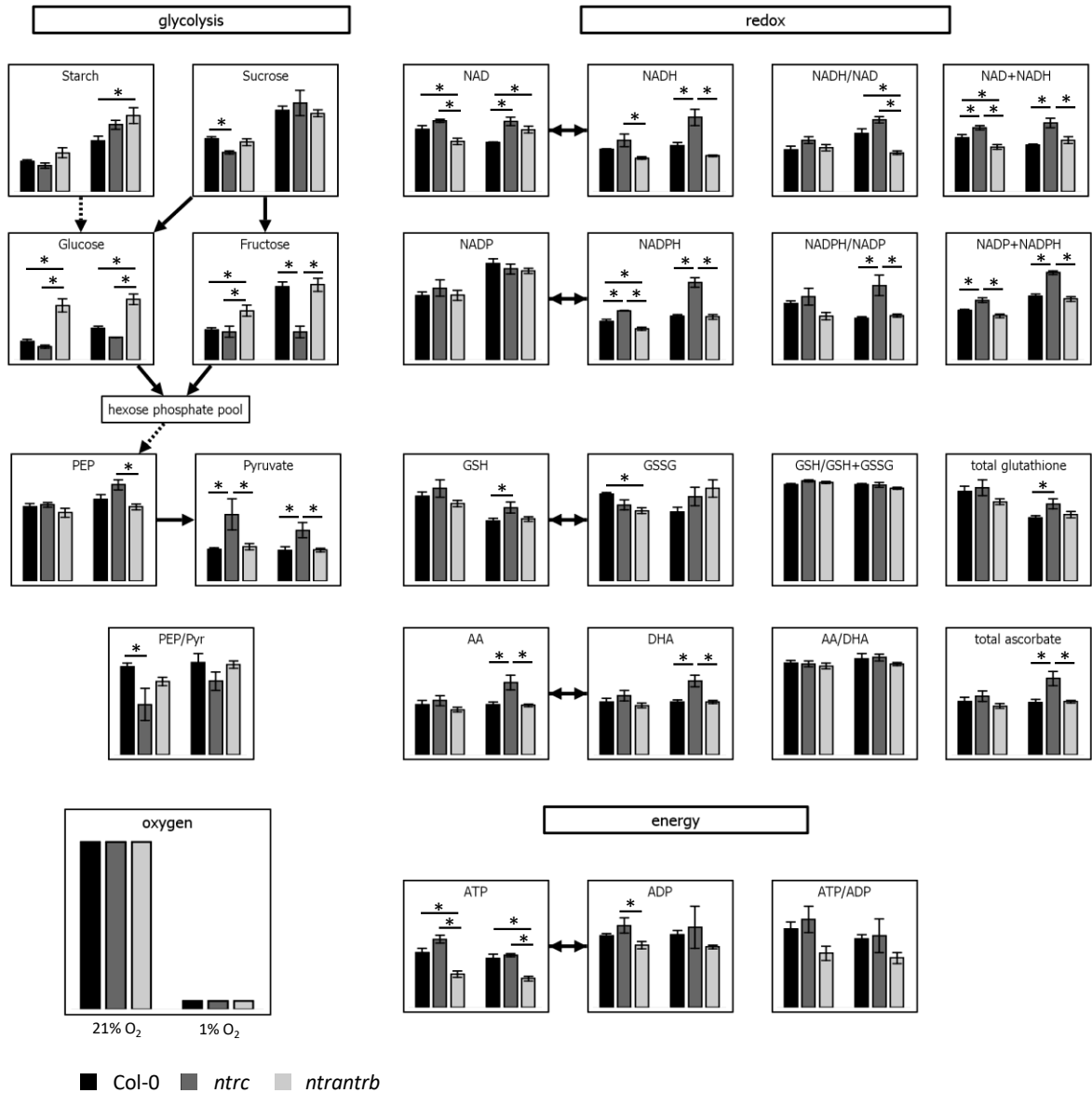
Fig. 3.18: Changes in the levels of metabolites in *ntrc* and *ntrantrb* seedlings compared to wild type Col-0 seedlings at different oxygen concentrations. Seedlings were grown for 2 weeks under long day conditions (16 h light /8 h dark with 100 µmol photons m² s⁻1) on vertical plates with 2% agar. Then, seedlings were exposed for 16 h to 21% and 1% (v/v) oxygen in the dark, and shoots were directly harvested in liquid nitrogen. Metabolite levels were measured by enzymatic assays and are nmol/g fw⁻¹ or µmol/g⁻ fw⁻¹, respectively. For details, see supplemental table 6. Results are the mean ± SE, *n* = 4-6 biological replicates. Significant changes between *ntrc, ntrantrb* and wild type were evaluated by using one-way ANOVA (p < 0.05) and are shown by asterisk.

Fig. 3.11 shows the metabolite levels of the *ntrc* and *ntrantrb* mutant compared to wild type at 21% and 1% oxygen.

3. Results

Both mutants display interesting changes in glycolytic intermediates at 21% oxygen relative to the wild type. Sucrose was decreased in the *ntrc* plants compared to wild type, while glucose and fructose were higher in the *ntrantrb* mutant relative to both, wild type and the *ntrc* mutant.

Pyruvate was increased in the *ntrc* mutant relative to the *ntrantrb* mutant and the wild type. Hence, the ratio of PEP to pyruvate was decreased in the *ntrc* plants compared to wild type.

The redox metabolites NAD, NADH, NADPH as well as the sum of NAD+NADH were decreased in the *ntrantrb* mutant relative to the *ntrc* mutant and the wild type. In the *ntrc* plants NADPH and the sum of NADP+NADPH were increased relative to wild type. Furthermore, the *ntrantrb* mutant showed decreased GSSG values, but no alterations in ascorbate levels in relation to the wild type. The nucleotides ATP and ADP were significantly lower in the *ntrantrb* mutant in comparison with the *ntrc* mutant and the wild type. On the other hand, *ntrc* plants had higher ATP and ADP levels than the *ntrantrb* mutant.

The decrease of oxygen from 21% to 1% revealed differences in sugars and glycolytic end products in *ntrc* plants as well as in *ntrantrb* plants compared to wild type. Glucose and fructose were significantly decreased in the *ntrc* mutant, while pyruvate was significantly increased with no changes of the PEP/pyruvate ratio relative to wild type. The *ntrantrb* plants only had higher levels of starch and glucose and no further changes in PEP or pyruvate compared to wild type. A direct comparison between the *ntrc* mutant and the *ntrantrb* mutant revealed differences in glucose and fructose being significantly higher in *ntrantrb* plants, while PEP and pyruvate were significantly lower in the *ntrantrb* plants than in the *ntrc* mutant. Furthermore, both mutants showed significant changes in redox metabolism. NAD, NADH, NAD+NADH, NADPH, NADPH+NADP and the ratio of NADPH/NADP were significantly higher in *ntrc* plants than in the wild type. On the other hand, the *ntrantrb* mutant showed a significant accumulation of NAD and a lower NADH/NAD ratio compared to wild type. In comparison with the *ntrc* plants NADH and the ratio of NADH to NAD was significantly decreased by 50% in *ntrantrb* plants. NADPH and NADP/NADP were also significantly decreased in the *ntrantrb* mutant compared to the *ntrc* mutant. Subsequently, the sums of NAD+NADH and NADP+NADPH were both significantly decreased in *ntrantrb* plants relative to *ntrc* plants. The most important antioxidants glutathione and ascorbate significantly accumulated in the *ntrc* mutant, but the ratio of the respective reduced vs. the oxidized form did not change in comparison to the wild type. The energy status under low-oxygen was only affected in the *ntrantrb* mutant. Moreover, ATP was significantly lower in *ntrantrb* plants compared to the *ntrc* mutant and the wild type. ADP and the ATP/ADP ratio was also decreased in the *ntrantrb* mutant compared to *ntrc* plants and the wild type, but only moderately by 20% and 30%, respectively (Fig. 3.18).

3.5 Characterization of the low-oxygen response of Arabidopsis lines with inducible silencing of the regulatory subunit of SNF1-related protein kinase in comparison to wild type

The results from chapter 3.4 show the influence of the cellular redox state on the adaptation to low-oxygen. Apart from changes in the redox state under hypoxia, the energy metabolism also plays a crucial role in the ability of plants to survive longer periods of oxygen deficit.

As pointed out in the introduction, the most prominent effect of hypoxia is the inhibition of respiration and subsequently the decreased energy generation through oxidative phosphorylation (Geigenberger 2003). As a consequence, the plant has to rebalance its metabolism to counteract the energy deficit. It has been postulated that the protein kinase SnRK1 functions as energy sensor, thereby controlling metabolic homeostasis (Polge & Thomas 2007; Baena-González & Sheen 2008; Ghillebert et al. 2011). SnRK1 is a heterotrimeric complex with catalytically α, regulatory β and γ subunits (Polge & Thomas 2007; Ghillebert et al. 2011). The γ subunit AKINβγ, also termed SNF4, is plant specific and the only subunit that complements yeast snf4Δ (Polge & Thomas 2007; Ramon et al. 2013). In order to study the function of the regulatory SNF4 subunit as part of the SnRK1 protein under low-oxygen conditions, Arabidopsis plants with transcriptional silencing of SNF4 were analyzed.

3.5.1 Measurement of SNF4 gene expression under normoxia in amiRSNF4 and wild type seedlings

Application of beta-estradiol to the plant induces the decrease in *SNF4* expression by artificial microRNA induced gene silencing. To study the effectiveness of the inducible silencing of *SNF4*, plants were harvested at different time points after applying beta-estradiol. In one group 10 µM beta-estradiol was applied directly into the agar before germination. So, induction of silencing took place with the beginning of germination of the seedlings. In the other group plants were grown for 9 or more days on agar without beta-estradiol and then transferred onto agar with 10 µM beta-estradiol, where they were grown another couple of days before harvesting. The gene expression of *SNF4* was checked using qRT-PCR.

3.5.1.1 Application of 10 µM beta-estradiol before germination

To check the effectiveness of *SNF4* silencing, 10 µM beta-estradiol was applied into the agar before the seeds were sown, and the *SNF4* expression was analyzed 5, 6, and 7 days after germination.
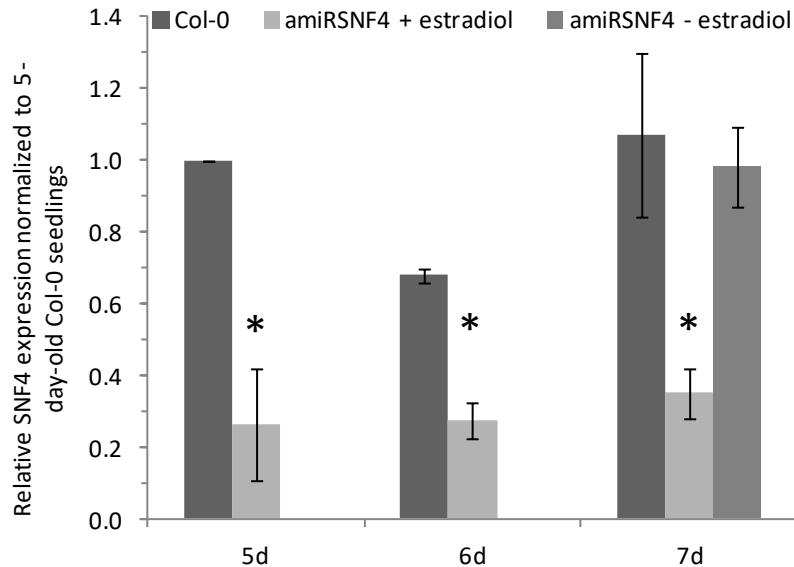
Fig. 3.19: Normalized fold *SNF4* expression of amiRSNF4 and wild type Col-0 seedlings. Seedlings were grown under long day conditions (16 h light/ 8 h dark with 100 µmol photons m² s^{-1}) on 0.8% agar medium including 10µM beta-estradiol (+ estradiol). On day 5, 6 and 7 after germination, seedlings were harvested to analyze SNF4 mRNA levels. Values are normalized against 5-day-old Col-0 seedlings. As a further control, 7-day-old amiRSNF4 seedlings growing on agar medium without beta-estradiol (- estradiol) are shown (medium-grey bar). A control with 5-and 6-day-old amiRSNF4 seedlings growing on agar medium without beta-estradiol was omitted. Results are the mean ± SE, *n* = 3-6 biological replicates. Significant changes between amiRSNF4 and wild type were evaluated by using Student's t-test ($p < 0.05$) and are shown by asterisks.

The expression of SNF4 in the amiRSNF4 line treated with beta-estradiol was significantly decreased by at least 50% when compared to the wild type. The greatest decrease in expression (80%) in beta-estradiol induced amiRSNF4 seedlings occurred 5 days after the start of the beta-estradiol treatment. 7-day-old beta-estradiol induced amiRSNF4 seedlings showed a decrease in SNF4 expression by 75% relative to wild type. 7-day-old amiRSNF4 plants without the inductor had similar SNF4 expression as the wild type control (Fig. 3.19).

3.5.1.2 Application of 10 µM beta-estradiol at different days after germination

As 7-days-old seedlings have a very small size, the amount of fresh weight for comprehensive biochemical analysis is limited. Therefore, 14-day-old seedlings were used for further experiments. In order to find the best time point of beta-estradiol application for efficient downregulation in 14-day-old plants, 10µM beta-estradiol was applied to 9-, 11-, and 13-day-old plants, and SNF4 expression was checked via qRT-PCR.
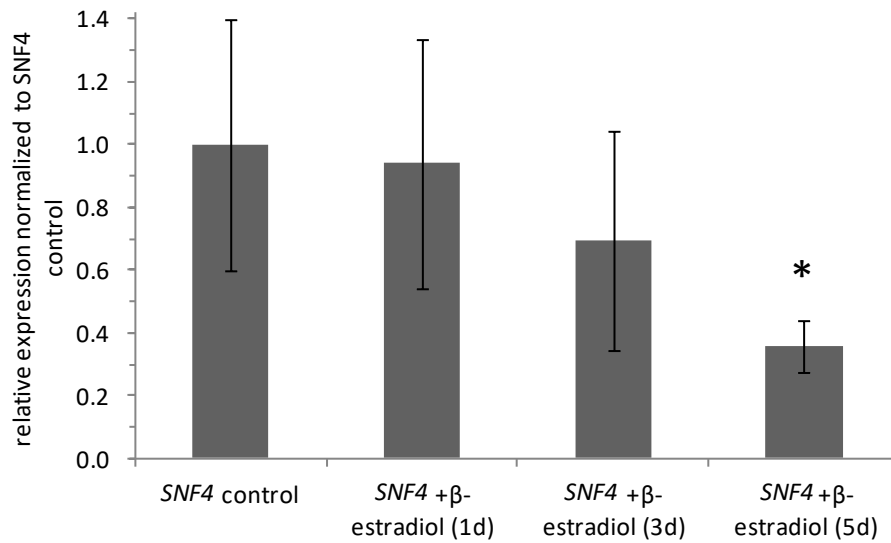
Fig. 3.20: Changes in SNF4 expression levels in amiRSNF4 seedlings in response to different time-periods of beta-estradiol treatment. AmiRSNF4 seedlings were grown under long day conditions (16 h light/8 h dark and 100 µmol photons m² s-1) on 2% agar plates containing 1% sucrose (but no beta-estradiol) for 9, 11 or 13 days, at which time-points seedlings were transferred to 2% agar plates containing 1% sucrose and 10 µM beta-estradiol. Seedlings were then harvested 14 days after germination (which means different time-periods of beta-estradiol treatments of 1, 3 and 5 days) to analyze SNF4 expression. AmiRSNF4 seedlings grown for 14 days on 2% agar containing 1% sucrose, but no estradiol, served as non-induced transgenic control to which values were normalized. Results are the mean of ± SE, n = 3 biological replicates. Significant changes between the treatments and the SNF4 control were evaluated by using Student's t-test ($p < 0.05$) and are shown by asterisks.

In comparison with the untreated control, application of 10 µM beta-estradiol to 9-day-old amiRSNF4 plants for 5 days led to a significant silencing of *SNF4* expression by about 65%. Shorter treatments of beta-estradiol had no significant effect on *SNF4* expression relative to the untreated control plants (Fig. 3.20).

3.5.2 Biomass analysis under normoxia in amiRSNF4 and wild type seedlings

In order to characterize the inducible amiRSNF4 line on a physiological level at 21% oxygen, the fresh weight of 7-day-old seedlings was determined. To induce silencing of the SNF4 subunit, 10µM beta-estradiol was added to the plant growth media before seed germination.
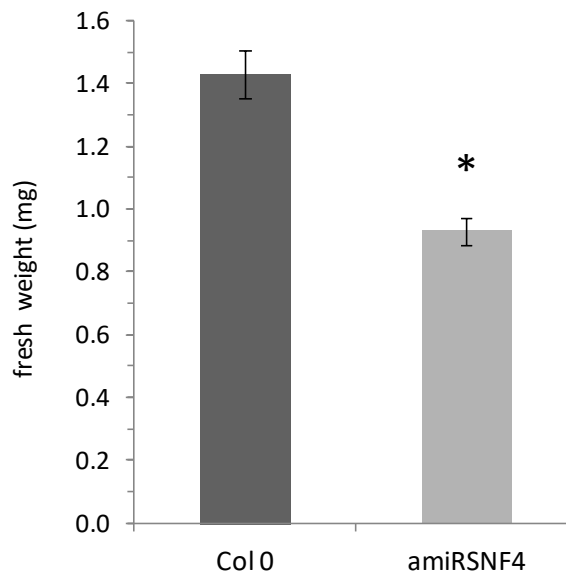
Fig. 3.21: Biomass of 7-day-old seedlings. AmiRSNF4 and wild type Col-0 seedlings were grown under long day conditions (16 h light /8 h dark with 100 µmol photons m² s-1) on plates with 2% Agar and 1% sucrose supplemented with 10µM of beta-estradiol. Results are the mean ± SE, n = 10 independent agar plates with 5 to 10 seedlings per plate. Significant changes between amiRSNF4 and wild type were evaluated by using Student's t-test ($p < 0.05$) and are shown by asterisks.

The weight of 7-day-old beta-estradiol induced amiRSNF4 seedlings was significantly decreased by 35% relative to the wild type (Fig. 3.21).

3.5.3 Root growth analysis under normoxia in amiRSNF4 and wild type seedlings

To test the influence of *SNF4* silencing on root growth, the root length of 7day-old-seedlings was measured. Therefore, 10 µM beta-estradiol was added to the plant growth media before seed germination to induce silencing of the SNF4 subunit.
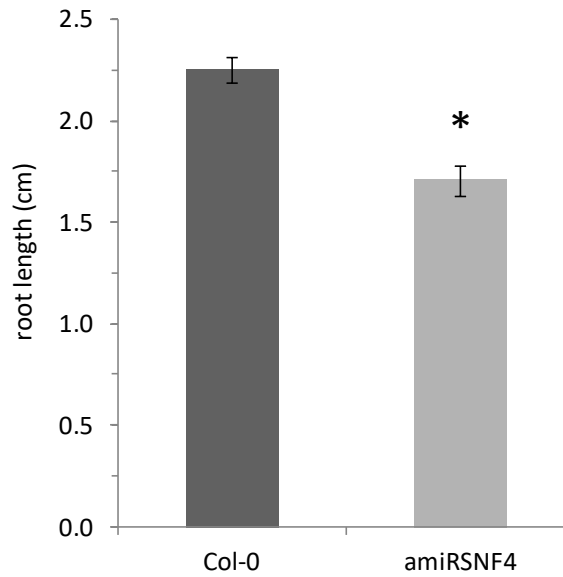
Fig. 3.22: Root length of 7-day-old seedlings. AmiRSNF4 and wild type Col-0 seedlings were grown under long day conditions (16 h light/ 8 h dark with 100 µmol photons m² s-1) on plates with 2% Agar and 1% sucrose supplemented with 10 µM of beta-estradiol. Results are the mean ± SE, n = 12 independent agar plates with 4 to 8 seedlings per plate. Significant changes between amiRSNF4 and wild type were evaluated by using Student's t-test ($p < 0.05$) and are shown by asterisks.

The root length in beta-estradiol induced amiRSNF4 plants was significantly decreased by 25% in comparison with the wild type (Fig. 3.22).

3.5.4 Anoxia tolerance assay in amiRSNF4 and wild type seedlings

The measurement of the survival rate after an anoxia treatment is a good indicator for an altered low-oxygen response of the amiRSNF4 plants in comparison with the wild type. As a further control, amiRNF4 plants without beta-estradiol were used as described in chapter 3.3.2.
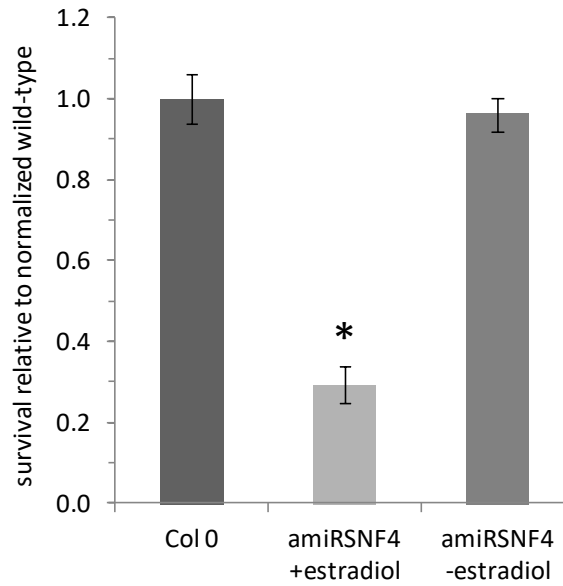
Fig. 3.23: Anoxic survival rate of amiRSNF4 seedlings relative to wild type Col-0. Seedlings were grown under long day conditions (16 h light/ 8 h dark with 100 µmol photons m² s-1) on 0.8% agar and 1% sucrose with or without 10 µM beta-estradiol. On day 7, seedlings were exposed for 8 h to anoxic conditions in the dark. Then, they were transferred back to the normoxic growth chamber at 21% oxygen for another 7 days and the surviving plants were counted. Results are the mean ± SE n = 12-15 plates, with each plate containing 30 seedlings. Significant changes between amiRSNF4 and wild type were evaluated by using Student's t-test ($p < 0.05$) and are shown by asterisks.

The anoxic survival rate of amiRSNF4 seedlings treated with beta-estradiol was significantly decreased by 70% compared to wild type. AmiRSNF4 seedlings without the inductor showed no difference to the wild type (Fig. 3.23).

3.5.5 Analysis of root growth in amiRSNF4 and wild type seedlings and across different oxygen concentrations

To elucidate the response of amiRSNF4 and wild-type plants to altered oxygen availability, the root growth under different low-oxygen concentrations was measured as described in chapter 3.3.1.3
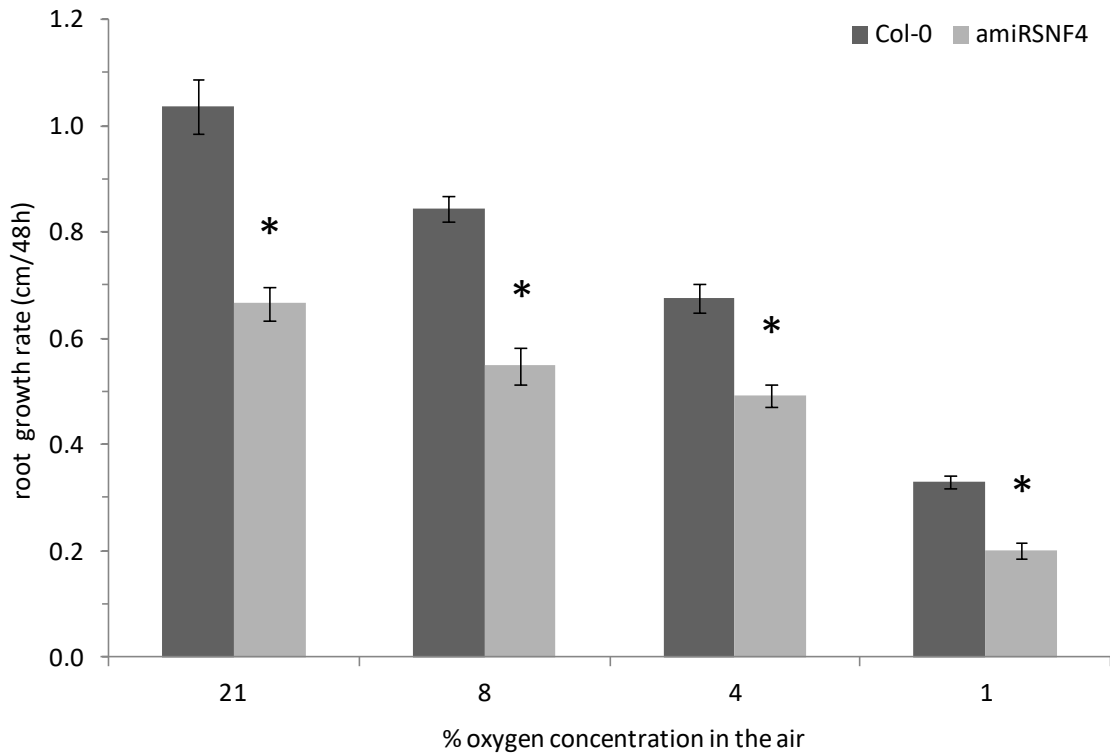
Fig. 3.24: Root growth rate of amiRSNF4 seedlings relative to wild type Col-0. Seedlings were grown for 9 days under long day conditions (16 h light /8 h dark with 100 μmol photons m² s⁻1) on vertical plates with 2% agar and 1% sucrose. Then, they were transferred to vertical plates with 2% agar, 1% sucrose and 10 μM beta-estradiol for additional 5 days, before they were exposed for 48 h to 21%, 8%, 4% and 1% (v/v) oxygen in the dark, and root growth was measured. Results are the mean ± SE n= 5-6 plates, with each plate containing 8-10 seedlings. Significant changes between amiRSNF4 and wild type were evaluated by using Student's t-test ($p < 0.05$) and are shown by asterisks.

The root extension rates gradually declined with the decrease in oxygen levels in both genotypes. In the amiRSNF4 plants root growth was already significantly decreased by 35% under normal oxygen conditions relative to wild type. This decrease in root growth in the amiRSNF4 seedlings relative to the wild type was maintained also under low-oxygen conditions (Fig. 3.24).

3.5.6 Transcript expression analysis of hypoxia marker genes in amiRSNF4 and wild type seedlings exposed for 24 h to different oxygen concentrations

The amiRSNF4 seedlings exhibited a severe decrease in anoxia survival rate, but showed no low-oxygen dependent decrease in root growth compared to wild type. Therefore, the expression of hypoxia marker genes at hypoxic (1% O_2) as well as anoxic (0% O_2) conditions was analyzed in amiRSNF4 and wild type seedlings. As mentioned in chapter 3.3.1.4
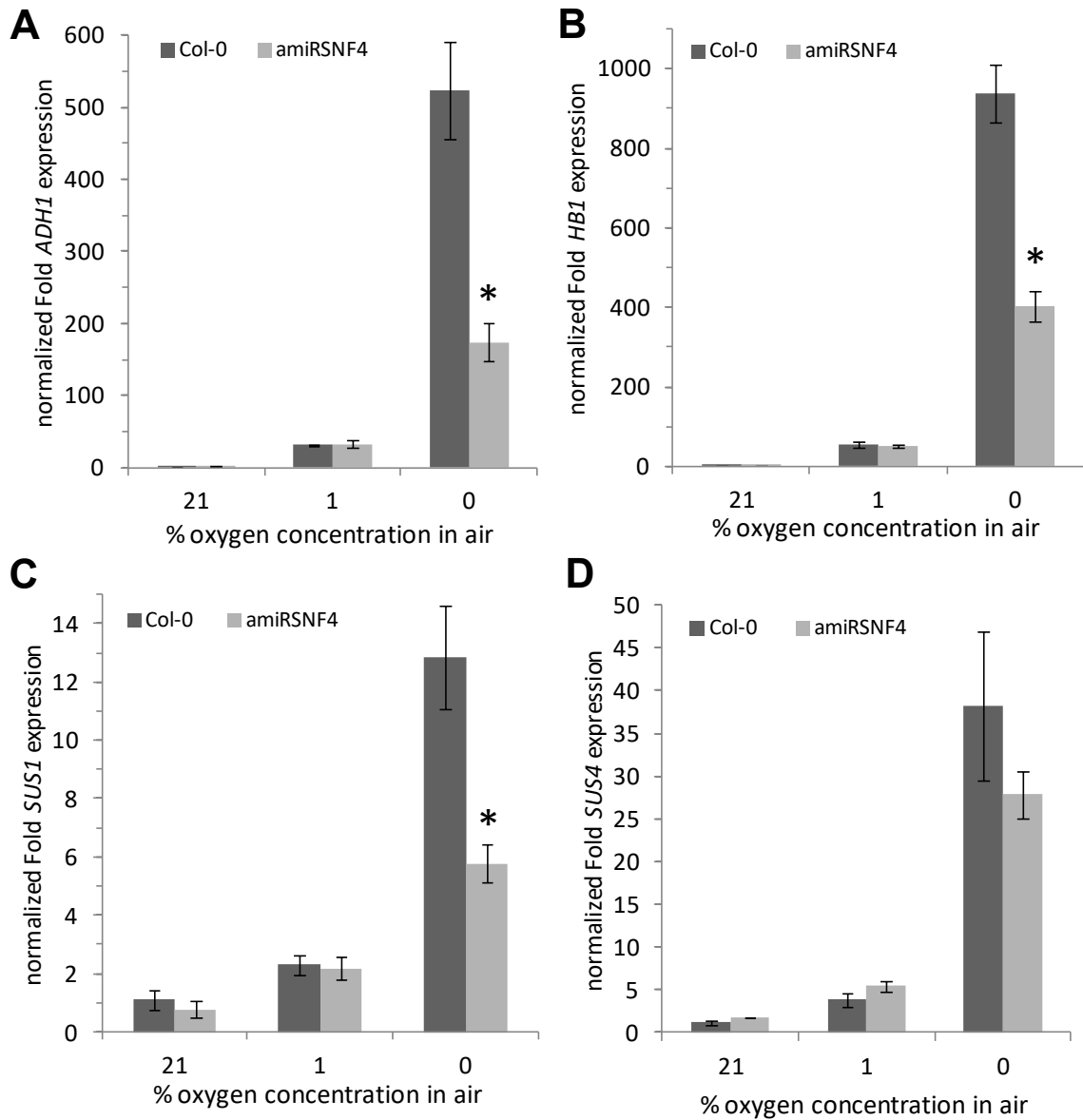
Fig. 3.25: Expression of the hypoxia marker genes *ADH1* (A), *HB1* (B), *SUS1* (C), and *SUS4* (D) in amiRSNF4 seedlings compared to wild type Col-0 at different oxygen concentrations. Marker gene expression was normalized to the housekeeping gene *RCE1* and is displayed as fold change. Seedlings were grown for 9 days under long day conditions (16 h light/ 8 h dark and 100 µmol photons m² s-1) on vertical plates containing 2% agar and 1% sucrose (but no beta-estradiol). Then, seedlings were transferred to vertical plates with 2% agar, 1% sucrose and 10µM beta-estradiol for additional 5 days, before they were exposed for 24 h to 21%, 1% and 0% (v/v) oxygen in the dark to analyze mRNA levels. Results are the mean ± SE, n = 3-4 biological replicates. Significant changes between amiRSNF4 and wild type were evaluated by using Student's t-test ($p < 0.05$) and are shown by asterisks.

Both genotypes showed an increase in induction of mRNA expression of hypoxia marker genes with a decrease in oxygen from 21% to 0% (Fig. 3.25). However, the expression of *ADH*, *HB1* and *SUS1* was significantly decreased in the amiRSNF4 plants compared to the wild type. The decrease in expression was 70%, 60% and 55%, respectively (Fig. 3.25A, B,

C). *SUS4* was decreased by 30% under anoxia in the amiRSNF4 plants relative to the wild type, although not significantly (Fig. 3.25D).

3.5.7 Metabolic analysis in amiRSNF4 and wild type seedlings exposed for 24 h to different oxygen concentrations

Previous results revealed alterations under normal oxygen conditions in the amiRSNF4 seedlings. Silencing of SNF4 led to inhibition of shoot and root growth in 7-day-old seedlings (see chapters 3.5.2 and 3.5.3) which is in line with the role of SNRK1 as an energy sensing protein controlling growth and development in Arabidopsis (Robaglia et al. 2012; Tome et al. 2014; Ghillebert et al. 2011). Moreover, silencing of SNF4 also negatively affects root growth under low-oxygen (see chapter 3.5.5) and the survival rate in response to anoxia (see chapter 3.5.4). This correlates with a decreased expression of hypoxia marker genes in amiRSNF4 seedlings (see chapter 3.5.6). To investigate the effect of SNF4 silencing on primary metabolism under low-oxygen, a metabolite profiling with GCMS and enzyme based assays was carried out. To get a comprehensive overview, metabolites of carbon and amino acid metabolism were measured, as well as glycolytic and TCA cycle intermediates. Furthermore, energy and redox related parameters were determined.

Fig. 3.26: Changes in the levels of metabolites in amiRSNF4 seedlings relative to wild type Col-0 at different oxygen concentrations. Seedlings were grown for 9 days under long day conditions (16 h light/ 8 h dark and 100 μmol photons m² s-1) on vertical plates containing 2% agar and 1% sucrose (but no estradiol). Then, seedlings were transferred to vertical plates with 2% agar, 1% sucrose and 10μM beta-estradiol for additional 5 days, before they were exposed for 24 h to 21%, 1% and 0% (v/v) oxygen in the dark, and shoots were directly harvested in liquid nitrogen. Metabolite levels were measured by profiling via GC-MS or by enzymatic assays. For details, see supplemental table 7. Results are the mean ± SE, *n* = 4-6 biological replicates. Significant changes between amiRSNF4 and wild type were evaluated by using Student's t-test (p < 0.05) and are shown by asterisks.

Fig. 3.11 shows the metabolite levels of the amiRNSF4 plants and the wild type at 21%, 1% and 0% oxygen.

It is not surprising to see changes in the metabolite profile under normoxic conditions relative to wild type, as the silencing of *SNF4* already had an effect on plant and root growth (see chapters 3.5.2 and 3.5.3). The TCA cycle intermediates citrate, isocitrate, succinate, malate, fumarate and aspartate which is an amino acid derived from oxaloacetate were significantly decreased in the amiRSNF4 seedlings relative to wild type. Furthermore, the glycolytic intermediate PEP was significantly decreased in amiRSNF4 plants compared to wild type. Serine, glycine and alanine which are amino acids produced from the glycolytic intermediates 3-PGA and pyruvate were also significantly lower in amiRSNF4 plants relative to wild type. Also, organic acids (3-hydroxybutyrate, 2-hydroxyglutarate) and sugars (myo-inositol and fucose) were significantly lower in amiRSNF4 plants than in the wild type. In contrast, uracil, beta-alanine and arabitol showed an increase in the amiRSNF4 compared to the wild type. The increase of the total amino acids pool in amiRSNF4 seedlings relative to the wild type can be attributed to the significant increases in the amino acids glutamine, arginine, ornithine and putrescine. Presumably, the higher abundance in amino acids in the amiRNSF4 plants is caused by an increased protein break down, as indicated by the 20% lower protein content in the amiRSNF4 seedlings relative to the wild type.

The decrease in oxygen concentration to 1% showed an interesting metabolic phenotype in the amiRSNF4 seedlings compared to the wild type. The amino acids serine and glycine as well as the organic acids 2-hydroxyglutarate, citrate, succinate and malate were significantly decreased in the amiRSNF4 seedlings relative to wild type. On the other hand, there was an increase in stress related amino acids like histidine, proline, beta-alanine and putrescine in the amiRSNF4 seedlings compared to wild type. However, the total amino acid pool was unchanged between both genotypes.

Starch, glucose and minor sugars (galactose, fucose, talose) were significantly higher in the amiRSNF4 plants relative to the wild type. At 1% oxygen the hexose phosphates are typically increased in the wild type Arabidopsis plants (see Fig. 3.26, Fig. 3.26). Interestingly, this was not the case in the amiRSNF4 plants. When compared to the wild type, G6P and F6P were significantly decreased in amiRSNF4 seedlings at 1% oxygen and unchanged at 21%

oxygen. Moreover, the ratio of NADPH to NADP was significantly higher in the amiRSNF4 plants compared to wild type.

The most significant difference in the metabolic profile between amiRSNF4 plants and the wild type was visible under anoxia. From the total 87 metabolites measured, 46 showed a significant difference in the amiRSNF4 seedlings relative to wild type. Most changes occurred in the amino acid and sugar metabolism in amiRSNF4 plants compared to wild type. The following amino acids were significantly increased in amiRSNF4 seedlings: Glutamine, proline, arginine, ornithine, aspartate, methionine, isoleucine, threonine, glycine, valine and the aromatic amino acids phenylalanine, threonine and tyrosine. Only serine and asparagine were significantly decreased in the amiRSNF4 seedlings. In addition, carbon availability was considerably enhanced in the amiRSNF4 plants under anoxia, as starch, maltose, sucrose, glucose and some minor sugars (trehalose, myo-inositol, arabitol) were significantly higher than in the wild type. Furthermore, the increase in PEP and the decrease in citrate in the amiRSNF4 plants compared to wild type suggest an inhibition of metabolism between glycolysis and the TCA cycle under anoxia. Moreover, lactate accumulation was significantly decreased by 50% in the amiRSNF4 seedlings compared to wild type. This decrease in fermentative activity may also explain the significant 50% increase in the NADH/NAD ratio in amiRSNF4 plants relative to the wild type. Another compound that typically accumulates under low-oxygen stress is GABA. The significant 20% increase of GABA in the amiRSNF4 plants relative to wild type could be indicative of increased anoxic stress in amiRSNF4 seedlings caused by the restriction of fermentation. Also, DNA and RNA metabolism might be compromised in amiRSNF4 seedlings under anoxia as uracil, guanine and uridine were strongly increased compared to wild type (Fig. 3.26).

4 Discussion

The aim of this thesis was to investigate the metabolic response of potato tuber and Arabidopsis to a low-oxygen atmosphere. Low-oxygen describes the limited availability of oxygen inside the plant cell. This can occur in highly metabolic active cells, bulky storage organs or under conditions of flooding (Geigenberger 2003; Licausi & Perata 2009).

Potato tuber tissue was treated with 4% oxygen, and the metabolic response was analyzed in a time dependent manner. Low-oxygen in potato tubers led to a rapid metabolic depression at various sites, but fermentation was induced at a later point of time. The results suggested PKc as a regulatory site in the adaptation of potato tubers to low-oxygen. PKc catalyses the final step in glycolysis and provides pyruvate as a substrate for fermentation and respiration. RNAi silenced transgenic potato tubers with decreased activity of PKc were treated with 4% oxygen and a comprehensive metabolic profile was performed. It turned out that PKc influenced the metabolic performance under hypoxia by regulating the supply of pyruvate that becomes available for fermentation. To circumvent the restrictions for genetic manipulations that are associated with the use of *Solanum tuberosum* as experimental system, *Arabidopsis thaliana* was chosen as an alternative. Arabidopsis plants that lack the catalytic subunit of IDH where used to study the importance of mitochondrial alpha-ketoglutarate production for the reorganization of the TCA cycle that occurs under hypoxia (Rocha et al. 2010). Indeed, transgenic *idhv* plants showed increased low-oxygen tolerance suggesting the importance of non-mitochondrial alpha-ketoglutarate production under hypoxia.

A further area that is affected by low-oxygen is the redox state of the cell. Under normoxic conditions oxygen is an important electron acceptor. With the decreased availability of oxygen under hypoxia, the cellular redox state becomes more reduced. Important redox regulating enzymes are the plastidial and extraplastidial NTRs. To investigate the role of this NTR system in response to hypoxia a knockout of the plastidial NTRC and a combined knockout of the extraplastidial NTRA and NTRB proteins were treated with low-oxygen, and the redox status related parameters were analyzed. The results reveal contrasting effects for the plastidial compared with the extraplastidial NTR system on hypoxic gene expression, metabolism and survival. Apart from the redox metabolism, the energy metabolism is also affected by low-oxygen. When respiration is inhibited under low-oxygen, ATP production slows down and the energy status decreases. In order to overcome the energy deficit, plant cells have to sense the energy status and initiate countermeasures. SnRK1 coordinates energy homeostasis through activation of energy producing anabolic processes and by limiting energy consuming processes (Baena-González & Sheen 2008). To study the function of SnRK1 under hypoxia, transgenic Arabidopsis plants with a beta-estradiol

inducible amiRNA transcriptional silencing of the regulatory SNF4 subunit were treated with low-oxygen. The transgenic plants showed decreased low-oxygen tolerance compared to wild type that was accompanied by a decreased expression of hypoxia induced marker genes and an altered metabolism suggesting a role of SnRK1 in the low-oxygen response in Arabidopsis plants.

4.1 Low-oxygen leads to a rapid metabolic depression in growing potato tubers

Treatment of potato tuber slices with low-oxygen revealed an immediate block of respiration within the first minute after applying low-oxygen conditions (Fig. 3.1). Apparently, potato tuber tissue can rapidly adjust its respiration rate to the oxygen concentration inside the cell. This hypothesis is supported by studies on barley, pea and Arabidopsis roots (Gupta et al. 2009; Zabalza et al. 2008). The inhibition of respiration during hypoxia cannot be easily explained by substrate limitation, as the K_m of COX for oxygen is 100 times lower than the oxygen concentration inside the cell at 4% oxygen (Mapson & Burton 1962; Drew 1997; Gupta et al. 2009). However, the underlying mechanisms leading to this rapid inhibition are yet unknown (Gupta et al. 2009). The inhibition of respiration also led to changes in the pool of nucleotides. For instance, ADP rose simultaneously to the inhibition of respiration pointing to a block of ATP synthase (Fig. 3.2). Subsequently, the ATP/ADP ratio dropped leading to an overall depression of many ATP-consuming pathways (Dongen et al. 2009; Geigenberger 2003). Apparently, the main action of low-oxygen is located in the mitochondrial electron transport chain as Geigenberger et al (2000) already speculated. The NADH/NAD ratio decreased in the same time frame indicating that not only electron transport was blocked, but also the production of NADH by glycolysis and TCA-cycle suggesting a general metabolic depression.

Tightly associated with the mitochondrial electron transport chain is the function of the TCA cycle. One important intermediate of the TCA cycle is aconitate which showed the earliest response to low-oxygen in potato tubers. It started to increase from minute 8 and accumulated around 3-fold at minute 60 (Fig. 3.2). Aconitate is produced by aconitase which is located in the mitochondria (Millar et al. 2001; Salvato et al. 2014) and readily inactivated by ROS like H_2O_2 (Verniquet et al. 1991) or NO (Gupta et al. 2012). Inhibition of aconitase under low-oxygen is part of the reorganization of the TCA cycle under these conditions (Rocha et al. 2010).

4. Discussion

The glycolytic pathway showed an immediate increase in FBP followed by a decrease in PEP in the first 10 minutes after the transfer of the potato tuber slices to low-oxygen conditions (Fig. 3.2). During minutes 8 to 60 of the hypoxic treatment FBP decreased and PEP increased (Fig. 3.2). The hexose phosphates being a precursor of FBP in glycolysis showed a similar kinetic to FBP, although with a short time delay (Fig. 3.2), suggesting that the control over the flux of glycolysis in potato tubers under low-oxygen conditions is shared between aldolase, PK and HK and/or fructokinase (FK). These results are in agreement with outcomes from Geigenberger et al. (2000) who treated potato tuber slices for 2 h under different oxygen conditions. They identified FK and PK as regulatory sites during low-oxygen stress in potato tubers. The experiments described and analyzed in this thesis revealed additional possible regulatory sites with aldolase and hexokinase, whereby aldolase could be identified as primary control site. Aldolase catalyzes the readily reversible conversion of FBP to glyceraldehyde-3-phosphate and dihydroxyacetone-phosphate in vivo and has not yet been considered as rate-limiting step or enzyme with a high flux control coefficient over glycolysis (Thomas et al. 1997). Nonetheless, aldolase is part of a glycolytic substrate channeling complex that is attached to the outer mitochondrial membrane according to Graham et al. (2007). The authors have shown that the degree of association is dependent on the respiration rate, and aldolase is strongly interacting with the outer mitochondrial membrane protein VDAC. Furthermore, Arabidopsis aldolase was found to be glutathionylated in a redox dependent manner in vitro and in vivo (Dixon et al. 2005; van der Linde et al. 2011). It can be speculated that the shift in the redox state occurring under low-oxygen triggers the glutathionylation of aldolase. This in turn could influence the activity and the interaction with the outer mitochondrial membrane of aldolase and, subsequently, alter glycolytic activity. The inhibition of aldolase in the first 5 minutes after the transfer of potato tubers to hypoxia was followed by the decrease of the hexose phosphates and FBP and the increase of PEP (Fig. 3.2). This indicates a shift from the primary control site aldolase to the secondary control sites HK, FK and PK. Geigenberger et al. (2000) have also identified PK and FK as control sites in the glycolysis of potato tuber under hypoxia. FK as well as HK regulates the entry of carbon into glycolysis whereas PK provides pyruvate for respiration. Interestingly, HK and FK are inhibited by ADP acting competitively to ATP (Renz & Stitt 1993). Therefore, the inhibition of both enzymes in potato tubers under low-oxygen can be explained by the increase in ADP being a consequence of the restriction of respiration and ATP synthesis under hypoxia. This provides a mechanism, whereby consumption of carbohydrates is restricted, if the energy status of the cell is too low to support biosynthesis (Geigenberger 2003).

Another regulatory enzyme in plants is PK. It catalyzes the final step of glycolysis and is believed to be a major control point of plant glycolysis (Hatzfeld & Stitt 1991; Plaxton 1996).

4. Discussion

Geigenberger et al (2000) already identified PK as one of the regulatory sites in potato tuber under low-oxygen. A possible explanation for the inhibition of PK under low-oxygen could be the increase in citrate (Fig. 3.2) which is a potent inhibitor of potato tuber PK (Auslender et al. 2015). As 95% of the citrate pool in potato tubers is stored in the vacuole (Farré et al. 2001), citrate might be released from the vacuole into the cytosol under hypoxia and thereby facilitating the inhibition of PK. The inhibition of PK by citrate is a mechanism by which the plant can control the intracellular pyruvate concentration under conditions where the mitochondrial respiration and the TCA cycle activity are compromised. This regulatory feedback loop can prevent the overaccumulation of pyruvate that otherwise would lead to unnecessary oxygen consumption under low-oxygen conditions (Gupta et al. 2009; Zabalza et al. 2008).

The alteration of the TCA cycle activity under low-oxygen is accompanied by the accumulation of GABA (van Dongen et al. 2003; Branco-Price et al. 2008; Narsai et al. 2009; Kreuzwieser et al. 2009; Zabalza et al. 2011). The experiments revealed that GABA increased immediately after the transfer of potato tubers to low-oxygen and accumulated after 60 minutes around 4-fold relative to the normoxic control (Fig. 3.2). The instantaneous rise of GABA preceded changes in alanine and lactate, indicating a different regulatory circuit for GABA metabolism in potato tubers under low-oxygen. A very rapid and strong increase in cellular GABA content was also visible in soybean and radish leaves after the feeding of glutamate and in response to stress (Streeter & Thompson 1972b; Wallace et al. 1984). In general, GABA is part of the so called GABA shunt comprised of three enzymatic reactions which bypasses the conversion of alpha-ketoglutarate to succinate in the TCA cycle (Bown & Shelp 1997; Fait et al. 2008). Thereby, it is clear that the GABA shunt and the TCA cycle activity are tightly linked (Fait et al. 2007; Araújo et al. 2008). The accumulation of GABA under low-oxygen is caused by an increased flux from glutamate to GABA (Streeter & Thompson 1972a; Tsushida & Murai 1987) through glutamate decarboxylase (GDC). GDC consumes glutamate and one proton to produce GABA and CO_2. It is located in the cytosol and regulated by Ca^{2+} and pH (Fait et al. 2008; Bown & Shelp 1997). Potato tuber GDC is maximally catalytically active at ph 5.8 and sensitive to thiol-directed agents (Satyanarayan & Nair 1985). The regulation of GDC via changes in cytosolic Ca^{2+} or H^+ concentration could explain the immediate increase of GABA under low-oxygen in potato tubers (Fig. 3.2), as changes in both ions occur within minutes after low-oxygen treatment (J. Roberts et al. 1984; J. K. Roberts et al. 1984; Roberts et al. 1992; Ratcliffe 1997; Gout et al. 2001) & (Subbaiah et al. 1994; Subbaiah et al. 1998; Subbaiah & Sachs 2003).

In addition to GABA glutamine is likewise a metabolite being derived from glutamate and being involved in nitrogen metabolism in potato tuber. When potato tubers were incubated with 4% oxygen, glutamine increased up to 12-fold in the first 8 minutes, but then declined

after 1 h to normoxic levels (Fig. 3.2). An initial increase in glutamine followed by a decrease was also observed in poplar roots, when plants were flooded up to 168 h (Kreuzwieser et al. 2009). While the exact reason for this behavior remains unclear, it shows that hypoxia leads to a very rapid rearrangement of flux through the GS/GOGAT pathway which is a common phenomenon under low-oxygen stress (Limami et al. 2008; Oliveira & Sodek 2013; Oliveira et al. 2013). The GS/GOGAT pathway is responsible for the incorporation of nitrogen in form of ammonium to produce glutamate which serves as substrate for most of the transamination reactions inside the cell. The increase of glutamine in the first minutes after transfer of potato tubers to low-oxygen (Fig. 3.2) is probably caused by the temporary inhibition of GOGAT or glutamine dependent asparagine synthetase (ASN) (Limami et al. 2008). The subsequent decrease in glutamine (Fig. 3.2) could be explained by the inhibition of GS, as this enzyme is sensitive to changes in the energy status (Limami et al. 2008; Kreuzwieser et al. 2009).

The increase in amino acids (arginine, tyrosine, valine, isoleucine and asparagine) 30 minutes after the transfer of potato tubers to low-oxygen (Fig. 3.2) is probably caused by the slowdown of protein synthesis being a common syndrome of low-oxygen stress in plants (Geigenberger et al. 2000; Geigenberger 2003; Branco-Price et al. 2008).

One of the most important metabolic alterations to promote survival under low-oxygen is the induction of fermentation. Fermentation is needed to oxidize excessive NADH that otherwise would inhibit glycolysis under low-oxygen conditions. There are 3 main fermentation routes in plants starting with pyruvate as substrate: 1) ethanol fermentation, 2) lactate fermentation and 3) alanine fermentation. While it was not possible to measure ethanol, lactate and alanine could be measured by GCMS. When potato tubers were treated with 4% oxygen, alanine and lactate started to rise at minute 7 and accumulated around 3-fold to 4-fold until minute 60 (Fig. 3.2). Strikingly, both metabolites showed a very similar kinetic pattern (Fig. 3.2) indicating a mutually regulation under low-oxygen. Similarly, NADH and the NADH/NAD ratio started to rise at minute 7 after the transfer of potato tuber to hypoxia (Fig. 3.2). So it might be possible that both fermentation processes are regulated by the NADH/NAD redox status. However, there are three reasons which do not support this hypothesis. First, the change in NADH and the NADH/NAD ratio started at the same time as the change in both fermentation products. If both reactions are regulated by the NADH/NAD ratio, it would be more plausible, if the change in NADH/NAD ratio precedes the onset of fermentation. Second, the main isoforms of LDH are located in the cytosol (Davies & Davies 1972; Asker & Davies 1984; Paventi et al. 2007), while the main isoform of AlaAT is located in the mitochondria (Salvato et al. 2014). Given the difference in NADH producing and consuming metabolic pathways, which occur in the mitochondria and the cytosol (TCA cycle and respiration versus glycolysis and gluconeogenesis), the mitochondrial NADH/NAD ratio is likely to be different from the cytosolic one (Hampp et al. 1985; Igamberdiev et al. 2001;

Igamberdiev & Gardeström 2003). Third, only the production of lactate via LDH is NADH dependent (Davies & Davies 1972; Asker & Davies 1984), whereas the production of alanine via AlaAT is not.

A second hypothesis explaining the common regulation of lactate and alanine fermentation under low-oxygen involves a similar substrate affinity to pyruvate of both enzymes. Unfortunately, a direct comparison of the kinetic parameters of LDH and AlaAT is not possible, as AlaAT has not been purified from potato tuber mitochondria until now. Still, there is a couple of arguments against the pyruvate availability hypothesis. First, as stated already before, LDH and AlaAT are located in different subcellular compartments (Davies & Davies 1972; Asker & Davies 1984; Paventi et al. 2007; Salvato et al. 2014). Hence, the Km of both enzymes has to match the pyruvate concentration in the respective compartment. Second, the concentration of pyruvate in potato tubers at 4% oxygen remained unchanged during the course of the experiment. If substrate availability plays a role in the induction of fermentation the substrate concentration has to change in order to alter enzyme activity. Indeed, Zabalza et al. (2009) fed pyruvate to pea roots and could demonstrate that the induction of fermentation was not dependent on the cellular pyruvate concentration, but rather on the ATP/ADP status.

4.2 Cytosolic pyruvate kinase affects metabolic performance under hypoxic conditions by regulating the supply of pyruvate for fermentative metabolism in growing potato tubers

Transgenic potato tubers with decreased expression of PKc showed no difference in the respiration rate at 21% oxygen compared to wild type (Fig. 3.5). This result is in agreement with earlier studies and confirms that PKc is probably not a primary control site of respiration in plants (Gottlob-McHugh et al. 1992; Grodzinski et al. 1999; Oliver et al. 2008).

Furthermore, the respiration rate at low-oxygen of the transgenic tubers is similar to wild type (Fig. 3.5). However, the metabolite profile of transgenic potato tubers with decreased expression of PKc at 4% oxygen revealed interesting changes in glycolysis and in the TCA cycle compared to wild type (Fig. 3.5). Particularly, the transgenic tubers showed a lower PEP to pyruvate ratio and less accumulation of the oxaloacetate derived metabolites aspartate and malate (Fig. 3.5). A possible explanation for the observed changes could be the increased flux through a bypass reaction of PKc which has a detrimental effect on low-oxygen metabolism. The bypass reactions start with the carboxylation of PEP through phosphoenolpyruvate carboxylase (PEPC) to yield oxaloacetate. Malate dehydrogenase

reduces oxaloacetate to malate being further decarboxylated to pyruvate via malic enzyme (ME). This bypass pathway does not produce ATP, which might explain the decrease in ATP content in the transgenic tubers under low-oxygen compared to wild type (Fig. 3.5). Although, oxaloacetate could not be measured, malate and aspartate which are derived from oxaloacetate were decreased in the transgenic tubers under low-oxygen relative to wild type (Fig. 3.5). Altogether, these alterations indicate a modified flux through the PEPC pathway.

A further reason for the abovementioned changes in the transgenic tubers with decreased expression of PKc under low-oxygen might be a change in the partitioning of pyruvate between the different metabolic pathways. Pyruvate can be found in all subcellular compartments, while the highest amount appears to be in the plastid of potato tubers (Farré et al. 2001). The main route of cytosolic pyruvate metabolism under normal oxygen conditions is the import into the mitochondria to feed into the TCA cycle as well as the import into the chloroplast to support branched chain amino and fatty acid synthesis in the plastid (Schulze-Siebert et al. 1984; Furumoto et al. 2011). However, plants are also able to synthesize pyruvate via a plastidial pyruvate kinase (PKp). Whereas the role of PKp in fatty acid biosynthesis is already known (Andre et al. 2007; Andre & Benning 2007), its role in the synthesis of branched chain amino acids is not yet clear. When plants face low-oxygen conditions, most of the available pyruvate is shuttled into the cytosolic ethanol and lactate fermentation pathways, whereas the remaining pyruvate pool is distributed between the mitochondria and the plastid to support mitochondrial respiration as well as amino and fatty acid synthesis (Geigenberger et al. 2000; Geigenberger 2003). Therefore, the plant has to regulate the amount of pyruvate available for respiration, fermentation and biosynthesis between the different compartments.

The inhibition of PKc in the transgenic potato tubers under low-oxygen led to a decrease in the TCA cycle intermediates citrate and aconitate (Fig. 3.5) indicating a decreased provision of pyruvate for the mitochondrial localized pathways. This finding is in agreement with the diminished accumulation of alanine in the transgenic PKc lines under low-oxygen (Fig. 3.5), as the main isoform of AlaAT is also localized in the mitochondria and, therefore, is dependent on the provision of pyruvate from the cytosol (Salvato et al. 2014). The importance of alanine fermentation for the production of ATP under hypoxia has been demonstrated in *Lotus japonicus* by Rocha et al. (2010). Indeed, the level of ATP and the ATP/ADP ratio at 4% oxygen were decreased in the transgenic PKC plants compared to wild type (Fig. 3.5), although the respiration was similar to wild type (Fig. 3.4). These findings suggest a decreased activity of the alanine fermentation pathway in the transgenic tubers under low-oxygen, resulting in a lower energy status. However, other important metabolites involved in this pathway (glutamine, glutamate, 2-oxoglutarate and succinate) were unaltered. Nevertheless, the synthesis of pyruvate derived branched chain amino acids

valine and isoleucine was also diminished in the transgenic potato tubers at 4% oxygen compared to wild type (Fig. 3.5). This decrease in the branched chain amino acid synthesis might explain the higher NADH/NAD ratio in the transgenic PKc tubers (Fig. 3.5), as the branched chain amino acid synthesis contributes to the regeneration of NAD under low-oxygen (Shimizu et al. 2010). The decrease in the pyruvate derived amino acids alanine, isoleucine and valine in the transgenic tubers under hypoxia could be indicative for a diminished partitioning of pyruvate into the mitochondria and into the amyloplast, while the provision of pyruvate for the cytosolic localized lactate fermentation is maintained (Davies & Davies 1972; Asker & Davies 1984; Paventi et al. 2007). Overall, this imbalance in pyruvate partitioning under hypoxia might explain the decrease in the energy status and the increase in the redox status in the transgenic potato tubers with decreased PKc expression.

4.3 Mitochondrial isocitrate dehydrogenase affects hypoxic metabolism and resistance in Arabidopsis plants

The characterization of an Arabidopsis mutant being deficient in the regulatory subunit of IDH revealed a 75% decrease in the maximum catalytic activity of IDH in mitochondrial enriched extracts compared to wild type (Fig. 3.6A). To check, whether other enzymes are compensating for the decrease in IDH activity in the *idhv* mutant, the maximum catalytic activity of ICDH was measured in the same extracts. The results show that there was no difference in ICDH activity between the *idhv* mutant and the wild type (Fig. 3.6B). These results are comparable with the findings of Lemaitre et al. (2007) using the same T-DNA insertion line.

To study the impact of decreased IDH activity on the low-oxygen response, root growth under hypoxia and anoxia survival rate was measured. The *idhv* mutant exhibited a consistent 10% decrease in root growth compared to wild type, when plants were treated for 48 h with 21%, 8%, or 4% oxygen (Fig. 3.8). However, a further oxygen decrease to 1% led to a 30% increase in root growth in the *idhv* mutant (Fig. 3.8). Apparently, diminished mitochondrial IDH activity leads to a better root growth, if oxygen availability is very low. To further investigate the response of *idhv* mutant and wild type to very low oxygen levels, anoxia survival experiments were carried out. The results showed a 50% increase in the anoxic survival rate of the *idhv* mutant relative to the wild type (Fig. 3.7). Possibly, the decrease in activity of IDH in the *idhv* mutant enhances the low-oxygen response compared to wild type. To verify whether the increased survival rate under anoxia in *idhv* plants is reflected by changes in hypoxia marker gene expression, wild type and *idhv* seedlings were

exposed for 16 h and 24 h to 21%, 1% and 0% oxygen in the dark. Surprisingly, the expression of *ADH1*, *SUS1* and *SUS4* at 0% oxygen was significantly lower in the *idhv* mutant compared to wild type at both time points (Fig. 3.9, Fig. 3.10). Hence, the increased anoxia survival rates in the *idhv* plants cannot be explained by an increase in hypoxia marker gene expression. Rather, it can be speculated that alterations in the metabolism of the *idhv* mutant are responsible for the increased low-oxygen tolerance compared to wild type.

To get an insight into the metabolic alterations in the *idhv* mutant, both genotypes were treated with 21%, 1% and 0% oxygen for 16 h and 24 h, and a comprehensive metabolite analysis was performed. The metabolite profile revealed an increase in starch and hexose phosphates (G6P, F6P) in the *idhv* mutant under low-oxygen compared to wild type (Fig. 3.11, Fig. 3.12). The increase in G6P and F6P is indicative for a decrease in glycolytic activity being characteristic for the response of plants to low-oxygen (Geigenberger et al. 2000; Vigeolas et al. 2003; Kreuzwieser et al. 2009; Matthew et al. 2009; Rocha et al. 2010). The lower glycolytic activity in the *idhv* mutant might also explain the increase in starch (Fig. 3.11, Fig. 3.12), as starch usually fuels glycolysis under low-oxygen conditions (Fukao & Bailey-Serres 2004). Altogether, these changes suggest that the *idhv* mutant has a more efficient carbon metabolism leading to an improved low-oxygen performance than the wild type.

Another indicator for an improved low-oxygen metabolism in the *idhv* mutant is the accumulation of alanine and succinate in the *idhv* plants relative to the wild type (Fig. 3.11, Fig. 3.12). Both metabolites are typically increased under low-oxygen conditions in plants being marker metabolites for the reorganization of the TCA cycle (Kennedy et al. 1992; Miyashita et al. 2007; Rocha et al. 2011; Narsai et al. 2011). Alanine and succinate are end products of the reorganized TCA cycle that bypasses the mitochondrial IDH reaction under low-oxygen conditions in plants (Rocha et al. 2010; António et al. 2015). The increase of succinate and alanine in the *idhv* mutant under low-oxygen (Fig. 3.11, Fig. 3.12) could be indicative for a higher activity of the bifurcated TCA cycle which additionally yields an extra ATP. Indeed, the energy status expressed as ATP/ADP ratio is higher in the *idhv* mutant under low-oxygen compared to wild type (Fig. 3.11, Fig. 3.12).

In addition to the increase of alanine and succinate, the *idhv* mutant had higher levels of aspartate, lysine and 2-hydroxyglutarate under low-oxygen conditions compared to wild type (Fig. 3.11, Fig. 3.12). These metabolites are part of an alternative pathway for the production of 2-oxoglutarate utilizing PEP to produce lysine via aspartate and oxaloacetate. Lysine is further converted to 2-hydroxyglutarate being the substrate for D2HGDH. 2-hydroxyglutarate is oxidized by D2HGDH to 2-oxoglutarate providing electrons for the electron transport chain in the mitochondria (Araújo et al. 2010; Boex-Fontvieille et al. 2013). The increased activity of this alternative pathway in the *idhv* plants can be beneficial under low-oxygen conditions, as

it couples the production of 2-oxoglutarate with the provision of electrons for the mETC, thereby, enhancing respiratory efficiency (Boex-Fontvieille et al. 2013).

The 2-hydroxyglutarate dependent pathway operating in the *idhv* mutant might also help to regulate the entry of electrons into the mETC that otherwise can lead to an over-reduction of the mETC, when respiration is inhibited, causing redox imbalances and the accumulation of ROS (Blokhina et al. 2003; Rhoads et al. 2006; Vanlerberghe 2013). A number of metabolites (Trehalose, γ-hydroxybutyrate, myo-inositol, proline and GABA) that contribute to ROS and redox homeostasis in plants (Allan et al. 2009;Szabados & Savouré 2010; Stiti et al. 2011; Valluru & Van den Ende 2012; Lunn et al. 2014; Ben Rejeb et al. 2014) are increased under low-oxygen in the *idhv* mutant relative to wild type (Fig. 3.11, Fig. 3.12). For instance, γ-hydroxybutyrate functions in the detoxification of succinic semialdehyde (SSA) which oxidizes membrane lipids, reacts with DNA and thereby causes cellular and developmental problems (Allan et al. 2009; Stiti et al. 2011). The nonproteinogenic amino acid GABA is able to scavenge ROS and helps to stabilize the cytoplasmic pH under low-oxygen conditions (Crawford et al. 1994; Liu et al. 2011; Narsai et al. 2011). In general, the detoxification of ROS is an important factor that determines plant survival under low-oxygen conditions and in the reoxygenation period (Blokhina et al. 2001; Blokhina et al. 2003; Pucciariello et al. 2012). Therefore, the increase in the aforementioned metabolites could be indicative for a higher activity of the ROS scavenging system leading to a better low-oxygen tolerance of the *idhv* mutant compared to wild-type.

An important cofactor for enzymes involved in the detoxification of ROS is NADPH which was increased in the *idhv* mutant under low-oxygen compared to wild type (Fig. 3.11, Fig. 3.12). NADPH in plants can be produced by ICDH which catalyzes the extramitochondrial oxidative decarboxylation of isocitrate to 2-oxoglutarate. Three genes encode for 4 different ICDH isoforms being located in plastids, peroxisomes and cytosol (Lemaitre & Hodges 2006; Boex-Fontvieille et al. 2013).The cytosolic isoform is responsible for up to 90% of the total cellular ICDH activity (Mhamdi, Mauve, et al. 2010) and is proposed to play a role in the regulation of the redox state of the cell (Mhamdi, Mauve, et al. 2010; Leterrier et al. 2012). Additionally, ICDH is suggested to support the scavenging of ROS under abiotic stress through supplying NADPH for the ascorbate-glutathione cycle (Marino et al. 2007; Mhamdi, Mauve, et al. 2010; Leterrier et al. 2012). Although the maximal catalytic activity of the ICDH isoforms were not different in *idhv* plants compared to wild type under normal conditions (Fig. 3.6), it cannot be ruled out that their activity *in vivo* is higher under low-oxygen conditions in the *idhv* mutant which would explain the increase of NADPH (Fig. 3.11, Fig. 3.12) and the higher low-oxygen tolerance of the *idhv* mutant compared to wild type (Fig. 3.7, Fig. 3.8).

4.4 Plastidial and extraplastidial NADPH-dependent thioredoxin reductases have contrasting effects on hypoxic gene expression, metabolism and survival in Arabidopsis plants

The results presented in this thesis provide evidence for a role of the NTR system in the response of Arabidopsis to low-oxygen. Perturbation of the cytosolic-mitochondrial NTR system in the *ntrantrb* mutant as well as perturbation of the plastidial NTR system in the *ntrc* mutant led to significant differences in the tolerance to low-oxygen compared to wild type. Anoxic survival experiments performed with both mutants revealed a 55% decrease in survival rate of the *ntrc* mutant, whereas there was a 75% increase in survival rate of the *ntrantrb* mutant compared to wild type (Fig. 3.13) suggesting a non-redundant function of both NTR systems in the low-oxygen response.

A possible reason for the lower survival rate of the *ntrc* mutant could be the decreased availability of carbohydrates for fermentation. In fact, the *ntrc* plants have decreased amounts of starch and soluble sugars under normal growth conditions (Michalska et al. 2009; Lepistö et al. 2013). However, treating the *ntrc* mutant with low-oxygen for 16 h led to an increase in starch, while glucose and fructose were clearly decreased (Fig. 3.18). Apparently, starch degradation is inhibited under low-oxygen in the *ntrc* plants. As a matter of fact, the degradation of starch is a redox regulated process (Kötting et al. 2010), and beta- amylase 1 is partly regulated by NTRC (Valerio et al. 2011) explaining the increase in starch under low-oxygen in the ntrc mutant compared to wild type (Fig. 3.18).

A decrease in starch breakdown can also affect the flux of carbon through glycolysis. Indeed, pyruvate being the end product of glycolysis was increased in the *ntrc* mutant (Fig. 3.18). It can be speculated that the increase in pyruvate is caused by lower fermentation rates under hypoxia in the *ntrc* plants. In fact, the expression of ADH under low-oxygen was lower in the *ntrc* plants compared to wild type (Fig. 3.15A) leading to an increase in the NADH/NAD ratio (Fig. 3.18) which can explain the lower anoxic survival rate of the *ntrc* mutant (Fig. 3.13) (Licausi et al. 2010; Ismond et al. 2003). The higher level of the NADH/NAD ratio under low-oxygen in the *ntrc* mutant can also be partly explained by the decrease in *HB1* expression (Fig. 3.16B), as *HB1* expression can influence the detoxification of nitric oxide in the haemoglobin/nitric oxide cycle (Hb/NO cycle) (Perazzolli et al. 2004; Igamberdiev et al. 2005). The detoxification of NO through Hb utilizes NADH, thereby decreasing the accumulation of NADH that otherwise would inhibit glycolysis under low-oxygen (Igamberdiev & Hill 2004). The decrease in activity of the Hb/NO cycle most likely triggers the accumulation of NO which is an important signaling molecule (Wilson et al. 2008) and

can inhibit the activity of the TCA cycle enzyme aconitase (Navarre et al. 2000; Gupta et al. 2012). Therefore, the accumulation of pyruvate in the *ntrc* mutant under low-oxygen could be a result of the inhibition of aconitase. However, a further analysis is necessary.

Moreover, the antioxidant ascorbate was increased in *ntrc* plants compared to wild type (Fig. 3.18). Its accumulation is associated with a disruption of flux through the TCA cycle or the mETC (Carrari et al. 2003; Nunes-Nesi et al. 2005; Zsigmond et al. 2011), as the terminal step of ascorbate synthesis is part of respiratory complex I (Schertl et al. 2012) and, thus, linked to mitochondrial function (Millar et al. 2003). The components of the mETC are organized in respiratory supercomplexes (Eubel et al. 2004; Boekema & Braun 2007) and contribute to mitochondrial ultrastructure formation (Dudkina et al. 2006). Treating plants with low-oxygen leads to mitochondrial deterioration (Shingaki-Wells et al. 2014) and dissociation of supercomplexes (Ramirez-Aguilar et al. 2011). Therefore, the increase in ascorbate in the *ntrc* plants relative to wild type (Fig. 3.18) is likely to be a consequence of altered mitochondrial function in the *ntrc* mutant under low-oxygen stress.

Additionally, ascorbate can activate G6PDH, thereby enhancing the production of NADPH under oxidative stress conditions (Córdoba-Pedregosa et al. 2005). Indeed, the *ntrc* mutant had higher NADPH levels and a higher NADPH/NADP ratio under low-oxygen (Fig. 3.18) as well as an increased activity of the plastidial G6PDH (Ina Thormählen personal communication) supporting a relationship between ascorbate levels and G6PDH (Debnam et al. 2004). Furthermore, G6PDH is a redox regulated enzyme (Wenderoth et al. 1997) that has been shown to have a higher activity under oxidative stress in the presence of H_2O_2 (Née et al. 2009).

A further reason for the increase of NADPH under low-oxygen in the *ntrc* plants is the decreased oxidation of NADPH to NADP, as NTRC is missing and the activity of the NADPH dependent 2-CP system is strongly diminished (Cejudo et al. 2012). These proteins usually use NADPH to oxidize their target enzymes or detoxify H_2O_2 (Pulido et al. 2010). Indeed, the *ntrc* mutant is characterized by higher levels of ROS and especially H_2O_2 (Pérez-Ruiz et al. 2006; Lepistö et al. 2013; Naranjo et al. 2016). The accumulation of ROS in the *ntrc* mutant could be even higher under low-oxygen conditions, as low-oxygen stress induces ROS formation (Blokhina et al. 2001; Blokhina et al. 2003; Pucciariello et al. 2012). The increase of glutathione under low-oxygen in the *ntrc* mutant compared to wild type could be caused by a potential increase of H_2O_2 in the *ntrc* plants, as H_2O_2 can also activate glutamate-cysteine ligase catalyzing the rate limiting step in glutathione biosynthesis (Hicks et al. 2007). Most likely, the increase in ascorbate and glutathione under low-oxygen in *ntrc* plants (Fig. 3.18) represents a compensation mechanism of the plant to counteract the decreased activity of NTRC regulated antioxidant enzymes (Pulido et al. 2010). A further factor that could contribute to an increase of ROS under low-oxygen is the decreased expression of AOX in

the *ntrc* mutant under hypoxia (Fig. 3.17). AOX is usually induced by altered mitochondrial function and by ROS (Juszczuk & Rychter 2003; Gray et al. 2004; Clifton et al. 2006; Bailey-Serres & Voesenek 2008) and may help in the reoxygenation phase to prevent ROS accumulation (Maxwell et al. 1999; Rhoads et al. 2006).

Surprisingly, the expression of Aox1a was repressed in *ntrc* seedlings under hypoxia (Fig. 3.17), although this gene is induced by ROS (Juszczuk & Rychter 2003; Gray et al. 2004; Clifton et al. 2006). A possible explanation for this discrepancy is the inhibition of the AOX1a gene expression by ABSCISIC ACIDINSENSITIVE-4 (ABI4) transcription factor (Kerchev et al. 2011; Foyer et al. 2012). ABI4 binds to the B element of the AOX1a promoter and represses it (Giraud et al. 2009). Intriguingly, ascorbate can regulate ABI4, thereby controlling plant growth and development (Kerchev et al. 2011; Foyer et al. 2012). Thus, the increase of ascorbate in the *ntrc* mutant under low-oxygen might be responsible for the repression of AOX1a gene induction (Fig. 3.17, Fig. 3.18). Taken together, the potential increase in ROS under low-oxygen in the *ntrc* mutant caused by the lack of NTRC might be the reason for the decrease in survival rate (Fig. 3.17).

Furthermore, the possible increase in ROS and NO in the *ntrc* mutant under low-oxygen can influence the stability of the transcription factor RAP 2.12. It belongs to the group VII ERF (Nakano et al. 2006) and is believed to be an oxygen sensor in plants (Licausi et al. 2011; Gibbs et al. 2011). RAP 2.12 is degraded via the N-end rule pathway, thereby including a step where an n-terminal cysteine is oxidized by a plant cysteine oxidase dependent on the cellular oxygen concentration (Weits et al. 2014; Kosmacz et al. 2015). In addition to oxygen availability, the presence or absence of NO can determine RAP2.12 stability (Gibbs et al. 2014). Also, increased levels of ROS can influence the oxidation of the n-terminal cysteine of RAP 2.12 (Licausi, Pucciariello, et al. 2013; van Dongen & Licausi 2014). An increase in ROS and NO in the *ntrc* mutant under low-oxygen would induce the degradation of RAP2.12 explaining the decreased expression of *ADH1* and *HB1* in the *ntrc* mutant under hypoxia (Fig. 3.15, Fig. 3.16).

In contrast to the knockout of NTRC in the chloroplast, the knockout of the cytosolic-mitochondrial NTR system in Arabidopsis led to the recovery of root growth under low-oxygen conditions and to a higher anoxic survival rate (Fig. 3.13, Fig. 3.14). These results are somewhat surprising, as both, the *ntrc* and the *ntrantrb* mutant, have less starch reserves under normal growth conditions (Michalska et al. 2009; Daloso et al. 2015), but accumulated starch at 1% oxygen indicating inhibition of starch breakdown (Fig. 3.18). However, NTRA and NTRB are not active in the chloroplast, so that a direct effect on starch breakdown can be excluded. Instead, a possible explanation for the decreased starch breakdown under low-oxygen in the *ntrantrb* plants might be found in a decrease of energy in the form of ATP (Fig. 3.18). This could be a consequence of a decreased activation of the mitochondrial ATP

synthase that is a potential target of the NTR dependent Trx o1 (Yoshida et al. 2013). As starch degradation requires phosphorylation (Silver et al. 2013), a decrease in the availability of ATP might inhibit a-glucan, water dikinase and phosphoglucan, water dikinase in the *ntrantrb* mutant under low-oxygen. Although starch degradation appears to be blocked, downstream metabolites like glucose, fructose, PEP and pyruvate were unaltered under low-oxygen in the *ntrantrb* mutant (Fig. 3.18). Moreover, the unchanged levels of pyruvate are rather surprising as Daloso et al. (2015) showed a strong deregulation of TCA cycle enzymes in the *ntrantrb* mutant and altered fluxes in glycolysis and in the TCA cycle. These changes are a consequence of an increased oxidation of Trx o and h, which are supposed to be the unique targets of NTRA and NTRB (Reichheld et al. 2007).

While the alterations in starch metabolism cannot explain the increased low-oxygen tolerance in the *ntrantrb* mutant, it is possible that the increase in *ADH1* expression under hypoxia (Fig. 3.15B) contributes to the increase in low-oxygen tolerance in *ntrantrb* plants. As *ADH1* is part of the ethanol fermentation pathway, increased ethanol fermentation helps the plant to survive low-oxygen conditions (Ellis et al. 1999; Licausi et al. 2010; Ismond et al. 2003). An indicator for increased ethanol fermentation is the lower NADH/NAD ratio under hypoxia in the *ntrantrb* mutant compared to wild type (Fig. 3.18), as the production of ethanol through ADH consumes NADH and helps the plant to sustain glycolytic activity under oxygen deprivation. Also, the operation of the Hb/NO cycle consumes NADH under hypoxic conditions (Igamberdiev et al. 2005), whereby overexpression of Hb increases low-oxygen survival (Hunt et al. 2002; Thiel et al. 2011). In fact, *HB1* expression was increased in the *ntrantrb* plants relative to wild type at 1% oxygen (Fig. 3.16B) contributing to the higher low-oxygen tolerance of the mutant.

Another important factor determining plant survival under oxygen deprivation is the ascorbate-glutathione cycle (Blokhina et al. 2003). Interestingly, both antioxidants were slightly decreased in the *ntrantrb* mutant at 21% oxygen, but recovered at 1% oxygen relative to wild type (Fig. 3.18). The relative increase in glutathione at the oxygen decrease from 21% to 1% in the *ntrantrb* mutant might also explain the recovery of root growth under low-oxygen (Fig. 3.18), as root growth is influenced by the level of glutathione in the root meristem (Bashandy et al. 2010). Although, the total glutathione pool recovered under low-oxygen in the *ntrantrb* mutant relative to wild type, GSSG increased at 1% oxygen concentration by 30% compared to 21% oxygen concentration in the *ntrantrb* mutant indicating an increased oxidation state of glutathione (Fig. 3.18).

The ratio of GSH to GSSG is determined by glutathione reductase (GR) which exists as two isoforms (GR1, GR2) being located in different subcellular compartments (Mhamdi, Hager, et al. 2010; Kataya & Reumann 2010; Yu et al. 2013). The increase in GSSG at 1% oxygen in the *ntrantrb* mutant points to a possible involvement of NTRA or NTRB in the regulation of

4. Discussion

GR activity in vivo. However, as of today, no data is available about the post-transcriptional regulation of GR.

The higher oxidation state of glutathione may also influence the activity of glutaredoxins which depend on the redox status of glutathione (Meyer et al. 2008; Meyer et al. 2012). Recent publications suggest an overlapping function of glutaredoxins and Trxs, possibly explaining the weak phenotype of the *ntrantrb* double mutant (Marty et al. 2009; Reichheld et al. 2007; Meyer et al. 2012). Indeed, glutaredoxins are able to reduce Trx-h3 which is the most abundant cytosolic Trx and also a target of NTRA and NTRB (Reichheld et al. 2007).

A putative target of the mitochondrial Trx system is AOX (Gelhaye et al. 2004; Yoshida et al. 2013). It contains two cysteins, whereby Cys_I, when reduced can interact with organic acids like pyruvate, thereby activating AOX (Umbach et al. 2006). Since the mitochondrial Trx system is more oxidized in the *ntrantrb* mutant than in the wild type (Bashandy et al. 2009; Reichheld et al. 2005; Reichheld et al. 2007), AOX should be less active in these plants. However, at least the expression of *AOX1a* under low-oxygen was not altered in the *ntrantrb* mutant in comparison with the wild type (Fig. 3.18). Also, pyruvate, being a potent activator of AOX, was not different in the *ntrantrb* plants relative to wild type (Fig. 3.18). It is unlikely that AOX activity is altered in the *ntrantrb* mutant, so this can also not explain the increased survival rates of the *ntrantrb* double knockout (Fig. 3.13).

Yet, the more oxidized Trx system in the *ntrantrb* mutant affects the activity of certain TCA cycle enzymes including IDH according to Daloso et al. (2015). The authors showed a 60% decrease in IDH activity in the *ntrantrb* mutant being comparable to the values obtained for the t-DNA insertion line used in this thesis (chapter 3.3). Thus, the superior performance under low-oxygen of the *ntrantrb* mutant compared to wild type can at least be partly attributed to the decrease in IDH activity which improves the survival of Arabidopsis under low-oxygen (see chapter 4.3).

4.5 Beta-estradiol inducible amiRNA *SNF4* silencing lines have a decreased low-oxygen tolerance than the wild type, suggesting a role of SnRK1 in regulating low-oxygen responsive gene expression, metabolism and survival in Arabidopsis plants

It has been shown that the regulatory SNF4 subunit influences the activity of the metabolic energy sensor SnRK1 (Polge & Thomas 2007; Robaglia et al. 2012; Crozet et al. 2014), thus, it is particularly interesting to study its role during hypoxia. Unfortunately, there is no T-DNA insertion line available, because disruption of *snf4* caused chromatid non-disjunction in male meiosis II (Csaba Koncz, unpublished). Therefore, Arabidopsis plants with a beta-estradiol inducible amiRNA SNF4 construct were used to explore the effect of transcriptional silencing of SNF4 during low-oxygen stress. First of all, those plants were characterized in terms of SNF4 silencing efficiency and growth. Applying beta-estradiol into the plant agar led to a 70% decrease after 7 days (Fig. 3.20) and, concomitantly, plant growth was inhibited by 35% and root growth by 25% (Fig. 3.21, Fig. 3.22). In comparison, altering SNF4 activity in *Medicago trunculata* seeds has no impact on the weight of fresh or dry seeds, but leads to a decreased seed longevity and changed stachyose and sucrose content, thus pointing to a role of SNF4 in regulating carbon metabolism (Rosnoblet et al. 2007). Thus, the decrease in growth in the amiRSNF4 plants could be explained by an imbalance between catabolism and anabolism. This seems plausible, as SnRK1 is suggested to regulate anabolism and catabolism under fluctuating conditions (Baena-González & Sheen 2008; Robaglia et al. 2012).

Treatment of amiRSNF4 plants with low-oxygen revealed a consistent 30% to 40% decrease in root growth under 8%, 4% and 1% oxygen relative to the wild type (Fig. 3.24). However, this decrease in root growth was as strong as the decrease at normoxic conditions in the amiRSNF4 plants compared to wild type (Fig. 3.24). Apparently, the low-oxygen stress was not severe enough to affect the amiRSNF4 plants any further. Indeed, the expression of the low-oxygen induced genes was not changed at 1% oxygen in the amiRSNF4 plants in comparison with the wild type (Fig. 3.25). Also, the metabolite profile in the amiRSNF4 plants under hypoxia revealed only minor changes compared to the drastic changes occurring under anoxic conditions relative to the wild type (Fig. 3.26). Concomitantly, amiRSNF4 plants showed a 70% decrease in anoxic survival rate relative to the wild type (Fig. 3.26). The inactivation of the catalytic KIN10 subunit of SnRK1 has a similar effect, as shown by Cho et al. (2012). Arabidopsis seedlings without functional catalytic subunit of SnRK1 could not withstand 37 days of submergence. The authors explained this observation with a lack of

induction in *PDC1* and *ADH1* expression. Both proteins are part of the ethanol pathway enhancing survival under low-oxygen conditions (Jacobs et al. 1988; Ellis et al. 1999). A decrease in overall fermentation activity could be responsible for the decrease in survival of the amiRSNF4 plants. In fact, there is evidence that fermentation is restricted in the amiRSNF4 plants. First of all, *ADH1* expression was decreased by 65% under anoxia in the amiRSFN4 plants relative to wild type (Fig. 3.25A). Secondly, the accumulation of lactate was 50% lower under the same conditions in amiRSNF4 plants in comparison with the wild type. Thirdly, sugars and starch were increased by 40% to 60% under anoxia in the amiRSNF4 line compared to wild type (Fig. 3.26). Thus, both lactate and ethanol fermentations were compromised in the amiRSNF4 plants. The decrease in *ADH1* mRNA could possibly be explained by SnRK1 not being able to associate with the chromatin sequence of *ADH1* without functional SNF4 subunit (Cho et al. 2012). Whether LDH activity is controlled by SnRK1 in a similar way or through posttranslational phosphorylation, is not yet clear. Nevertheless, the restriction of fermentation in the amiRSNF4 plants should lead to an accumulation of pyruvate, as it is the only substrate for both fermentation pathways. Conversely, PEP was increased, while pyruvate was slightly decreased and downstream metabolites like citrate and isocitrate in the TCA cycle were significantly decreased under anoxia in the amiRSNF4 plants compared to wild type (Fig. 3.26). These findings indicate a regulation of cytosolic pyruvate kinase by SnRK1. Indeed, Beczner et al. (2010) could demonstrate an interaction between SnRK's and a PKc in potato. However, further studies in Arabidopsis are necessary to determine the interaction between SnRK1 and PKc.

In addition to the potential role of SnRK1 in the control of glycolysis, Lee et al. (2009) have shown that SnRK1 is responsible to provide sugars for fermentation under low-oxygen in rice. They provided evidence that SnRk1 and its upstream kinase CIPK15 are needed to transcribe an amylase which is necessary to produce sugars from the stored starch reserves for fermentation under submergence. In addition to starch, the supply of sucrose likewise supports fermentation under low-oxygen conditions. In the amiRSNF4 plants sucrose accumulated more than 2-fold and the expression of *SUS1* was decreased by 55% and *SUS4* by 25% under anoxia relative to the wild type (Fig. 3.25C and D, Fig. 3.26). Both isoforms of SuSy are highly induced under low-oxygen (Santaniello et al. 2014) being important for plant survival under low-oxygen conditions, as they provide an energy benefit in the cleavage of sucrose compared to invertase (Stitt 1998). The data presented in chapter 3.5 provide evidence that SnRK1 might be involved in the regulation of SuSy transcription under anoxia. An involvement of SnRK's in SuSy function was already shown by Purcell et al. (1998) and McKibbin et al. (2006). Antisense lines of potato sucrose nonfermenting-1 (SNF1)-related protein kinase displayed lower SuSy transcript level and activity, whereas

SNRK1 over-expressor lines had increased SuSy transcript level and activity (Purcell et al. 1998; McKibbin et al. 2006).

In addition to the fermentation products ethanol and lactate, GABA usually accumulates in plants under low-oxygen (van Dongen et al. 2003; Branco-Price et al. 2008; Narsai et al. 2009; Kreuzwieser et al. 2009; Zabalza et al. 2011). In the amiRSNF4 plants the accumulation of GABA under anoxia was even increased in comparison with the wild type (Fig. 3.26). One of its function is the stabilization of cytoplasmic pH, as GABA synthesis from glutamate consumes one proton (Crawford et al. 1994). This reaction which is catalyzed by glutamate decarboxylase depends on the Ca^{2+}/calmodulin system (Snedden et al. 1995; Baum et al. 1996) and contributes to Ca^{2+} homeostasis under low-oxygen stress (Shabala et al. 2014). The hypoxic induced release of Ca^{2+} into the cytosol (Subbaiah et al. 1998) activates plasma membrane NADPH oxidases (Lecourieux et al. 2002) that produce H_2O_2 and eventually damage the cell. GABA is able to restore normal Ca^{2+} levels via multiple mechanisms (Demidchik et al. 2007) circumventing the increase of H_2O_2. Another explanation for the higher GABA levels in the amiRSNF4 mutant (Fig. 3.26) is the possible inhibition of GABA transaminase which catalyzes the conversion of GABA to SSA. SSA itself is used by succinate semialdehyde dehydrogenase (SSADH), being part of the GABA shunt, to produce succinate for the TCA cycle. The increase in the NADH/NAD ratio under anoxia in the amiRSNF4 plants relative to wild type (Fig. 3.26) can inhibit SSADH (Busch & Fromm 1999) leading to the accumulation of γ-hydroxybutyrate in the amiRSNF4 plants under anoxia (Fig. 3.26). This could be a protective mechanism against the overaccumulation of ROS which is caused by dysfunction of SSADH (Bouché et al. 2003). Also, conversion of SSA to γ-hydroxybutyrate regenerates NAD being needed to sustain glycolysis (Breitkreuz et al. 2003).

A higher NADH/NAD ratio in the amiRSNF4 plants under anoxia may also be related to the lower expression of *HB1* (Fig. 3.25B, Fig. 3.26). Hypoxic conditions induce the expression of *HB1* (Dordas, Rivoal, et al. 2003; Licausi et al. 2010) functioning in the detoxification of NO (Perazzolli et al. 2004). The proposed Hb/NO cycle helps the plant to maintain NADH oxidation, when mitochondrial respiration is inhibited (Igamberdiev & Hill 2004; Dordas, Rivoal, et al. 2003). Furthermore, increased Hb expression leads to a higher ATP/ADP ratio and, subsequently, to improved survival under low-oxygen conditions (Sowa et al. 1998; Hunt et al. 2002; Dordas, Hasinoff, et al. 2003; Thiel et al. 2011). Whereas the ATP/ADP ratio was unaltered under anoxia in the amiRSNF4 seedlings relative to wild type (Fig. 3.26), it is likely that the decreased *HB1* expression contributes to the higher redox state and, as a consequence, leads to the lower anoxia tolerance of amiRSNF4 plants (Fig. 3.23, Fig. 3.25B).

4. Discussion

While there is no evidence in the literature for a direct regulation of Hb by SnRK1, SnRK1 and Hb could be linked through the activity of nitrate reductase producing NO. NR is the main producer of NO under low-oxygen (Planchet et al. 2005; Gupta et al. 2012) and the activity of NR is highly induced in Arabidopsis plants under anoxia (personal communication by Martin Gänsheimer). As NR is one of the putative targets of SnRK1 (Christopher Sugden et al. 1999), activity measurements of NR revealed an inhibition of NR in the amiRSNF4 plants (personal communication by Martin Gänsheimer). The decreased activity of NR could lead to lower NO production and, hence, to lower induction of Hb. A general coordinated regulation of NR and Hb expression as well as activity could be already demonstrated in two studies (Trevisan et al. 2011; Thiel et al. 2011).

In addition to its function in the production of NO, NR also plays an important role in nitrogen metabolism reducing nitrate to nitrite. NR activity is regulated by asparagine (Oaks et al. 1977; Sivasankar et al. 1995) which is another important nitrogen storage and transport compound.

In the amiRSNF4 plants asparagine was decreased, whereas its precursor aspartate was increased at 0% oxygen compared to wild type (Fig. 3.26) pointing to an inhibition of asparagine synthesis under anoxia. The majority of the asparagine pool in plants is synthesized by the glutamine-dependent asparagine synthase 1 (ASN1) (Lam et al. 2003; Gaufichon et al. 2010) being induced by various stresses like darkness and hypoxia (Baena-González et al. 2007). Interestingly, Baena-Gonzales et al (2007) could show that ASN1 is specifically activated by SnRK1 under energy/sugar starvation conditions. It can be speculated that decreased SNF4 expression in the amiRSNF4 plants leads to an inefficient activation of ASN1. This would also explain the increase in all the other amino acids in the amiRSNF4 plants under anoxia as compensatory mechanism (Fig. 3.26). Lam et al. (2003) have demonstrated that overexpression of ASN1 in Arabidopsis leads to a change in amino acid composition between aspartate and glutamate derived amino acids. Another explanation for the increase in amino acids in the amiRSFN4 plants under anoxia is the potential crosstalk of SnRK1 with the target of rapamycin (TOR) (Robaglia et al. 2012; Tome et al. 2014). TOR is a serine/threonine kinase involved in seed yield, cell size and stress resistance (Ren et al. 2012). Tomé et al. (2014) could show a substantial overlap of genes that are upregulated by the SnRk1 subunit KIN10 and downregulated by TOR and vice versa. The overlapping genes have functions in amino acid and carbon metabolism (Tome et al. 2014). It is possible that silencing of SNF4 disturbs the putative interaction of SnRK1 with TOR leading to the accumulation of amino acids under anoxia in amiRSNF4 plants caused by inhibition of TOR (Moreau et al. 2012; Ren et al. 2012).

5 Appendix

Supplemental Table 1: Dataset of time-resolved changes in the levels of metabolites in wild type potato tubers incubated with 21% oxygen. Potato plants were grown in the greenhouse under long day conditions (16 h light/8 h dark). Tubers were harvested from 12-week-old plants. After 60 min of pre-incubation in buffer equilibrated with 21% oxygen, half of the potato tuber slices were transferred to 4% oxygen. The remaining potato tuber slices were further incubated with 21% oxygen, and tuber discs were sampled at the indicated time points. Tuber discs were sampled by shock-freezing in liquid nitrogen to immediately quench the metabolism in the tissue. Metabolite levels were measured by profiling via GC-MS (relative response ratio) or by enzymatic assays (nmol/g fw^{-1} or µmol/g fw^{-1}). Results are the mean ± SE, n = 3 biological replicates.

metabolite	unit	0 min			15 min			30 min			60 min		
sugars													
Fructose	nmol/g fw^{-1}	70.00	±	9.31	41.81	±	5.32	48.13	±	5.80	45.83	±	5.51
Glucose	nmol/g fw^{-1}	116.72	±	26.38	169.75	±	115.05	155.90	±	110.08	120.00	±	86.41
Sucrose	µmol/g fw^{-1}	2.76	±	0.27	1.93	±	0.02	2.20	±	0.14	1.96	±	0.23
sugar alcohols													
Galactinol	relative response ratio	6.06	±	1.65	6.56	±	0.12	5.57	±	0.67	6.55	±	1.89
Mannitol	relative response ratio	3.66	±	0.41	3.57	±	0.20	3.09	±	0.15	2.93	±	0.62
Myo-Inositol	relative response ratio	2.25	±	0.20	2.36	±	0.08	2.07	±	0.03	1.70	±	0.29
Phosphate ester													
3-Phosphoglycerate	nmol/g fw^{-1}	40.01	±	5.70	34.74	±	7.11	38.85	±	2.77	36.20	±	2.76
Dihydroxyacetone phosphate	nmol/g fw^{-1}	3.19	±	0.06	2.85	±	0.06	2.85	±	0.11	2.97	±	0.30
Fructose 1,6-bisphosphate	nmol/g fw^{-1}	0.86	±	0.10	0.91	±	0.15	1.20	±	0.36	1.31	±	0.06
Fructose-6-phosphate	relative response ratio	5.33	±	1.73	7.16	±	0.63	6.87	±	1.15	9.23	±	0.69
Glucose-6-phosphate	relative response ratio	5.05	±	1.69	5.76	±	0.06	5.37	±	0.25	7.56	±	1.05
Glyceraldehyde 3-phosphate	nmol/g fw^{-1}	1.03	±	0.10	0.97	±	0.06	1.48	±	0.11	1.88	±	0.36
Glycerol-3-phosphate	relative response ratio	6.82	±	0.55	7.44	±	0.70	8.30	±	0.48	6.65	±	0.84
Phosphoenolpyruvate	nmol/g fw^{-1}	5.45	±	0.16	3.92	±	0.58	3.38	±	0.23	2.80	±	0.32
UDP-glucose	nmol/g fw^{-1}	44.65	±	0.65	39.58	±	5.02	41.75	±	1.55	35.92	±	1.45
Organic acids													
2-Oxoglutarate	nmol/g fw^{-1}	22.74	±	2.45	24.09	±	0.24	25.71	±	1.80	31.77	±	5.50
Aconitate	relative response ratio	5.57	±	0.71	6.79	±	0.73	6.82	±	0.99	3.16	±	1.16
Benzoate	relative response ratio	4.92	±	1.50	5.77	±	2.42	3.77	±	0.84	2.27	±	0.40
Citrate	relative response ratio	13.66	±	3.04	14.66	±	4.60	10.35	±	0.51	10.78	±	1.38
Fumarate	relative response ratio	12.05	±	1.04	13.27	±	1.83	12.46	±	0.32	11.44	±	3.14
Galactarate	relative response ratio	5.14	±	0.54	5.77	±	0.24	5.80	±	1.42	5.24	±	1.36
Glycerate	relative response ratio	5.89	±	0.74	10.20	±	1.96	9.62	±	2.72	8.87	±	2.01
Isocitrate	nmol/g fw^{-1}	290.19	±	41.07	294.57	±	30.93	276.72	±	15.25	263.77	±	40.26
Itaconate	relative response ratio	5.04	±	1.19	7.41	±	2.16	4.48	±	0.24	3.79	±	2.28
Lactate	relative response ratio	2.87	±	0.98	2.54	±	1.12	1.36	±	0.34	1.34	±	0.15
Malate	relative response ratio	8.12	±	1.17	8.23	±	1.02	9.23	±	1.42	9.44	±	1.49
Nicotinate	relative response ratio	11.61	±	0.99	10.88	±	0.86	10.98	±	0.25	8.54	±	0.90
Oxalate	relative response ratio	11.19	±	3.60	10.76	±	1.39	8.77	±	1.14	7.88	±	0.82
Pyruvate	nmol/g fw^{-1}	5.30	±	0.30	5.50	±	0.40	7.96	±	1.01	8.34	±	0.50
Quinate	relative response ratio	6.32	±	0.32	7.43	±	0.29	6.34	±	0.91	7.47	±	0.91
Shikimate	relative response ratio	6.62	±	1.05	7.41	±	0.90	9.12	±	1.33	6.53	±	0.95
Succinate	relative response ratio	6.08	±	1.49	6.94	±	0.78	8.03	±	1.15	7.54	±	0.41
Threonate	relative response ratio	4.41	±	0.96	5.73	±	0.62	5.99	±	1.02	5.17	±	1.01

5. Appendix

Amino Acids

Alanine	relative response ratio	8.09	±	2.42	7.09	±	0.94	8.05	±	1.99	4.71	±	0.52
Arginine	relative response ratio	3.69	±	2.28	2.96	±	1.52	6.54	±	2.36	3.50	±	0.86
Asparagine	relative response ratio	6.72	±	3.54	4.63	±	0.50	5.81	±	1.34	3.45	±	0.23
Aspartate	relative response ratio	7.58	±	1.89	6.86	±	0.70	5.63	±	1.47	4.78	±	0.55
beta-Alanine	relative response ratio	3.04	±	0.48	3.27	±	0.24	2.61	±	0.48	2.75	±	0.38
Gaba	relative response ratio	1.50	±	0.30	3.27	±	0.81	1.15	±	0.95	2.19	±	0.47
Glutamate	relative response ratio	5.21	±	1.01	4.20	±	0.57	4.39	±	0.96	3.58	±	0.51
Glutamine	relative response ratio	0.33	±	0.08	0.48	±	0.10	0.73	±	0.09	0.26	±	0.02
Glycine	relative response ratio	1.50	±	0.27	1.39	±	0.02	1.55	±	0.21	1.23	±	0.10
Isoleucine	relative response ratio	5.85	±	2.74	3.46	±	0.66	5.11	±	3.40	1.76	±	1.13
Lysine	relative response ratio	2.50	±	0.48	2.58	±	0.14	3.15	±	0.74	2.04	±	0.33
Methionine	relative response ratio	6.37	±	1.71	5.06	±	1.66	5.66	±	3.10	3.40	±	1.05
Ornithine	relative response ratio	2.16	±	0.76	2.95	±	0.59	3.14	±	1.61	3.86	±	0.50
Phenylalanine	relative response ratio	3.98	±	0.56	4.23	±	0.41	4.26	±	1.07	3.68	±	0.29
Pyroglutamate	relative response ratio	7.31	±	0.74	5.72	±	0.43	5.62	±	0.50	4.46	±	0.36
Serine	relative response ratio	6.38	±	1.84	6.42	±	0.86	7.57	±	1.12	5.02	±	0.74
Threonine	relative response ratio	10.78	±	2.70	9.98	±	1.28	11.86	±	1.70	8.40	±	1.21
Tryptophane	relative response ratio	3.48	±	1.45	5.12	±	1.73	5.07	±	0.98	1.77	±	0.59
Tyrosine	relative response ratio	2.22	±	0.55	2.88	±	0.45	3.71	±	0.54	2.93	±	0.30
Valine	relative response ratio	7.98	±	2.68	9.88	±	1.90	8.80	±	1.59	6.24	±	0.24

Nucleotides

ADP	nmol/g fw^{-1}	7.39	±	0.12	6.14	±	0.51	6.10	±	0.91	5.52	±	0.36
ATP	nmol/g fw^{-1}	48.18	±	1.60	51.70	±	6.83	54.36	±	1.20	53.25	±	1.85
GDP	nmol/g fw^{-1}	1.63	±	0.28	0.97	±	0.25	1.28	±	0.14	0.83	±	0.10
GTP	nmol/g fw^{-1}	6.96	±	0.27	6.19	±	0.52	6.76	±	0.14	6.41	±	0.15
NAD	nmol/g fw^{-1}	76.18	±	3.28	70.80	±	3.55	70.27	±	2.14	74.04	±	5.14
NADH	nmol/g fw^{-1}	7.52	±	0.33	5.25	±	0.45	4.75	±	0.35	5.14	±	0.47
NADP	nmol/g fw^{-1}	6.00	±	0.24	5.98	±	0.28	6.17	±	0.20	6.42	±	0.20
NADPH	nmol/g fw^{-1}	10.64	±	0.72	7.27	±	0.43	7.37	±	0.34	6.57	±	1.07
UDP	nmol/g fw^{-1}	1.04	±	0.18	1.01	±	0.03	0.89	±	0.13	0.56	±	0.14
UTP	nmol/g fw^{-1}	10.34	±	0.43	7.47	±	2.25	7.08	±	0.58	4.43	±	0.55

Others

Uracil	relative response ratio	1.06	±	0.43	1.34	±	0.45	1.08	±	0.13	0.95	±	0.39
Putrescine	relative response ratio	1.70	±	0.18	1.42	±	0.11	1.48	±	0.79	1.29	±	0.29

Metabolite ratios

ATP/ADP	ratio	6.52	±	0.11	7.52	±	0.93	9.43	±	1.74	9.76	±	0.90
GTP/GDP	ratio	4.22	±	0.64	5.72	±	0.47	7.55	±	1.53	11.90	±	0.33
NADH/NAD	ratio	0.10	±	0.00	0.07	±	0.01	0.07	±	0.01	0.07	±	0.01
NADPH/NADP	ratio	1.78	±	0.19	1.22	±	0.04	1.20	±	0.02	1.04	±	0.20
PEP/Pyr	ratio	1.04	±	0.08	0.71	±	0.06	0.43	±	0.03	0.34	±	0.05
UTP/UDP	ratio	7.37	±	1.88	5.23	±	0.50	7.91	±	1.05	13.46	±	4.02

Supplemental Table 2: Dataset of time-resolved changes in the levels of metabolites in wild type potato tubers incubated with 4% oxygen. Potato plants were grown in the greenhouse under long day conditions (16 h light/8 h dark). Tubers were harvested from 12-week-old plants. After 60 min of pre-incubation in buffer equilibrated with 21% oxygen, potato tuber slices were transferred to 4% oxygen and sampled at different time points (1, 2, 3, 4, 5, 6, 7, 15, 30, 60 min). Tuber discs were sampled by direct shock-freezing in liquid nitrogen to immediately quench the metabolism in the tissue. Metabolite levels were measured by profiling via GC-MS (relative response ratio) or by enzymatic assays (nmol/g fw^{-1} or µmol/g fw^{-1}). Results are the mean ± SE, n = 3 biological replicates.

Metabolite	unit	1 min	2 min	3 min	4 min	5 min	6 min	7 min	8 min	15 min	30 min	60 min
sugars												
Fructose	nmol/g fw^{-1}	42.21 ± 1.40	68.19 ± 22.29	131.66 ± 63.13	66.22 ± 5.87	103.16 ± 44.64	44.07 ± 11.29	60.79 ± 7.06	44.02 ± 13.88	50.19 ± 3.91	50.64 ± 8.75	39.51 ± 5.84
Glucose	nmol/g fw^{-1}	218.56 ± 120.98	89.48 ± 17.73	204.60 ± 83.48	282.31 ± 179.15	129.01 ± 99.33	108.82 ± 56.21	77.85 ± 16.12	93.03 ± 25.65	148.75 ± 53.02	77.21 ± 22.21	219.38 ± 110.68
Sucrose	µmol/g fw^{-1}	2.50 ± 0.19	2.55 ± 0.15	2.22 ± 0.23	2.74 ± 0.05	2.57 ± 0.11	2.16 ± 0.21	2.51 ± 0.18	2.33 ± 0.11	2.29 ± 0.04	2.09 ± 0.13	2.01 ± 0.28
sugar alcohols												
Galactinol	relative response ratio	6.91 ± 3.19	7.49 ± 1.62	6.65 ± 0.97	9.93 ± 2.71	7.75 ± 1.04	7.25 ± 1.51	7.72 ± 1.22	7.30 ± 1.04	6.54 ± 1.02	6.41 ± 1.23	7.23 ± 1.66
Mannitol	relative response ratio	3.94 ± 1.09	3.33 ± 0.30	3.67 ± 0.37	4.28 ± 0.19	3.52 ± 0.19	3.58 ± 0.57	3.61 ± 0.14	3.45 ± 0.15	3.43 ± 0.41	3.28 ± 0.37	3.03 ± 0.38
Myo-Inositol	relative response ratio	2.94 ± 1.04	2.48 ± 0.25	2.60 ± 0.21	2.92 ± 0.35	2.91 ± 0.31	2.97 ± 0.70	2.83 ± 0.09	2.53 ± 0.26	2.54 ± 0.41	2.43 ± 0.49	2.65 ± 0.30
Phosphate ester												
3-Phosphoglycerate	nmol/g fw^{-1}	43.40 ± 4.41	51.88 ± 2.44	30.69 ± 2.40	43.95 ± 5.32	44.01 ± 7.19	30.43 ± 6.22	59.67 ± 6.97	30.24 ± 4.44	39.32 ± 4.61	28.72 ± 3.88	33.50 ± 2.20
Dihydroxyacetone phosphate	nmol/g fw^{-1}	3.06 ± 0.18	2.97 ± 0.41	2.51 ± 0.11	2.62 ± 0.23	2.74 ± 0.00	2.62 ± 0.23	3.48 ± 0.32	3.82 ± 0.15	3.16 ± 0.30	2.70 ± 0.11	2.94 ± 0.30
Fructose 1,6-bisphosphate	nmol/g fw^{-1}	0.64 ± 0.04	0.86 ± 0.17	1.20 ± 0.10	1.20 ± 0.10	1.37 ± 0.36	1.20 ± 0.10	1.71 ± 0.00	1.54 ± 0.10	1.34 ± 0.18	1.45 ± 0.09	1.41 ± 0.09
Fructose-6-phosphate	relative response ratio	14.68 ± 4.71	6.15 ± 1.33	10.08 ± 0.93	12.03 ± 5.19	9.81 ± 2.87	7.62 ± 2.94	9.56 ± 1.59	15.10 ± 4.44	9.12 ± 1.72	8.78 ± 1.81	7.78 ± 1.81
Glucose-6-phosphate	relative response ratio	11.33 ± 3.39	4.97 ± 0.81	8.68 ± 0.15	11.14 ± 3.66	8.24 ± 2.48	6.00 ± 2.40	8.08 ± 1.36	10.45 ± 4.98	8.14 ± 1.24	7.59 ± 1.72	6.90 ± 1.16
Glyceraldehyde 3-phosphate	nmol/g fw^{-1}	1.00 ± 0.03	0.91 ± 0.11	1.03 ± 0.00	1.14 ± 0.11	1.20 ± 0.17	1.37 ± 0.10	1.20 ± 0.10	1.14 ± 0.11	1.56 ± 0.23	1.17 ± 0.10	1.47 ± 0.11
Glycerol-3-phosphate	relative response ratio	8.17 ± 0.91	9.31 ± 0.97	9.12 ± 2.56	8.03 ± 0.75	10.11 ± 3.55	11.61 ± 2.95	11.15 ± 1.60	9.80 ± 1.02	10.20 ± 2.06	10.37 ± 1.91	8.48 ± 1.83
Phosphoenolpyruvate	nmol/g fw^{-1}	4.49 ± 0.42	5.10 ± 0.46	4.86 ± 0.29	4.61 ± 0.57	3.59 ± 0.77	3.54 ± 0.49	4.09 ± 0.20	3.66 ± 0.39	3.01 ± 0.38	2.71 ± 0.29	3.37 ± 0.30
UDP-glucose	nmol/g fw^{-1}	45.30 ± 4.78	42.56 ± 3.59	44.06 ± 2.44	47.17 ± 4.74	50.30 ± 2.64	44.47 ± 5.79	51.31 ± 7.85	49.57 ± 3.94	47.55 ± 2.54	44.92 ± 1.28	46.63 ± 1.43
Organic acids												
2-Oxoglutarate	nmol/g fw^{-1}	20.74 ± 3.51	23.81 ± 2.17	24.44 ± 1.81	25.39 ± 1.02	21.11 ± 1.42	22.08 ± 2.82	16.05 ± 1.56	19.62 ± 2.42	23.29 ± 2.04	18.75 ± 2.50	31.48 ± 2.09
Aconitate	relative response ratio	7.26 ± 1.31	4.88 ± 1.43	7.25 ± 4.35	4.29 ± 1.10	8.99 ± 3.71	9.07 ± 2.48	6.38 ± 1.84	7.37 ± 1.10	9.29 ± 2.03	10.73 ± 2.29	10.20 ± 0.38
Benzoate	relative response ratio	4.55 ± 0.17	2.92 ± 0.85	8.00 ± 2.91	4.09 ± 1.10	11.15 ± 8.25	4.09 ± 0.84	2.07 ± 0.24	4.78 ± 2.17	3.66 ± 0.48	7.40 ± 2.22	2.52 ± 0.07
Citrate	relative response ratio	14.94 ± 2.70	12.83 ± 1.53	13.53 ± 1.93	14.65 ± 1.32	15.12 ± 3.73	16.22 ± 4.64	12.45 ± 1.21	14.04 ± 0.87	16.92 ± 0.48	12.85 ± 3.48	24.09 ± 5.91
Fumarate	relative response ratio	17.94 ± 1.00	11.60 ± 0.68	15.47 ± 7.73	11.99 ± 3.14	14.46 ± 2.20	15.24 ± 5.01	11.54 ± 1.94	12.62 ± 1.18	15.22 ± 2.58	16.05 ± 3.58	14.97 ± 0.97
Galactarate	relative response ratio	6.65 ± 1.81	6.92 ± 0.13	7.11 ± 1.31	8.55 ± 1.75	7.55 ± 0.91	6.55 ± 1.33	7.48 ± 1.02	6.55 ± 1.17	7.31 ± 1.01	6.74 ± 1.62	6.54 ± 0.52
Glycerate	relative response ratio	10.30 ± 0.63	9.15 ± 1.85	20.36 ± 10.36	14.12 ± 1.77	11.01 ± 4.40	7.35 ± 1.23	9.36 ± 1.21	7.98 ± 2.73	12.36 ± 0.41	10.72 ± 2.66	13.75 ± 1.08
Isocitrate	nmol/g fw^{-1}	265.85 ± 14.25	343.47 ± 11.78	328.16 ± 8.89	296.97 ± 10.69	337.51 ± 4.45	315.87 ± 3.63	353.84 ± 5.43	320.73 ± 2.11	285.36 ± 3.35	374.92 ± 12.22	329.74 ± 13.95
Itaconate	relative response ratio	9.12 ± 3.93	5.19 ± 2.50	7.14 ± 3.38	3.08 ± 1.58	9.23 ± 4.05	6.20 ± 0.77	5.57 ± 2.61	5.85 ± 1.94	10.00 ± 2.36	13.29 ± 3.14	3.30 ± 0.79
Lactate	relative response ratio	2.49 ± 0.76	1.73 ± 0.16	3.26 ± 0.12	2.79 ± 0.28	3.04 ± 0.57	1.91 ± 0.52	1.64 ± 0.40	2.70 ± 0.78	6.73 ± 2.15	3.36 ± 0.98	5.24 ± 1.13
Malate	relative response ratio	10.65 ± 1.93	9.44 ± 1.04	13.93 ± 3.67	10.18 ± 0.88	10.75 ± 2.21	11.16 ± 2.91	9.55 ± 1.11	9.66 ± 1.33	11.75 ± 0.14	10.16 ± 1.97	12.33 ± 0.16
Nicotinate	relative response ratio	13.42 ± 0.13	11.08 ± 0.20	13.84 ± 6.88	11.04 ± 3.17	10.06 ± 3.34	12.34 ± 3.47	10.73 ± 1.62	11.41 ± 0.55	13.17 ± 1.92	12.69 ± 2.37	12.13 ± 1.59
Oxalate	relative response ratio	12.12 ± 1.11	8.96 ± 1.43	19.33 ± 7.22	14.34 ± 3.05	13.19 ± 2.88	16.05 ± 6.70	8.85 ± 0.59	11.29 ± 1.93	14.93 ± 0.98	14.01 ± 4.05	9.52 ± 1.79
Pyruvate	nmol/g fw^{-1}	5.97 ± 0.65	6.11 ± 0.18	5.52 ± 0.04	5.43 ± 0.11	5.98 ± 1.13	5.74 ± 0.35	6.15 ± 0.65	5.95 ± 0.27	6.30 ± 0.65	7.35 ± 0.37	8.02 ± 0.03
Quinate	relative response ratio	7.98 ± 0.16	6.94 ± 0.59	9.24 ± 1.66	7.97 ± 0.91	7.96 ± 0.18	8.34 ± 0.35	7.87 ± 0.78	7.37 ± 0.62	8.47 ± 0.82	7.10 ± 0.82	5.41 ± 0.63
Shikimate	relative response ratio	7.83 ± 1.01	8.37 ± 0.95	8.18 ± 2.26	8.05 ± 1.59	7.90 ± 3.01	10.58 ± 2.28	8.19 ± 1.73	8.40 ± 0.98	9.05 ± 1.01	9.33 ± 0.99	7.21 ± 1.94
Succinate	relative response ratio	7.08 ± 0.19	5.85 ± 0.78	8.87 ± 3.57	6.84 ± 1.50	6.65 ± 0.92	5.60 ± 0.68	5.12 ± 0.21	6.60 ± 2.00	7.92 ± 1.11	6.35 ± 0.18	8.09 ± 0.16
Threonate	relative response ratio	6.85 ± 0.32	5.76 ± 1.12	7.45 ± 0.20	5.90 ± 1.44	5.57 ± 2.08	4.46 ± 0.12	4.75 ± 0.56	5.18 ± 0.98	6.76 ± 0.42	5.97 ± 1.09	6.73 ± 0.27

Amino Acids

Alanine	relative response ratio	8.13 ± 2.18	9.43 ± 2.84	12.84 ± 2.41	10.00 ± 2.81	11.44 ± 2.07	8.05 ± 1.83	6.75 ± 0.70	8.59 ± 0.77	10.92 ± 1.27	10.61 ± 1.68	13.20 ± 1.77
Arginine	relative response ratio	2.29 ± 0.10	6.66 ± 0.86	5.59 ± 2.26	4.75 ± 1.40	5.54 ± 3.13	5.23 ± 2.54	6.59 ± 4.92	5.97 ± 0.48	5.57 ± 2.19	4.25 ± 0.71	7.45 ± 0.49
Asparagine	relative response ratio	4.90 ± 0.11	6.58 ± 2.48	6.83 ± 1.45	6.40 ± 0.65	8.33 ± 3.36	8.00 ± 2.79	6.26 ± 3.25	6.71 ± 0.40	8.17 ± 1.86	6.68 ± 0.93	13.95 ± 2.81
Aspartate	relative response ratio	8.34 ± 0.38	7.71 ± 1.95	9.03 ± 1.86	7.84 ± 1.21	9.05 ± 2.31	8.65 ± 1.58	6.58 ± 2.04	7.71 ± 0.48	7.50 ± 0.50	7.60 ± 1.14	5.17 ± 0.65
beta-Alanine	relative response ratio	4.09 ± 0.69	2.32 ± 0.03	4.01 ± 0.83	3.40 ± 1.41	3.14 ± 0.18	3.93 ± 0.66	2.52 ± 0.33	3.32 ± 0.58	3.49 ± 0.40	3.54 ± 0.60	2.19 ± 0.07
Gaba	relative response ratio	2.25 ± 0.87	3.54 ± 2.88	5.44 ± 2.84	4.92 ± 0.96	7.46 ± 1.62	7.22 ± 2.82	3.00 ± 2.09	6.53 ± 1.56	5.98 ± 1.60	5.56 ± 0.12	8.22 ± 2.10
Glutamate	relative response ratio	5.50 ± 0.05	5.18 ± 0.31	6.06 ± 0.31	5.19 ± 0.63	5.49 ± 1.10	5.67 ± 1.59	4.77 ± 0.85	5.58 ± 0.58	5.57 ± 0.41	5.04 ± 0.82	4.68 ± 0.15
Glutamine	relative response ratio	0.39 ± 0.10	2.33 ± 1.66	1.71 ± 0.57	3.19 ± 1.22	2.79 ± 2.16	4.63 ± 2.85	2.14 ± 1.78	4.16 ± 0.20	2.87 ± 1.17	2.47 ± 1.35	0.48 ± 0.15
Glycine	relative response ratio	1.57 ± 0.10	1.12 ± 0.05	1.85 ± 0.82	1.68 ± 0.64	1.14 ± 0.20	1.52 ± 0.33	1.17 ± 0.13	1.68 ± 0.41	1.63 ± 0.10	1.41 ± 0.10	1.40 ± 0.10
Isoleucine	relative response ratio	7.27 ± 0.72	4.77 ± 2.25	4.01 ± 1.01	7.46 ± 3.70	9.35 ± 2.83	6.51 ± 2.63	4.48 ± 2.64	6.70 ± 1.13	8.14 ± 2.53	4.67 ± 1.17	10.84 ± 2.42
Lysine	relative response ratio	2.42 ± 0.46	2.34 ± 0.26	2.76 ± 0.77	3.11 ± 0.56	3.25 ± 0.79	4.16 ± 1.53	2.47 ± 0.60	3.23 ± 0.11	2.95 ± 0.37	2.87 ± 0.08	2.37 ± 0.44
Methionine	relative response ratio	5.60 ± 0.74	3.24 ± 0.57	3.34 ± 0.88	4.60 ± 2.43	7.52 ± 3.70	7.73 ± 3.36	4.94 ± 3.36	7.42 ± 1.58	4.91 ± 0.62	5.45 ± 1.39	4.58 ± 1.93
Ornithine	relative response ratio	3.19 ± 0.55	3.90 ± 1.75	2.85 ± 0.82	1.55 ± 0.31	1.44 ± 0.19	2.56 ± 1.20	3.08 ± 0.95	2.40 ± 0.31	1.96 ± 0.82	1.81 ± 0.54	1.86 ± 0.57
Phenylalanine	relative response ratio	4.78 ± 0.83	4.08 ± 0.42	4.49 ± 0.74	3.46 ± 0.46	5.35 ± 0.96	4.46 ± 1.34	3.62 ± 0.83	4.71 ± 0.60	5.03 ± 0.66	4.35 ± 0.01	6.19 ± 1.98
Pyroglutamate	relative response ratio	8.94 ± 0.32	7.17 ± 0.39	7.42 ± 1.32	6.07 ± 0.95	6.88 ± 1.75	6.71 ± 1.64	5.69 ± 1.33	6.87 ± 0.99	7.54 ± 0.28	5.80 ± 1.23	7.02 ± 0.90
Serine	relative response ratio	7.03 ± 1.25	5.50 ± 1.75	9.73 ± 3.74	7.73 ± 2.19	9.18 ± 2.16	7.83 ± 2.46	6.31 ± 1.57	8.29 ± 0.31	9.41 ± 0.63	6.16 ± 1.43	6.37 ± 1.53
Threonine	relative response ratio	12.36 ± 0.98	8.98 ± 2.75	14.60 ± 6.32	13.21 ± 4.11	11.53 ± 3.92	13.77 ± 4.67	11.26 ± 2.65	13.62 ± 0.24	14.45 ± 1.24	11.39 ± 3.02	12.69 ± 1.43
Tryptophane	relative response ratio	4.19 ± 2.34	5.59 ± 1.57	5.70 ± 3.05	5.54 ± 2.39	9.13 ± 4.93	5.52 ± 2.21	7.88 ± 4.90	8.48 ± 0.67	8.61 ± 3.19	4.95 ± 0.15	2.99 ± 0.93
Tyrosine	relative response ratio	2.99 ± 0.98	3.17 ± 0.35	2.87 ± 0.78	3.15 ± 0.94	4.49 ± 1.89	3.90 ± 1.37	3.49 ± 1.08	3.88 ± 0.40	3.72 ± 0.80	3.19 ± 0.35	7.43 ± 1.98
Valine	relative response ratio	12.13 ± 0.90	10.50 ± 1.03	13.91 ± 3.29	11.16 ± 4.14	12.82 ± 3.17	12.01 ± 4.50	8.06 ± 1.63	11.20 ± 0.72	14.46 ± 1.01	8.06 ± 2.82	19.77 ± 5.05

Nucleotides

ADP	nmol/g fw^{-1}	7.18 ± 0.93	7.27 ± 1.05	8.09 ± 0.56	8.85 ± 0.40	9.14 ± 0.37	8.77 ± 0.84	9.55 ± 1.56	9.22 ± 1.00	9.10 ± 0.61	10.59 ± 1.15	11.54 ± 0.47
ATP	nmol/g fw^{-1}	44.69 ± 3.68	47.70 ± 2.08	46.89 ± 2.14	47.02 ± 4.87	51.54 ± 8.04	43.81 ± 4.25	49.33 ± 6.26	44.24 ± 4.02	41.35 ± 1.59	45.10 ± 3.77	47.67 ± 3.25
GDP	nmol/g fw^{-1}	1.51 ± 0.21	1.30 ± 0.12	1.62 ± 0.15	1.47 ± 0.06	1.45 ± 0.03	1.49 ± 0.09	1.85 ± 0.31	1.80 ± 0.14	1.66 ± 0.09	2.39 ± 0.20	1.88 ± 0.33
GTP	nmol/g fw^{-1}	7.08 ± 0.61	6.49 ± 0.51	7.19 ± 0.46	6.31 ± 0.42	7.68 ± 1.57	6.57 ± 0.72	7.68 ± 1.08	6.39 ± 0.73	6.66 ± 0.58	6.63 ± 0.58	8.05 ± 0.63
NAD	nmol/g fw^{-1}	74.28 ± 7.70	75.49 ± 3.88	73.81 ± 1.99	88.62 ± 6.27	78.67 ± 2.82	76.91 ± 5.76	77.38 ± 4.40	76.10 ± 2.07	74.09 ± 3.28	69.25 ± 4.38	66.71 ± 3.86
NADH	nmol/g fw^{-1}	5.77 ± 0.38	4.72 ± 0.32	5.67 ± 0.36	6.16 ± 0.61	4.81 ± 0.20	5.82 ± 0.39	5.19 ± 0.21	6.46 ± 0.75	6.22 ± 0.08	5.00 ± 0.30	5.78 ± 0.35
NADP	nmol/g fw^{-1}	6.62 ± 0.38	6.25 ± 0.74	5.95 ± 0.15	7.23 ± 0.99	6.27 ± 0.09	6.85 ± 0.53	6.23 ± 0.34	5.96 ± 0.34	6.11 ± 0.47	5.60 ± 0.84	6.15 ± 0.83
NADPH	nmol/g fw^{-1}	7.59 ± 0.40	7.20 ± 0.53	7.98 ± 0.38	9.00 ± 0.80	6.46 ± 0.59	7.04 ± 0.97	7.50 ± 0.48	7.87 ± 0.41	7.68 ± 0.70	7.89 ± 0.75	5.41 ± 0.44
UDP	nmol/g fw^{-1}	1.30 ± 0.29	0.88 ± 0.06	1.26 ± 0.45	1.52 ± 0.48	1.84 ± 0.54	0.96 ± 0.21	1.46 ± 0.40	1.28 ± 0.54	1.18 ± 0.27	1.48 ± 0.26	2.00 ± 0.14
UTP	nmol/g fw^{-1}	10.17 ± 1.41	9.68 ± 1.22	9.13 ± 0.96	8.50 ± 1.55	8.40 ± 1.28	7.68 ± 1.36	7.22 ± 1.45	8.04 ± 0.84	7.66 ± 0.07	7.56 ± 0.76	7.43 ± 0.59

Others

Uracil	relative response ratio	2.02 ± 0.37	0.78 ± 0.46	2.53 ± 0.71	1.29 ± 0.50	1.87 ± 0.78	1.41 ± 0.08	0.95 ± 0.56	1.43 ± 0.68	2.21 ± 0.27	2.47 ± 0.49	0.85 ± 0.37
Putrescine	relative response ratio	1.60 ± 0.03	1.14 ± 0.43	1.50 ± 0.45	2.01 ± 0.44	1.61 ± 0.50	2.06 ± 0.25	1.84 ± 0.35	1.87 ± 0.31	1.66 ± 0.09	1.79 ± 0.17	1.11 ± 0.14

Metabolite ratios

ATP/ADP	ratio	6.32 ± 0.44	6.81 ± 0.86	5.84 ± 0.40	5.29 ± 0.33	4.86 ± 0.59	4.99 ± 0.02	5.25 ± 0.33	4.82 ± 0.11	4.57 ± 0.01	4.32 ± 0.40	4.14 ± 0.32
GTP/GDP	ratio	4.42 ± 0.83	5.27 ± 0.47	3.72 ± 0.60	3.63 ± 0.36	2.47 ± 0.93	3.37 ± 0.19	3.01 ± 0.58	2.72 ± 0.27	2.15 ± 0.77	1.83 ± 0.23	2.33 ± 0.38
NADH/NAD	ratio	0.08 ± 0.01	0.06 ± 0.00	0.08 ± 0.01	0.07 ± 0.01	0.06 ± 0.00	0.07 ± 0.02	0.07 ± 0.00	0.09 ± 0.01	0.09 ± 0.00	0.08 ± 0.01	0.08 ± 0.00
NADPH/NADP	ratio	1.16 ± 0.10	1.21 ± 0.25	1.34 ± 0.04	1.27 ± 0.05	1.03 ± 0.11	1.06 ± 0.23	1.20 ± 0.01	1.34 ± 0.14	1.26 ± 0.05	1.47 ± 0.16	0.93 ± 0.18
PEP/Pyr	ratio	0.78 ± 0.12	0.83 ± 0.05	0.88 ± 0.06	0.85 ± 0.09	0.69 ± 0.22	0.62 ± 0.08	0.67 ± 0.04	0.63 ± 0.04	0.49 ± 0.07	0.37 ± 0.05	0.38 ± 0.02
UTP/UDP	ratio	5.89 ± 1.15	7.53 ± 1.03	7.81 ± 3.19	4.86 ± 1.15	4.40 ± 0.52	7.70 ± 2.10	5.65 ± 0.70	7.57 ± 3.18	6.34 ± 1.55	4.82 ± 1.02	4.22 ± 0.79

Supplemental Table 3: Dataset of low-oxygen induced changes in the levels of metabolites in PKc transgenic line 6 and 15 and wild type. Potato plants were grown in the greenhouse under long day conditions (16 h light/8 h dark). Tubers were harvested from 12-week-old plants. After 60 min of pre-incubation in buffer equilibrated with 21% oxygen, potato tuber slices were transferred into 4% oxygen and harvested after another hour. Sampling of the discs was performed in order to immediately quench the metabolism of the discs by direct shock-freezing in liquid nitrogen. Metabolite levels were measured by GC-MS profiling (relative response ratio) or by enzymatic assays (nmol/g fw^{-1} or μmol/g fw^{-1}). Results are expressed as fold change of metabolite level in 4% oxygen relative to 21% oxygen in all genotypes. Results are the mean ± SE, n = 3 biological replicates. Significant changes between the transgenic lines PKC-6, PKC-15 and wild type were evaluated by using Student's t-test ($p < 0.05$) and are indicated in bold.

	Wild type			PKC-6			PKC-15		
Metabolites	ratio 4% O_2/21% O_2								
sugars									
Glucose	1.83	±	1.13	1.03	±	0.24	0.81	±	0.54
Fructose	0.86	±	0.13	1.06	±	0.27	0.77	±	0.07
Sucrose	1.02	±	0.14	0.85	±	0.07	1.13	±	0.14
sugar alcohols									
Galactinol	1.10	±	0.25	1.31	±	0.13	0.98	±	0.28
Mannitol	1.03	±	0.13	0.96	±	0.07	1.11	±	0.08
Myo-Inositol	1.56	±	0.18	1.36	±	0.13	1.50	±	0.51
UDP-glucose	1.30	±	0.04	**0.94**	**±**	**0.07**	1.12	±	0.06
Phosphate ester									
3-Phosphoglycerate	0.93	±	0.06	0.81	±	0.10	**1.39**	**±**	**0.11**
Fructose-6-phosphate	0.84	±	0.20	1.45	±	0.24	0.65	±	0.00
Glucose-6-phosphate	0.91	±	0.15	1.55	±	0.39	0.62	±	0.06
Glycerol-3-phosphate	1.28	±	0.34	1.51	±	0.26	1.25	±	0.49
Phosphoenolpyruvate	1.20	±	0.11	0.90	±	0.09	1.11	±	0.11
Organic acids									
2-Oxoglutarate	0.99	±	0.07	1.23	±	0.12	0.98	±	0.13
Aconitate	3.23	±	0.12	**0.86**	**±**	**0.23**	**0.70**	**±**	**0.01**
Benzoate	1.11	±	0.04	**0.50**	**±**	**0.10**	1.19	±	0.06
Citrate	2.24	±	0.55	1.09	±	0.08	0.89	±	0.02
Fumarate	1.31	±	0.10	1.01	±	0.19	**0.69**	**±**	**0.07**
Isocitrate	1.25	±	0.05	**0.87**	**±**	**0.10**	1.07	±	0.10
Itaconate	0.87	±	0.21	0.73	±	0.26	0.65	±	0.11
Galactarate	1.25	±	0.10	1.44	±	0.13	1.16	±	0.25
Glycerate	1.55	±	0.12	**1.12**	**±**	**0.02**	1.12	±	0.13
Lactate	3.91	±	0.85	4.22	±	1.96	2.96	±	0.13

Malate	1.31	±	0.02	1.15	±	0.11	**0.81**	±	**0.08**
Nicotinate	1.42	±	0.23	1.19	±	0.03	1.18	±	0.38
Oxalate	1.21	±	0.28	1.09	±	0.22	1.16	±	0.56
Pyruvate	1.09	±	0.13	1.28	±	0.09	1.42	±	0.21
Quinate	0.72	±	0.10	1.06	±	0.12	1.07	±	0.09
Shikimate	1.10	±	0.36	1.11	±	0.11	0.85	±	0.02
Succinate	1.07	±	0.03	0.93	±	0.10	0.81	±	0.13
Threonate	1.30	±	0.05	0.97	±	0.06	1.12	±	0.12

Amino Acids

Alanine	2.80	±	0.38	**0.86**	±	**0.33**	**0.77**	±	**0.08**
Arginine	2.13	±	0.14	**1.39**	±	**0.01**	2.02	±	0.23
Asparagine	4.05	±	0.82	**1.28**	±	**0.09**	0.85	±	0.36
Aspartate	1.08	±	0.17	**0.45**	±	**0.10**	0.51	±	0.16
beta-Alanine	0.80	±	0.03	1.05	±	0.06	0.79	±	0.09
Gaba	3.76	±	0.96	0.71	±	0.28	0.53	±	0.38
Glutamate	1.31	±	0.05	1.25	±	0.05	1.40	±	0.54
Glutamine	1.84	±	0.56	1.07	±	0.19	2.02	±	0.81
Glycine	1.14	±	0.09	0.99	±	0.18	0.96	±	0.14
Isoleucine	6.15	±	1.37	**1.12**	±	**0.24**	1.34	±	0.28
Lysine	1.17	±	0.27	1.12	±	0.05	0.82	±	0.19
Methionine	1.35	±	0.70	1.38	±	0.03	1.60	±	0.79
Ornithine	0.48	±	0.18	1.02	±	0.26	0.94	±	0.12
Phenylalanine	1.68	±	0.54	0.96	±	0.20	1.16	±	0.35
Pyroglutamate	1.58	±	0.25	1.03	±	0.13	1.17	±	0.07
Serine	1.27	±	0.37	1.35	±	0.09	1.21	±	0.38
Threonine	1.51	±	0.21	1.41	±	0.09	0.86	±	0.15
Tyrosine	2.53	±	0.68	1.23	±	0.10	1.23	±	0.18
Tryptophan	1.69	±	0.53	1.64	±	0.12	2.12	±	0.25
Valine	3.17	±	0.81	1.48	±	0.13	0.88	±	0.12

Nucleotides

ADP	2.09	±	0.09	**1.73**	**±**	**0.09**	**1.78**	**±**	**0.06**
ATP	0.90	±	0.06	**0.61**	**±**	**0.06**	**0.61**	**±**	**0.02**
GDP	2.28	±	0.40	1.44	±	0.05	1.57	±	0.20
GTP	1.26	±	0.10	**0.82**	**±**	**0.06**	**0.82**	**±**	**0.04**
NAD	0.90	±	0.05	1.03	±	0.06	1.06	±	0.12
NADH	1.13	±	0.07	**1.67**	**±**	**0.09**	**1.49**	**±**	**0.09**
NADP	0.96	±	0.13	1.17	±	0.07	0.98	±	0.08
NADPH	0.82	±	0.07	0.83	±	0.10	0.98	±	0.03
UDP	2.87	±	0.20	**1.09**	**±**	**0.27**	2.06	±	0.21
UTP	1.68	±	0.13	**1.12**	**±**	**0.06**	1.36	±	0.16

Others

Putrescine	0.86	±	0.14	0.53	±	0.09	1.87	±	0.64
Uracil	0.90	±	0.39	0.56	±	0.20	1.15	±	0.17

Metabolite ratios

ATP/ADP	0.42	±	0.03	0.35	±	0.02	0.34	±	0.02
GTP/GDP	0.20	±	0.03	0.22	±	0.01	0.22	±	0.02
NADH/NAD	1.20	±	0.04	**1.53**	**±**	**0.01**	1.42	±	0.09
NADPH/NADP	0.90	±	0.17	0.73	±	0.11	1.01	±	0.09
PEP/Pyr	1.12	±	0.06	**0.71**	**±**	**0.10**	**0.75**	**±**	**0.04**
UTP/UDP	0.45	±	0.08	0.85	±	0.34	0.39	±	0.06

Supplemental Table 4: Dataset of changes in the levels of metabolites in idhv seedlings relative to wild type Col-0 at different oxygen concentrations. Seedlings were grown for 2 weeks under long day conditions (16 h light /8 h dark with 100 µmol photons m² s-1) on vertical plates with 2% agar and 1% sucrose. Then, seedlings were exposed for 16 h to 21%, 1% and 0% (v/v) oxygen in the dark. For harvesting plant material, seedlings on vertical plates were directly shock-frozen in liquid nitrogen and shoots were harvested from the frozen seedling. Metabolite levels were measured by profiling via GC-MS (relative response ratio) or by enzymatic assays (nmol/g fw-1 or µmol/g fw-1). Results are the mean ± SE, n = 4-6 biological replicates. Significant changes between idhv and wild type were evaluated by using Student's t-test (p < 0.05) and are indicated in bold.

Metabolite	unit	21% O_2 Wild type	21% O_2 idhv	1% O_2 Wild type	1% O_2 idhv	0% O_2 Wild type	0% O_2 idhv
sugars & starch							
1-Methyl-D-galactopyranoside	relative response ratio	9.67 ± 2.12	4.66 ± 2.22	6.55 ± 1.25	4.81 ± 0.94	1.65 ± 0.55	2.14 ± 1.04
alpha-D-Galactopyranosyl-(1,4)-D-galactopyranoside	relative response ratio	0.66 ± 0.05	0.60 ± 0.06	0.44 ± 0.03	**0.60 ± 0.04**	0.89 ± 0.02	0.94 ± 0.08
alpha-D-Glucopyranosyl-(1,6)-D-mannitol	relative response ratio	0.15 ± 0.01	0.13 ± 0.02	0.23 ± 0.08	0.16 ± 0.02	0.13 ± 0.02	0.14 ± 0.02
Arabinose	relative response ratio	22.20 ± 1.17	22.77 ± 1.09	21.77 ± 1.65	23.31 ± 2.09	32.04 ± 0.88	**37.35 ± 1.95**
Fucose	relative response ratio	8.08 ± 0.18	7.65 ± 0.49	7.76 ± 0.32	8.44 ± 0.65	7.29 ± 0.50	7.68 ± 0.95
Fructose	µmol/g fw^{-1}	0.49 ± 0.06	0.57 ± 0.07	0.72 ± 0.06	0.67 ± 0.02	1.16 ± 0.06	1.29 ± 0.09
Galactose	relative response ratio	7.55 ± 0.86	9.02 ± 0.88	9.91 ± 0.59	10.23 ± 1.71	19.38 ± 1.20	22.81 ± 2.23
Glucose	µmol/g fw^{-1}	0.59 ± 0.06	**0.86 ± 0.09**	1.05 ± 0.11	1.02 ± 0.09	3.07 ± 0.21	3.55 ± 0.19
Glucoheptose	relative response ratio	0.24 ± 0.02	0.28 ± 0.02	0.28 ± 0.03	0.34 ± 0.02	0.29 ± 0.02	**0.36 ± 0.03**
Lactulose	relative response ratio	1.17 ± 0.06	1.01 ± 0.07	0.89 ± 0.09	1.01 ± 0.08	0.94 ± 0.04	0.98 ± 0.08
Maltose	relative response ratio	14.64 ± 1.44	**7.50 ± 0.81**	12.15 ± 1.31	14.15 ± 1.64	55.23 ± 3.79	56.97 ± 6.70
Mannose	relative response ratio	4.67 ± 0.67	5.66 ± 0.46	8.32 ± 1.25	9.19 ± 1.44	14.45 ± 0.90	15.97 ± 1.66
Melezitose	relative response ratio	5.50 ± 0.52	5.20 ± 1.04	3.33 ± 0.33	4.12 ± 0.94	6.54 ± 1.14	9.77 ± 3.05
N-acetyl-Mannosamine	relative response ratio	2.73 ± 0.25	2.80 ± 0.22	2.75 ± 0.16	3.13 ± 0.34	2.41 ± 0.18	3.02 ± 0.41
Palatinose	relative response ratio	2.15 ± 0.04	**1.65 ± 0.16**	1.61 ± 0.11	1.69 ± 0.09	1.32 ± 0.11	1.51 ± 0.18
Ribose	relative response ratio	0.67 ± 0.03	0.62 ± 0.06	0.54 ± 0.05	0.60 ± 0.07	0.52 ± 0.06	0.55 ± 0.06
Sorbose	relative response ratio	22.42 ± 2.03	27.00 ± 2.10	31.59 ± 3.30	34.23 ± 3.86	43.71 ± 1.41	50.17 ± 5.26
Starch	µmol/g fw^{-1}	1.59 ± 0.14	1.71 ± 0.21	3.25 ± 0.33	**4.76 ± 0.53**	5.18 ± 0.35	**7.12 ± 0.70**
Sucrose	µmol/g fw^{-1}	1.20 ± 0.10	**1.61 ± 0.08**	1.72 ± 0.17	1.67 ± 0.12	1.34 ± 0.11	1.51 ± 0.08
Talose	relative response ratio	2.13 ± 0.24	**0.74 ± 0.24**	1.04 ± 0.20	1.01 ± 0.30	3.16 ± 0.21	3.40 ± 0.59
Trehalose	relative response ratio	0.28 ± 0.01	0.27 ± 0.03	0.23 ± 0.01	0.28 ± 0.03	0.29 ± 0.01	**0.36 ± 0.01**
Trehalose-alpha-beta	relative response ratio	0.94 ± 0.04	0.94 ± 0.09	0.87 ± 0.05	**1.11 ± 0.09**	7.29 ± 0.79	7.17 ± 0.71
Trehalose-beta-beta	relative response ratio	4.74 ± 0.20	3.99 ± 0.34	3.74 ± 0.25	4.38 ± 0.25	3.32 ± 0.19	3.65 ± 0.44
Xylose	relative response ratio	5.15 ± 0.19	4.92 ± 0.24	4.83 ± 0.30	5.02 ± 0.43	7.21 ± 0.46	7.70 ± 0.40
Xylulose	relative response ratio	6.73 ± 0.41	5.85 ± 0.34	5.45 ± 0.37	**6.84 ± 0.44**	6.02 ± 0.22	6.27 ± 0.49

sugar alcohols							
Arabitol	relative response ratio	0.22 ± 0.02	0.21 ± 0.02	0.16 ± 0.01	0.19 ± 0.01	0.10 ± 0.02	0.10 ± 0.02
Erythritol	relative response ratio	0.17 ± 0.01	0.16 ± 0.01	0.14 ± 0.01	0.16 ± 0.01	0.11 ± 0.01	**0.13 ± 0.01**
Galactinol	relative response ratio	3.86 ± 0.34	3.52 ± 0.72	1.90 ± 0.12	2.36 ± 0.49	2.02 ± 0.23	3.21 ± 0.99
Glycerol	relative response ratio	48.48 ± 3.16	42.13 ± 0.81	39.99 ± 1.18	39.28 ± 0.81	28.64 ± 0.56	31.46 ± 3.51
Maltitol	relative response ratio	0.11 ± 0.01	0.10 ± 0.01	0.09 ± 0.01	0.10 ± 0.01	0.37 ± 0.03	0.51 ± 0.07
myo-Inositol	relative response ratio	111.46 ± 13.58	77.67 ± 5.70	114.27 ± 8.85	**153.88 ± 12.87**	142.90 ± 10.18	184.96 ± 25.31
Xylitol	relative response ratio	0.21 ± 0.03	0.20 ± 0.02	0.16 ± 0.01	0.19 ± 0.02	0.33 ± 0.02	0.32 ± 0.03
Phosphate ester							
Fructose-6-phosphate	relative response ratio	2.37 ± 0.20	2.20 ± 0.18	2.79 ± 0.20	**3.58 ± 0.25**	0.36 ± 0.04	0.35 ± 0.04
Glucose-6-phosphate	relative response ratio	4.16 ± 0.34	4.15 ± 0.30	5.01 ± 0.23	**6.11 ± 0.43**	0.86 ± 0.09	0.81 ± 0.08
Monomethyl-phosphate	relative response ratio	0.44 ± 0.07	**0.21 ± 0.05**	0.29 ± 0.05	0.31 ± 0.05	0.26 ± 0.02	0.22 ± 0.04
Myo-Inositol-1-phosphate	relative response ratio	0.40 ± 0.03	0.31 ± 0.03	0.34 ± 0.05	0.37 ± 0.03	0.47 ± 0.06	0.47 ± 0.04
Phosphoenolpyruvate	nmol/g fw^{-1}	36.68 ± 4.98	34.30 ± 3.99	20.94 ± 4.09	29.46 ± 3.96	10.04 ± 2.80	9.75 ± 1.82
Organic acids							
2-hydroxyglutarate	relative response ratio	2.79 ± 0.12	**2.21 ± 0.08**	2.22 ± 0.18	**2.78 ± 0.17**	1.56 ± 0.09	1.50 ± 0.18
2-oxoglutarate	µmol/g fw^{-1}	0.51 ± 0.02	0.48 ± 0.01	0.56 ± 0.04	0.47 ± 0.04	0.54 ± 0.02	0.52 ± 0.08
2,4-dihydroxybutyrate	relative response ratio	2.42 ± 0.43	**1.30 ± 0.21**	1.66 ± 0.46	1.30 ± 0.23	1.71 ± 0.32	1.78 ± 0.65
3-hydroxybutyrate	relative response ratio	0.58 ± 0.08	0.52 ± 0.04	0.53 ± 0.05	0.53 ± 0.06	0.48 ± 0.04	0.46 ± 0.04
4-hydroxybutyrate	relative response ratio	0.85 ± 0.04	0.77 ± 0.04	0.74 ± 0.05	**1.01 ± 0.09**	20.37 ± 1.76	**28.91 ± 1.86**
Benzoate	relative response ratio	4.15 ± 0.16	**3.54 ± 0.17**	3.08 ± 0.20	3.53 ± 0.20	4.72 ± 0.51	4.65 ± 0.36
Borate	relative response ratio	6.02 ± 1.21	5.52 ± 1.91	4.38 ± 1.29	4.32 ± 1.07	2.75 ± 0.81	4.28 ± 2.07
Citrate	relative response ratio	62.36 ± 2.91	**49.20 ± 3.96**	44.46 ± 8.66	**71.21 ± 5.07**	8.26 ± 0.70	7.09 ± 0.99
Fumarate	relative response ratio	159.21 ± 8.15	**113.65 ± 6.65**	121.26 ± 23.14	186.02 ± 22.23	97.67 ± 4.92	86.13 ± 9.17
Galactarate	relative response ratio	2.20 ± 0.09	**1.48 ± 0.14**	1.67 ± 0.15	1.90 ± 0.13	1.88 ± 0.17	1.62 ± 0.23
Galactonate	relative response ratio	5.48 ± 0.18	**4.51 ± 0.27**	4.39 ± 0.25	**5.64 ± 0.44**	4.44 ± 0.28	4.67 ± 0.55
Glycerate	relative response ratio	6.81 ± 0.70	**4.29 ± 0.32**	6.54 ± 0.39	7.93 ± 0.79	16.03 ± 0.32	**18.75 ± 0.98**
Glycolate	relative response ratio	0.42 ± 0.14	0.46 ± 0.13	0.47 ± 0.06	0.36 ± 0.06	0.80 ± 0.10	1.03 ± 0.25
Isocitrate	nmol/g fw^{-1}	91.89 ± 2.34	92.74 ± 2.85	96.47 ± 3.23	**71.00 ± 6.65**	74.37 ± 1.93	68.80 ± 7.67
Lactate	relative response ratio	n.d.	n.d.	n.d.	n.d.	645.24 ± 28.29	613.05 ± 68.52
Malate	relative response ratio	28.24 ± 1.97	**18.92 ± 0.97**	20.05 ± 2.10	**28.40 ± 2.20**	20.31 ± 1.63	22.80 ± 0.88
Malonate	relative response ratio	0.48 ± 0.13	0.35 ± 0.10	0.38 ± 0.08	0.46 ± 0.07	0.63 ± 0.10	**1.10 ± 0.08**

Pyruvate	nmol/g fw^{-1}	26.93 ± 3.54	26.07 ± 7.05	38.48 ± 5.69	36.78 ± 9.02	34.52 ± 2.47	**49.18 ± 5.81**
Ribonate	relative response ratio	6.55 ± 0.36	**8.23 ± 0.50**	5.33 ± 0.30	**7.65 ± 0.79**	4.45 ± 0.52	5.98 ± 0.50
Succinate	relative response ratio	0.99 ± 0.03	0.97 ± 0.03	0.67 ± 0.07	**0.96 ± 0.08**	10.69 ± 0.54	**13.78 ± 0.13**
Shikimate	relative response ratio	3.07 ± 0.28	2.72 ± 0.48	3.05 ± 0.54	3.62 ± 0.68	1.55 ± 0.35	1.69 ± 0.11
trans-Aconitate	relative response ratio	22.34 ± 0.83	19.93 ± 1.29	17.38 ± 0.82	**22.44 ± 1.46**	15.81 ± 0.74	16.85 ± 1.27
Amino Acids							
3-cyanoalanine	relative response ratio	24.30 ± 2.50	23.02 ± 3.69	21.81 ± 5.69	21.56 ± 3.45	12.66 ± 1.42	14.26 ± 3.24
Alanine	relative response ratio	11.50 ± 0.63	**8.52 ± 0.66**	19.17 ± 1.85	**27.44 ± 2.14**	109.19 ± 4.80	113.24 ± 10.44
Arginine	relative response ratio	1.07 ± 0.08	**0.57 ± 0.09**	0.65 ± 0.03	**0.52 ± 0.05**	0.44 ± 0.08	0.42 ± 0.08
Asparagine	relative response ratio	81.23 ± 9.19	91.67 ± 12.23	68.05 ± 17.03	85.05 ± 15.36	37.34 ± 7.72	30.55 ± 10.64
Aspartate	relative response ratio	364.02 ± 13.13	**277.39 ± 16.17**	247.75 ± 20.23	**335.37 ± 22.14**	36.06 ± 3.55	31.03 ± 2.50
beta-Alanine	relative response ratio	14.11 ± 0.77	**9.83 ± 0.56**	14.32 ± 1.11	16.55 ± 0.78	13.12 ± 0.86	14.66 ± 1.56
beta-Homoserine	relative response ratio	0.87 ± 0.10	1.05 ± 0.53	1.25 ± 0.36	1.43 ± 0.24	8.39 ± 2.18	6.73 ± 2.21
Cycloleucine	relative response ratio	5.50 ± 0.60	**2.79 ± 0.87**	4.86 ± 1.20	3.81 ± 1.02	4.57 ± 0.34	4.71 ± 0.45
GABA	relative response ratio	2.72 ± 0.30	2.89 ± 0.39	2.97 ± 0.33	**5.56 ± 1.00**	151.00 ± 9.96	165.17 ± 16.57
Glutamate	relative response ratio	536.88 ± 8.85	**401.51 ± 30.17**	405.44 ± 18.15	445.02 ± 22.28	37.56 ± 0.93	33.55 ± 4.90
Glutamine	relative response ratio	389.45 ± 48.09	411.64 ± 87.47	359.51 ± 18.55	**62.33 ± 9.25**	27.78 ± 3.10	16.58 ± 4.41
Glycine	relative response ratio	35.39 ± 1.94	33.47 ± 3.42	70.51 ± 4.49	77.35 ± 10.21	285.13 ± 30.66	347.63 ± 18.95
Histidine	relative response ratio	10.40 ± 2.39	10.19 ± 1.81	5.78 ± 1.36	4.53 ± 0.65	5.14 ± 1.08	3.60 ± 0.89
Homoserine	relative response ratio	0.61 ± 0.02	**0.46 ± 0.05**	0.61 ± 0.08	0.62 ± 0.07	0.61 ± 0.09	0.57 ± 0.07
Isoleucine	relative response ratio	143.02 ± 6.58	**76.25 ± 9.53**	104.16 ± 7.81	106.79 ± 10.04	97.76 ± 9.31	98.65 ± 10.19
Lysine	relative response ratio	6.54 ± 0.81	6.00 ± 0.43	4.66 ± 0.26	**7.26 ± 0.80**	5.51 ± 0.45	**7.11 ± 0.11**
Methionine	relative response ratio	24.22 ± 1.74	**17.82 ± 1.99**	15.41 ± 0.58	17.98 ± 1.50	14.74 ± 1.24	15.59 ± 1.24
O-acetylserine	relative response ratio	1.56 ± 0.05	1.47 ± 0.10	0.96 ± 0.05	**1.58 ± 0.24**	81.18 ± 9.11	88.47 ± 9.42
Ornithine	relative response ratio	8.32 ± 0.34	**6.39 ± 0.66**	7.06 ± 0.84	7.21 ± 0.62	6.48 ± 0.60	5.43 ± 0.77
Phenylalanine	relative response ratio	29.89 ± 1.71	**18.57 ± 1.94**	22.26 ± 1.01	20.75 ± 2.03	24.18 ± 2.05	23.46 ± 2.27
Proline	relative response ratio	128.24 ± 17.60	**70.02 ± 10.38**	127.55 ± 14.00	**207.63 ± 30.45**	271.19 ± 36.12	368.31 ± 69.66
Serine	relative response ratio	57.25 ± 1.94	**44.40 ± 4.28**	51.90 ± 2.02	54.42 ± 3.01	38.11 ± 2.43	42.08 ± 5.44
Threonine	relative response ratio	126.35 ± 6.35	**90.69 ± 8.49**	97.33 ± 5.00	106.34 ± 8.67	94.65 ± 7.05	95.30 ± 11.70
Tryptophane	relative response ratio	8.75 ± 1.31	**2.59 ± 0.70**	5.46 ± 0.55	4.13 ± 0.45	8.00 ± 1.59	6.39 ± 0.81
Tyrosine	relative response ratio	36.80 ± 3.14	**17.36 ± 2.66**	33.66 ± 3.20	29.92 ± 2.74	50.27 ± 6.81	46.45 ± 5.79
Valine	relative response ratio	29.61 ± 1.44	**17.37 ± 2.31**	21.82 ± 1.39	22.71 ± 1.95	23.51 ± 2.13	23.97 ± 2.56
total amino acids	µmol/g fw^{-1}	14.07 ± 0.65	**12.04 ± 0.29**	12.57 ± 1.42	12.86 ± 1.90	16.49 ± 0.74	18.25 ± 1.30

5. Appendix

		Col1		Col2		Col3		Col4		Col5		Col6	
Nucleotides													
ADP	nmol/g fw^{-1}	17.78	± 1.61	17.86	± 1.53	12.85	± 0.58	**7.52**	± **0.98**	10.20	± 0.19	**6.14**	± **0.94**
ATP	nmol/g fw^{-1}	21.28	± 1.44	21.75	± 1.67	20.04	± 1.27	17.70	± 2.55	2.74	± 0.78	4.32	± 0.25
NAD	nmol/g fw^{-1}	60.83	± 2.63	55.69	± 2.10	50.10	± 3.15	**58.94**	± **2.26**	61.23	± 1.88	54.75	± 2.54
NADH	nmol/g fw^{-1}	29.93	± 2.75	27.38	± 0.81	28.51	± 1.49	31.28	± 1.20	29.07	± 1.93	31.15	± 2.50
NADP	nmol/g fw^{-1}	12.70	± 1.69	10.28	± 0.47	13.62	± 1.69	13.25	± 0.54	12.27	± 0.95	11.54	± 0.34
NADPH	nmol/g fw^{-1}	19.05	± 1.25	19.65	± 0.86	21.07	± 1.19	22.23	± 1.16	11.55	± 0.45	14.34	± 1.65
Others													
2-hydroxy-pyridine	relative response ratio	8.83	± 1.38	10.96	± 1.37	8.43	± 1.22	10.21	± 1.89	8.78	± 1.55	13.17	± 3.47
Ascorbate	relative response ratio	4.51	± 1.14	**1.11**	± **0.47**	1.78	± 0.45	2.89	± 0.78	0.97	± 0.33	0.91	± 0.31
Butyro-1,4-lactam	relative response ratio	0.21	± 0.10	0.35	± 0.03	0.38	± 0.22	0.24	± 0.06	0.18	± 0.08	0.12	± 0.07
Cellobiitol	relative response ratio	1.27	± 0.08	1.29	± 0.09	1.12	± 0.09	1.36	± 0.12	1.31	± 0.03	1.34	± 0.06
Dehydroascorbate	relative response ratio	48.61	± 5.89	40.68	± 5.89	27.94	± 4.10	**49.88**	± **6.90**	37.25	± 5.27	46.54	± 7.03
Dihydrosphingosine	relative response ratio	n.d.		n.d.		n.d.		n.d.		0.07	± 0.01	0.08	± 0.01
Ethanolamine	relative response ratio	115.16	± 33.21	**32.25**	± **8.48**	54.41	± 16.90	59.38	± 19.31	165.47	± 15.46	171.31	± 26.22
Galactono-1,4-lactone	relative response ratio	0.16	± 0.01	0.15	± 0.01	0.14	± 0.01	0.15	± 0.01	1.36	± 0.10	1.53	± 0.10
Guanine	relative response ratio	0.38	± 0.02	0.38	± 0.02	0.40	± 0.02	**0.49**	± **0.03**	0.59	± 0.03	**0.78**	± **0.05**
Hydroxyquinol	relative response ratio	1.45	± 0.28	1.18	± 0.25	1.39	± 0.28	1.35	± 0.28	0.92	± 0.39	1.04	± 0.34
Isopropyl beta-D-1-thiogalactopyranoside	relative response ratio	6.59	± 0.16	**5.31**	± **0.20**	4.53	± 0.27	**5.38**	± **0.24**	4.23	± 0.34	4.14	± 0.55
Ornithine-1,5-lactam	relative response ratio	46.20	± 6.48	32.41	± 4.84	29.25	± 2.47	26.72	± 3.43	26.72	± 5.58	19.49	± 7.33
Palmitate	relative response ratio	3.48	± 1.02	3.04	± 1.09	2.22	± 0.75	3.01	± 0.62	0.57	± 0.06	0.41	± 0.16
Phosphate	relative response ratio	2390.73	± 446.57	2540.05	± 509.35	1382.24	± 168.27	**2254.20**	± **241.54**	3141.30	± 651.03	2493.15	± 354.62
Putrescine	relative response ratio	91.96	± 11.97	64.78	± 5.57	95.26	± 9.42	98.30	± 7.83	112.14	± 9.77	92.46	± 6.37
Threonolactone	relative response ratio	7.02	± 0.43	6.27	± 0.22	5.57	± 0.14	5.71	± 0.34	3.62	± 0.22	4.08	± 0.31
total proteins	µmol/g fw^{-1}	9.39	± 0.70	9.21	± 0.45	10.10	± 0.68	9.42	± 0.53	12.66	± 0.37	12.56	± 0.51
Uracil	relative response ratio	4.10	± 0.69	3.65	± 0.48	3.85	± 0.99	3.67	± 0.64	24.80	± 1.04	24.99	± 1.80
Uridine	relative response ratio	4.50	± 0.46	**3.21**	± **0.25**	2.57	± 0.22	3.21	± 0.45	2.83	± 0.30	2.88	± 0.19
Metabolite ratios													
Ascorbate/Dehydroascorbate	ratio	0.10	± 0.03	**0.02**	± **0.01**	0.04	± 0.01	0.04	± 0.01	0.02	± 0.00	0.01	± 0.00
ATP/ADP	ratio	1.25	± 0.17	1.17	± 0.15	1.50	± 0.15	**2.69**	± **0.46**	0.28	± 0.07	**0.77**	± **0.12**
isocitrate/2-oxoglutarate	ratio	0.18	± 0.01	0.18	± 0.02	0.17	± 0.02	0.15	± 0.03	0.14	± 0.01	0.14	± 0.01
NADH/NAD	ratio	0.50	± 0.06	0.50	± 0.03	0.58	± 0.04	0.54	± 0.03	0.48	± 0.04	0.60	± 0.08
NADPH/NADP	ratio	1.86	± 0.37	1.93	± 0.10	1.59	± 0.24	1.69	± 0.10	1.00	± 0.09	1.24	± 0.14
Phosphoenolpyruvate/Pyruvate	ratio	1.37	± 0.32		± 0.37	0.53	± 0.09	0.90	± 0.22	0.31	± 0.11	0.22	± 0.00

Supplemental Table 5: Dataset of changes in the levels of metabolites in *idhv* seedlings relative to wild type Col-0 at different oxygen concentrations. Seedlings were grown for 2 weeks under long day conditions (16 h light /8 h dark with 100 µmol photons m² s⁻1) on vertical plates with 2% agar and 1% sucrose. Then, seedlings were exposed for 24 h to 21%, 1% and 0% (v/v) oxygen in the dark. For harvesting plant material, seedlings on vertical plates were directly shock-frozen in liquid nitrogen and shoots were harvested from the frozen seedling. Metabolite levels were measured by profiling via GC-MS (relative response ratio) or by enzymatic assays (nmol/g fw^{-1} or µmol/g fw^{-1}). Results are the mean ± SE, *n* = 4-6 biological replicates. Significant changes between *idhv* and wild type were evaluated by using Student's t-test (p < 0.05) and are indicated in bold.

Metabolite	unit	21% O$_2$ Wild type	21% O$_2$ *idhv*	1% O$_2$ Wild type	1% O$_2$ *idhv*	0% O$_2$ Wild type	0% O$_2$ *idhv*
sugars & starch							
alpha-D-Galactopyranosyl-(1,4)-D-galactopyranoside	relative response ratio	0.21 ± 0.02	0.27 ± 0.03	0.21 ± 0.01	0.24 ± 0.01	0.54 ± 0.08	0.69 ± 0.15
alpha-D-Glucopyranosyl-(1,6)-D-mannitol	relative response ratio	0.28 ± 0.03	0.38 ± 0.04	0.29 ± 0.03	0.27 ± 0.07	0.26 ± 0.04	**1.24 ± 0.31**
1-Methyl-D-galactopyranoside	relative response ratio	5.54 ± 2.11	26.61 ± 19.94	5.94 ± 1.10	6.60 ± 3.30	1.24 ± 0.32	1.03 ± 0.41
Arabinose	relative response ratio	20.71 ± 1.01	21.62 ± 2.79	20.85 ± 2.58	22.98 ± 2.29	31.37 ± 1.40	34.80 ± 1.91
Fucose	relative response ratio	6.59 ± 0.84	5.91 ± 0.80	6.55 ± 0.55	6.43 ± 0.26	5.45 ± 0.39	**7.33 ± 0.43**
Fructose	µmol/g fw^{-1}	0.36 ± 0.04	0.37 ± 0.02	0.46 ± 0.03	0.65 ± 0.17	1.71 ± 0.14	1.93 ± 0.28
Galactose	relative response ratio	4.85 ± 0.45	5.93 ± 1.30	6.33 ± 1.00	10.69 ± 3.02	17.61 ± 1.15	16.74 ± 1.44
Glucose	µmol/g fw^{-1}	0.30 ± 0.02	**0.43 ± 0.04**	0.46 ± 0.05	0.76 ± 0.18	3.53 ± 0.37	4.25 ± 0.61
Glucoheptose	relative response ratio	0.21 ± 0.01	0.25 ± 0.04	0.22 ± 0.01	**0.32 ± 0.05**	0.33 ± 0.02	**0.42 ± 0.04**
Lactulose	relative response ratio	0.79 ± 0.05	0.76 ± 0.08	0.74 ± 0.07	0.69 ± 0.05	0.66 ± 0.01	**0.81 ± 0.04**
Maltose	relative response ratio	5.85 ± 0.65	6.91 ± 0.99	7.12 ± 0.93	5.42 ± 0.51	13.98 ± 1.29	13.64 ± 2.22
Mannose	relative response ratio	2.93 ± 0.32	3.08 ± 0.58	3.65 ± 0.32	**8.16 ± 2.21**	11.39 ± 1.11	11.53 ± 0.96
Melezitose	relative response ratio	0.96 ± 0.14	1.95 ± 0.39	1.05 ± 0.18	6.60 ± 5.78	1.53 ± 0.21	2.32 ± 0.30
N-acetyl-Mannosamine	relative response ratio	2.25 ± 0.24	1.95 ± 0.28	2.21 ± 0.10	2.19 ± 0.16	2.05 ± 0.07	**2.52 ± 0.13**
Palatinose	relative response ratio	1.56 ± 0.10	1.53 ± 0.19	1.47 ± 0.10	1.30 ± 0.08	1.05 ± 0.02	**1.32 ± 0.06**
Ribose	relative response ratio	0.51 ± 0.05	0.51 ± 0.07	0.45 ± 0.03	0.49 ± 0.04	0.63 ± 0.05	**1.01 ± 0.12**
Sorbose	relative response ratio	14.65 ± 1.29	14.76 ± 2.29	20.19 ± 2.96	28.00 ± 5.50	29.22 ± 1.33	30.19 ± 1.85
Starch	µmol/g fw^{-1}	0.18 ± 0.02	**0.51 ± 0.04**	0.18 ± 0.02	**0.47 ± 0.13**	0.53 ± 0.04	**0.90 ± 0.10**
Sucrose	µmol/g fw^{-1}	0.48 ± 0.04	**0.61 ± 0.02**	0.56 ± 0.02	**0.80 ± 0.10**	0.42 ± 0.01	0.41 ± 0.03
Talose	relative response ratio	2.43 ± 0.32	2.35 ± 0.37	1.53 ± 0.33	1.69 ± 0.17	2.05 ± 0.11	1.95 ± 0.21
Trehalose	relative response ratio	0.20 ± 0.01	0.22 ± 0.04	0.18 ± 0.01	0.19 ± 0.02	0.20 ± 0.01	**0.30 ± 0.04**
Trehalose-alpha-beta	relative response ratio	0.68 ± 0.04	0.72 ± 0.09	0.65 ± 0.02	0.71 ± 0.11	2.49 ± 0.31	2.83 ± 0.58
Trehalose-beta-beta	relative response ratio	3.42 ± 0.21	4.14 ± 0.40	3.46 ± 0.21	3.63 ± 0.14	2.47 ± 0.08	**3.32 ± 0.28**
Xylose	relative response ratio	4.65 ± 0.23	4.86 ± 0.56	4.65 ± 0.58	4.95 ± 0.35	6.70 ± 0.30	7.29 ± 0.36
Xylulose	relative response ratio	4.76 ± 0.14	4.88 ± 0.44	4.67 ± 0.26	5.00 ± 0.26	4.60 ± 0.19	4.76 ± 0.32

sugar alcohols

Arabitol	relative response ratio	0.19 ± 0.01	0.17 ± 0.02	0.16 ± 0.02	0.17 ± 0.02	0.07 ± 0.01	0.08 ± 0.01
Erythritol	relative response ratio	0.08 ± 0.00	0.08 ± 0.01	0.08 ± 0.00	0.09 ± 0.00	0.06 ± 0.00	**0.09 ± 0.01**
Galactinol	relative response ratio	0.70 ± 0.11	**1.40 ± 0.31**	0.83 ± 0.06	0.99 ± 0.15	0.89 ± 0.04	**1.83 ± 0.38**
Glycerol	relative response ratio	28.54 ± 0.34	28.62 ± 0.63	26.87 ± 1.72	23.11 ± 2.37	20.22 ± 1.10	20.40 ± 1.34
Maltitol	relative response ratio	0.09 ± 0.00	**0.14 ± 0.01**	0.08 ± 0.01	0.10 ± 0.01	0.57 ± 0.07	**1.10 ± 0.11**
myo-Inositol	relative response ratio	25.40 ± 2.89	**34.97 ± 2.11**	76.73 ± 4.28	**97.87 ± 5.70**	99.29 ± 5.71	**119.57 ± 5.71**
Xylitol	relative response ratio	0.11 ± 0.01	0.12 ± 0.02	0.10 ± 0.01	**0.15 ± 0.02**	0.25 ± 0.01	**0.31 ± 0.02**

Phosphate ester

Fructose-6-phosphate	relative response ratio	1.03 ± 0.08	1.17 ± 0.23	1.29 ± 0.07	**1.72 ± 0.19**	0.06 ± 0.01	0.06 ± 0.01
Glucose-6-phosphate	relative response ratio	1.67 ± 0.15	1.81 ± 0.40	2.01 ± 0.10	**2.67 ± 0.30**	0.11 ± 0.02	0.12 ± 0.01
Monomethyl-phosphate	relative response ratio	0.19 ± 0.01	0.17 ± 0.02	0.16 ± 0.01	0.16 ± 0.03	0.09 ± 0.01	0.09 ± 0.00
myo-Inositol-1-phosphate	relative response ratio	0.18 ± 0.01	0.22 ± 0.04	0.17 ± 0.02	0.17 ± 0.02	0.37 ± 0.01	**0.48 ± 0.03**
Phosphoenolpyruvate	nmol/g fw^{-1}	34.93 ± 2.65	38.09 ± 2.07	40.45 ± 4.93	42.31 ± 4.25	5.34 ± 0.69	5.17 ± 1.32

Organic acids

2-hydroxyglutarate	relative response ratio	4.17 ± 0.25	**2.59 ± 0.41**	2.04 ± 0.18	1.72 ± 0.07	0.75 ± 0.03	**1.07 ± 0.11**
2-oxoglutarate	µmol/g fw^{-1}	0.30 ± 0.02	0.27 ± 0.03	0.35 ± 0.04	0.33 ± 0.06	0.54 ± 0.04	0.49 ± 0.05
2,4-dihydroxybutyrate	relative response ratio	1.46 ± 0.18	1.51 ± 0.35	1.18 ± 0.14	0.91 ± 0.25	0.74 ± 0.04	0.70 ± 0.07
3-hydroxybutyrate	relative response ratio	8.65 ± 1.38	7.40 ± 1.73	1.87 ± 0.42	0.74 ± 0.15	0.55 ± 0.03	0.59 ± 0.02
4-hydroxybutyrate	relative response ratio	0.55 ± 0.04	0.62 ± 0.07	0.53 ± 0.02	**0.67 ± 0.06**	14.32 ± 2.47	**27.69 ± 5.02**
Benzoate	relative response ratio	4.49 ± 0.32	4.28 ± 0.55	3.88 ± 0.52	3.39 ± 0.53	4.76 ± 0.24	5.03 ± 0.49
Borate	relative response ratio	3.55 ± 0.25	**1.99 ± 0.54**	3.05 ± 0.74	3.64 ± 0.67	0.87 ± 0.27	0.95 ± 0.24
Citrate	relative response ratio	83.83 ± 7.05	81.89 ± 9.46	81.69 ± 7.05	71.53 ± 9.09	9.69 ± 0.83	**18.55 ± 2.79**
Fumarate	relative response ratio	89.24 ± 4.19	76.10 ± 3.55	95.11 ± 9.65	87.87 ± 4.59	46.26 ± 4.76	**67.67 ± 5.92**
Galactarate	relative response ratio	1.47 ± 0.07	1.73 ± 0.20	1.39 ± 0.06	1.56 ± 0.08	1.45 ± 0.05	**2.00 ± 0.14**
Galactonate	relative response ratio	3.79 ± 0.35	4.06 ± 0.58	3.86 ± 0.25	3.88 ± 0.08	3.42 ± 0.14	**4.51 ± 0.28**
Glycerate	relative response ratio	4.61 ± 0.24	**3.29 ± 0.14**	5.13 ± 0.62	5.02 ± 0.76	8.15 ± 0.69	**10.59 ± 0.58**
Glycolate	relative response ratio	0.23 ± 0.04	0.28 ± 0.07	0.23 ± 0.07	0.20 ± 0.04	0.58 ± 0.07	0.66 ± 0.13
Isocitrate	nmol/g fw^{-1}	50.02 ± 2.69	53.01 ± 2.13	42.46 ± 2.68	52.94 ± 5.66	28.13 ± 2.14	26.70 ± 5.57
Lactate	relative response ratio	1.89 ± 0.66	1.60 ± 0.55	1.06 ± 0.03	1.91 ±	573.28 ± 24.00	546.41 ± 55.27
Malate	relative response ratio	24.08 ± 1.38	24.31 ± 3.88	21.25 ± 1.35	19.66 ± 0.99	13.99 ± 0.59	**23.80 ± 1.97**
Malonate	relative response ratio	0.37 ± 0.06	0.68 ± 0.21	0.28 ± 0.07	0.53 ± 0.25	0.90 ± 0.20	**2.62 ± 0.63**
Pyruvate	nmol/g fw^{-1}	12.08 ± 1.57	13.41 ± 1.11	14.08 ± 0.91	**9.94 ± 1.19**	30.92 ± 2.26	**42.70 ± 0.46**
Ribonate	relative response ratio	6.46 ± 0.34	6.68 ± 0.64	6.20 ± 0.27	7.46 ± 1.24	5.80 ± 0.19	**7.27 ± 0.41**
Succinate	relative response ratio	0.83 ± 0.06	0.77 ± 0.11	0.63 ± 0.06	0.62 ± 0.06	6.25 ± 0.38	**11.06 ± 0.87**
Shikimate	relative response ratio	2.56 ± 0.45	2.54 ± 0.50	2.81 ± 0.27	3.01 ± 0.49	1.29 ± 0.05	1.43 ± 0.08
trans-Aconitate	relative response ratio	16.87 ± 0.70	17.69 ± 1.16	17.20 ± 0.56	18.35 ± 1.02	14.25 ± 0.47	**15.85 ± 0.50**

Amino Acids

		1	2	3	4	5	6
3-cyanoalanine	relative response ratio	60.09 ± 17.54	37.39 ± 6.70	45.52 ± 11.40	28.63 ± 13.76	18.71 ± 3.99	15.19 ± 5.38
Alanine	relative response ratio	3.94 ± 0.26	**3.04 ± 0.24**	5.46 ± 0.46	**9.21 ± 1.74**	69.99 ± 2.80	71.43 ± 3.96
Arginine	relative response ratio	0.70 ± 0.04	0.52 ± 0.08	0.60 ± 0.04	0.66 ± 0.05	0.32 ± 0.05	0.33 ± 0.05
Asparagine	relative response ratio	135.30 ± 40.91	73.70 ± 18.55	110.71 ± 29.78	65.91 ± 30.06	33.48 ± 10.47	30.26 ± 11.67
Aspartate	relative response ratio	104.01 ± 4.77	104.82 ± 9.81	138.31 ± 10.36	137.11 ± 8.47	29.95 ± 0.72	**38.80 ± 3.72**
beta-Alanine	relative response ratio	16.45 ± 0.85	16.64 ± 2.05	14.99 ± 1.26	14.99 ± 1.12	8.27 ± 0.31	**11.18 ± 0.36**
beta-Homoserine	relative response ratio	0.26 ± 0.05	0.23 ± 0.02	0.47 ± 0.10	0.39 ± 0.09	5.97 ± 1.51	5.09 ± 1.22
Cycloleucine	relative response ratio	2.69 ± 0.25	2.24 ± 0.18	3.08 ± 0.32	3.25 ± 0.15	2.65 ± 0.11	2.54 ± 0.11
GABA	relative response ratio	3.38 ± 0.50	3.27 ± 0.51	2.30 ± 0.24	**8.31 ± 4.54**	99.16 ± 4.35	109.65 ± 6.16
Glutamate	relative response ratio	350.83 ± 9.13	349.72 ± 8.48	310.96 ± 17.92	283.38 ± 24.37	14.80 ± 1.34	**19.08 ± 1.07**
Glutamine	relative response ratio	144.85 ± 42.06	200.16 ± 47.18	76.27 ± 16.35	**198.12 ± 5.09**	3.42 ± 0.85	**1.40 ± 0.09**
Glycine	relative response ratio	19.76 ± 2.53	14.97 ± 1.44	19.63 ± 1.21	21.07 ± 0.53	128.96 ± 8.08	**202.43 ± 33.43**
Histidine	relative response ratio	12.27 ± 2.73	12.40 ± 1.57	7.08 ± 1.57	11.64 ± 0.77	3.42 ± 0.72	3.39 ± 0.36
Homoserine	relative response ratio	0.67 ± 0.05	0.84 ± 0.08	0.69 ± 0.07	0.74 ± 0.02	0.28 ± 0.02	**0.38 ± 0.02**
Isoleucine	relative response ratio	151.58 ± 9.32	148.88 ± 14.26	154.12 ± 12.09	147.91 ± 12.71	95.70 ± 8.76	102.95 ± 9.70
Lysine	relative response ratio	5.98 ± 0.89	6.26 ± 0.62	6.45 ± 0.72	4.93 ± 0.79	6.87 ± 0.54	**10.89 ± 1.69**
Methionine	relative response ratio	28.11 ± 1.46	25.69 ± 3.23	21.24 ± 1.81	21.54 ± 2.35	18.30 ± 1.69	21.95 ± 1.92
O-acetylserine	relative response ratio	0.51 ± 0.07	0.47 ± 0.07	0.44 ± 0.04	0.46 ± 0.07	14.76 ± 1.73	14.56 ± 2.57
Ornithine	relative response ratio	8.28 ± 0.75	5.22 ± 1.15	6.93 ± 0.84	5.88 ± 0.58	5.65 ± 0.38	5.30 ± 0.49
Phenylalanine	relative response ratio	58.25 ± 3.85	52.12 ± 6.77	40.26 ± 3.23	34.71 ± 2.44	25.66 ± 1.83	**33.66 ± 2.21**
Proline	relative response ratio	90.63 ± 4.66	84.53 ± 1.63	94.71 ± 6.56	**146.77 ± 27.69**	155.39 ± 11.63	167.99 ± 16.23
Serine	relative response ratio	22.42 ± 1.28	**14.86 ± 2.31**	22.67 ± 0.86	23.67 ± 1.26	13.19 ± 0.77	12.38 ± 0.86
Threonine	relative response ratio	87.81 ± 5.74	82.31 ± 8.28	97.25 ± 5.63	94.11 ± 5.32	62.07 ± 1.75	68.87 ± 4.56
Tryptophane	relative response ratio	17.79 ± 1.98	18.67 ± 0.42	10.79 ± 1.65	11.77 ± 0.92	8.37 ± 1.09	8.60 ± 1.08
Tyrosine	relative response ratio	51.35 ± 3.60	57.42 ± 3.68	65.60 ± 5.21	64.09 ± 3.54	55.68 ± 6.88	60.42 ± 6.07
Valine	relative response ratio	46.46 ± 2.94	42.45 ± 3.45	39.12 ± 2.68	37.99 ± 2.87	24.75 ± 2.44	32.14 ± 2.77
total amino acids	μmol/g fw^{-1}	7.47 ± 0.43	7.59 ± 0.35	9.06 ± 0.58	10.69 ± 1.30	9.74 ± 0.68	**12.40 ± 0.73**

Nucleotides

ADP	nmol/g fw^{-1}	15.28 ± 1.94	15.16 ± 2.05	15.68 ± 1.12	18.93 ± 1.69	16.46 ± 1.75	**10.92 ± 1.37**
ATP	nmol/g fw^{-1}	12.64 ± 1.16	10.81 ± 0.97	10.02 ± 0.71	14.00 ± 2.77	2.52 ± 0.44	2.94 ± 0.25
NAD	nmol/g fw^{-1}	45.80 ± 1.32	54.04 ± 4.38	41.15 ± 1.09	43.56 ± 1.36	25.56 ± 1.82	28.57 ± 5.74
NADH	nmol/g fw^{-1}	13.06 ± 0.53	14.08 ± 0.74	12.39 ± 0.38	13.35 ± 0.29	11.85 ± 0.45	**14.36 ± 0.60**
NADP	nmol/g fw^{-1}	29.01 ± 2.84	34.46 ± 8.62	35.36 ± 6.11	37.38 ± 5.57	38.97 ± 8.60	32.83 ± 1.96
NADPH	nmol/g fw^{-1}	16.69 ± 0.39	19.06 ± 1.59	21.48 ± 1.14	21.05 ± 1.71	5.08 ± 0.15	**7.28 ± 0.72**

Others

2-hydroxy-pyridine	relative response ratio	7.83 ± 1.68	8.24 ± 1.73	9.00 ± 3.15	6.94 ± 2.41	9.14 ± 1.46	10.96 ± 3.03
Ascorbate	relative response ratio	4.46 ± 0.90	**0.65 ± 0.16**	2.51 ± 0.50	1.93 ± 1.04	0.28 ± 0.06	0.36 ± 0.07
Butyro-1,4-lactam	relative response ratio	0.94 ± 0.17	0.73 ± 0.10	0.63 ± 0.07	0.58 ± 0.15	0.51 ± 0.09	**0.21 ± 0.02**
Cellobiitol	relative response ratio	1.04 ± 0.05	1.15 ± 0.16	1.02 ± 0.04	1.03 ± 0.11	1.06 ± 0.07	**1.59 ± 0.12**
Dehydroascorbate	relative response ratio	30.92 ± 4.61	38.82 ± 5.03	19.31 ± 3.61	20.80 ± 3.27	25.10 ± 5.30	37.17 ± 8.82
Dihydrosphingosine	relative response ratio	n.d.	n.d.	n.d.	n.d.	0.04 ± 0.00	0.06 ± 0.01
Ethanolamine	relative response ratio	35.36 ± 4.41	**16.94 ± 3.84**	20.44 ± 3.86	26.35 ± 4.91	147.33 ± 14.39	153.70 ± 14.18
Galactono-1,4-lactone	relative response ratio	0.10 ± 0.01	0.11 ± 0.01	0.11 ± 0.02	0.12 ± 0.02	1.32 ± 0.08	1.41 ± 0.10
Guanine	relative response ratio	0.27 ± 0.02	0.28 ± 0.03	0.28 ± 0.01	**0.38 ± 0.05**	0.65 ± 0.06	**0.87 ± 0.07**
Hydroxyquinol	relative response ratio	0.36 ± 0.09	0.20 ± 0.02	0.31 ± 0.04	0.20 ± 0.02	0.23 ± 0.03	0.19 ± 0.03
Isopropyl beta-D-1-thiogalactopyranoside	relative response ratio	4.25 ± 0.33	3.76 ± 0.36	4.01 ± 0.43	3.35 ± 0.39	2.82 ± 0.30	2.94 ± 0.24
Ornithine-1,5-lactam	relative response ratio	30.55 ± 4.12	22.42 ± 2.86	24.38 ± 3.71	18.08 ± 5.15	9.22 ± 1.83	8.02 ± 1.58
Palmitate	relative response ratio	1.96 ± 0.22	1.61 ± 0.21	1.63 ± 0.28	2.57 ± 0.32	0.64 ± 0.11	1.00 ± 0.21
Phosphate	relative response ratio	606.87 ± 83.27	968.24 ± 199.59	445.47 ± 83.00	**1186.26 ± 56.77**	711.66 ± 98.45	**1116.36 ± 25.82**
Putrescine	relative response ratio	72.71 ± 5.95	71.42 ± 5.14	82.68 ± 4.17	85.02 ± 9.01	118.22 ± 4.69	**137.48 ± 4.03**
Threonolactone	relative response ratio	3.53 ± 0.28	3.12 ± 0.36	3.68 ± 0.45	2.99 ± 0.25	2.41 ± 0.23	2.76 ± 0.11
total proteins	µmol/g fw^{-1}	5.87 ± 0.44	5.36 ± 0.53	6.08 ± 0.41	5.72 ± 0.54	7.12 ± 0.46	**9.98 ± 0.36**
Uracil	relative response ratio	8.87 ± 0.56	**5.97 ± 1.16**	6.84 ± 1.15	5.28 ± 1.63	22.30 ± 1.50	24.57 ± 1.47
Uridine	relative response ratio	2.58 ± 0.15	1.99 ± 0.26	2.03 ± 0.17	2.01 ± 0.15	1.94 ± 0.23	1.97 ± 0.20

Metabolite ratios

Ascorbate/Dehydroascorbate	ratio	0.16 ± 0.02	**0.01 ± 0.01**	0.06 ± 0.02	0.06 ± 0.04	0.01 ± 0.00	0.01 ± 0.00
ATP/ADP	ratio	0.79 ± 0.12	0.77 ± 0.17	0.52 ± 0.04	0.65 ± 0.15	0.18 ± 0.02	0.27 ± 0.06
isocitrate/2-oxoglutarate	ratio	0.14 ± 0.02	0.18 ± 0.03	0.14 ± 0.01	0.17 ± 0.04	0.05 ± 0.00	0.04 ± 0.01
NADH/NAD	ratio	0.29 ± 0.01	0.26 ± 0.01	0.30 ± 0.01	0.31 ± 0.02	0.48 ± 0.05	0.47 ± 0.06
NADPH/NADP	ratio	0.53 ± 0.07	0.54 ± 0.15	0.69 ± 0.11	0.62 ± 0.14	0.13 ± 0.03	0.18 ± 0.02
Phosphoenolpyruvate/Pyruvate	ratio	3.02 ± 0.47	2.86 ± 0.10	2.50 ± 0.37	**4.31 ± 0.27**	0.19 ± 0.03	0.13 ± 0.05

Supplemental Table 6: Dataset of changes in the levels of metabolites in *ntrc* and *ntrantrb* plants compared to wild type Col-0 seedlings at different oxygen concentrations. Seedlings were grown for 2 weeks under long day conditions (16 h light /8 h dark with 100 µmol photons m² s⁻1) on vertical plates with 2% agar. Then, seedlings were exposed for 16 h to 21% and 1% (v/v) oxygen in the dark. For harvesting plant material, seedlings on vertical plates were directly shock-frozen in liquid nitrogen and shoots were harvested from the frozen seedling. Metabolite levels were measured by enzymatic assays and are nmol/g fw⁻¹ or µmol/g fw-¹, respectively. Results are the mean ± SE, *n* = 4-6 biological replicates. Significant changes between all genotypes (wt/*ntrc*; wt/*ntrantrb*; *ntrc*/*ntrantrb*) were evaluated by using one-way ANOVA (p < 0.05) and are denoted as sig.

Metabolite	unit	21% O₂ Wild type	*ntrc*	*ntrantrb*	wt ntrc	wt ntrantrb	ntrc ntrantrb	1% O₂ Wild type	*ntrc*	*ntrantrb*	wt ntrc	wt ntrantrb	ntrc ntrantrb
sugars & starch													
Fructose	µmol/g fw⁻¹	0.17 ± 0.01	0.16 ± 0.03	0.28 ± 0.03		sig	sig	0.41 ± 0.03	0.16 ± 0.03	0.42 ± 0.04	sig		sig
Glucose	µmol/g fw⁻¹	0.22 ± 0.02	0.16 ± 0.02	0.64 ± 0.08		sig	sig	0.37 ± 0.02	0.26 ± 0.01	0.71 ± 0.06	sig		sig
Starch	µmol/g fw⁻¹	1.68 ± 0.10	1.44 ± 0.14	2.18 ± 0.29				2.85 ± 0.27	3.76 ± 0.26	4.29 ± 0.45		sig	
Sucrose	µmol/g fw⁻¹	0.68 ± 0.03	0.50 ± 0.02	0.64 ± 0.05	sig			1.05 ± 0.05	1.14 ± 0.17	1.01 ± 0.04			
Phosphate ester													
Phosphoenolpyruvate	nmol/g fw⁻¹	34.98 ± 1.61	35.96 ± 1.12	32.24 ± 2.11				38.51 ± 2.21	45.36 ± 2.36	34.93 ± 1.31			sig
Organic acids													
Pyruvate	nmol/g fw⁻¹	20.73 ± 0.92	43.83 ± 10.20	22.38 ± 2.04	sig		sig	19.93 ± 2.55	33.36 ± 5.13	20.36 ± 1.26	sig		sig
Nucleotides													
ADP	nmol/g fw⁻¹	22.88 ± 0.64	26.11 ± 2.39	19.81 ± 1.12			sig	23.24 ± 1.34	25.51 ± 6.78	19.26 ± 0.60			
ATP	nmol/g fw⁻¹	7.71 ± 0.59	9.60 ± 0.57	4.70 ± 0.44		sig	sig	6.88 ± 0.61	7.36 ± 0.23	4.05 ± 0.35		sig	sig
NAD	nmol/g fw⁻¹	58.46 ± 3.69	66.46 ± 1.63	46.88 ± 2.91		sig	sig	45.80 ± 0.70	65.92 ± 4.01	58.18 ± 3.24	sig	sig	
NADH	nmol/g fw⁻¹	11.83 ± 0.24	14.40 ± 1.79	9.36 ± 0.36			sig	12.96 ± 0.91	20.89 ± 2.25	10.02 ± 0.26	sig		sig
NAD+NADH	nmol/g fw⁻¹	68.27 ± 3.80	80.86 ± 2.41	56.39 ± 2.85	sig	sig	sig	59.03 ± 1.26	86.81 ± 6.00	65.13 ± 4.59	sig		sig
NADP	nmol/g fw⁻¹	14.95 ± 0.80	16.64 ± 1.89	15.01 ± 1.16				22.41 ± 1.09	21.11 ± 1.17	20.65 ± 0.59			
NADPH	nmol/g fw⁻¹	19.81 ± 1.01	25.44 ± 0.20	15.99 ± 0.91	sig	sig	sig	22.58 ± 0.80	40.00 ± 2.52	22.25 ± 1.18	sig		sig
NADP+NADPH	nmol/g fw⁻¹	34.76 ± 1.05	42.08 ± 1.73	31.00 ± 1.42	sig		sig	44.99 ± 1.57	61.56 ± 1.26	42.90 ± 1.51	sig		sig
Antioxidants													
AA	µmol/g fw⁻¹	1.64 ± 0.13	1.78 ± 0.16	1.48 ± 0.08				1.64 ± 0.09	2.38 ± 0.24	1.62 ± 0.04	sig		sig
DHA	µmol/g fw⁻¹	0.87 ± 0.06	0.97 ± 0.09	0.81 ± 0.04				0.86 ± 0.03	1.21 ± 0.10	0.87 ± 0.02	sig		sig
total ascorbate	µmol/g fw⁻¹	2.51 ± 0.19	2.75 ± 0.24	2.29 ± 0.12				2.45 ± 0.14	3.59 ± 0.33	2.49 ± 0.06	sig		sig
GSH	µmol/g fw⁻¹	3.21 ± 0.17	3.50 ± 0.33	2.93 ± 0.12				2.27 ± 0.11	2.78 ± 0.21	2.35 ± 0.09	sig		
GSSG	µmol/g fw⁻¹	0.51 ± 0.01	0.44 ± 0.03	0.41 ± 0.02		sig		0.40 ± 0.03	0.49 ± 0.05	0.54 ± 0.05			
total Glutathione	µmol/g fw⁻¹	3.78 ± 0.23	3.95 ± 0.33	3.36 ± 0.11				2.67 ± 0.10	3.27 ± 0.21	2.81 ± 0.14	sig		
Metabolite ratios													
AA/DHA	ratio	1.89 ± 0.05	1.87 ± 0.06	1.83 ± 0.06				1.98 ± 0.11	2.01 ± 0.07	1.87 ± 0.03			
ATP/ADP	ratio	0.34 ± 0.03	0.38 ± 0.06	0.23 ± 0.03				0.30 ± 0.02	0.31 ± 0.07	0.21 ± 0.02			
GSH/GSH+GSSG	ratio	0.85 ± 0.01	0.88 ± 0.01	0.87 ± 0.01				0.85 ± 0.01	0.85 ± 0.02	0.82 ± 0.01			
NADH/NAD	ratio	0.20 ± 0.02	0.24 ± 0.02	0.21 ± 0.01				0.27 ± 0.02	0.34 ± 0.01	0.18 ± 0.01		sig	sig
NADPH/NADP	ratio	1.43 ± 0.07	1.60 ± 0.22	1.11 ± 0.10				1.05 ± 0.04	1.89 ± 0.26	1.12 ± 0.04	sig		sig
Phosphoenolpyruvate/pyruvate	ratio	1.69 ± 0.07	0.97 ± 0.31	1.41 ± 0.08	sig			1.77 ± 0.18	1.41 ± 0.18	1.73 ± 0.07			

Supplemental Table 7: Dataset of changes in the levels of metabolites in amiRSNF4 seedlings compared to wild type Col-0 at different oxygen concentrations. Seedlings were grown for 9 days under long day conditions (16 h light/ 8 h dark and 100 µmol photons m² s-1) on vertical plates containing 2% agar and 1% sucrose (but no estradiol). Then seedlings were transferred to vertical plates with 2% agar, 1% sucrose and 10µM beta-estradiol for additional 5 days, before they were exposed for 24 h to 21%, 1% and 0% (v/v) oxygen in the dark. For harvesting plant material, seedlings on vertical plates were directly shock-frozen in liquid nitrogen, and shoots were harvested from the frozen seedling. Metabolite levels were measured by profiling via GC-MS (relative response ratio) or by enzymatic assays (nmol/g fw^{-1} or µmol/g fw^{-1}). Results are the mean ± SE, n = 4-6 biological replicates. Significant changes between *amiRSNF4* and wild type were evaluated by using Student's t-test ($p < 0.05$) and are indicated in bold.

Metabolites	unit	21% O$_2$ Wild type	21% O$_2$ amiRSNF4	1% O$_2$ Wild type	1% O$_2$ amiRSNF4	0% O$_2$ Wild type	0% O$_2$ amiRSNF4
sugars & starch							
alpha-D-Galactopyranosyl-(1,4)-D-galactopyranoside	relative response ratio	0.23 ± 0.02	0.23 ± 0.03	0.20 ± 0.02	0.21 ± 0.02	0.21 ± 0.04	0.22 ± 0.05
alpha-D-Glucopyranosyl-(1,6)-D-mannitol	relative response ratio	0.30 ± 0.07	0.34 ± 0.02	0.27 ± 0.02	0.37 ± 0.05	0.21 ± 0.02	0.23 ± 0.01
1-Methyl-D-galactopyranoside	relative response ratio	2.78 ± 0.23	2.79 ± 0.74	3.89 ± 0.88	2.85 ± 0.39	0.45 ± 0.06	0.59 ± 0.05
Arabinose	relative response ratio	14.41 ± 1.82	15.55 ± 1.62	17.94 ± 0.74	14.89 ± 1.30	23.90 ± 1.29	27.34 ± 2.33
Fucose	relative response ratio	7.61 ± 0.16	**5.97 ± 0.35**	8.37 ± 0.94	**6.05 ± 0.36**	7.84 ± 0.96	6.33 ± 0.44
Fructose	µmol/g fw^{-1}	0.16 ± 0.03	0.16 ± 0.03	0.08 ± 0.02	0.09 ± 0.02	0.14 ± 0.02	0.13 ± 0.02
Galactose	relative response ratio	2.04 ± 0.62	2.86 ± 0.35	2.27 ± 0.43	**5.78 ± 1.31**	15.08 ± 1.23	**22.69 ± 0.42**
Glucose	µmol/g fw^{-1}	0.87 ± 0.11	0.81 ± 0.11	0.79 ± 0.08	**1.15 ± 0.07**	1.69 ± 0.16	**2.63 ± 0.31**
Glucoheptose	relative response ratio	0.15 ± 0.02	0.17 ± 0.01	0.15 ± 0.01	0.16 ± 0.02	0.19 ± 0.02	0.19 ± 0.02
Lactulose	relative response ratio	0.67 ± 0.08	0.69 ± 0.03	0.69 ± 0.05	0.66 ± 0.05	0.63 ± 0.06	0.67 ± 0.04
Maltose	relative response ratio	8.68 ± 1.14	6.84 ± 0.52	7.60 ± 1.48	7.93 ± 1.26	4.16 ± 0.62	**7.39 ± 1.02**
Mannose	relative response ratio	0.33 ± 0.08	0.49 ± 0.10	0.47 ± 0.08	0.74 ± 0.16	2.26 ± 0.39	3.06 ± 0.53
Melezitose	relative response ratio	0.32 ± 0.18	0.25 ± 0.04	0.24 ± 0.03	0.64 ± 0.35	0.23 ± 0.01	0.64 ± 0.25
N-acetyl-Mannosamine	relative response ratio	2.49 ± 0.18	2.34 ± 0.15	2.56 ± 0.24	2.17 ± 0.20	2.55 ± 0.17	2.36 ± 0.09
Palatinose	relative response ratio	2.01 ± 0.09	1.99 ± 0.11	1.69 ± 0.15	1.90 ± 0.16	1.26 ± 0.12	1.29 ± 0.11
Ribose	relative response ratio	0.55 ± 0.04	0.51 ± 0.04	0.54 ± 0.06	0.56 ± 0.05	0.58 ± 0.04	**1.01 ± 0.09**
Sorbose	relative response ratio	2.58 ± 0.48	3.61 ± 0.64	4.10 ± 0.74	4.48 ± 0.82	12.70 ± 1.81	16.37 ± 2.35
Starch	µmol/g fw^{-1}	0.16 ± 0.01	**0.26 ± 0.03**	0.22 ± 0.01	**0.44 ± 0.05**	0.25 ± 0.02	**0.35 ± 0.03**
Sucrose	µmol/g fw^{-1}	0.19 ± 0.05	0.20 ± 0.05	0.18 ± 0.04	0.22 ± 0.05	0.31 ± 0.05	**0.85 ± 0.18**
Talose	relative response ratio	4.28 ± 0.34	4.18 ± 0.14	3.78 ± 0.33	**2.83 ± 0.17**	0.80 ± 0.09	**1.31 ± 0.07**
Trehalose	relative response ratio	0.18 ± 0.01	0.21 ± 0.01	0.19 ± 0.02	0.19 ± 0.02	0.17 ± 0.01	**0.21 ± 0.01**
Trehalose-alpha-beta	relative response ratio	0.59 ± 0.04	0.61 ± 0.04	0.65 ± 0.07	0.59 ± 0.05	0.55 ± 0.03	**1.18 ± 0.21**
Trehalose-beta-beta	relative response ratio	4.38 ± 0.30	4.29 ± 0.32	4.07 ± 0.25	4.15 ± 0.29	2.66 ± 0.30	**4.29 ± 0.32**
Xylose	relative response ratio	3.43 ± 0.36	3.59 ± 0.34	3.75 ± 0.32	3.52 ± 0.32	5.92 ± 0.63	5.99 ± 0.46
Xylulose	relative response ratio	4.29 ± 0.26	4.12 ± 0.32	5.23 ± 0.32	**4.05 ± 0.19**	4.71 ± 0.42	4.50 ± 0.29

sugar alcohols

Arabitol	relative response ratio	0.20	±	0.01	**0.25**	±	**0.01**	0.20	±	0.02	0.21	±	0.02	0.08	±	0.00	**0.11**	±	**0.01**
Erythritol	relative response ratio	0.10	±	0.01	0.10	±	0.01	0.12	±	0.01	0.11	±	0.01	0.08	±	0.01	0.08	±	0.00
Galactinol	relative response ratio	0.51	±	0.12	0.44	±	0.07	0.43	±	0.03	0.51	±	0.18	0.30	±	0.04	0.45	±	0.07
Glycerol	relative response ratio	31.49	±	1.39	29.49	±	2.16	35.93	±	1.14	**31.01**	±	**1.19**	29.95	±	2.74	**23.09**	±	**0.80**
Maltitol	relative response ratio	0.12	±	0.01	0.11	±	0.01	0.12	±	0.01	0.10	±	0.01	0.38	±	0.01	**0.72**	±	**0.12**
myo-Inositol	relative response ratio	23.64	±	1.52	**17.48**	±	**1.29**	57.87	±	3.12	47.34	±	4.06	76.82	±	2.30	**96.07**	±	**6.99**
Xylitol	relative response ratio	0.13	±	0.01	0.15	±	0.01	0.13	±	0.01	0.15	±	0.01	0.23	±	0.03	0.16	±	0.02

Phosphate ester

Fructose-6-phosphate	relative response ratio	0.84	±	0.06	0.88	±	0.04	1.21	±	0.09	**0.90**	±	**0.09**	n.d.			n.d.		
Glucose-6-phosphate	relative response ratio	1.59	±	0.17	1.65	±	0.07	2.27	±	0.17	**1.77**	±	**0.13**	0.10	±	0.01	0.09	±	0.01
Monomethyl-phosphate	relative response ratio	0.37	±	0.05	0.32	±	0.03	0.32	±	0.04	0.30	±	0.03	0.15	±	0.02	0.13	±	0.02
myo-Inositol-1-phosphate	relative response ratio	0.21	±	0.02	0.21	±	0.02	0.21	±	0.02	0.19	±	0.02	0.46	±	0.02	0.47	±	0.02
Phosphoenolpyruvate	nmol/g fw^{-1}	44.13	±	1.93	**36.19**	±	**2.38**	31.37	±	3.41	28.11	±	2.76	4.83	±	0.50	**7.69**	±	**0.38**

Organic acids

2-hydroxyglutarate	relative response ratio	3.23	±	0.33	**2.11**	±	**0.20**	2.07	±	0.15	**1.28**	±	**0.07**	0.70	±	0.05	**0.55**	±	**0.02**
2,4-dihydroxybutyrate	relative response ratio	1.78	±	0.24	1.59	±	0.19	1.86	±	0.34	2.13	±	0.47	0.67	±	0.08	1.00	±	0.22
3-hydroxybutyrate	relative response ratio	5.97	±	0.92	3.14	±	0.36	1.64	±	0.21	2.88	±	0.84	0.52	±	0.04	0.46	±	0.03
4-hydroxybutyrate	relative response ratio	0.57	±	0.06	0.53	±	0.04	0.56	±	0.04	0.55	±	0.03	8.24	±	0.62	**10.68**	±	**0.82**
Benzoate	relative response ratio	4.34	±	0.38	4.29	±	0.40	4.34	±	0.44	4.43	±	0.31	6.14	±	0.80	5.91	±	0.63
Borate	relative response ratio	3.87	±	0.47	3.96	±	0.68	4.61	±	0.35	3.19	±	0.69	1.67	±	0.49	0.96	±	0.31
Citrate	relative response ratio	101.43	±	10.16	**61.80**	±	**6.76**	107.31	±	9.95	**70.75**	±	**5.24**	12.77	±	1.65	**8.73**	±	**0.73**
Fumarate	relative response ratio	101.62	±	6.35	**77.63**	±	**6.12**	123.33	±	12.25	107.53	±	10.90	45.91	±	3.41	50.18	±	3.35
Galactarate	relative response ratio	1.61	±	0.05	**1.28**	±	**0.08**	1.51	±	0.11	1.42	±	0.07	1.30	±	0.10	1.25	±	0.07
Galactonate	relative response ratio	3.30	±	0.15	2.92	±	0.21	3.21	±	0.18	3.20	±	0.21	2.63	±	0.12	2.87	±	0.10
Glycerate	relative response ratio	3.45	±	1.08	3.07	±	0.62	3.27	±	0.39	3.26	±	0.67	8.36	±	0.99	**5.99**	±	**0.31**
Glycolate	relative response ratio	0.07	±	0.03	0.09	±	0.02	0.08	±	0.02	0.10	±	0.02	0.27	±	0.02	0.25	±	0.02
Isocitrate	nmol/g fw^{-1}	75.36	±	2.68	**46.19**	±	**5.45**	68.44	±	5.26	62.37	±	4.16	58.84	±	2.92	**47.92**	±	**3.19**
Lactate	relative response ratio	n.d.			n.d.			n.d.			n.d.			377.07	±	45.82	**174.94**	±	**21.83**
Malate	relative response ratio	18.24	±	1.34	**9.06**	±	**0.78**	20.41	±	2.10	**9.71**	±	**0.43**	16.18	±	2.28	18.37	±	0.79
Malonate	relative response ratio	0.61	±	0.08	0.55	±	0.07	0.53	±	0.04	0.60	±	0.06	1.37	±	0.14	1.49	±	0.06
Pyruvate	nmol/g fw^{-1}	16.99	±	1.68	17.42	±	1.56	16.04	±	0.87	17.88	±	1.01	25.04	±	1.35	23.00	±	1.37
Ribonate	relative response ratio	4.49	±	0.60	3.61	±	0.29	4.80	±	0.34	**2.84**	±	**0.12**	3.45	±	0.18	**2.85**	±	**0.14**
Succinate	relative response ratio	0.88	±	0.06	**0.56**	±	**0.04**	0.87	±	0.03	**0.66**	±	**0.06**	3.34	±	0.27	3.31	±	0.07
Shikimate	relative response ratio	1.65	±	0.10	1.73	±	0.20	2.05	±	0.19	1.88	±	0.18	1.20	±	0.04	**1.56**	±	**0.12**
trans-Aconitate	relative response ratio	15.24	±	1.18	13.20	±	1.01	16.89	±	1.06	**12.70**	±	**0.80**	13.08	±	1.53	11.09	±	0.61

Amino Acids

3-cyanoalanine	relative response ratio	60.09	±	17.54	37.39	±	6.70	45.52	±	11.40	28.63	±	13.76	18.71	±	3.99	15.19 ± 5.38
Alanine	relative response ratio	3.94	±	0.26	**3.04**	±	**0.24**	5.46	±	0.46	**9.21**	±	**1.74**	69.99	±	2.80	71.43 ± 3.96
Arginine	relative response ratio	0.70	±	0.04	0.52	±	0.08	0.60	±	0.04	0.66	±	0.05	0.32	±	0.05	0.33 ± 0.05
Asparagine	relative response ratio	135.30	±	40.91	73.70	±	18.55	110.71	±	29.78	65.91	±	30.06	33.48	±	10.47	30.26 ± 11.67
Aspartate	relative response ratio	104.01	±	4.77	104.82	±	9.81	138.31	±	10.36	137.11	±	8.47	29.95	±	0.72	**38.80** ± **3.72**
beta-Alanine	relative response ratio	16.45	±	0.85	16.64	±	2.05	14.99	±	1.26	14.99	±	1.12	8.27	±	0.31	**11.18** ± **0.36**
beta-Homoserine	relative response ratio	0.26	±	0.05	0.23	±	0.02	0.47	±	0.10	0.39	±	0.09	5.97	±	1.51	5.09 ± 1.22
Cycloleucine	relative response ratio	2.69	±	0.25	2.24	±	0.18	3.08	±	0.32	3.25	±	0.15	2.65	±	0.11	2.54 ± 0.11
GABA	relative response ratio	3.38	±	0.50	3.27	±	0.51	2.30	±	0.24	**8.31**	±	**4.54**	99.16	±	4.35	109.65 ± 6.16
Glutamate	relative response ratio	350.83	±	9.13	349.72	±	8.48	310.96	±	17.92	283.38	±	24.37	14.80	±	1.34	**19.08** ± **1.07**
Glutamine	relative response ratio	144.85	±	42.06	200.16	±	47.18	76.27	±	16.35	**198.12**	±	**5.09**	3.42	±	0.85	**1.40** ± **0.09**
Glycine	relative response ratio	19.76	±	2.53	14.97	±	1.44	19.63	±	1.21	21.07	±	0.53	128.96	±	8.08	**202.43** ± **33.43**
Histidine	relative response ratio	12.27	±	2.73	12.40	±	1.57	7.08	±	1.57	11.64	±	0.77	3.42	±	0.72	3.39 ± 0.36
Homoserine	relative response ratio	0.67	±	0.05	0.84	±	0.08	0.69	±	0.07	0.74	±	0.02	0.28	±	0.02	**0.38** ± **0.02**
Isoleucine	relative response ratio	151.58	±	9.32	148.88	±	14.26	154.12	±	12.09	147.91	±	12.71	95.70	±	8.76	102.95 ± 9.70
Lysine	relative response ratio	5.98	±	0.89	6.26	±	0.62	6.45	±	0.72	4.93	±	0.79	6.87	±	0.54	**10.89** ± **1.69**
Methionine	relative response ratio	28.11	±	1.46	25.69	±	3.23	21.24	±	1.81	21.54	±	2.35	18.30	±	1.69	21.95 ± 1.92
O-acetylserine	relative response ratio	0.51	±	0.07	0.47	±	0.07	0.44	±	0.04	0.46	±	0.07	14.76	±	1.73	14.56 ± 2.57
Ornithine	relative response ratio	8.28	±	0.75	5.22	±	1.15	6.93	±	0.84	5.88	±	0.58	5.65	±	0.38	5.30 ± 0.49
Phenylalanine	relative response ratio	58.25	±	3.85	52.12	±	6.77	40.26	±	3.23	34.71	±	2.44	25.66	±	1.83	**33.66** ± **2.21**
Proline	relative response ratio	90.63	±	4.66	84.53	±	1.63	94.71	±	6.56	**146.77**	±	**27.69**	155.39	±	11.63	167.99 ± 16.23
Serine	relative response ratio	22.42	±	1.28	**14.86**	±	**2.31**	22.67	±	0.86	23.67	±	1.26	13.19	±	0.77	12.38 ± 0.86
Threonine	relative response ratio	87.81	±	5.74	82.31	±	8.28	97.25	±	5.63	94.11	±	5.32	62.07	±	1.75	68.87 ± 4.56
Tryptophane	relative response ratio	17.79	±	1.98	18.67	±	0.42	10.79	±	1.65	11.77	±	0.92	8.37	±	1.09	8.60 ± 1.08
Tyrosine	relative response ratio	51.35	±	3.60	57.42	±	3.68	65.60	±	5.21	64.09	±	3.54	55.68	±	6.88	60.42 ± 6.07
Valine	relative response ratio	46.46	±	2.94	42.45	±	3.45	39.12	±	2.68	37.99	±	2.87	24.75	±	2.44	32.14 ± 2.77
total amino acids	µmol/g fw^{-1}	7.47	±	0.43	7.59	±	0.35	9.06	±	0.58	10.69	±	1.30	9.74	±	0.68	**12.40** ± **0.73**

Nucleotides

ADP	nmol/g fw^{-1}	15.28	±	1.94	15.16	±	2.05	15.68	±	1.12	18.93	±	1.69	16.46	±	1.75	**10.92** ± **1.37**
ATP	nmol/g fw^{-1}	12.64	±	1.16	10.81	±	0.97	10.02	±	0.71	14.00	±	2.77	2.52	±	0.44	2.94 ± 0.25
NAD	nmol/g fw^{-1}	45.80	±	1.32	54.04	±	4.38	41.15	±	1.09	43.56	±	1.36	25.56	±	1.82	28.57 ± 5.74
NADH	nmol/g fw^{-1}	13.06	±	0.53	14.08	±	0.74	12.39	±	0.38	13.35	±	0.29	11.85	±	0.45	**14.36** ± **0.60**
NADP	nmol/g fw^{-1}	29.01	±	2.84	34.46	±	8.62	35.36	±	6.11	37.38	±	5.57	38.97	±	8.60	32.83 ± 1.96
NADPH	nmol/g fw^{-1}	16.69	±	0.39	19.06	±	1.59	21.48	±	1.14	21.05	±	1.71	5.08	±	0.15	**7.28** ± **0.72**

Others

Ascorbate	relative response ratio	0.97 ± 0.30	0.77 ± 0.24	0.56 ± 0.24	0.61 ± 0.10	0.39 ± 0.06	0.37 ± 0.04
Cellobiitol	relative response ratio	0.85 ± 0.06	0.92 ± 0.07	0.93 ± 0.09	0.86 ± 0.07	0.91 ± 0.08	**1.28** ± **0.03**
Dehydroascorbate	relative response ratio	17.24 ± 1.31	16.65 ± 1.76	12.01 ± 0.43	10.82 ± 2.12	22.66 ± 2.47	21.10 ± 2.99
Ethanolamine	relative response ratio	128.96 ± 25.21	98.47 ± 5.60	86.17 ± 13.24	60.99 ± 8.53	184.60 ± 7.14	**224.01** ± **14.46**
Galactono-1,4-lactone	relative response ratio	0.10 ± 0.01	0.11 ± 0.01	0.11 ± 0.01	0.11 ± 0.01	1.96 ± 0.08	**2.27** ± **0.07**
Guanine	relative response ratio	0.18 ± 0.03	0.20 ± 0.01	0.20 ± 0.03	0.22 ± 0.02	0.64 ± 0.05	**0.96** ± **0.06**
Hydroxyquinol	relative response ratio	0.35 ± 0.02	0.35 ± 0.03	0.42 ± 0.04	0.46 ± 0.08	0.27 ± 0.04	0.25 ± 0.02
Isopropyl beta-D-1-thiogalactopyranoside	relative response ratio	4.60 ± 0.51	4.45 ± 0.36	4.66 ± 0.43	4.46 ± 0.36	3.20 ± 0.26	3.43 ± 0.39
Ornithine-1,5-lactam	relative response ratio	28.69 ± 2.72	**52.78** ± **7.12**	40.30 ± 7.90	41.82 ± 7.59	16.38 ± 1.99	27.91 ± 6.73
Palmitate	relative response ratio	1.04 ± 0.24	1.11 ± 0.16	1.00 ± 0.24	0.84 ± 0.14	0.62 ± 0.30	0.40 ± 0.12
Phosphate	relative response ratio	1494.01 ± 122.04	1649.93 ± 127.47	1718.74 ± 170.80	**1201.83** ± **133.22**	1237.80 ± 100.30	1327.30 ± 47.91
Putrescine	relative response ratio	54.80 ± 6.91	**75.70** ± **5.23**	67.56 ± 6.21	**99.43** ± **9.70**	108.45 ± 12.16	**157.67** ± **7.82**
Threonolactone	relative response ratio	3.43 ± 0.34	3.00 ± 0.19	2.78 ± 0.16	2.65 ± 0.21	3.12 ± 0.17	2.87 ± 0.23
total proteins	$\mu mol/g\ fw^{-1}$	2.89 ± 0.12	**2.34** ± **0.09**	2.83 ± 0.31	2.91 ± 0.17	2.68 ± 0.47	2.53 ± 0.22
Uracil	relative response ratio	8.72 ± 1.03	**11.83** ± **0.77**	10.48 ± 1.55	12.69 ± 0.71	22.55 ± 0.91	**27.99** ± **1.60**
Uridine	relative response ratio	1.79 ± 0.08	2.01 ± 0.23	1.62 ± 0.07	1.73 ± 0.13	1.31 ± 0.07	**2.84** ± **0.24**

Metabolite ratios

Ascorbate/Dehydroascorbate	ratio	0.11 ± 0.04	0.06 ± 0.01	0.08 ± 0.03	0.06 ± 0.02	0.03 ± 0.01	0.02 ± 0.00
ATP/ADP	ratio	0.62 ± 0.07	0.57 ± 0.06	0.53 ± 0.04	0.41 ± 0.05	0.20 ± 0.02	0.19 ± 0.00
NADH/NAD	ratio	0.63 ± 0.05	0.70 ± 0.10	0.77 ± 0.12	0.76 ± 0.08	1.00 ± 0.09	**1.49** ± **0.12**
NADPH/NADP	ratio	0.53 ± 0.07	**0.67** ± **0.04**	0.70 ± 0.02	**0.91** ± **0.05**	0.08 ± 0.02	0.11 ± 0.03
Phosphoenolpyruvate/Pyruvate	ratio	2.70 ± 0.26	2.03 ± 0.24	1.91 ± 0.10	1.66 ± 0.22	0.23 ± 0.02	**0.37** ± **0.03**

6 References

Albrecht, G., Mustroph, A. & Fox, T., 2004. Sugar and fructan accumulation during metabolic adjustment between respiration and fermentation under low oxygen conditions in wheat roots. *Physiologia Plantarum*, 120(1), pp.93–105.

Allan, W.L. et al., 2009. Role of plant glyoxylate reductases during stress: a hypothesis. *Biochem. J*, 423(1), pp.15–22.

Allan, W.L.W. et al., 2008. g-Hydroxybutyrate accumulation in Arabidopsis and tobacco plants is a general response to abiotic stress: Putative regulation by redox balance and glyoxylate reductase isoforms. *Journal of Experimental Botany*, 59(9), pp.2555–2564.

Alonso, A.A.P. et al., 2007. Substrate cycles in the central metabolism of maize root tips under hypoxia. *Phytochemistry*, 68(16–18), pp.2222–2231.

Andre, C. et al., 2007. A heteromeric plastidic pyruvate kinase complex involved in seed oil biosynthesis in Arabidopsis. *Plant Cell*, 19(6), pp.2006–2022.

Andre, C. & Benning, C., 2007. Arabidopsis seedlings deficient in a plastidic pyruvate kinase are unable to utilize seed storage compounds for germination and establishment. *Plant physiology*, 145(4), pp.1670–1680.

António, C. et al., 2015. Regulation of Primary Metabolism in Response to Low Oxygen Availability as Revealed by Carbon and Nitrogen Isotope Redistribution. *Plant physiology*, 170(1), pp.43–56.

Araújo, W. et al., 2011. Antisense inhibition of the iron-sulphur subunit of succinate dehydrogenase enhances photosynthesis and growth in tomato via an organic acid–mediated effect on. *The Plant Cell*, 23(February), pp.600–627.

Araújo, W.L. et al., 2014. 2-Oxoglutarate: linking TCA cycle function with amino acid, glucosinolate, flavonoid, alkaloid, and gibberellin biosynthesis. *Frontiers in plant science*, 5(October), p.552.

Araújo, W.L.W. et al., 2010. Identification of the 2-hydroxyglutarate and isovaleryl-CoA dehydrogenases as alternative electron donors linking lysine catabolism to the electron transport chain of. *The Plant Cell*, 22(5), pp.1549–1563.

Araújo, W.L.W. et al., 2008. Inhibition of 2-oxoglutarate dehydrogenase in potato tuber suggests the enzyme is limiting for respiration and confirms its importance in nitrogen assimilation. *Plant physiology*, 148(December), pp.1782–1796.

Araújo, W.L.W. et al., 2011. Metabolic control and regulation of the tricarboxylic acid cycle in photosynthetic and heterotrophic plant tissues. *Plant, cell & environment*, 35(1), pp.1–21.

Armstrong, W. et al., 2009. Measuring and interpreting respiratory critical oxygen pressures in roots. *Annals of Botany*, 103(2), pp.281–293.

Arrivault, S. et al., 2009. chromatography, linked to tandem mass spectrometry, to profile the Calvin cycle and other metabolic intermediates in Arabidopsis rosettes at different carbon. *The Plant Journal*, 59(5), pp.824–839.

Asker, H. & Davies, D., 1984. The physiological role of the isoenzymes of lactate dehydrogenase in potatoes. *Planta*, pp.272–280.

Atwell, B.J., Greenway, H. & Colmer, T.D., 2015. Efficient use of energy in anoxia-tolerant plants with focus on germinating rice seedlings. *New Phytologist*, 206(1), pp.36–56.

Auslender, E.L. et al., 2015. Expression, purification and characterization of Solanum tuberosum recombinant cytosolic pyruvate kinase. *Protein Expression and Purification*, 110(January), pp.7–13.

Baena-González, E. et al., 2007. A central integrator of transcription networks in plant stress and energy signalling. *Nature*, 448(7156), pp.938–42.

Baena-González, E. & Sheen, J., 2008. Convergent energy and stress signaling. *Trends in plant science*, (August), pp.18–25.

Bailey-Serres, J. et al., 2012. Making sense of low oxygen sensing. *Trends in plant science*, 17(3), pp.129–138.

Bailey-Serres, J. & Voesenek, L.A.C.J. a C.J., 2008. Flooding Stress: Acclimations and

6. References

Genetic Diversity. *Annual Review of Plant Biology*, 59(1), pp.313–339.

Banti, V. et al., 2010. The Heat-Inducible Transcription Factor HsfA2 Enhances Anoxia Tolerance in Arabidopsis. *Plant Physiology*, 152(3), pp.1471–1483.

Bashandy, T. et al., 2009. Accumulation of flavonoids in an ntra ntrb mutant leads to tolerance to UV-C. *Molecular Plant*, 2(2), pp.249–258.

Bashandy, T. et al., 2010. Interplay between the NADP-linked thioredoxin and glutathione systems in Arabidopsis auxin signaling. *The Plant cell*, 22(2), pp.376–391.

Baum, G. et al., 1996. Calmodulin binding to glutamate decarboxylase is required for regulation of glutamate and GABA metabolism and normal development in plants. *The EMBO journal*, 15(12), pp.2988–2996.

Baxter-Burrell, A. et al., 2002. RopGAP4-dependent Rop GTPase rheostat control of Arabidopsis oxygen deprivation tolerance. *Science (New York, N.Y.)*, 296, pp.2026–2028.

Beczner, F. et al., 2010. Interaction between SNF1-related kinases and a cytosolic pyruvate kinase of potato. *Journal of Plant Physiology*, 167(13), pp.1046–1051.

Beligni, M.V. et al., 2002. Nitric oxide acts as an antioxidant and delays programmed cell death in barley aleurone layers. *Plant physiology*, 129(4), pp.1642–50.

Belin, C. et al., 2014. A comprehensive study of thiol reduction gene expression under stress conditions in Arabidopsis thaliana. *Plant, Cell and Environment*, pp.299–314.

Biais, B. et al., 2010. Metabolic acclimation to hypoxia revealed by metabolite gradients in melon fruit. *Journal of plant physiology*, 167(3), pp.242–245.

Bitrián, M. et al., 2011. BAC-recombineering for studying plant gene regulation: Developmental control and cellular localization of SnRK1 kinase subunits. *Plant Journal*, 65(5), pp.829–842.

Blokhina, O., Virolainen, E. & Fagerstedt, K. V., 2003. Antioxidants, oxidative damage and oxygen deprivation stress: A review. *Annals of Botany*, 91(SPEC. ISS. JAN.), pp.179–194.

Blokhina, O.B., Chirkova, T. V & Fagerstedt, K. V, 2001. Anoxic stress leads to hydrogen peroxide formation in plant cells. *Journal of Experimental Botany*, 52(359), pp.1179–1190.

Boekema, E.J. & Braun, H.-P., 2007. Supramolecular structure of the mitochondrial oxidative phosphorylation system. *The Journal of biological chemistry*, 282(1), pp.1–4.

Boex-Fontvieille, E.R.A. et al., 2013. A new anaplerotic respiratory pathway involving lysine biosynthesis in isocitrate dehydrogenase-deficient Arabidopsis mutants. *New Phytologist*, 199(3), pp.673–682.

Bologa, L.K. et al., 2003. A bypass of sucrose synthase leads to low internal oxygen and impaired metabolic performance in growing potato tubers. *Plant physiology*, 132(4), pp.2058–2072.

Borisjuk, L. & Rolletschek, H., 2009. The oxygen status of the developing seed. *New Phytologist*, 182(1), pp.17–30.

Bouché, N. et al., 2003. Mitochondrial succinic-semialdehyde dehydrogenase of the gamma-aminobutyrate shunt is required to restrict levels of reactive oxygen intermediates in plants. *Proceedings of the National Academy of Sciences of the United States of America*, 100(11), pp.6843–6848.

Bouny, J.M. & Saglio, P., 1996. Glycolytic Flux and Hexokinase Activities in Anoxic Maize Root Tips Acclimated by Hypoxic Pretreatment. *Plant Physiology*, 111(1 996), pp.187–194.

Bown, A.W. & Shelp, B.J., 1997. The Metabolism and Functions of y-Aminobutyric Acid. *Plant Physiology*, 1(115), pp.1–5.

Branco-Price, C. et al., 2005. Genome-wide analysis of transcript abundance and translation in Arabidopsis seedlings subjected to oxygen deprivation. *Annals of botany*, 96(4), pp.647–60.

Branco-Price, C. et al., 2008. Selective mRNA translation coordinates energetic and metabolic adjustments to cellular oxygen deprivation and reoxygenation in Arabidopsis thaliana. *The Plant Journal*, 56(5), pp.743–755.

Breitkreuz, K.E. et al., 2003. A novel gamma-hydroxybutyrate dehydrogenase: identification

and expression of an Arabidopsis cDNA and potential role under oxygen deficiency. *The Journal of biological chemistry*, 278(42), pp.41552–6.

Bright, J. et al., 2006. ABA-induced NO generation and stomatal closure in Arabidopsis are dependent on H2O2 synthesis. *Plant Journal*, 45(1), pp.113–122.

de Bruxelles, G.L. et al., 1996. Abscisic acid induces the alcohol dehydrogenase gene in Arabidopsis. *Plant physiology*, 111, pp.381–391.

Bui, L.T. et al., 2015. activate the core anaerobic response in Arabidopsis thaliana. *Plant Science*, pp.1–7.

Busch, K.B. & Fromm, H., 1999. Plant succinic semialdehyde dehydrogenase. Cloning, purification, localization in mitochondria, and regulation by adenine nucleotides. *Plant Physiology*, 121(October), pp.589–597.

Carrari, F. et al., 2003. Reduced expression of aconitase results in an enhanced rate of photosynthesis and marked shifts in carbon partitioning in illuminated leaves of wild species tomato. *Plant Physiology*, 133(November), pp.1322–1335.

Cejudo, F.J. et al., 2012. The function of the NADPH thioredoxin reductase C-2-Cys peroxiredoxin system in plastid redox regulation and signalling. *FEBS Letters*, 586(18), pp.2974–2980.

Cha, J.Y. et al., 2014. NADPH-dependent thioredoxin reductase A (NTRA) confers elevated tolerance to oxidative stress and drought. *Plant Physiology and Biochemistry*, 80, pp.184–191.

Cha, J.-Y. et al., 2015. Stress defense mechanisms of NADPH-dependent thioredoxin reductases (NTRs) in plants. *Plant signaling & behavior*, 10(5), p.e1017698.

Cho, Y.-H. et al., 2012. Regulatory Functions of SnRK1 in Stress-Responsive Gene Expression and in Plant Growth and Development. *Plant physiology*, 158(April), pp.1955–1964.

Christianson, J. a et al., 2010. Comparisons of early transcriptome responses to low-oxygen environments in three dicotyledonous plant species. *Plant signaling & behavior*, 5(February 2015), pp.1006–1009.

Clifton, R., Millar, a. H.A. & Whelan, J., 2006. Alternative oxidases in Arabidopsis: A comparative analysis of differential expression in the gene family provides new insights into function of non-phosphorylating bypasses. *Biochimica et Biophysica Acta - Bioenergetics*, 1757(7), pp.730–741.

Confraria, A. et al., 2013. miRNAs mediate SnRK1-dependent energy signaling in Arabidopsis. *Frontiers in plant science*, 4(June), p.197.

Córdoba-Pedregosa, M.D.C. et al., 2005. Changes in intracellular and apoplastic peroxidase activity, ascorbate redox status, and root elongation induced by enhanced ascorbate content in Allium cepa L. *Journal of Experimental Botany*, 56(412), pp.685–694.

Correa-Aragunde, N., Cejudo, F.J. & Lamattina, L., 2015. Nitric oxide is required for the auxin-induced activation of NADPH-dependent thioredoxin reductase and protein denitrosylation during root growth responses in arabidopsis. *Annals of Botany*, 116(4), pp.695–702.

Crawford, L. et al., 1994. The synthesis of γ-aminobutyric acid in response to treatments reducing cytosolic pH. *Plant physiology*, 104, pp.865–871.

Crozet, P. et al., 2010. Cross-phosphorylation between Arabidopsis thaliana sucrose nonfermenting 1-related protein kinase 1 (AtSnRK1) and its activating kinase (AtSnAK) determines their catalytic activities. *Journal of Biological Chemistry*, 285(16), pp.12071–12077.

Crozet, P. et al., 2014. Mechanisms of regulation of SNF1/AMPK/SnRK1 protein kinases. *Frontiers in plant science*, 5(May), pp.1–17.

Daloso, D.M. et al., 2015. Thioredoxin, a master regulator of the tricarboxylic acid cycle in plant mitochondria. *Proceedings of the National Academy of Sciences*, p.201424840.

Davies, D. & Davies, S., 1972. Purification and properties of l(+)-lactate dehydrogenase from potato tubers. *Biochem. J*, 129, pp.831–839.

Davies, D.D., Grego, S. & Kenworthy, P., 1974. The control of the production of lactate and ethanol by higher plants. *Planta*, 118(4), pp.297–310.

Debnam, P.M. et al., 2004. Altered activity of the P2 isoform of plastidic glucose 6-phosphate

dehydrogenase in tobacco (Nicotiana tabacum cv. Samsun) causes changes in carbohydrate metabolism and response to oxidative stress in leaves. *Plant Journal*, 38(1), pp.49–59.

Demidchik, V., Shabala, S.N. & Davies, J.M., 2007. Spatial variation in H2O2 response of Arabidopsis thaliana root epidermal Ca2+ flux and plasma membrane Ca2+ channels. *The Plant journal*, 49(3), pp.377–86.

Desikan, R. et al., 2002. A new role for an old enzyme: nitrate reductase-mediated nitric oxide generation is required for abscisic acid-induced stomatal closure in Arabidopsis thaliana. *Proceedings of the National Academy of Sciences of the United States of America*, 99(25), pp.16314–8.

Dietrich, K. et al., 2011. Heterodimers of the Arabidopsis transcription factors bZIP1 and bZIP53 reprogram amino acid metabolism during low energy stress. *The Plant cell*, 23(1), pp.381–395.

Dixon, D.P. et al., 2005. Stress-Induced Protein S -Glutathionylation in Arabidopsis 1. *Plant physiology*, 138(August), pp.2233–2244.

Dolferus, R. et al., 1994. Differential interactions of promoter elements in stress responses of the Arabidopsis Adh gene. *Plant physiology*, 105, pp.1075–1087.

Dolferus, R. et al., 2008. Functional analysis of lactate dehydrogenase during hypoxic stress in \textit{Arabidopsis}. *Functional Plant Biology*, 35(2), pp.131–140.

van Dongen, J. et al., 2003. Phloem metabolism and function have to cope with low internal oxygen. *Plant physiology*, 131(4), pp.1529–1543.

Dongen, J. Van et al., 2009. Transcript and metabolite profiling of the adaptive response to mild decreases in oxygen concentration in the roots of Arabidopsis plants. *Annals of Botany*, 103(2), pp.269–280.

van Dongen, J.T. & Licausi, F., 2014. Oxygen Sensing and Signaling. *Annual Review of Plant Biology*, 66(December 2014), pp.1–23.

van Dongen, J.T.J. et al., 2004. Phloem import and storage metabolism are highly coordinated by the low oxygen concentrations within developing wheat seeds. *Plant physiology*, 135(3), pp.1809–1821.

Dordas, C., Hasinoff, B.B., et al., 2003. Expression of a stress-induced hemoglobin affects NO levels produced by alfalfa root cultures under hypoxic stress. *The Plant Journal*, 35(6), pp.763–770.

Dordas, C., Rivoal, J. & Hill, R.D., 2003. Plant haemoglobins, nitric oxide and hypoxic stress. *Annals of Botany*, 91(SPEC. ISS. JAN.), pp.173–178.

Drew, M.C., 1997. OXYGEN DEFICIENCY AND ROOT METABOLISM: Injury and Acclimation Under Hypoxia and Anoxia. *Annual Review of Plant Physiology and Plant Molecular Biology*, 48(1), pp.223–250.

Du, H. et al., 2015. A Cytosolic Thioredoxin Acts as a Molecular Chaperone for Peroxisome Matrix Proteins as Well as Antioxidant in Peroxisome. *Molecular Cell*, 38(2), pp.187–194.

Dudkina, N. V. et al., 2006. Respiratory chain supercomplexes in the plant mitochondrial membrane. *Trends in Plant Science*, 11(5), pp.232–240.

Ellis, M.H., Dennis, E.S. & Peacock, W.J., 1999. Arabidopsis roots and shoots have different mechanisms for hypoxic stress tolerance. *Plant Physiology*, 119(1), pp.57–64.

Emanuelle, S. et al., 2015. SnRK1 from Arabidopsis thaliana is an atypical AMPK. *Plant Journal*, 82(2), pp.183–192.

Erban, A. et al., 2007. Nonsupervised construction and application of mass spectral and retention time index libraries from time-of-flight gas chromatography-mass spectrometry metabolite. *Metabolomics*, 358, pp.19–38.

Eubel, H. et al., 2004. Respiratory chain supercomplexes in plant mitochondria. *Plant Physiology and Biochemistry*, 42(12), pp.937–942.

Fait, A. et al., 2008. Highway or byway: the metabolic role of the GABA shunt in plants. *Trends in plant science*, 13(1), pp.14–19.

Fait, A. et al., 2007. Reduced expression of succinyl-coenzyme A ligase can be compensated for by up-regulation of the gamma-aminobutyrate shunt in illuminated tomato leaves. *Plant physiology*, 145(November), pp.626–639.

6. References

Farré, E. et al., 2001. Analysis of compartmentation of glycolytic intermediates, nucleotides, sugars, organic acids, amino acids, and sugar alcohols in potato tubers using a nonaqueous fractionation. *Plant Physiology*, 127(2), pp.685–700.

Felle, H.H., 2005. pH regulation in anoxic plants. *Annals of Botany*, 96(4), pp.519–532.

Foyer, C.H., Kerchev, P.I. & Hancock, R.D., 2012. The ABA-INSENSITIVE-4 (ABI4) transcription factor links redox, hormone and sugar signaling pathways. *Plant Signaling & Behavior*, 7(March 2015), pp.276–281.

Fragoso, S. et al., 2009. SnRK1 isoforms AKIN10 and AKIN11 are differentially regulated in Arabidopsis plants under phosphate starvation. *Plant physiology*, 149(April), pp.1906–1916.

Fukao, T. & Bailey-Serres, J., 2004. Plant responses to hypoxia - Is survival a balancing act? *Trends in Plant Science*, 9(9), pp.449–456.

Furumoto, T. et al., 2011. A plastidial sodium-dependent pyruvate transporter. *Nature*, 476(7361), pp.472–475.

Gasch, P. et al., 2015. Redundant ERF-VII transcription factors bind an evolutionarily-conserved cis-motif to regulate hypoxia-responsive gene expression in Arabidopsis. *The Plant Cell*, p.TPC2015-00866-RA.

Gaufichon, L. et al., 2010. Biological functions of asparagine synthetase in plants. *Plant Science*, 179(3), pp.141–153.

Geigenberger, P. et al., 2000. Metabolic activity decreases as an adaptive response to low internal oxygen in growing potato tubers. *Biological chemistry*, 381(8), pp.723–740.

Geigenberger, P. et al., 1996. Phloem-specific expression of pyrophosphatase inhibits long distance transport of carbohydrates and amino acids in tobacco plants. *Plant, cell & environment*, 19, pp.43–55.

Geigenberger, P., 2003. Response of plant metabolism to too little oxygen. *Current opinion in plant biology*, 6(3), pp.247–256.

Geigenberger, P. & Fernie, A., 2014. Metabolic control of redox and redox control of metabolism in plants. *Antioxidants & redox signaling*, 0(0), pp.1–75.

Geigenberger, P., Geiger, M. & Stitt, M., 1998. High-Temperature Perturbation of Starch Synthesis Is Attributable to Inhibition of ADP-Glucose Pyrophosphorylase by Decreased Levels of Glycerate-3-Phosphate in Growing Potato Tubers1. *Plant physiology*, 117(4), pp.1307–1316.

Gelhaye, E. et al., 2004. A specific form of thioredoxin h occurs in plant mitochondria and regulates the alternative oxidase. *Proceedings of the National Academy of Sciences of the United States of America*, 101(40), pp.14545–14550.

Ghillebert, R. et al., 2011. The AMPK/SNF1/SnRK1 fuel gauge and energy regulator: structure, function and regulation. *FEBS Journal*, 278(21), pp.3978–3990.

Gibbs, D. et al., 2015. Group VII Ethylene Response Factors co-ordinate oxygen and nitric oxide signal transduction and stress responses in plants. *Plant Physiology*, 169(September), p.pp.00338.2015.

Gibbs, D.D.J. et al., 2011. Homeostatic response to hypoxia is regulated by the N-end rule pathway in plants. *Nature*, 479(7373), pp.415–418.

Gibbs, D.J. et al., 2014. Nitric Oxide Sensing in Plants Is Mediated by Proteolytic Control of Group VII ERF Transcription Factors. *Molecular Cell*, 53(3), pp.369–379.

Gibbs, J. & Greenway, H., 2003. Mechanisms of anoxia tolerance in plants . I . Growth , survival and anaerobic catabolism. *Functional Plant Biology*, 30(1), pp.1–47.

Gibon, Y. et al., 2002. Sensitive and high throughput metabolite assays for inorganic pyrophosphate, ADPGlc, nucleotide phosphates, and glycolytic intermediates based on a novel enzymic cycling system. *Plant Journal*, 30(2), pp.221–235.

Giraud, E. et al., 2009. The transcription factor ABI4 is a regulator of mitochondrial retrograde expression of ALTERNATIVE OXIDASE1a. *Plant physiology*, 150(3), pp.1286–1296.

Givan, C., 1999. Evolving concepts in plant glycolysis: two centuries of progress. *Biological Reviews*, 74, pp.277–309.

Gonzali, S. et al., 2005. The use of microarrays to study the anaerobic response in Arabidopsis. *Annals of Botany*, 96(4), pp.661–668.

6. References

Gonzali, S. et al., 2015. Universal stress protein HRU1 mediates ROS homeostasis under anoxia. *Nature Plants*, 1, p.15151.

Good, A. & Muench, D., 1993. Long-term anaerobic metabolism in root tissue (metabolic products of pyruvate metabolism). *Plant Physiology*, pp.1163–1168.

Gottlob-McHugh, S.G. et al., 1992. Normal growth of transgenic tobacco plants in the absence of cytosolic pyruvate kinase. *Plant physiology*, 100(2), pp.820–825.

Gout, E. et al., 2001. Origin of the cytoplasmic pH changes during anaerobic stress in higher plant cells. Carbon-13 and phosphorous-31 nuclear magnetic resonance studies. *Plant physiology*, 125(2), pp.912–925.

Graham, J.W. a J. et al., 2007. Glycolytic enzymes associate dynamically with mitochondria in response to respiratory demand and support substrate channeling. *The Plant cell*, 19(11), pp.3723–3738.

Gray, G.R. et al., 2004. Mitochondria/nuclear signaling of alternative oxidase gene expression occurs through distinct pathways involving organic acids and reactive oxygen species. *Plant Cell Reports*, 23(7), pp.497–503.

Griffith, O.W., 1980. Determination of glutathione and glutathione disulfide using glutathione reductase and 2-vinylpyridine. *Analytical biochemistry*, 106(1), pp.207–212.

Grodzinski, B. et al., 1999. Photosynthesis and carbon partitioning in transgenic tobacco plants deficient in leaf cytosolic pyruvate kinase. *Plant physiology*, 120(3), pp.887–896.

Gupta, K.J. et al., 2012. Inhibition of aconitase by nitric oxide leads to induction of the alternative oxidase and to a shift of metabolism towards biosynthesis of amino acids. *Journal of Experimental Botany*, 63(4), pp.1773–1784.

Gupta, K.J. et al., 2011. On the origins of nitric oxide. *Trends in Plant Science*, 16(3), pp.160–168.

Gupta, K.J. et al., 2009. Regulation of respiration when the oxygen availability changes. *Physiologia Plantarum*, 137(4), pp.383–391.

Gupta, K.J. & Kaiser, W.M., 2010. Production and scavenging of nitric oxide by barley root mitochondria. *Plant and Cell Physiology*, 51(4), pp.576–584.

Hampp, R. et al., 1985. Pyridine and Adenine Nudeotide Status , and Pool Sizes of a Range of Metabolites in Chloroplasts , Mitochondria and the Cytosol / Vacuole of Avena Mesophyll Protoplasts during Dark / Light Transition: Effect of Pyridoxal Phosphate. *Plant Cell Physiology*, 26(1), pp.99–108.

Hatzfeld, W.D. & Stitt, M., 1991. Regulation of Glycolysis in Heterotrophic Cell-Suspension Cultures of Chenopodium-Rubrum in Response To Proton Fluxes At the Plasmalemma. *Physiologia Plantarum*, 81(1), pp.103–110.

Heazlewood, J.L. et al., 2004. Experimental analysis of the Arabidopsis mitochondrial proteome highlights signaling and regulatory components, provides assessment of targeting prediction programs, and indicates plant-specific mitochondrial proteins. *The Plant cell*, 16(January), pp.241–256.

Hess, N. et al., 2011. The hypoxia responsive transcription factor genes ERF71/HRE2 and ERF73/HRE1 of Arabidopsis are differentially regulated by ethylene. *Physiologia Plantarum*, 143(1), pp.41–49.

Hicks, L.M. et al., 2007. Thiol-based regulation of redox-active glutamate-cysteine ligase from Arabidopsis thaliana. *The Plant cell*, 19(August), pp.2653–2661.

Hill, R.D., 2012. Non-symbiotic haemoglobins-What's happening beyond nitric oxide scavenging? *AoB plants*, 2012, p.pls004.

Hinz, M. et al., 2010. Arabidopsis RAP2.2: An Ethylene Response Transcription Factor That Is Important for Hypoxia Survival. *Plant Physiology*, 153(2), pp.757–772.

Ho, Q.T. et al., 2010. Genotype effects on internal gas gradients in apple fruit. *Journal of Experimental Botany*, 61(10), pp.2745–2755.

Hochachka, P. et al., 1996. Unifying theory of hypoxia tolerance: molecular/metabolic defense and rescue mechanisms for surviving oxygen lack. *Proceedings of the National Academy of Sciences*, 93(September), pp.9493–9498.

Hodges, M. et al., 2003. Higher plant NADP+-dependent isocitrate dehydrogenases, ammonium assimilation and NADPH production. *Plant Physiology and Biochemistry*, 41, pp.577–585.

6. References

Hsu, F. et al., 2011. Insights into hypoxic systemic responses based on analyses of transcriptional regulation in Arabidopsis. *PloS one*, 6(12), p.e28888.

Hunt, P.W. et al., 2002. Increased level of hemoglobin 1 enhances survival of hypoxic stress and promotes early growth in Arabidopsis thaliana. *Proceedings of the National Academy of Sciences of the United States of America*, 99(26), pp.17197–202.

Igamberdiev, A. et al., 2005. The haemoglobin/nitric oxide cycle: involvement in flooding stress and effects on hormone signalling. *Annals of Botany*, 96(4), pp.557–564.

Igamberdiev, A.U. et al., 2010. Anoxic nitric oxide cycling in plants: Participating reactions and possible mechanisms. *Physiologia Plantarum*, 138(4), pp.393–404.

Igamberdiev, A.U. et al., 2001. The role of photorespiration in redox and energy balance of photosynthetic plant cells: A study with a barley mutant deficient in glycine decarboxylase. *Physiologia plantarum*, 111(4), pp.427–438.

Igamberdiev, A.U. & Gardeström, P., 2003. Regulation of NAD- and NADP-dependent isocitrate dehydrogenases by reduction levels of pyridine nucleotides in mitochondria and cytosol of pea leaves. *Biochimica et Biophysica Acta - Bioenergetics*, 1606(1–3), pp.117–125.

Igamberdiev, A.U. & Hill, R.D., 2004. Nitrate, NO and haemoglobin in plant adaptation to hypoxia: an alternative to classic fermentation pathways. *Journal of Experimental Botany*, 55(408), pp.2473–2482.

Ismond, K.P.K.K.P. et al., 2003. Enhanced low oxygen survival in Arabidopsis through increased metabolic flux in the fermentative pathway. *Plant physiology*, 132(3), pp.1292–1302.

Jacobs, M. et al., 1988. Isolation and Biochemical Analysis of Ethyl Methanesulfonate-Induced Alcohol Dehydrogenase Null Mutants of Arabidopsis thaliana (L .) Heynh . *Biochemical Genetics*, 26, pp.105–122.

Jelitto, T. et al., 1992. Inorganic pyrophosphate content and metabolites in potato and tobacco plants expressing E. coli pyrophosphatase in their cytosol. *Planta*, 188(2), pp.238–244.

Juszczuk, I. & Rychter, A., 2003. Alternative oxidase in higher plants. *ACTA BIOCHIMICA POLONICA*, 50(4), pp.1257–1271.

Kalamaki, M. et al., 2009. Overexpression of a tomato N-acetyl-L-glutamate synthase gene (SlNAGS1) in Arabidopsis thaliana results in high ornithine levels and increased tolerance in salt and drought stresses. *Journal of experimental botany*, 60(6), pp.1859–1871.

Kataya, A.R.A. & Reumann, S., 2010. Arabidopsis glutathione reductase 1 is dually targeted to peroxisomes and the cytosol. *Plant signaling & behavior*, 5(2), pp.171–175.

Kennedy, R., Rumpho, M. & Fox, T., 1992. Anaerobic metabolism in plants. *Plant Physiology*, (8387), pp.1–6.

Kerchev, P.I. et al., 2011. The transcription factor ABI4 Is required for the ascorbic acid-dependent regulation of growth and regulation of jasmonate-dependent defense signaling pathways in Arabidopsis. *The Plant cell*, 23(9), pp.3319–34.

Kleine, T. et al., 2007. Genome-wide gene expression analysis reveals a critical role for CRYPTOCHROME1 in the response of Arabidopsis to high irradiance. *Plant physiology*, 144(3), pp.1391–1406.

Kleinow, T. et al., 2000. Functional identification of an Arabidopsis Snf4 ortholog by screening for heterologous multicopy suppressors of snf4 deficiency in yeast. *Plant Journal*, 23(1), pp.115–122.

Klok, E.J. et al., 2002. Expression profile analysis of the low-oxygen response in Arabidopsis root cultures. *The Plant cell*, 14(10), pp.2481–2494.

Knowles, V.L. et al., 1998. Altered growth of transgenic tobacco lacking leaf cytosolic pyruvate kinase. *Plant physiology*, 116(1), pp.45–51.

Kosmacz, M. et al., 2015. The stability and nuclear localization of the transcription factor RAP2.12 are dynamically regulated by oxygen concentration. *Plant, Cell and Environment*, 38(6), pp.1094–1103.

Kötting, O. et al., 2010. Regulation of starch metabolism: The age of enlightenment? *Current Opinion in Plant Biology*, 13(3), pp.321–329.

6. References

Kreuzwieser, J. et al., 2009. Differential response of gray poplar leaves and roots underpins stress adaptation during hypoxia. *Plant physiology*, 149(1), pp.461–473.

Kursteiner, O. et al., 2003. The Pyruvate decarboxylase1 Gene of Arabidopsis Is Required during Anoxia But Not Other Environmental Stresses. *Plant Physiology*, 132(2), pp.968–978.

Laisk, A., Oja, V. & Eichelmann, H., 2007. Kinetics of leaf oxygen uptake represent in planta activities of respiratory electron transport and terminal oxidases. *Physiologia Plantarum*, 131(1), pp.1–9.

Lam, H. et al., 2003. Overexpression of the ASN1 Gene Enhances Nitrogen Status in Seeds of Arabidopsis 1. *Plant physiology*, 132, pp.926–935.

Lecourieux, D. et al., 2002. Analysis and effects of cytosolic free calcium increases in response to elicitors in Nicotiana plumbaginifolia cells. *The Plant Cell*, 14(October), pp.2627–2641.

Lee, K.K.-W. et al., 2009. Coordinated responses to oxygen and sugar deficiency allow rice seedlings to tolerate flooding. *Science signaling*, 2(91), p.ra61.

Lee, K.W., Chen, P.W. & Yu, S.-M., 2014. Metabolic adaptation to sugar/O2 deficiency for anaerobic germination and seedling growth in rice. *Plant, cell & environment*, 37(10), pp.2234–2244.

Lee, M. et al., 2003. AMP-activated protein kinase activity is critical for hypoxia-inducible factor-1 transcriptional activity and its target gene expression under hypoxic conditions in DU145 cells. *Journal of Biological Chemistry*, 278(41), pp.39653–39661.

Lemaitre, T. et al., 2007. NAD-dependent isocitrate dehydrogenase mutants of Arabidopsis suggest the enzyme is not limiting for nitrogen assimilation. *Plant physiology*, 144(July), pp.1546–1558.

Lemaitre, T. & Hodges, M., 2006. Expression analysis of Arabidopsis thaliana NAD-dependent isocitrate dehydrogenase genes shows the presence of a functional subunit that is mainly expressed in the pollen and absent from vegetative organs. *Plant and Cell Physiology*, 47(5), pp.634–643.

Lepistö, A. et al., 2013. Deletion of chloroplast NADPH-dependent thioredoxin reductase results in inability to regulate starch synthesis and causes stunted growth under short-day photoperiods. *Journal of Experimental Botany*, 64(12), pp.3843–3854.

Lepistö, A. et al., 2009. Implication of chlorophyll biosynthesis on chloroplast-to-nucleus retrograde signaling. *Plant Signal Behav*, 4(6), pp.545–547.

Leterrier, M. et al., 2012. NADP-dependent isocitrate dehydrogenase from Arabidopsis roots contributes in the mechanism of defence against the nitro-oxidative stress induced by salinity. *The Scientific World Journal*, 2012, pp.1–9.

Liao, Y.-D. et al., 2004. Removal of N-terminal methionine from recombinant proteins by engineered E. coli methionine aminopeptidase. *Protein science: a publication of the Protein Society*, 13(7), pp.1802–10.

Licausi, F. et al., 2010. HRE1 and HRE2, two hypoxia inducible ethylene response factors, affect anaerobic responses in Arabidopsis thaliana. *The Plant Journal*, 62(2), pp.302–315.

Licausi, F., 2013. Molecular elements of low-oxygen signaling in plants. *Physiologia Plantarum*, 148, pp.1–8.

Licausi, F. et al., 2011. Oxygen sensing in plants is mediated by an N-end rule pathway for protein destabilization. *Nature*, 479(7373), pp.419–422.

Licausi, F., Ohme-Takagi, M. & Perata, P., 2013. APETALA2/Ethylene Responsive Factor (AP2/ERF) transcription factors: Mediators of stress responses and developmental programs. *New Phytologist*, pp.639–649.

Licausi, F. & Perata, P., 2009. Low oxygen signaling and tolerance in plants. *Advances in Botanical Research*.

Licausi, F., Pucciariello, C. & Perata, P., 2013. New Role for an Old Rule: N-end Rule-Mediated Degradation of Ethylene Responsive Factor Proteins Governs Low Oxygen Response in Plants. *Journal of Integrative Plant Biology*, 55(1), pp.31–39.

Limami, A.M. et al., 2008. Concerted modulation of alanine and glutamate metabolism in young Medicago truncatula seedlings under hypoxic stress. *Journal of Experimental*

6. References

    Botany, 59(9), pp.2325–2335.

van der Linde, K. et al., 2011. Regulation of plant cytosolic aldolase functions by redox-modifications. *Plant Physiology and Biochemistry*, 49(9), pp.946–957.

Lindermayr, C., Saalbach, G. & Durner, J., 2005. Proteomic Identification of S -Nitrosylated Proteins. *Plant physiology*, 137(March), pp.921–930.

Lintala, M. et al., 2014. Arabidopsis tic62 trol mutant lacking thylakoid-bound ferredoxin-NADP + Oxidoredu shows distinct metabolic phenotype. *Molecular Plant*, 7(1), pp.45–57.

Lisec, J. et al., 2006. Gas chromatography mass spectrometry–based metabolite profiling in plants. *Nature protocols*, 1(1), pp.387–396.

Liu, C., Zhao, L. & Yu, G., 2011. The dominant glutamic acid metabolic flux to produce γ-amino butyric acid over proline in nicotiana tabacum leaves under water stress relates to its significant role in antioxidant activity. *Journal of Integrative Plant Biology*, 53(8), pp.608–618.

Liu, F. et al., 2005. Global transcription profiling reveals comprehensive insights into hypoxic response in Arabidopsis. *Plant physiology*, 137(3), pp.1115–1129.

Luedemann, A. et al., 2008. TagFinder for the quantitative analysis of gas chromatography - Mass spectrometry (GC-MS)-based metabolite profiling experiments. *Bioinformatics*, 24(5), pp.732–737.

Lumbreras, V. et al., 2001. Domain fusion between SNF1-related kinase subunits during plant evolution. *EMBO reports*, 2(1), pp.55–60.

Mapson, L.W. & Burton, W.G., 1962. The terminal oxidases of the potato tuber. *Biochemical Journal*, 82, pp.19–25.

Maricle, B.R. & Lee, R.W., 2007. Root respiration and oxygen flux in salt marsh grasses from different elevational zones. *Marine Biology*, 151(2), pp.413–423.

Marino, D. et al., 2007. NADPH recycling systems in oxidative stressed pea nodules: a key role for the NADP+-dependent isocitrate dehydrogenase. *Planta*, 225(2), pp.413–421.

Marsin, A.S. et al., 2002. The stimulation of glycolysis by hypoxia in activated monocytes is mediated by AMP-activated protein kinase and inducible 6-phosphofructo-2-kinase. *Journal of Biological Chemistry*, 277(34), pp.30778–30783.

Marty, L. et al., 2009. The NADPH-dependent thioredoxin system constitutes a functional backup for cytosolic glutathione reductase in Arabidopsis. *Proceedings of the National Academy of Sciences of the United States of America*, 106(22), pp.9109–9114.

Matthew, T. et al., 2009. The Metabolome of Chlamydomonas reinhardtii following Induction of Anaerobic H2 Production by Sulfur Depletion. *Journal of Biological Chemistry*, 284(35), pp.23415–23425.

Maxwell, D.P., Wang, Y. & McIntosh, L., 1999. The alternative oxidase lowers mitochondrial reactive oxygen production in plant cells. *Proceedings of the National Academy of Sciences of the United States of America*, 96(14), pp.8271–8276.

McKibbin, R.S. et al., 2006. Production of high-starch, low-glucose potatoes through over-expression of the metabolic regulator SnRK1. *Plant biotechnology journal*, 4(4), pp.409–18.

Meyer, Y. et al., 2008. Glutaredoxins and thioredoxins in plants. *Biochimica et Biophysica Acta - Molecular Cell Research*, 1783(4), pp.589–600.

Meyer, Y. et al., 2012. Thioredoxin and Glutaredoxin Systems in Plants: Molecular Mechanisms, Crosstalks, and Functional Significance. *Antioxidants & Redox Signaling*, 17(8), pp.1124–1160.

Mhamdi, A., Hager, J., et al., 2010. Arabidopsis GLUTATHIONE REDUCTASE1 plays a crucial role in leaf responses to intracellular hydrogen peroxide and in ensuring appropriate gene expression through both salicylic acid and jasmonic acid signaling pathways. *Plant physiology*, 153(3), pp.1144–1160.

Mhamdi, A., Mauve, C., et al., 2010. Cytosolic NADP- dependent isocitrate dehydrogenase contributes to redox homeostasis and the regulation of pathogen responses in Arabidopsis leaves. *Plant, Cell and Environment*, 33(7), pp.1112–1123.

Michalska, J. et al., 2009. NTRC links built-in thioredoxin to light and sucrose in regulating starch synthesis in chloroplasts and amyloplasts. *Proceedings of the National Academy*

of Sciences of the United States of America, 106(24), pp.9908–9913.

Millar, a H. et al., 2001. Analysis of the Arabidopsis mitochondrial proteome. *Plant physiology*, 127(4), pp.1711–1727.

Millar, a H. et al., 2003. Control of ascorbate synthesis by respiration and its implications for stress responses. *Plant physiology*, 133(2), pp.443–447.

Mithran, M. et al., 2014. Analysis of the role of the pyruvate decarboxylase gene family in Arabidopsis thaliana under low- oxygen conditions. *Plant Biology*, pp.1–7.

Miyashita, Y. et al., 2007. Alanine aminotransferase catalyses the breakdown of alanine after hypoxia in Arabidopsis thaliana. *The Plant Journal*, 49(6), pp.1108–1121.

Mizoi, J., Shinozaki, K. & Yamaguchi-Shinozaki, K., 2012. AP2/ERF family transcription factors in plant abiotic stress responses. *Biochimica et Biophysica Acta (BBA) - Gene Regulatory Mechanisms*, 1819(2), pp.86–96.

Mock, H.-P. & Dietz, K.-J., 2016. Redox proteomics for the assessment of redox-related posttranslational regulation in plants. *Biochimica et Biophysica Acta (BBA) - Proteins and Proteomics*, pp.1–7.

Mohannath, G. et al., 2014. A complex containing SNF1-related kinase (SnRK1) and adenosine kinase in Arabidopsis. *PloS one*, 9(1), p.e87592.

Montrichard, F. et al., 2009. Thioredoxin targets in plants: The first 30 years. *Journal of Proteomics*, 72(3), pp.452–474.

Moreau, M. et al., 2012. Mutations in the Arabidopsis homolog of LST8/GβL, a partner of the target of Rapamycin kinase, impair plant growth, flowering, and metabolic adaptation to long days. *The Plant cell*, 24(2), pp.463–81.

Mustroph, A. et al., 2009. Profiling translatomes of discrete cell populations resolves altered cellular priorities during hypoxia in Arabidopsis. *Proceedings of the National Academy of Sciences*, 106(44), pp.18843–18848.

Nakano, T. et al., 2006. Genome-Wide Analysis of the ERF Gene Family. *Plant Physiology*, 140(February), pp.411–432.

Naranjo, B. et al., 2016. The chloroplast NADPH thioredoxin reductase C, NTRC, controls non-photochemical quenching of light energy and photosynthetic electron transport in Arabidopsis. *Plant, Cell & Environment*, 39(4), pp.804–822.

Narsai, R. et al., 2011. Comparative analysis between plant species of transcriptional and metabolic responses to hypoxia. *New Phytologist*, 190(2), pp.472–487.

Narsai, R. et al., 2009. Defining Core Metabolic and Transcriptomic Responses to Oxygen Availability in Rice Embryos and Young Seedlings. *Plant Physiology*, 151(1), pp.306–322.

Navarre, D. a et al., 2000. Nitric oxide modulates the activity of tobacco aconitase. *Plant physiology*, 122(February), pp.573–582.

Née, G. et al., 2009. Redox regulation of chloroplastic glucose-6-phosphate dehydrogenase: A new role for f-type thioredoxin. *FEBS Letters*, 583(17), pp.2827–2832.

Nikoloski, Z. & van Dongen, J.T., 2011. Modeling alternatives for interpreting the change in oxygen-consumption rates during hypoxic conditions. *New Phytologist*, 190(2), pp.273–276.

Nunes-Nesi, A. et al., 2005. Enhanced photosynthetic performance and growth as a consequence of decreasing mitochondrial malate dehydrogenase activity in transgenic tomato plants. *Plant physiology*, 137(February), pp.611–622.

Oaks, A.N.N., Aslam, M. & Boesel, I., 1977. Ammonium Regulators Nitrate. , pp.391–394.

Oliveira, H., Freschi, L. & Sodek, L., 2013. Nitrogen metabolism and translocation in soybean plants subjected to root oxygen deficiency. *Plant Physiology and Biochemistry*, 66, pp.141–149.

Oliveira, H.C.H. & Sodek, L., 2013. Effect of oxygen deficiency on nitrogen assimilation and amino acid metabolism of soybean root segments. *Amino acids*, 44(2), pp.743–755.

Oliver, S.N. et al., 2008. Decreased expression of cytosolic pyruvate kinase in potato tubers leads to a decline in pyruvate resulting in an in vivo repression of the alternative oxidase. *Plant physiology*, 148(3), pp.1640–1654.

Papdi, C. et al., 2015. The low oxygen, oxidative and osmotic stress responses synergistically act through the ethylene response factor VII genes RAP2.12, RAP2.2

and RAP2.3. *The Plant Journal*, 82(5), pp.772–784.

Paventi, G. et al., 2007. L- Lactate metabolism in potato tuber mitochondria. *FEBS Journal*, 274(6), pp.1459–1469.

Perazzolli, M. et al., 2004. Arabidopsis nonsymbiotic hemoglobin AHb1 modulates nitric oxide bioactivity. *The Plant Cell*, 16(10), pp.2785–2794.

Perez-Ruiz, J.M. et al., 2014. NADPH thioredoxin reductase C is involved in redox regulation of the Mg-chelatase I subunit in Arabidopsis thaliana chloroplasts. *Molecular Plant*, 7(7), pp.1252–1255.

Pérez-Ruiz, J.M.J. et al., 2006. Rice NTRC is a high-efficiency redox system for chloroplast protection against oxidative damage. *The Plant Cell*, 18(9), pp.2356–2368.

Planchet, E. et al., 2005. Nitric oxide emission from tobacco leaves and cell suspensions: rate limiting factors and evidence for the involvement of mitochondrial electron transport. *The Plant journal*, 41(5), pp.732–43.

Plaxton, W.C. & Podestá, F.E., 2006. The Functional Organization and Control of Plant Respiration. *Critical Reviews in Plant Sciences*, 25, pp.159–198.

Plaxton, W.C. & Tran, H.T., 2011. Metabolic Adaptations of Phosphate-Starved Plants. *Plant physiology*, 156(July), pp.1006–1015.

Plaxton, W.C.W., 1996. The organization and regulation of plant glycolysis. *Annual review of plant biology*, 47(1), pp.185–214.

Polge, C. & Thomas, M., 2007. SNF1/AMPK/SnRK1 kinases, global regulators at the heart of energy control? *Trends in plant science*, 12(1), pp.20–8.

Pucciariello, C. et al., 2012. Reactive Oxygen Species-Driven Transcription in Arabidopsis under Oxygen Deprivation. *Plant Physiology*, 159(1), pp.184–196.

Pucciariello, C. & Perata, P., 2016. New insights into reactive oxygen species and nitric oxide signalling under low oxygen in plants. *Plant, Cell & Environment*.

Pulido, P. et al., 2010. Functional analysis of the pathways for 2-Cys peroxiredoxin reduction in Arabidopsis thaliana chloroplasts. *Journal of Experimental Botany*, 61(14), pp.4043–4054.

Purcell, P., Smith, A. & Halford, N., 1998. Antisense expression of a sucrose non- fermenting- 1- related protein kinase sequence in potato results in decreased expression of sucrose synthase in tubers and. *The Plant Journal*, 14(January), pp.195–202.

Purcell, P.C., Smith, A.M. & Halford, N.G., 1998. Antisense expression of a sucrose non fermenting 1 related protein kinase sequence in potato results in decreased expression of sucrose synthase in tubers and loss of sucrose inducibility of sucrose synthase transcripts in leaves. *The Plant Journal*, 14(2), pp.195–202.

Queval, G. & Noctor, G., 2007. A plate reader method for the measurement of NAD, NADP, glutathione, and ascorbate in tissue extracts: Application to redox profiling during Arabidopsis rosette development. *Analytical Biochemistry*, 363(1), pp.58–69.

Ramirez-Aguilar, S.J. et al., 2011. The composition of plant mitochondrial supercomplexes changes with oxygen availability. *Journal of Biological Chemistry*, 286(50), pp.43045–43053.

Ramon, M. et al., 2013. The hybrid Four CBS Domain KINβγ subunit functions as the canonical γ subunit of the plant energy sensor SnRK1. *The Plant Journal*, 75(1), pp.11–25.

Ratcliffe, R., 1997. In vivo NMR studies of the metabolic response of plant tissues to anoxia. *Annals of Botany*, 79(January 1996), pp.39–48.

REGGIANI, R., 1985. Effect of exogenous nitrate on anaerobic metabolism in excised rice roots I. Nitrate reduction and pyridine nucleotide pools. *Journal of Experimental Botany*, 36(169), pp.1193–1199.

Reichheld, J.P.J. et al., 2005. AtNTRB is the major mitochondrial thioredoxin reductase in Arabidopsis thaliana. *FEBS letters*, 579(2), pp.337–342.

Reichheld, J.-P.J. et al., 2007. Inactivation of thioredoxin reductases reveals a complex interplay between thioredoxin and glutathione pathways in Arabidopsis development. *The Plant cell*, 19(6), pp.1851–1865.

Ben Rejeb, K., Abdelly, C. & Savouré, A., 2014. How reactive oxygen species and proline

face stress together. *Plant physiology and biochemistry*, 80C, pp.278–284.

Ren, M. et al., 2012. Target of rapamycin signaling regulates metabolism, growth, and life span in Arabidopsis. *The Plant Cell*, 24(December), pp.4850–4874.

Renz, A. & Stitt, M., 1993. Substrate specificity and product inhibition of different forms of fructokinases and hexokinases in developing potato tubers. *Planta*, 49(6221), pp.166–175.

Rhoads, D.M. et al., 2006. Mitochondrial reactive oxygen species. Contribution to oxidative stress and interorganellar signaling. *Plant physiology*, 141(2), pp.357–366.

Ribas-Carbo, M. et al., 1994. The reaction of the plant mitochondrial cyanide-resistant alternative oxidase with oxygen. *Biochimica et biophysica acta*, 1188, pp.205–212.

Ricard, B. et al., 1994. Plant Metabolism Under Hypoxia and Anoxia. *Plant Physiology and Biochemistry*, 32(1), pp.1–10.

Richter, A.S. et al., 2013. Posttranslational influence of NADPH-dependent thioredoxin reductase C on enzymes in tetrapyrrole synthesis. *Plant physiology*, 162(1), pp.63–73.

Robaglia, C., Thomas, M. & Meyer, C., 2012. Sensing nutrient and energy status by SnRK1 and TOR kinases. *Current opinion in plant biology*, 15(3), pp.1–7.

Roberts, J. et al., 1984. Mechanisms of cytoplasmic pH regulation in hypoxic maize root tips and its role in survival under hypoxia. *Proceedings of the National Academy of Sciences of the United States of America*, 81(11), pp.3379–3383.

Roberts, J., Andrade, F. & Anderson, I., 1985. Further evidence that cytoplasmic acidosis is a determinant of flooding intolerance in plants. *Plant Physiology*, pp.492–494.

Roberts, J.K. et al., 1992. Contribution of malate and amino acid metabolism to cytoplasmic pH regulation in hypoxic maize root tips studied using nuclear magnetic resonance spectroscopy. *Plant physiology*, 98(2), pp.480–487.

Roberts, J.K. et al., 1984. Cytoplasmic acidosis as a determinant of flooding intolerance in plants. *Proceedings of the National Academy of Sciences of the United States of America*, 81(October), pp.6029–6033.

Rocha, M. et al., 2010. Glycolysis and the tricarboxylic acid cycle are linked by alanine aminotransferase during hypoxia induced by waterlogging of Lotus japonicus. *Plant physiology*, 152(3), pp.1501–1513.

Roessner, U. et al., 2001. Metabolic profiling allows comprehensive phenotyping of genetically or environmentally modified plant systems. *The Plant Cell*, 13(January), pp.11–29.

Rosnoblet, C. et al., 2007. SNF4b of the sucrose non- fermenting- related kinase complex is involved in longevity and stachyose accumulation during maturation of Medicago truncatula. *The Plant Journal*, 51, pp.47–59.

Salvato, F. et al., 2013. The Potato Tuber Mitochondrial Proteome. *Plant Physiology*, 164(2), pp.637–653.

Salvato, F. et al., 2014. The potato tuber mitochondrial proteome. *Plant physiology*, 164(February), pp.637–53.

Santaniello, A. et al., 2014. A reassessment of the role of sucrose synthase in the hypoxic sucrose-ethanol transition in Arabidopsis. *Plant, cell & environment*, 37(10), pp.2294–2302.

Sasidharan, R. & Mustroph, A., 2011. Plant oxygen sensing is mediated by the N-end rule pathway: a milestone in plant anaerobiosis. *The Plant Cell Online*, 23(12), pp.4173–83.

Satyanarayan, V. & Nair, M., 1985. Purification and characterization of glutamate decarboxylase from Solanum tuberosum. *European Journal of Biochemistry*, 150, pp.53–60.

Schertl, P. et al., 2012. L-galactono-1, 4-lactone dehydrogenase (GLDH) forms part of three subcomplexes of mitochondrial complex I in Arabidopsis thaliana. *Journal of Biological Chemistry*, 287(18), pp.14412–14419.

Schulze-Siebert, D. et al., 1984. Pyruvate-Derived Amino Acids in Spinach Chloroplasts. *Plant Physiology*, 76, pp.465–471.

Serrato, A.J. et al., 2004. A novel NADPH thioredoxin reductase, localized in the chloroplast, which deficiency causes hypersensitivity to abiotic stress in Arabidopsis thaliana. *The Journal of biological chemistry*, 279(42), pp.43821–43827.

6. References

Setter, T.L. & Waters, I., 2003. Review of prospects for germplasm improvement for waterlogging tolerance in wheat, barley and oats. *Plant and Soil*, 253(1), pp.1–34.

Shabala, S. et al., 2014. Membrane transporters mediating root signalling and adaptive responses to oxygen deprivation and soil flooding. *Plant, cell & environment*, 37(10), pp.2216–33.

Shen, W. & Hanley-Bowdoin, L., 2006. Geminivirus infection up-regulates the expression of two Arabidopsis protein kinases related to yeast SNF1- and mammalian AMPK-activating kinases. *Plant physiology*, 142(4), pp.1642–1655.

Shigeoka, S. & Maruta, T., 2014. Cellular redox regulation, signaling, and stress response in plants. *Biosci Biotechnol Biochem*, 78(9), pp.1457–1470.

Shimizu, M. et al., 2010. Mechanism of De Novo Branched-Chain Amino Acid Synthesis as an Alternative Electron Sink in Hypoxic Aspergillus nidulans Cells. *Applied and Environmental Microbiology*, 76(5), pp.1507–1515.

Shingaki-Wells, R. et al., 2014. What happens to plant mitochondria under low oxygen? An omics review of the responses to low oxygen and re-oxygenation. *Plant, cell & environment*, pp.2260–2277.

Siddiqui, M.H., Al-Whaibi, M.H. & Basalah, M.O., 2011. Role of nitric oxide in tolerance of plants to abiotic stress. *Protoplasma*, 248(3), pp.447–455.

Sienkiewicz-Porzucek, A. et al., 2010. Mild reductions in mitochondrial NAD-dependent isocitrate dehydrogenase activity result in altered nitrate assimilation and pigmentation but do not impact growth. *Molecular Plant*, 3(1), pp.156–173.

Silver, D.M. et al., 2013. Insight into the redox regulation of the phosphoglucan phosphatase SEX4 involved in starch degradation. *FEBS Journal*, 280(2), pp.538–548.

Sivasankar, S., Oaks, A. & Science, N., 1995. Regulation of Nitrate Reductase during Early Seedling Growth '. *Plant physiology*, 107(4), pp.1225–1231.

Smith, C., 2000. Purification and characterization of cytosolic pyruvate kinase from Brassica napus (rapeseed) suspension cell cultures. *European Journal of Biochemistry*, 267(14), pp.4477–4485.

Snedden, W.A. et al., 1995. Calcium / Calmodulin Activation of Soybean Glutamate Decarboxylase. *Plant physiology*, 108(2), pp.543–549.

Sousa, C. & Sodek, L., 2002. The metabolic response of plants to oxygen deficiency. *Brazilian Journal of Plant Physiology*, 14(2), pp.83–94.

Sowa, A. et al., 1998. Altering hemoglobin levels changes energy status in maize cells under hypoxia. *Proceedings of the National Academy of Sciences*, 95(August), pp.10317–10321.

Steffens, B., Geske, T. & Sauter, M., 2011. Aerenchyma formation in the rice stem and its promotion by H2O2. *New Phytologist*, 190(2), pp.369–378.

Steffens, B., Steffen-Heins, A. & Sauter, M., 2013. Reactive oxygen species mediate growth and death in submerged plants. *Frontiers in plant science*, 4(June), p.179.

Stiti, N. et al., 2011. Aldehyde Dehydrogenases in Arabidopsis thaliana: Biochemical Requirements, Metabolic Pathways, and Functional Analysis. *Frontiers in plant science*, 2(October), p.Article 65: 1-11.

Stitt, M., 1998. Pyrophosphate as an energy donor in the cytosol of plant cells: an enigmatic alternative to ATP. *Botanica Acta*, 111, pp.167–175.

Streeter, J.G. & Thompson, J.F., 1972a. Anaerobic Accumulation of gamma-Aminobutyric Acid and Alanine in Radish Leaves (Raphanus sativus, L.). *Plant physiology*, 49(4), pp.572–578.

Streeter, J.G. & Thompson, J.F., 1972b. In Vivo and In Vitro Studies on gamma-Aminobutyric Acid Metabolism with the Radish Plant (Raphanus sativus, L.). *Plant physiology*, 49(4), pp.579–584.

Subbaiah, C.C., Bush, D.S. & Sachs, M.M., 1994. Elevation of cytosolic calcium precedes anoxic gene expression in maize suspension-cultured cells. *The Plant cell*, 6(12), pp.1747–1762.

Subbaiah, C.C., Bush, D.S. & Sachs, M.M., 1998. Mitochondrial contribution to the anoxic Ca2+ signal in maize suspension-cultured cells. *Plant Physiology*, 61801, pp.759–771.

Subbaiah, C.C. & Sachs, M.M., 2003. Calcium-mediated responses of maize to oxygen

deprivation. *Russian Journal of Plant Physiology*, 50(6), pp.752–761.

Sugden, C. et al., 1999. Regulation of spinach SNF1-related (SnRK1) kinases by protein kinases and phosphatases is associated with phosphorylation of the T loop and is regulated. *The Plant Journal*, 19(June), pp.433–439.

Sugden, C. et al., 1999. Two SNF1-Related Protein Kinases from Spinach Leaf Phosphorylate and Inactivate 3-Hydroxy-3-Methylglutaryl- Coenzyme A Reductase , Nitrate Reductase , and Sucrose Phosphate Synthase in Vitro. *Plant physiology*, 120(May), pp.257–274.

Sweetlove, L.J.L. et al., 2010. Not just a circle: Flux modes in the plant TCA cycle. *Trends in plant …*, 15(8), pp.1–9.

Szabados, L. & Savouré, A., 2010. Proline: a multifunctional amino acid. *Trends in Plant Science*, 15(December), pp.89–97.

Szecowka, M. et al., 2013. Metabolic fluxes in an illuminated Arabidopsis rosette. *The Plant Cell*, 25(2), pp.694–714.

Tadege, M., Dupuis, I. & Kuhlemeier, C., 1999. Ethanolic fermentation: new functions for an old pathway. *Trends in plant science*, 4(8), pp.320–325.

Tasaki, T. et al., 2012. The N-End Rule Pathway. , 81(1), pp.261–289.

Taylor, N., Heazlewood, J. & Millar, A., 2011. thaliana 2-D gel mitochondrial proteome: Refining the value of reference maps for assessing protein abundance, contaminants and post-translational modifications. *Proteomics*, 11(9), pp.1720–1733.

Thiel, J. et al., 2011. Seed-specific elevation of non-symbiotic hemoglobin AtHb1: beneficial effects and underlying molecular networks in Arabidopsis thaliana. *BMC plant biology*, 11(1), p.48.

Thomas, S. et al., 1997. Metabolic control analysis of glycolysis in tuber tissue of potato (Solanum tuberosum): explanation for the low control coefficient of phosphofructokinase over respiratory flux. *Biochem. J*, 127, pp.119–127.

Thormählen, I. et al., 2013. Inactivation of thioredoxin f1 leads to decreased light activation of ADP-glucose pyrophosphorylase and altered diurnal starch turnover in leaves of Arabidopsis plants. *Plant, cell & environment*, 36(1), pp.16–29.

Toivola, J. et al., 2013. Overexpression of chloroplast NADPH-dependent thioredoxin reductase in Arabidopsis enhances leaf growth and elucidates in vivo function of reductase and thioredoxin domains. *Frontiers in plant science*, 4(October), p.389.

Tome, F. et al., 2014. The low energy signaling network. *Frontiers in Plant Science*, 5(July), p.353.

Torres, M.A., Dangl, J.L. & Jones, J.D.G., 2002. Arabidopsis gp91phox homologues AtrbohD and AtrbohF are required for accumulation of reactive oxygen intermediates in the plant defense response. *Proceedings of the National Academy of Sciences*, 99(1), pp.517–522.

Trevisan, S. et al., 2011. Transcriptome analysis reveals coordinated spatiotemporal regulation of hemoglobin and nitrate reductase in response to nitrate in maize roots. *The New phytologist*, 192(2), pp.338–52.

Tsushida, T. & Murai, T., 1987. Conversion of glutamic acid to γ-aminobutyric acid in tea leaves under anaerobic conditions. *Agricultural and Biological Chemistry*, 51(11), pp.2865–2871.

Turner, W. & Plaxton, W., 2000. Purification and characterization of cytosolic pyruvate kinase from banana fruit. *Biochem. J*, 352 Pt 3, pp.875–882.

Turner, W.L.W., Knowles, V.V.L. & Plaxton, W.C.W., 2005. Cytosolic pyruvate kinase: Subunit composition, activity, and amount in developing castor and soybean seeds, and biochemical characterization of the purified castor seed enzyme. *Planta*, 222(6), pp.1051–1062.

Umbach, A.L., Ng, V.S. & Siedow, J.N., 2006. Regulation of plant alternative oxidase activity: a tale of two cysteines. *Biochimica et biophysica acta*, 1757(2), pp.135–42.

Valerio, C. et al., 2011. Thioredoxin-regulated beta-amylase (BAM1) triggers diurnal starch degradation in guard cells, and in mesophyll cells under osmotic stress. *Journal of Experimental Botany*, 62(2), pp.545–555.

Valluru, R. & Van den Ende, W., 2012. Plant Science Erratum to " Myo -inositol and beyond

6. References

– Emerging networks under stress .” *Plant Science*, 185–186, pp.340–341.

Vanlerberghe, G.C., 2013. Alternative oxidase: A mitochondrial respiratory pathway to maintain metabolic and signaling homeostasis during abiotic and biotic stress in plants. *International Journal of Molecular Sciences*, 14(4), pp.6805–6847.

Vartapetian, B.B.B. & Jackson, M.B., 1997. Plant adaptations to anaerobic stress. *Annals of Botany*, 79(suppl 1), pp.3–20.

Verniquet, F. et al., 1991. Rapid inactivation of plant aconitase by hydrogen peroxide. *The Biochemical journal*, 276 (Pt 3, pp.643–648.

Vigeolas, H. et al., 2003. Lipid storage metabolism is limited by the prevailing low oxygen concentrations within developing seeds of oilseed rape. *Plant Journal*, 133(4), pp.2048–2060.

Voesenek, L. a C.J. & Bailey-Serres, J., 2013. Flooding tolerance: O2 sensing and survival strategies. *Current Opinion in Plant Biology*, 16(5), pp.647–653.

Wallace, W., Secor, J. & Schrader, L.E., 1984. Rapid Accumulation of gamma-Aminobutyric Acid and Alanine in Soybean Leaves in Response to an Abrupt Transfer to Lower Temperature, Darkness, or Mechanical Manipulation. *Plant physiology*, 75(1), pp.170–175.

Weits, D.A. et al., 2014. Plant cysteine oxidases control the oxygen-dependent branch of the N-end-rule pathway. *Nature Communications*, 5, p.3425.

Wenderoth, I., Scheibe, R. & Von Schaewen, A., 1997. Identification of the cysteine residues involved in redox modification of plant plastidic glucose-6-phosphate dehydrogenase. *Journal of Biological Chemistry*, 272(43), pp.26985–26990.

Wilson, I.D., Neill, S.J. & Hancock, J.T., 2008. Nitric oxide synthesis and signalling in plants. *Plant, Cell & Environment*, 31(5), pp.622–631.

Yamasaki, H. & Sakihama, Y., 2000. Simultaneous production of nitric oxide and peroxynitrite by plant nitrate reductase: In vitro evidence for the NR-dependent formation of active nitrogen species. *FEBS Letters*, 468(1), pp.89–92.

Yoshida, K. et al., 2013. Systematic exploration of thioredoxin target proteins in plant mitochondria. *Plant & cell physiology*, 54(6), pp.875–92.

Yu, X. et al., 2013. Plastid-Localized Glutathione Reductase2 – Regulated Glutathione Redox Status Is Essential for Arabidopsis Root Apical Meristem Maintenance. *The Plant cell*, 25(November), pp.1–19.

Zabalza, A. et al., 2008. Regulation of Respiration and Fermentation to Control the Plant Internal Oxygen Concentration. *Plant Physiology*, 149(2), pp.1087–1098.

Zabalza, A. et al., 2011. Unraveling the role of fermentation in the mode of action of acetolactate synthase inhibitors by metabolic profiling. *Journal of plant physiology*, 168(13), pp.1568–1575.

Zhang, Y. et al., 2012. Downregulation of OsPK1, a cytosolic pyruvate kinase, by T-DNA insertion causes dwarfism and panicle enclosure in rice. *Planta*, 235(1), pp.25–38.

Zsigmond, L. et al., 2011. Enhanced activity of galactono-1,4-lactone dehydrogenase and ascorbate-glutathione cycle in mitochondria from complex III deficient Arabidopsis. *Plant Physiology and Biochemistry*, 49(8), pp.809–815.

Acknowledgements

I would like to give my sincere thanks to Prof. Peter Geigenberger for giving me the opportunity to do my PhD thesis at the LMU in Munich and also for the supervision and support during the years of my PhD project.

I'd also like to thank Prof. Joost van Dongen and Dr. Francesco Licausi for their support and advices especially in the beginning of my thesis. Furthermore, I want to thank all collaboration partners for the provision of the mutant plant material and specifically Dr. Martin Lehmann and Jennifer Lindstadt for the GCMS profiling data.

Additionally, I am very grateful to my bachelor and master students as well as my summer school and research course students Ana Luz, Alexandra, Kate, Michael and Sri who did all the work I did not have the time to do or was too lazy…☺

My special thanks go to all former and present lab members of the AG Geigenberger, namely Alexandra, Anne, Chrissi, Ina, Jessy, Luke, Martin, Matthias, Melanie, Sabrina, Ulrike and Uta. I will remember the friendly atmosphere in the office and in the lab as well as the fun we had during the numerous activities like sledging and hiking in the mountains, riding with the bike to the Bodensee, playing soccer, going to the Oktoberfest and Christmas markets and just sitting outside in the summer for a "short" break during work. Furthermore, I want to thank Dr. Michael Sandmann for correcting my thesis and the fun time we had during our studies in biology.

Last but not least, I should like to express my sincere thanks to my family for the support and encouragement during the last years and especially my sister for proofreading my thesis manuscript.

Curriculum vitae

Personal data

Name: Benjamin Faix

Date of birth: 13.02.1983

Place of birth: Erfurt

Citizenship: German

Research experience

Since 2010   PhD thesis "Adaptation of plants to low-oxygen"

Ludwig-Maximillians-University Munich

Faculty of Biology (Botany)

Research group plant metabolism of Prof. Peter Geigenberger

2009-2010   Scientific assistant

Max-Planck-Institute of Molecular Plant Physiology Golm

Research group storage carbohydrate metabolism of Prof. Peter

Geigenberger

Education

2002-2009   Diploma in biology

University of Potsdam

Specialization: biochemistry/physiology

Final grade 1.9

1996-2002   A-levels

Humboldt-Gymnasium Potsdam

Grade 2.1

Research publications

Faix B, Radchuk V, Hümmer C, Radchuk R, Emery RJ, Keller H, Götz KP, Weschke W, Geigenberger P, Weber H. (2012) Barley grains, deficient in cytosolic small subunit of ADP-glucose pyrophosphorylase, reveal coordinate adjustment of C:N metabolism mediated by an overlapping metabolic-hormonal control. *Plant J.* Mar; 69 (6):1077-93

Tiessen A, Nerlich A, Faix B, Hümmer C, Fox S, Trafford K, Weber H, Weschke W, Geigenberger P. Subcellular analysis of starch metabolism in developing barley seeds using a non-aqeous fractionation method. *J Exp Bot.* Mar; 63 (5):2071-87

Zabalza A, van Dongen JT, Froehlich A, Oliver SN, Faix B, Gupta KJ, Schmälzlin E, Igal M, Orcaray L, Royuela M, Geigenberger P. (2009) Regulation of respiration and fermentation to control the plant internal oxygen concentration. *Plant Physiol.* Feb; 149(2):1087-98

Oliver SN, Lunn JE, Urbanczyk-Wochniak E, Lytovchenko A, van Dongen JT, Faix B, Schmälzlin E, Fernie AR, Geigenberger P. (2008) Decreased expression of cytosolic pyruvate kinase in potato tubers leads to a decline in pyruvate resulting in an in vivo repression of the alternative oxidase. *Plant Physiol.* Nov; 148(3):1640-54

Eidesstattliche Erklärung

Ich versichere hiermit an Eides statt, dass die vorgelegte Dissertation von mir selbständig und ohne unerlaubte Hilfe angefertigt ist. Der Autor hat zuvor nicht versucht, anderweitig eine Dissertation einzureichen oder sich einer Doktorprüfung zu unterziehen. Die Dissertation wurde keiner weiteren Prüfungskommission weder in Teilen noch als Ganzes vorgelegt.

München, den 29.09.2016

_____

Benjamin Faix